National Research Council Canada | Conseil national de recherches Canada
Environmental Secretariat | Secretariat de l'environnement
Associate Committee on Scientific Criteria for Environmental Quality | Comité associé sur les critères scientifiques concernant l'état de l'environnement
Ottawa Canada
K1A 0R6

ANNOUNCEMENT
OF
PUBLICATION

EFFECTS OF AEROSOLS ON ATMOSPHERIC PROCESSES

This document deals with various aspects of aerosols in the atmosphere: particle characteristics; sources and emissions; effects on optical properties of the atmosphere; effects on clouds, fog, precipitation and atmospheric electricity; and effects on climate.

The presence of particles in the atmosphere results from the activities of both nature and man. The relative proportions of the total atmospheric particle burden generated by each source category has yet to be elucidated. The routine measurement and control of airborne particles have been traditionally based on the concept of total suspended particulate matter with little regard for an airborne particle's intrinsic characteristics or the factors dictating its behavior in an atmospheric aerosol. It has been demonstrated that atmospheric aerosols are composed of a spectrum of airborne particles, having characteristics such as particle size, shape, density, surface area, light scattering properties, etc. which are dependent upon mechanisms of particle formation, atmospheric transport, transformation and removal. The most important parameter to characterize airborne particles is considered to be particle size, and, of the numerous expressions used to denote it, aerodynamic diameter is the most widely accepted.

The distribution of particle sizes in an atmospheric aerosol fluctuates dramatically, depending upon such influences as source(s), age of the aerosol and meteorological conditions. Atmospheric aerosols relatively far removed from specific sources normally have a bimodal size distribution according to mass; these modes are fine (0.1-1.0 μm) and coarse (2-100 μm). The division between fine and coarse particle modes is in the range of 1-3 μm, but is commonly assumed to be 2 μm. However, this separation is neither sharp nor fixed and significant overlap may occur.

The scattering and absorption of light by aerosols is dependent upon particle size distribution, refractive index and shape, and on the relative humidity and wavelength of incident light. The reduction in visible light intensity is due primarily to the presence of fine particles (particularly those with diameters 0.1-1.0 μm). Although airborne fine particles are generally considered responsible for much of the reduced visibility, especially in areas of relatively low particle mass loadings, the concentration and chemical composition of such particles can vary significantly in space and in time. Despite numerous attempts to correlate particle chemical composition with visibility reduction, such a correlation must be considered tenuous since a chemical constituent's contribution to aerosol mass loading may not equal its contribution to visibility degradation. Some field studies have demonstrated significant positive correlations between sulfate concentrations and visibility, especially in nonurban areas.

Aerosols may affect clouds, fog, precipitation and electric properties of the atmosphere. Climate models indicate that an increase in aerosol loading in the stratosphere will warm the aerosol layer and may decrease the temperature at the earth's surface. However, the effects of aerosols (both stratospheric and tropospheric) on the earth's surface temperature have not yet been clearly established.

English version (208 pages)
Publication No. NRCC 18473
Available through prepaid
purchase orders from

Version française
Publication no CNRC 18474
En vente, moyennant commandes
prépayées, au Service des

Publications, NRCC/CNRC
Ottawa, Ontario, Canada K1A 0R6

Price/Prix: $8.00

Canada

National Research Council Canada
Conseil national de recherches Canada

Environmental Secretariat
Secrétariat de l'environnement

Associate Committee on Scientific Criteria for Environmental Quality
Comité associé sur les critères scientifiques concernant l'état de l'environnement

Ottawa, Canada
K1A 0R6

NOUVELLE
PUBLICATION

EFFETS DES AEROSOLS SUR LES PROCESSUS ATMOSPHERIQUES

Ce document traite des divers aspects des aérosols dans l'atmosphère: caractéristiques des particules; sources et émissions; effets sur les propriétés optiques de l'atmosphère; effets sur les nuages, la brume, les précipités, l'électricité atmosphérique et le climat.

La présence des particules dans l'atmosphère résultent des activités naturelles et anthropiques. L'importance relative de chaque source reste toujours à élucider. Les mesures et le contrôle des particules dans les airs sont basés traditionnellement sur le concept de la matière particulaire totale en suspension, sans tenir beaucoup compte des caractéristiques intrinsèques de la particule ou des facteurs régissant son comportement. Par contre, les aérosols atmosphériques se composent de toute une gamme de particules, ayant des caractéristiques (dimensions, morphologie, densité, superficie, etc.) qui dépendent des mécanismes mêmes de leur formation, transport, transformation et élimination. L'on considère que la caractéristique la plus importante de ces particules est leur taille, et notamment le diamètre aérodynamique.

Les sources, l'âge de l'aérosol, les conditions météorologiques entre autres font varier considérablement la répartition des particules quant à leurs dimensions. Les aérosols relativement éloignés des sources ont normalement une répartition, selon la masse, consistant de particules fines (0.1-1.0 μm) et grossières (2-100 μm), la limite, se situant entre 1 et 3 μm, est souvent considérée comme 2 μm. Toutefois, cette démarcation n'est pas du tout bien définie.

La dispersion et l'absorption de la lumière par les aérosols dépendent de la morphologie, l'indice de réfraction, la répartition des particules selon leurs dimensions ainsi que de l'humidité relative et de la longueur d'onde de la lumière incidente. La présence des particules fines est principalement responsable de la réduction de la visibilité, particulièrement, croit-on, dans les régions où l'apport des particules, selon leur masse, est relativement faible; toutefois, leur concentration et leur composition chimique peuvent varier sensiblement avec le temps et l'espace. L'on doit considérer les nombreuses tentatives de mettre en corrélation la composition chimique des particules et la réduction de la visibilité toujours suspectes puisque l'apport d'un constituant chimique à la charge (quant à la masse) d'un aérosol pourrait ne pas égaler son apport à la réduction de la visibilité. D'après des études *in situ*, lorsque la concentration des sulfates augmente, la visibilité diminue, surtout dans les régions urbaines.

Les aérosols peuvent avoir un effet sur les nuages, la brume, les précipitations et les propriétés électriques de l'atmosphère. D'après des simulations de climat, si la quantité des aérosols dans la stratosphère augmente, la couche des aérosols deviendra plus chaude, et la température à la surface de la terre pourra donc s'abaisser. Cependent, les effets des aérosols (qu'ils soient stratosphérique ou troposphérique) restent à préciser.

Version anglaise (208 pages)
Publication No. NRCC 18473
Available through prepaid purchase orders from

Version française (à paraître)
Publication nº CNRC 18474
En vente, moyennant commandes prépayées, au Service des

Publications, NRCC/CNRC
Ottawa, Ontario, Canada K1A 0R6

Prix/Price: $8.00

Canada

NATIONAL RESEARCH COUNCIL OF CANADA

NRCC ASSOCIATE COMMITTEE ON SCIENTIFIC CRITERIA

FOR

ENVIRONMENTAL QUALITY

EFFECTS OF AEROSOLS ON ATMOSPHERIC PROCESSES

PANEL ON ATMOSPHERIC AEROSOLS
SUBCOMMITTEE ON AIR

Publication No. NRCC 18473
of the
Environmental Secretariat

Crown Copyright Reserved
1982

Available through prepaid
orders only from:

Publications, NRCC/CNRC
Ottawa, Canada K1A 0R6

Price: $8.00

The Associate Committee on Scientific Criteria for Environmental Quality was established by the National Research Council of Canada in response to a mandate provided by the Federal Government to develop scientific guidelines for defining the quality of the environment. The concern of the NRCC Associate Committee is strictly with scientific criteria. Pollution standards and objectives are the responsibility of the regulatory authorities and are set for the purpose of pollution control. These may be based on scientific criteria as a starting point but they also take into account the optimal socioeconomic impact of proposed measures as well as the state of existing technology.

The Associate Committee's program includes the evaluation of available information on the probability of effects of contaminants on receptors together with the related fundamental principles and scientific knowledge. In this work particular attention is directed to receptors and contaminants (and their interactions) important to Canada. This Canadian approach is necessary because evaluations made in other countries or regions will not always be applicable to the particular circumstances prevailing in Canada.

Members of the Associate Committee, its Subcommittees and Expert Panels, serve voluntarily and are selected for their individual competence and relevant experience with due consideration for a balance among all sectors in Canada. Responsibility for the quality of study documents rests with the Associate Committee. Each report is carefully reviewed according to a multistage procedure established and monitored by the National Research Council of Canada in order to preserve objectivity in presentation of the scientific knowledge. Publication and distribution of the report are undertaken only after completion of this review process.

Comments on Associate Committee documents are welcome and will be carefully reviewed by the Expert Panels. It is foreseen that these scientific criteria may be revised from time to time, as new knowledge becomes available.

All documents published by the Associate Committee are published in both French and English.

SUBCOMMITTEE ON AIR

PANEL ON EFFECTS OF AEROSOLS ON ATMOSPHERIC PROCESSES

Dr. J.W.S. Young (Chairman),
Air Quality and Inter-Environmental Research Branch,
Atmospheric Environment Service,
Downsview, Ontario
M3H 5T4

Dr. R.C. Pierce (Secretary),
Environmental Secretariat,
Division of Biological Sciences,
National Research Council of Canada,
100 Sussex Drive,
Ottawa, Ontario
K1A 0R6

Dr. S. Bhartendu,
Scientific Services Division,
Ontario Region,
Atmospheric Environment Service,
Toronto, Ontario
M4T 1M2

Mr. R. Berry,
Atmospheric Chemistry,
Criteria and Standards Division,
Atmospheric Environment Service,
Downsview, Ontario
M3H 5T4

Mr. A.J. Chandler,
Beak Consultants,
Mississauga, Ontario
L4V 1L9

Dr. A.L. Christie,
Air Quality and Inter-Environmental Research Branch,
Atmospheric Environment Service,
Downsview, Ontario
M3H 5T4

Dr. J. Davies,
Department of Geography,
McMaster University,
Hamilton, Ontario
L8S 4J9

Dr. R. Hoff,
Atmospheric Dispersion Division,
Atmospheric Environment Service,
Downsview, Ontario
M3H 5T4

Dr. G.A. Isaac,
Cloud Physics Research Division,
Atmospheric Environment Service,
Downsview, Ontario
M3H 5T4

Dr. E. Lozowski,
Department of Geography,
University of Alberta,
Edmonton, Alberta
T6G 2H4

Mr. B. McArthur,
Department of Geography,
McMaster University,
Hamilton, Ontario
L8S 4T9

Mr. I.R. McCracken,
Environmental Secretariat,
National Research Council of Canada,
100 Sussex Drive,
Ottawa, Ontario,
K1A 0R6

Mr. B.E. Sheppard,
Atmospheric Sounding Systems Section,
Atmospheric Environment Services,
Downsview, Ontario
M3H 5T4

Mr. E. Witushek,
Environmental Protection Service,
Department of the Environment,
West Vancouver, British Columbia
V7T 1A2

ACKNOWLEDGEMENTS

The Panel gratefully acknowledges the assistance of Mr. E. Maser and Ms. P. Curry for the editorial review and Ms. K. O'Connor and Ms. M. Given for typing the manuscript.

Special thanks to Mr. A. Sheffield, Data Analysis Division, Air Pollution Control Directorate, for supplying the Canada emissions data and reviewing the manuscript.

SUMMARY

It has long been known that the presence of particles in the atmospheric environment results from the activities of both nature and man. There has been a continuing discussion regarding the relative proportions of the total atmospheric particle burden that each of these two source categories generates. The routine measurement and control of airborne particles have been based on the concept of total suspended particulate matter with little regard for an airborne particle's intrinsic characteristics or the factors that dictate its behavior in an atmospheric aerosol. It has been demonstrated that atmospheric aerosols are composed of a spectrum of airborne particles, having characteristics such as particle size, shape, density, surface area, light scattering properties, etc. which are dependent upon mechanisms of particle formation, atmospheric transport, transformation and removal.

1.0 PARTICLE CHARACTERISTICS (see Chapter 2.0)

1.1 PHYSICAL PROPERTIES (see Section 2.1-2.4)

Along with the recent growth in interest in the study of airborne particles, there has evolved an apparent complex terminology to describe an airborne particle's source(s), formation, transformation, transport and effects. The following is a brief overview of the salient features of airborne particles as they relate to effects on atmospheric processes.

A particle is any minute piece of solid or liquid matter, larger then individual molecules (0.01-100 μm). An aerosol is a mixture of particles and gases that exhibits some stabilization in a gravitational field. Primary particles are those particles that are emitted directly into the air and do not change form in the atmosphere. Secondary particles are those particles that form in the atmosphere as a result of chemical and physical reactions. Most of the reactants are emitted as gases.

The most important parameter used for the characterization of airborne particles is considered to be particle size. Although numerous expressions have been used to denote particle size, aerodynamic diameter is currently the most widely accepted.

The distribution of particle sizes in an atmospheric aerosol fluctuates dramatically, depending upon such influences as source(s), age of the aerosol and meteorological conditions. However, it is generally accepted that atmospheric aerosols have a trimodal size distribution based on mass; the three modes are 1) nuclei (<0.1 μm diameter) 2) accumulation (>0.1 to <2.0 μm diameter) and 3) coarse (>2.0 μm diameter). The nuclei mode is usually observed near combustion sources or other high temperature sources and coagulates into

EFFECTS OF AEROSOLS ON ATMOSPHERIC PROCESSES

NRCC No. 18473

accumulation mode particles. Consequently, atmospheric aerosols relatively far removed from specific sources normally have a bimodal size distribution according to mass; these modes are fine (0.1-1.0 μm) and coarse (2-100 μm). The division between fine and coarse particle modes is in the range of 1-3 μm but is commonly assumed to be 2 μm. However, this separation is neither sharp nor fixed and significant overlap may occur, depending upon such factors as source strength and meteorological conditions. In addition, the reported particle size distribution of an atmospheric aerosol is oftentimes a function of the methods of particle collection and data presentation. In order to completely describe the particle size distribution of an atmospheric aerosol, it would be necessary to employ a number of different sampling instruments and measurement techniques.

The shape and density of airborne particles are highly variable; particle shape often differs dramatically from sphericity while the density of individual particles can differ from 0.5 to 6.5 $g.cm^{-3}$. Although surface properties of airborne particles have received little attention, these particles have large surface areas, as a result of their small size and their rough and porous surfaces.

1.2 CHEMICAL PROPERTIES (see Section 2.7)

Depending upon the substance, the mass concentration of chemical constituents is usually found in only one of the two modes, although some overlap between the two modes does occur. This difference in chemical composition between the two particle modes is usually attributable to the different mechanisms of particle formation. Particle mass in the fine particle mode is composed of sulfates, nitrates, ammonium, lead, bromine, elemental carbon and condensed organic matter. A significant portion of trace inorganic and organic constituents are present at or near the surface of airborne fine particles. In addition, submicrometre particles can contain significant amounts of water and, hence, it has been suggested that many gas-particle reactions in the atmosphere involve a gas-liquid interface.

The chemical composition of coarse particles typically reflects the composition of the earth's crust, containing such predominate elements as calcium, aluminum, silicon and iron. Depending upon the sampling location and meteorological conditions, sea salt and vegetation-derived components may also be present in the coarse mode.

1.3 PARTICLE FORMATION, TRANSPORT, TRANSFORMATION AND REMOVAL (see Sections 2.5 and 2.6)

Most fine particles present in the atmospheric environment are formed by a complex series of gas and particle phase reactions. Nuclei mode particles are formed in or near sources and in the atmosphere by various nucleation processes which include 1) condensation of hot, supersaturated vapor via homogeneous nucleation and 2) condensation of cold, supersaturated vapor via homogeneous and heterogeneous nucleation. Once formed, such particles undergo extensive heterogeneous nucleation as well as homogeneous and heterogeneous particle coagulation. The dynamics of fine particle growth usually prevent such particles from becoming larger than about 1.0 μm. Larger particles are formed mainly via mechanical processes (e.g. windblown dust, sea spray, grinding, crushing, etc). Such particles do not undergo significant gas-particle and particle-particle interactions in the atmosphere.

Fine particles are transported through the atmosphere via eddy diffusion and advection and, in the absence of precipitation, may be transported long distances without being deposited. Wet deposition processes, such as rain out and wash out, are significant methods of removal of fine particles. Coarse particles, which are usually emitted close to the surface, are in most cases removed from the atmosphere without being transported long distances. In special circumstances, such as volcanic emissions, coarse particles may be transmitted far from their point of origin.

2.0 SOURCES AND EMISSIONS (see Chapter 3.0)

The relative contributions of particles to the atmospheric environment by both nature and man depends upon the location, season, type of activity, etc. Sources of airborne particles may be grouped into two general categories: direct sources referring to particles emitted in a gas stream and indirect sources (fugitive sources), involving particles emitted without first passing through a stack or duct which directs and controls their flow.

A diverse range of particles are emitted to the atmosphere from natural processes, including emissions from soils, combustion, sea spray, vegetation and volcanoes. Particles injected into the atmosphere from man-made activities are derived from industrial processes, fuel combustion, transportation, solid waste incineration and a host of other processes such as slash burning, fertilizer application, etc. The following briefly summarizes the salient features of the size range and chemical compositions of particles emitted from both natural and man-made sources and includes estimates of particle emissions to the atmosphere.

2.1 PARTICLE SIZE DISTRIBUTION AND CHEMICAL COMPOSITION (see Section 3.3)

2.1.1 Natural Aerosols (see Section 3.3.1.1)

Soil-derived aerosols usually have a bimodal distribution (1-10 μm and 50 μm) with over 90% of the aerosol mass residing in particles > 1 μm. The chemical composition of these aerosols, which reflects that of the earth's surface, consists predominately of silicon, aluminum, iron, sodium, potassium, calcium and magnesium. There is considerable variation in size distribution and chemical composition of aerosols derived from natural combustion sources, such as forest fires. Forest fires usually produce particles of 0.1 to 1 μm, although the absolute size range may be 0.01 to 200 μm. Approximately 80% of the aerosol mass is < 1 μm, while the average particle size is 0.1 μm. Particles generated from temperate forest fires contain approximately 50% benzene soluble material, 40% elemental carbon and 10% minerals.

Sea spray aerosols are characterized by the following typical mass distribution: 24% > 10 μm, 54% 3-10 μm, 20% 1-3 μm and 2% < 1 μm. Particles derived from sea spray are composed mainly of water along with dissolved and suspended materials, primarily sodium chloride. Trace amounts potassium, calcium, magnesium, organic matter, sulfates and carbonates are also present.

Particles emitted to the atmosphere from vegetation may be derived from the emission of pollen and spores and vapors that undergo physical and chemical reactions in the atmosphere to produce particles. The size range of pollen and spores is 10-50 μm and 5-10 μm, respectively. Although the emissions of volatile organic compounds from vegetation are substantial, the portion of vapor converted to particles is not yet known. Isoprene derivatives are believed to make up the majority of these emissions.

Volcanic-derived aerosols have a particle size range of 0.01 to > 60 μm; more than 95% of the aerosol mass resides in primary particles > 5 μm. Although chemical composition is highly variable, major components include silicon, aluminum, magnesium, calcium and iron.

2.1.2 Man-Made Aerosols (see Section 3.3.2.1)

In man-made aerosols, both particle size distribution and chemical composition are highly variable as a result of the influence of several factors including source type, operating conditions, general maintenance, cleanliness, type of emission control equipment, etc. In general, the size and chemical composition of emitted particles reflect the materials used and the activity concerned. Particles may be emitted from both direct and indirect sources; indirect sources include both industrial and nonindustrial emissions. Industrial fugitive emissions include 1) dust emissions from wind erosion of storage piles and unpaved plant roads and from vehicular traffic over paved roads and 2) process emissions from industry-related operations such as material handling, loading, unloading and transfer operations.

Very little information is available on the size distribution and chemical composition of aerosols derived from indirect sources. In addition, most investigations have been confined to primary particles with little or no study of the potential for the generation of secondary particles. Although the study of primary particle emissions from both direct and indirect sources is important in the determination of source contributions and ultimately emission controls, from the perspective of ambient air quality, secondary particle formations should be investigated as well.

One factor that does have a significant effect on the size and chemical composition of primary particles emitted from man-made sources is the type and degree of emission control. Although conventional emission controls are responsible for reducing the overall particle mass loading, the portion of mass loading attributed to fine particle mass has increased. It is informative to note that of the 38 industrial source categories identified in Canada in 1978, 21 sources emitted at least half of their total particle mass loading as particles < 2.5 μm. The efficiency of particle removal for most types of collection equipment varies inversely with particle size, so that the overall removal efficiency of such equipment will be high on a particle mass basis, but will be considerably lower on a particle number basis.

2.2 ESTIMATED EMISSIONS (see Sections 3.2, 3.3.1.2 and 3.3.2.2)

On a global basis, it is estimated that particle emissions range from (1 to 4) x 10^{12} $kg.a^{-1}$ with 7-19% from man-made sources and 81-93% from natural sources. Man-made emissions consist of 5-41% primary and 59-95% secondary particles, whereas natural emissions consist of 48-73% primary and 27-52% secondary particles.

Emission estimates have been generated for both Canada and the United States; although designation of source categories are somewhat different between the two countries, it is informative to compare estimated emissions on a North American scale. In addition, because of the numerous assumptions and extrapolations that were required, all natural emission estimates should be regarded as order of magnitude approximations.

Total emissions of primary particles from natural sources in Canada are estimated to be 748 x 10^9 $kg.a^{-1}$, with 42 and 58% originating from terrestrial and marine sources, respectively. Of the terrestrial mass emission rate of 314 x 10^9 $kg.a^{-1}$, 95% of the particles were > 2.5 μm. Of the marine mass emission rate of 434 x 10^9 $kg.a^{-1}$, 85% of the particles were > 2.5 μm. Emissions of soil-derived particles were the largest contributors (304 x 10^9 $kg.a^{-1}$) to the terrestrial mass flux. Most soil-derived particles originate from grassland agricultural biomes, primarily as a result of soils exposed during cultivations. Lesser quantities originate from nonvegetated tundra regions while forested biomes emit negligible quantities.

Total particle emissions from natural sources in the United States are estimated to be 84 x 10^9 $kg.a^{-1}$. This total is composed of 57 x 10^9 $kg.a^{-1}$ for terrestrial dust, 5.5 x 10^9 $kg.a^{-1}$ for sea spray, 20 x 10^9 $kg.a^{-1}$ for vegetation, and (0.5-0.7) x 10^9 $kg.a^{-1}$ for wildfires. It must be noted that estimates of total natural emissions for Canada and the United States are not directly comparable, since the U.S. total does not take into account emissions from agricultural tilling, wind erosion from croplands, entrained dust from paved and unpaved roads, etc. In the United States, these sources are classified as non-industrial man-made fugitive sources and estimates of emissions differ from 112 x 10^9 to 369 x 10^9 $kg.a^{-1}$. Average global particle emissions from volcanos are estimated at 3.6 x 10^9 $kg.a^{-1}$, although the 1976 eruption of the St. Augustine volcano in Alaska generated approximately 7 x 10^9 kg of particles.

Based on 1976 data, emissions of primary particles from man-made sources in Canada total 2,330 x 10^6 $kg.a^{-1}$. This total consists of: 1,192 x 10^6 $kg.a^{-1}$ for industrial processes, 301 x 10^6 $kg.a^{-1}$ for fuel combustion (stationary sources), 74 x 10^6 $kg.a^{-1}$ for transportation, 34 x 10^6 $kg.a^{-1}$ for solid waste incineration and 682 x 10^6 $kg.a^{-1}$ for miscellaneous sources (e.g. forest fires, slash burning).

Based on preliminary data for 1978, industrial emissions in Canada total 1,439 x 10^6 $kg.a^{-1}$. Iron ore mining and beneficiation along with mining and rock quarrying contribute 19 and 13%, respectively, to this total. In comparison, industrial emissions in the United States, based on 1978 data, total 6,190 x 10^6 $kg.a^{-1}$ with the source categories identified as metals and mineral processing, contributing 25 and 54%, respectively, to this total.

Utility power generation accounts for 187 x 10^6 $kg.a^{-1}$ (62%) of the total Canadian fuel combustion primary particle emissions, based on 1976 data. Based on preliminary 1978 data, this source accounts for 57% of total fuel combustion emissions. The emissions of particles from stationary combustion sources in the United States (1978) total 3,770 x 10^6 $kg.a^{-1}$, with utility power generation contributing 2,500 x 10^6 $kg.a^{-1}$.

Total Canadian emissions for 1976 for the transportation sector (74 x 10^6 $kg.a-^1$) are composed of 62% for gasoline-powered engines, 18% for diesel-powered engines, 3% for tire wear and 17% for other forms of transportation. Engine-related particle emissions in the United States are estimated at 1.3 x 10^9 $kg.a^{-1}$.

Total emissions for solid waste incineration approximate 34 x 10^6 $kg.a^{-1}$ in Canada and 500 x 10^3 $kg.a^{-1}$ in the United States.

Very little information is available for estimated emissions from indirect sources. Preliminary Canadian estimates (1978) have been prepared for several sources including unpaved and paved roads, agricultural tilling, agricultural wind erosion, construction sites and mine tailings. Of a total of approximately 40 x 10^9 kg.a^{-1}, construction activity (44%) and unpaved roads (40%) were the two highest emitters. Uncontrolled industrial fugitive primary particle emissions for the United States are estimated to total 3,370 x 10^6 kg.a^{-1}. Of the two United States studies available for the estimation of primary particle emissions from nonindustrial fugitive sources, the total emission ranges from 112 x 10^9 kg.a^{-1} to 369 x 10^9 kg.a^{-1}, the difference being largely due to the different estimated emissions from unpaved roads.

3.0 EFFECTS ON OPTICAL PROPERTIES OF THE ATMOSPHERE (see Chapter 4.0)

Atmospheric aerosols have a unique characteristic in that they may be sensed by the unaided eye. This characteristic, which indicates the reduction of visibility as aerosol loading increases, can be considered along with the climatic effects due to subsequent radiative energy reduction, to be the principal optical effects of atmospheric aerosols.

3.1 OPTICAL PROPERTIES OF AIRBORNE PARTICLES (see Section 4.2)

Atmospheric visibility is a function of the transmission of light through air and the ability of the eye to identify an object by its contrast with the background. When the eye can no longer distinguish this contrast, the object is considered to be beyond the limit of visibility. The change in contrast or light intensity is due to scattering and absorption of light by the atmosphere.

The intensity, I, of light over a homogeneous path, x, is given by the Beer-Lambert law:

$$I(x) = I(o)\exp(-b_{ext}x) \qquad (1)$$

where b_{ext} is the volume extinction coefficient of the atmosphere and has units of inverse distance. The volume extinction coefficient is the sum of the extinction coefficients for gases ($b_{ext\text{-}gas}$) and particles ($b_{ext\text{-}part}$). In addition, the extinction coefficient for gases is composed of extinction coefficients for Rayleigh scattering and gas scattering. The extinction coefficient for particles includes extinction due to the particle scattering and absorption.

A particle-free atmosphere at sea level has a Rayleigh scattering coefficient of approximately 12 x 10^{-6} m^{-1} (λ=550 nm). As the particle loading increases from very low levels, where Rayleigh scattering predominates, the particle scattering coefficient increases until it is larger than the Rayleigh scattering coefficient. Typical values of the particle scattering coefficient approximate 10^{-4} m^{-1} with tropospheric minima and maxima of 10^{-7} m^{-1} and 10^{-3} m^{-1}, respectively. In rural areas, the particle absorption coefficient is approximately 10% of the particle scattering coefficient, although its contribution may increase to 50% in urban areas.

The scattering and absorption of light by aerosols is dependent upon particle size distribution, refractive index and shape as well as upon relative humidity and wavelength of incident light. It has been demonstrated that the reduction in visible light intensity is due primarily to the presence of fine particles, particularly those with diameters 0.1-1.0 μm. Particles smaller than 0.1 μm, although sometimes present in high number concentrations, are inefficient at scattering light and hence contribute only marginally to visibility reduction. In addition, particles larger than 1-3 μm, though efficient at scattering light on a single particle basis, usually have relatively low number concentrations in the atmosphere and therefore contribute only a small amount to visibility reduction. In areas where the concentration of fine particles is low, that of coarse particles may contribute significantly to visibility impairment.

Under certain defined conditions, the measurement of visibility is a reliable measure of the mass loading of airborne particles. It has been demonstrated that a nonabsorbing aerosol composed of particles 0.1-1.0 μm with a mass loading, M, will give rise to a volume scattering coefficient (b_{scat}) such that:

$$\frac{M}{b_{scat}} = 0.32 \pm 0.02 \text{ g.m}^{-2} \qquad (2)$$

Visibility, V, is related to the volume extinction coefficient by:

$$V = \frac{3.91}{b_{ext}} \qquad (3)$$

Where Rayleigh scattering is less than scattering by particles and absorption by gases and particles is not significant, b_{ext} may be approximated by b_{scat} and:

$$M = \frac{1.25}{V} \times 10^3 \ \mu\text{g.m}^{-3} \qquad (4)$$

where V is measured in km and aerosol mass loading is measured in $\mu g.m^{-3}$. From equation (4) it is evident that the resultant visibility reduction for a given incremental increase in fine particle mass loading will be greater for areas of high visibility than for areas of relatively lower visibility.

Although it has been generally accepted that airborne fine particles are responsible for much of the reduction in visibility, especially in areas of relatively low particle mass loadings, the concentration and chemical composition of such particles can vary significantly on both a spatial and temporal basis. Numerous attempts have been made to correlate particle chemical composition with visibility reduction; however, such a correlation must be considered tenuous since a chemical constituent's contribution to aerosol mass loading may not equal its contribution to visibility degradation. Some field studies have demonstrated that there are significant positive correlations between sulfate concentrations and visibility, especially in nonurban areas.

3.2 MEASUREMENTS OF VISIBILITY AND TURBIDITY (see Sections 4.3 and 4.4)

The relative changes in incident light intensity given by the Beer-Lambert equation (equation 1) may be determined by the measurement of the total atmospheric extinction coefficient (b_{ext}) over long path-lengths. Such measurements are usually made in the horizontal or vertical plane. Horizontal extinction is more difficult to measure but it is more useful, since it is related to optical behavior parallel to the earth's surface. The measurement of vertical extinction permits the determination of atmospheric turbidity, i.e., the reduction in direct solar radiation.

While various refined methods for measuring horizontal extinction are available for the determination of changes in visibility and fine particle mass loading, a relatively crude haze index is all that has been used to determine temporal and spatial trends in visibility in Canada. Values for the haze index have increased consistently from about 1950, for most areas of Canada, with higher values having been recorded in summer and lower values in winter. On a spatial scale, the values reflect relatively higher pollution levels in the populous eastern sector of Canada as well as in Alberta and around Vancouver, British Columbia. However, on a nationwide scale, the index is clearly not sensitive enough to adequately delineate the occurrence of haze and elevated loadings. There has been a significant increase from 1948-52 to 1970-74 in the atmospheric extinction coefficient, with a corresponding dramatic decrease in visibility for the spring, summer and fall months in the eastern United States. A moderate decrease in visibility was observed for the winter months.

Atmospheric turbidity has been measured at several locations in Canada since 1974. A spring-to-summer maximum and a winter minimum with a max/min ratio of 2-4 have been recorded at these locations. Sites located in western Canada usually have lower measured turbidity than sites in eastern Canada. Because of the lack of long-term data collected at a representative number of locations, the interpretation of an overall increase in turbidity in Canada is open to question, although long-term increases in turbidity at widely separate locations throughout the world indicate these temporal increases in turbidity might be expected.

4.0 EFFECTS ON CLOUDS, FOG, PRECIPITATION AND ATMOSPHERIC ELECTRICITY (see Chapter 5.0)

Virtually all atmospheric cloud and fog particles are formed by heterogeneous nucleation, which is stimulated by cloud condensation nuclei and ice nuclei. The addition of such nuclei to a cloud affects its microphysical structure which, in turn, may increase or decrease the probability of precipitation. In addition, the introduction of particles into the atmosphere may result in some alterations of the electrical properties of the atmosphere.

4.1 CLOUDS, FOGS AND PRECIPITATION (see Section 5.2)

Under normal conditions in the absence of local sources the cloud condensation nuclei concentration is approximately 100-500 cm^{-3} at a relative humidity of 101% (1% supersaturation), with the nuclei being typically < 1 μm. Although much harder to measure accurately, the ice nuclei concentration is approximately 1 L^{-1} at -20°C and increases by a factor of 10 for each 3-5°C decrease in temperature. Depending upon the mechanism of formation and temperature of activation, ice nuclei may be as small as a few molecules or as large as several micrometres.

Clouds form as air rises and cools, and water condenses around available nuclei. Precipitation may be formed either through warm-rain or cold-rain processes. In warm-rain processes, droplets which are formed around cloud condensation nuclei grow at a rate controlled by the supersaturation with respect to water. The resulting droplets coalesce until they reach a size where they fall through the sustaining updraft and reach cloud base as precipitation. Cold-rain processes usually occur more rapidly than warm-rain processes and involve ice nuclei. Ice crystals, activated from ice nuclei, grow, fall and accrete surrounding supercooled droplets. If the air below cloud base is above 0°C the ice particles fall as rain, although some graupel and hail may be large enough to reach the ground in solid form.

Condensation on active cloud condensation nuclei may also occur at lower relative humidities ($< 70\%$) depending upon the size and number of nuclei present. As relative humidity increases, the initial droplets grow in size to become fog droplets with a resultant decrease in visibility.

Numerous investigations have been carried out to examine the effects of both planned and inadvertent weather modification. Planned weather modification experiments include increasing rain and snow producing efficiency of clouds, dissipating fogs and thin-layer clouds, suppressing hail formation and modifying hurricanes. Although such procedures are feasible under some circumstances, only a few experiments which have attempted to increase rainfall have withstood statistical verification.

It is well known that urban areas, some industries and natural phenomena can generate large quantities of particles. Despite the existence of a large volume of data in the man-made generation of weather-modifying nuclei, the causal relationships between sources and altered weather have not been established. Although there is a general consensus that urban areas enhance rainfall in downwind areas, the significance of modifying factors such as nuclei generation, urban heat island and urban topography have not yet been quantified.

4.2 EFFECTS ON ATMOSPHERIC ELECTRICITY (see Section 5.3)

Electrical processes are constantly occurring in the lower atmosphere and may be attributed to two sources: 1) intense electrification accompanying local storms and 2) global fair-weather electrical activity due to electrical storms, cosmic rays and radioactive gases and particles. Both positive and negative ions, consisting of gas molecules, molecular clusters and small particles, are present in the atmosphere and are responsible for the electrical conductivity of the atmosphere and, hence, the fair-weather electrical activity. It has been usual practice to subdivide these ions into either small (i.e. those having mobilities within range of 1-2 $cm^2.volt^{-1}.s^{-1}$) or large ions (i.e. those having mobilities in the range of 10^{-1} to 10^{-3} $cm^2.volt^{-1}.s^{-1}$). In remote regions over the oceans, ionizing radiation produces approximately 2 ion $pairs.cm^{-3}.s^{-1}$ and a resulting small ion concentration and electrical conductivity of 10^3 $ions.cm^{-3}$ and 2.5 x 10^{-4} $ohm.m^{-1}$, respectively. The lifetime of these small ions is governed by removal via homogeneous coagulation of oppositely charged ions and heterogeneous coagulation with larger charged or neutral particles. Such large particles provide relatively immobile surfaces for the diffusional attachment of highly mobile, small ions, thereby resulting in a reduction in atmospheric electrical conductivity.

Measurements of electrical conductivity have been carried out since about 1900 in remote regions as well as in areas experiencing elevated particle loadings. Electrical conductivity, although displaying diurnal variation, has remained relatively constant since 1900 in remote areas over the oceans; however, in the atmosphere over the North Atlantic it has decreased by at least 20%, with the majority of this reduction occurring after 1929. The electrical conductivity over the oceans decreases upon approaching land. The historical trends in global electrical conductivity have been complicated by the direct introduction of man-made radioactive aerosols since 1945.

In continental areas, atmospheric electrical conductivity is influenced by domestic, urban and industrial activities. Although there are few Canadian studies on the effects of aerosols on atmospheric electrical conductivity, there is a general consensus that increased particle loading in the atmosphere contributes to a decrease in electrical conductivity on a local or regional scale.

The consequences of either short- or long-term changes in atmospheric electrical properties are presently unknown, although it has been postulated that processes such as thunderstorm activity, cloud formation and particle transport and transformation may be altered.

5.0 EFFECTS ON CLIMATE (see Chapter 6.0)

Aerosols, present in both the stratosphere and the troposphere, are believed to cause changes in the radiant energy that reaches the earth's surface. If atmospheric processes, such as light scattering and absorption, are systematically influenced by the presence of airborne particles, then both weather, the instantaneous state of the atmosphere, and climate, the long-term average of weather, may be modified. Climate may be considered as the mean thermal state of the earth-atmosphere system. Numerous investigations have attempted to either estimate the quantitative change in temperature at the earth's surface or determine whether the temperature has been increasing or decreasing.

Many attempts have been made to establish a relationship between the presence of airborne particles in the atmosphere and climate, but to date it cannot be stated unequivocally that changes in aerosol loading have caused observable changes in world surface temperatures. Partly because of the difficulty in obtaining measured responses, climate models have been used to simulate the possible influences of aerosols on climate. Such models have been applied on both global and regional scales. The increasing complexity of the earth-atmosphere system from the planetary to the regional scale requires a hierarchy of models ranging from simple zero-dimensional energy balance statements to three-dimensional general circulation models. Current studies of aerosol effects on temperature have been restricted mainly to zero- and one-dimensional models.

Early climate models considered the effects of aerosols on climate in terms of effects on solar radiation; cooling of the earth's surface was generally assumed to be the result of an increase in aerosol loading, since the airborne particles making up the aerosol were considered to only scatter radiation. However, later models considered the possibility that aerosols might also absorb radiation, thereby leading to a warming effect.

At present, there is a general consensus that an increase in the stratospheric aerosol loading (primarily sulfate and silicate particles) will warm the aerosol layer and may lower the temperature at the earth's surface. Such a warming has been observed following major volcanic eruptions; however subsequent surface cooling has not been clearly established from temperature records. Northern hemisphere temperature variations since the late 19th century may be accounted for in terms of increases in atmospheric carbon dioxide concentration and volcanic activity, but they may equally well be due to the natural variability of the unperturbed system. Over long-term periods, volcanic activity may account for temperature variations in glacial periods, but not for the initiation of glaciation.

There is increasing evidence that tropospheric aerosols, especially those of man-made origin, are efficient absorbers of solar radiation and may have a significant effect on the lower atmosphere, thus augmenting warming due to the presence of carbon dioxide. However, the effects on the earth's surface temperature have not yet been clearly established.

RECOMMENDATIONS

The Panel on Aerosols was given the responsibility for developing and evaluating the scientific criteria for aerosols in the atmospheric environment and for identifying critical gaps in knowledge. The following is a list of recommendations that, in the opinion of the Panel, need to be addressed. Recommendations are not ordered according to priority, but by chapter content.

1. Along with the increase over the last several years in the scientific study of airborne particles in the environment, there has arisen a complex and apparently confusing terminology that has attempted to describe the various aspects of aerosols, such as source identification, modes of formation, transformation and transport, modes of deposition and effects. Since different disciplines often label the same aspect in different ways, it is recommended that:

> A STANDARDIZED TERMINOLOGY TO DESCRIBE ALL ASPECTS OF AIRBORNE PARTICLES BE INTERNATIONALLY ADOPTED FOR ONGOING MONITORING AND SURVEILLANCE PROGRAMS.

Numerous assumptions and approximations were required to arrive at estimated emissions from natural sources, and hence all natural emission estimates should be regarded as order-of-magnitude approximations. In addition, such estimates for Canada and the United States were developed using somewhat different methodologies and hence are not directly comparable. It is therefore recommended that:

> STANDARDIZED METHODOLOGIES FOR ESTIMATING EMISSIONS FROM NATURAL SOURCES BE PREPARED AND ADOPTED INTERNATIONALLY.

2. There is a general consensus that atmospheric aerosols are composed of two distinct distributions of airborne particles: 1) those particles formed by condensation, having a size range below 2 μm and 2) those particles formed by comminution, having a size range above 2 μm. Although there is some overlap, a minimum in aerosol mass occurs at approximately 2 μm. Distinctions between fine and coarse particle modes with respect to formation, atmospheric transformation, removal, effects and oftentimes chemical composition, can be established. It is generally considered that fine particles are responsible for most of the atmospheric effects addressed in this document. Owing to the complex and nonuniform (both on micro and macro scales) nature of the atmospheric aerosol, it is recognized that no collection of instruments will provide a complete description of the aerosol. We can however classify airborne particles according to their diffusivity, aerodynamic properties, electrical mobility, conductivity, light scattering ability, gravitational settling, appearance under microscopic examination, nucleating ability, mass and chemical composition. Each of these techniques, except for the final two, yields some information about the size of the aerosol, however, because of the nonuniformity of the natural aerosol, the relationship is not independent of all of the other parameters. It is therefore recommended that:

> STANDARD REFERENCE METHODS FOR THE MEASUREMENT OF THE SIZE DISTRIBUTION OF ATMOSPHERIC AEROSOLS BE DEVELOPED. IN DEVISING THESE REFERENCE METHODS SEVERAL TECHNIQUES SHOULD BE EMPLOYED AND "NATURAL" AS WELL AS ARTIFICIAL AEROSOLS SHOULD BE USED AS TEST SOURCES. SIZE DISTRIBUTION MEASUREMENTS SHOULD BE COMPARED WITH MASS AND CHEMICAL DETERMINATIONS TO ENSURE THAT MASS IS CONSERVED. ALL FIELD PROGRAMS SHOULD INCLUDE SIZE DISTRIBUTION MEASUREMENTS COINCIDENTAL WITH MASS AND CHEMICAL DETERMINATION. THE LATTER SHOULD BE SEPARATED INTO AT LEAST TWO FRACTIONS, FINE (<2 μm) AND COARSE (>2 μm). MEASUREMENT OF A MORE COMPLETE NUMBER SIZE DISTRIBUTION AND ITS VERTICAL DISTRIBUTION ARE DESIRABLE, ESPECIALLY FOR CLIMATE STUDIES.

Because of the highly variable nature and anthropogenic sources of atmospheric aerosols one must be very careful in interpreting measurements from other regions of the world. It is therefore recommended that:

> MONITORING AND SURVEILLANCE FIELD PROGRAMS (WITH INSTRUMENTATATION AS DESCRIBED ABOVE) BE IMPLEMENTED ON LOCAL, REGIONAL AND NATIONAL LEVELS. A GLOBAL MONITORING SYSTEM WOULD ASSIST IN THE INTERPRETATION OF THE CLIMATIC EFFECTS OF AEROSOLS AND ALLOW FOR A MORE DIRECT ASSESSMENT OF THE IMPACT OF ANTHROPOGENIC PARTICLES.

3. There is only limited information available concerning the size and chemical composition of particles emitted from either natural or man-made sources in Canada. Most of the available information deals with the emissions of primary particles from direct sources; the significance of secondary particles, emitted during both natural and man-made activities, has not been adequately elucidated. On a global scale, 25-50% of natural and 60-95% of man-made airborne particles are secondary in nature. It is recommended that:

> THE RELATIVE CONTRIBUTIONS TO THE TOTAL ATMOSPHERIC PARTICLE LOADING OF PRIMARY AND SECONDARY PARTICLES, ESPECIALLY THOSE LESS THAN 2 μm, FROM DIRECT AND INDIRECT (FUGITIVE) SOURCES BE QUANTIFIED. SPECIAL EMPHASIS SHOULD BE GIVEN TO THE EMISSIONS OF MAN-MADE FINE PARTICLES AND THE EMISSIONS OF FINE PARTICLES FROM FORESTED AND AGRICULTURAL AREAS (VAPOR-PARTICLE CONVERSION AND COMBUSTION) IN CANADA.

4. Based on scientific knowledge to date, only the effects on atmospheric visibility can be related numerically to aerosol loading. Visibility reduction can be correlated with the atmospheric mass loading of fine particles, depending on certain conditions, e.g. geographical location, relative humidity and type of aerosol. Since the relative contributions of fine and course particles to total aerosol mass loadings are highly variable, even at the same sampling location, the

measurement of total suspended particulate matter does not provide a useful measure of atmospheric fine particle loading. Current air quality objectives in Canada for "suspended particulates" are based, in part, on visibility reduction. Atmospheric particle loading is estimated by the measurement of "total suspended particulates". In light of new information concerning both optical effects and size distribution-chemical composition of aerosols, it is recommended that:

> THE CANADIAN AIR QUALITY OBJECTIVE FOR "SUSPENDED PARTICULATES", THAT IS BASED ON VISIBILITY IMPAIRMENT AS A CRITERION, BE MODIFIED TO REFLECT THE RELATIONSHIP BETWEEN VISIBILITY AND ATMOSPHERIC FINE PARTICLE CONCENTRATION.

5. Aside from visibility reduction, all other manifestations of atmospheric aerosols are qualitative in nature. Further scientific information is required before quantitative relationships between cause and effect can be established. Although numerous studies have attempted to define cause and effect relationships between atmospheric particle loading and planned or inadvertent weather modification, very few have demonstrated statistically significant results. There is a general consensus that urban areas enhance rainfall in downwind areas; however, the significance of modifying factors such as particle generation, urban heat island and urban topography have not yet been quantified. Atmospheric electrical properties may be altered by the introduction of airborne particles, although the consequences of either short- or long-term alterations are not known. It is therefore recommended that:

> THE ROLE OF ATMOSPHERIC FINE PARTICLES IN PROCESSES SUCH AS RAIN AND SNOW ALTERATION, FOG DISSIPATION, HAIL SUPPRESSION AND THE ALTERATION OF ATMOSPHERIC CONDUCTIVITY BE FURTHER EXAMINED UNDER CANADIAN CLIMATIC CONDITIONS. THE SIGNIFICANCE OF MAN-MADE FINE PARTICLES SHOULD BE INVESTIGATED.

6. There is concern that the injection of particles, along with carbon dioxide, into the atmospheric environment will effect climate. Although numerous studies have attempted to establish a relationship between atmospheric aerosols and climate modification, the role of airborne particles with respect to effects on climate is unclear. In the absence of readily observable climatic changes attributable to atmospheric aerosols, many researchers have relied upon climate models of various degrees of sophistication to simulate possible interactions. To date, the effects on surface temperature have not been established and must await further development and use of radiation-dynamic models; several gaps in knowledge require research:

EXPERIMENTAL STUDIES ARE NEEDED TO DETERMINE SPECTRAL VALUES FOR THE IMAGINARY PART OF THE COMPLEX INDEX OF REFRACTION FOR BETTER DEFINITION OF THE SINGLE SCATTERING ALBEDO. VALUES FOR THE RATIO OF ABSORPTION TO SCATTER SHOULD BE DETERMINED FROM RADIATION MEASUREMENTS IN CANADA. MEASUREMENTS OF BOTH DIRECT AND DIFFUSE RADIATION ARE REQUIRED.

7. In general, there is a need for integrated studies that incorprate several of the recommendations outlined above. These studies include:

(A) DETERMINATION OF THE RELATIONSHIP BETWEEEN VISIBILITY AND PARTICLE MASS LOADING.

(B) EXAMINATION OF THE ROLE OF AIRBORNE PARTICLES ON THE POTENTIAL ALTERATION OF PRECIPITATION DOWNWIND OF URBAN SOURCES.

(C) ASSESSMENT OF AEROSOL EFFECTS ON THE RADIATION AND ENERGY BUDGETS OF URBAN AREAS.

TABLE OF CONTENTS

		PAGE
SUMMARY		7
RECOMMENDATIONS		21
LIST OF FIGURES		27
LIST OF TABLES		30
LIST OF APPENDICES		31
1.0	INTRODUCTION	33
2.0	PARTICLE CHARACTERISTICS	35
2.1	Terminology	35
2.2	Particle Size	35
2.3	Particle Shape and Density	38
2.4	Particle Surface Properties	40
2.5	Particle Formation	40
2.6	Particle Transport and Removal	41
2.7	Chemical Composition	42
2.7.1	Artifact Formation During Sampling	43
3.0	SOURCES AND EMISSIONS	45
3.1	Introduction	45
3.2	Global Perspective	45
3.3	Canada and the United States	45
3.3.1	Natural Sources and Emissions	45
3.3.1.1	Particle Size and Chemical Composition	47
3.3.1.2	Estimated Emissions	48
3.3.2	Man-Made Sources and Emissions	51
3.3.2.1	Particle Size and Chemical Composition	51
3.3.2.2	Estimated Emissions	63
4.0	EFFECTS ON OPTICAL PROPERTIES OF THE ATMOSPHERE	69
4.1	Introduction	69
4.2	Scattering of Light by Aerosols	69
4.3	Measures of Visibility and Atmospheric Turbidity	73
4.4	Aerosol Geographical Distribution and Trends in Haziness	77

TABLE OF CONTENTS (CONT'D)

PAGE

5.0 EFFECTS ON CLOUDS, FOG, PRECIPITATION AND ATMOSPHERIC ELECTRICITY 91

5.1 Introduction 91
5.2 Effects on Clouds, Fog and Precipitation 91
5.2.1 Pertinent Particle Measurements 91
5.2.1.1 Cloud Condensation Nuclei (CCN) 91
5.2.1.2 Ice Nuclei (IN) 93
5.2.2 Theoretically Predicted Effects 93
5.2.2.1 Warm Rain Processes 93
5.2.2.2 Cold Rain Processes 94
5.2.2.3 Warm, Supercooled and Ice Fogs 97
5.2.3 Observed Effects 97
5.2.3.1 Planned Weather Modification 97
5.2.3.2 Inadvertent Weather Modification 98
5.3 Effects on Atmospheric Electricity 100

6.0 EFFECTS ON CLIMATE 107

6.1 Introduction 107
6.2 Climate Variation and Models 107
6.2.1 Global Scale Models 108
6.2.1.1 Planetary Energy Balance 108
6.2.1.2 Radiative Convective Model 109
6.2.1.3 Surface Energy Balance Model 110
6.2.2 Regional Models 110
6.3 Radiative Transfer 113
6.4 Radiative and Thermal Effects of Aerosols 114
6.4.1 Climatic Effects of Stratospheric Aerosols 115
6.4.2 Climatic Effects of Tropospheric Aerosols 126

REFERENCES 185

LIST OF FIGURES

FIGURE		PAGE
2-1	Schematic representation of an atmospheric aerosol surface area distribution	37
2-2	Normalized frequency plots of number, surface and volume distributions for the grand average 1969 Pasadena smog aerosol	39
4-1	Scattering efficiency as a function of particle size for a single nonabsorbing particle	70
4-2	Volume scattering coefficient per unit volume of particles	72
4-3	Computed relative extinction coefficient as a function of relative humidity at a power law exponent of $\nu = 3.5$	74
4-4	Fraction of extinction efficiency contributed by absorption as a function of particle size parameter	75
4-5a	Canadian haze index for the summer months, 1967-1974	79
4-5b	Canadian haze index for the winter months, 1967-1974	80
4-6	Spatial distribution of 5-year average extinction coefficients for the eastern United States	81
4-7	Three-year moving average summer extinction coefficient for the eastern United States	82
4-8	Geographic distribution of CANSAP, BAPMoN and CAAPP stations in Canada, 1981	85
4-9	Mean monthly atmospheric turbidity coefficients over the period 1974-1979 for selected Canadian locations	86
4-10	Trend in annual turbidity for five Canadian stations during the years 1975-1979	87
4-11	Nephelometer data from the Canadian Arctic Air Pollution Program	89
4-12	Aerosol light scattering in relation to excess sulfate levels for two stations in the Canadian Arctic	90

LIST OF FIGURES (CONT'D)

FIGURE		PAGE
5-1	Median concentration of cloud condensation nuclei (CCN) as a function of supersaturation over water for observations over land and the oceans	92
5-2	Schematic diagram showing the evolution of warm and cold rain, starting from cloud condensation nuclei (CCN) and ice nuclei (IN)	95
5-3	Distribution of particles, in relation to particle size, in air of high nuclei content	101
5-4	Worldwide oceanic measurements of atmospheric conductivity	104
6-1	Schematic diagram showing multiple reflections between the ground and an aerosol layer	112
6-2a	Change in mean surface temperature as a function of the visible optical thickness of a stratospheric aerosol	119
6-2b	Change in mean surface temperature as a function of optical depth perturbation of sulfuric acid droplets and aerosols	120
6-3	Change in the effective blackbody radiative temperature of the atmosphere (K) with addition of an aerosol layer with $\tau_{vis} = 0.1$	122
6-4a	Optical depth perturbations of the atmosphere at a wavelength of 550 nm as a function of time and volcanic explosion that Lamb (1970) has judged to have injected significant quantities of particles into the stratosphere	124
6-4b	Comparison between the observed temperature change for the northern hemisphere over the last century and those expected from changes in the level of volcanic activity and carbon dioxide content of the atmosphere	125
6-5a	Influence of aerosol absorption to backscatter ratio (a/b) on the shortwave radiation balance as a function of surface albedo	128

LIST OF FIGURES (CONT'D)

FIGURE		PAGE
6-5b(i)	Values of $(a/b)_{crit}$ as a function of albedo with three distributions of aerosol. Surface reflectivity is 0.12 with variable cloud optical depth	131
6-5b(ii)	Values of $(a/b)_{crit}$ as a function of albedo with three distributions of aerosol. Cloud optical depth is fixed at 2.0	132
6-5c	Values of $(a/b)_{crit}$ as a function of surface albedo	133
II-1	Particle size ranges for soil types and soil movements	141
II-2	Mean annual number of days with 0.01 inches or more of rainfall for Canada (1941-1970)	145
II-3	Reduction factor for wind erosion over vegetative cover	150
II-4	Thornthwaite's Annual Precipitation-Evaporation Index for Canada (1941-1970)	152
III-1	Scattering geometry for the interaction of a photon with a particle	156
III-2	Scattering efficiency as a function of scattering angle	158
III-3	Contributions to luminosity seen by an observer	160
IV-1	The role of precipitation scavenging in the overall regional material balance	170
IV-2	Relationship between the rain scavenging rate and particle size	179
IV-3	Surface area distribution of particles measured at ground level before, at the beginning of, and during a rain in Ft. Collins, Colorado	181

LIST OF TABLES

TABLE		PAGE
3-1	Estimated global production of particles from natural and man-made sources	46
3-2	Estimated Canadian annual terrestrial emissions of primary natural particles	49
3-3	Estimated annual emissions of salts from Canadian marine environments	50
3-4	Summary of size distributions and chemical composition of particles emitted from various sources	52
3-5	Size distribution of primary particles emitted from various sources identified in the Canada nationwide inventory	55
3-6	Estimated Canadian annual emissions of man-made primary particles, 1976	58
3-7	Estimated United States emissions of primary particles from industrial processes, 1978	65
3-8	Estimated United States emissions of primary particles from fuel combustion (stationary sources),1978	66
3-9	Estimated emissions of primary particles from uncontrolled industrial fugitive sources, 1978	68
4-1	Turbidity parameters observed at Canadian BAPMoN sites	84
5-1	The appearance of rain in 87 summer cumulus clouds in 1976, 1977 and 1978 taken from observations made near Yellowknife, N.W.T. and Thunder Bay, Ontario	96
6-1	Change in planetary albedo and effective reduction in solar constant due to a change in optical depth	117
II-1	Erodibility and average percent by weight of suspended particles for different soil types	140
II-2	Various control strategies used to reduce emissions from unpaved roads	146
II-3	Values of equivalent vegetative cover for common field crops	151

LIST OF APPENDICES

APPENDIX		PAGE
I.0	GLOSSARY	137
II.0	EMISSION FACTORS FOR FUGITIVE EMISSIONS OF PARTICLES	139
II.1	Parameters	139
II.2	Emission Factor Equations	143
II.3	Conversion Factors	153
III.0	OPTICAL PROPERTIES OF AEROSOLS AND MEASUREMENT TECHNIQUES	155
III.1	Parameterization	155
III.2	Solutions for Light Scattering by Spherical Particles	155
III.3	The Relationship of the Extinction Coefficient to Visibility	159
III.4	Turbidity Parameters	163
III.5	Methods of Measurement	164
IV.0	AEROSOL SCAVENGING	169
IV.1	Introduction	169
IV.2	Scavenging Mechanisms	169
IV.2.1	Nucleation Scavenging	171
IV.2.2	Brownian or Convective Diffusion Scavenging	172
IV.2.3	Turbulence Scavenging	172
IV.2.4	Thermo- and Diffusiophoretic Scavenging	172
IV.2.5	Gravitational or Inertial Impaction Scavenging	173
IV.2.6	Electrostatic Scavenging	173
IV.2.7	Combining Individual Scavenging Mechanisms	174
IV.3	Integral Scavenging Effects	175
IV.4	Laboratory Measurements of Scavenging	177
IV.5	Theoretical Estimates and Field Measurements of Scavenging	178
IV.6	Scavenging Models	180
IV.7	Snow Scavenging	183
IV.8	Precipitation Chemistry	183
IV.9	Indirect Effects of Precipitation Mechanisms	184

1.0 INTRODUCTION

Deterioration in the quality of the atmospheric environment in the presence of airborne particles may oftentimes be readily discerned with the unaided eye and, as a result, citizen concern regarding such deterioration has been notable. From an historical perspective, efforts to record and control such airborne particles have been based on the concept of total suspended particulate matter with little or no discrimination on the basis of particle size, shape, origin, chemical characteristics, physical behavior, light scattering properties, etc. In recent years, scientific understanding of such characteristics of airborne particles has been greatly expanded and refined. This document examines that new knowledge in order to provide scientific criteria for assessing the effects of aerosols on atmospheric processes.

Particle characteristics (size, shape, density, surface properties, chemical composition) together with particle formation, transport and removal are examined in Chapter 2. The sources (natural and anthropogenic) and emission inventories of particles for Canada and the United States are detailed in Chapter 3. Where data are available, both direct and indirect (fugitive) sources are examined. The effects of aerosols on optical properties of the atmosphere are detailed in Chapter 4 and the effects on clouds, fog, precipitation and atmospheric electricity are discussed in Chapter 5. Chapter 6 is devoted to an examination of the effects of aerosols on climate. Several appendices are included dealing with such areas as emission factors for fugitive emissions of particles, optical properties of aerosols and measurement techniques, and aerosol scavenging. Literature up to and including January 1982 was examined and an extensive reference section is included.

2.0 PARTICLE CHARACTERISTICS

2.1 TERMINOLOGY

The study of atmospheric particles has dramatically increased in the past several years, resulting in the development of a complex terminology to describe their various formations, sources, transformations, transport and effects. Because the study of particles involves many disciplines, each apparently with its own system of nomenclature to differentiate particles according to size, physical state, origin, etc., much of the literature contains numerous ill-defined and inappropriately-used terms. This document will attempt to conform to a relatively simple nomenclature and, where necessary, define the terms commonly used.

A particle is any minute piece of solid or liquid matter that is larger than an individual molecule. The usual size range is 0.001-100 μm (Lodge et al. 1981). An aerosol is a mixture of particles and gases that exhibits some stabilization in a gravitational field (Hidy and Brock 1970). An atmospheric aerosol consists of solid or liquid particles suspended in air. The term particulate matter usually refers to matter divided into particles having a size range of 0.001 to 100 μm (Lodge et al. 1981). Suspended particulate matter (SPM) is composed of particles which were airborne in the vicinity of a collection apparatus during the time of sampling (Corn 1976).

Primary particles are those particles that are emitted directly into the air and that do not change form in the atmosphere (e.g. windblown dust, sea salt spray) (U.S. NAS 1979). Secondary particles are those particles that form in the atmosphere as a result of physical and chemical reactions, often involving gases (e.g. sulfate particles produced by the photochemical oxidation of sulfur dioxide) (U.S. NAS 1979).

Numerous other terms used to describe particles appear in the scientific literature and the interested reader is referred to the Glossary in Appendix I.0 for relevant definitions.

2.2 PARTICLE SIZE

Although atmospheric particles have been characterized by many different physical and chemical properties as well as sampling techniques, particle size has emerged in recent years as the single most important parameter in characterizing atmospheric aerosols. For the purpose of this document, the term particle size refers to particle diameter.

Although several expressions are used to denote particle size, the aerodynamic diameter is currently the most widely used. This term derives from the study of solid particle motion in a stagnant medium (Hidy and Brock 1970). When a spherical object is released at a height above the ground it will accelerate towards the ground under the force of gravity. When the gravitational force is balanced by the drag of air on the object, the settling velocity of the object becomes constant. The expression of this velocity is given by Stoke's Law and is applicable for airborne particles between 1 and 100 μm in diameter. For particles with diameters <1 μm, the Cunningham correction factor must be included to account for particle slip between air molecules. Approximate settling velocities for solid spheres of density 1 $g.cm^{-3}$ in still air at 0°C and 101.3 kPa range downward from 25 $cm.s^{-1}$ for 100 μm particles to 8×10^{-5} $cm.s^{-1}$ for 0.1 μm particles (U.S. HEW 1969).

The design of numerous size-selective sampling devices used for the collection of atmospheric particles is theoretically based on Stoke's Law and hence it is possible to compute the diameters of the collected particles. If the density of the collected particles is known, the computed diameter is called the Stoke's diameter; however, if the density of the collected particles is not known but assumed to be 1 $g.cm^{-3}$, then the computed diameter is called the equivalent aerodynamic diameter. As will be discussed later, atmospheric particles are not all spherical, solid or of unit density. Unless otherwise specified, in this document particle size refers to equivalent aerodynamic diameter.

It is now generally accepted that atmospheric aerosols have a multimodal distribution with respect to particle size. Depending upon source influences, age of the aerosol, sampling methodology, etc. atmospheric aerosols are considered to have a trimodal distribution (Figure 2-1) with the three modes being nuclei (<0.1 μm diameter), accumulation (>0.1 to <2.0 μm diameter) and coarse (>2.0 μm diameter). The nuclei mode is usually observed near combustion sources or other high temperature sources and coagulates into accumulation mode particles. Consequently, atmospheric particles relatively far from specific sources usually have a bimodal size distribution with one mode in a fine particle size range (0.1-1.0 μm diameter) and another in a coarse particle size range (2-100 μm). Distinct trimodal surface area and volume distributions have been verified in the field (Whitby 1975; Whitby *et al.* 1976).

The division between fine and coarse particle modes is in the range of 1-3 μm and is commonly assumed to be 2 μm (UN-ECE 1979). It is convenient to differentiate atmospheric particles into fine and coarse modes, since each mode is usually different chemically and has different origins and fates in the atmospheric environment.

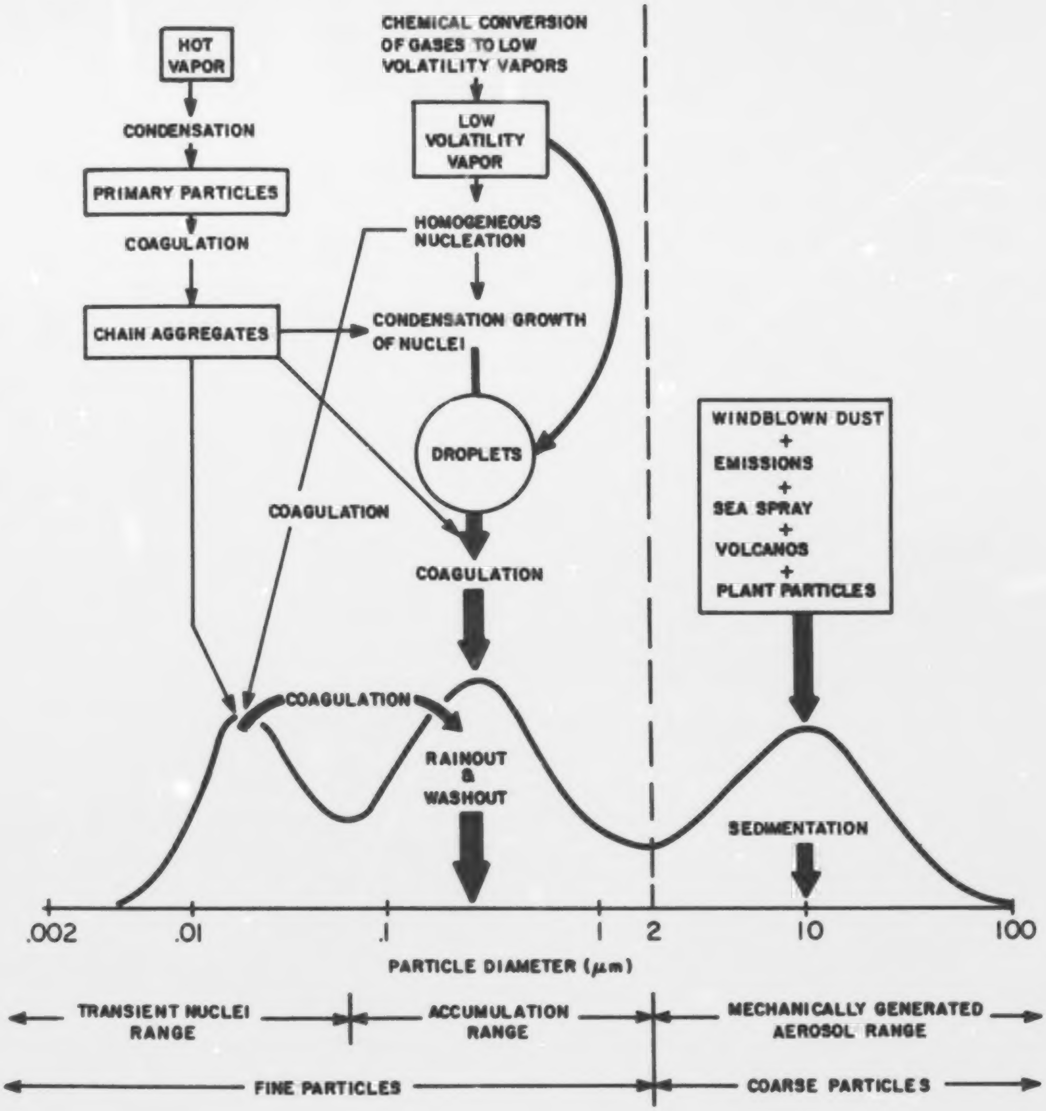
HOT VAPOR
CONDENSATION
PRIMARY PARTICLES
COAGULATION
CHAIN AGGREGATES
CHEMICAL CONVERSION OF GASES TO LOW VOLATILITY VAPORS
LOW VOLATILITY VAPOR
HOMOGENEOUS NUCLEATION
CONDENSATION GROWTH OF NUCLEI
DROPLETS
COAGULATION
COAGULATION
COAGULATION
RAINOUT & WASHOUT
WINDBLOWN DUST + EMISSIONS + SEA SPRAY + VOLCANOS + PLANT PARTICLES
SEDIMENTATION
.002
.01
.1
1
2
10
100
PARTICLE DIAMETER (μm)
TRANSIENT NUCLEI RANGE
ACCUMULATION RANGE
MECHANICALLY GENERATED AEROSOL RANGE
FINE PARTICLES
COARSE PARTICLES

Figure 2-1. Schematic representation of an atmospheric aerosol surface area distribution (from Whitby 1975).

It must be emphasized that the reported particle size distribution of an atmospheric aerosol will also be dependent upon the methods of particle collection and data presentation. Figure 2-2 presents normalized frequency plots of number, surface area and volume distributions for a smog aerosol (Whitby 1975). Maxima in the number and surface area distribution occur at approximately 0.01 and 0.2 μm diameter, respectively. Two maxima, 0.3 and 10.0 μm, occur in the aerosol volume distribution. Thus, in order to completely describe the particle size distribution of an atmospheric aerosol it is usually necessary to employ a number of different sampling instruments and techniques since no one method can fully characterize the approximate five orders of magnitude range (i.e. < 0.01-10 μm) of particle sizes.

2.3 PARTICLE SHAPE AND DENSITY

The fact that the shape of airborne particles may vary dramatically from sphericity cannot be ignored. The shape of particles in an atmospheric aerosol will be dependent upon the source, age of aerosol, etc. Some commonly encountered highly nonspherical particles include talc, mica, vermiculite, asbestos, glass fibers, organic fibers and synthetic fibers (for a detailed discussion of particle size and shape characteristics and the various methods used to examine such characteristics see NRCC 1982).

Agglomerates of particles can form via particle coagulation in or near combustion sources or in the ambient environment. They are often formed during incomplete combustion of fuels and contain a large amount of carbon (Corn 1976).

The behavior of a particle in an atmospheric aerosol is also affected by its density. For particles of spherical or other regular shapes, the density of an individual particle is usually equivalent to the density of the collected bulk material. However, particles that exist as agglomerates or that are porous have a significant portion of their volume as voids filled with gas or air. Hence, the apparent density of such particles can be 2-10 times lower than the density of particles if the pore volume is excluded (Hesketh 1972). The density of individual particles in atmospheric aerosols has been estimated to differ from 0.5 to 6.5 $g.cm^{-3}$ (Corn 1976).

Because of the large number of atmospheric particles that have irregular shapes and unknown densities, it has become common practice to represent such parameters in terms of dynamically equivalent spheres of unit density (i.e. equivalent aerodynamic diameter, see Section 2.2).

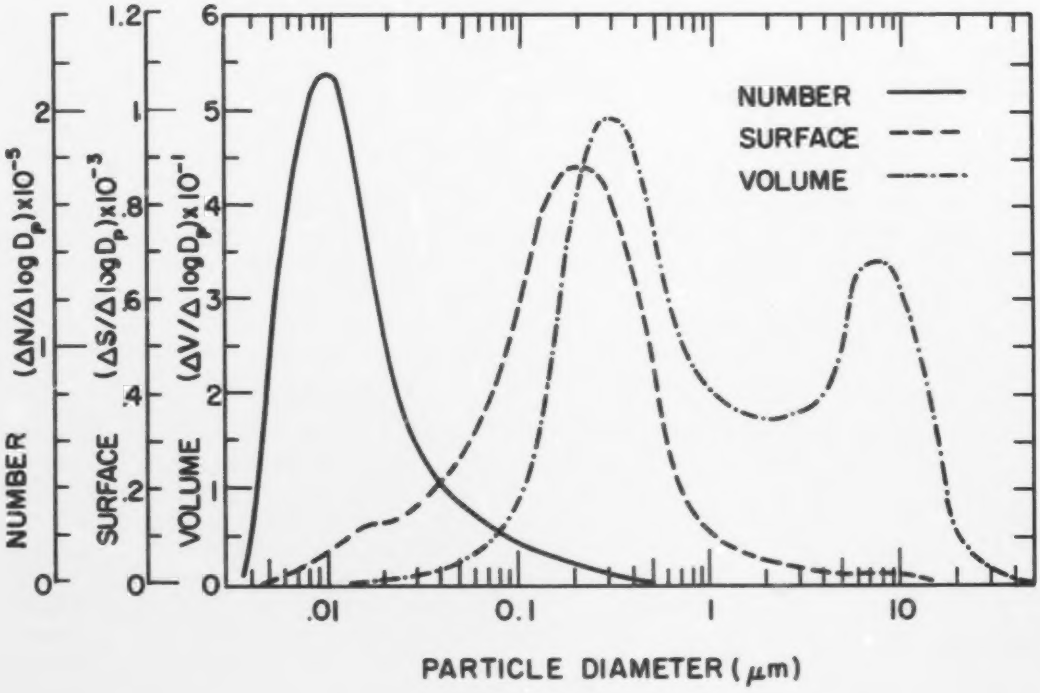

Figure 2-2. Normalized frequency plots of number, surface and volume distributions for the grand average 1969 Pasadena smog aerosol (from Whitby 1975).

2.4 PARTICLE SURFACE PROPERTIES

Because of their small size and the presence of surface roughness and porosity, airborne particles have large surface areas. Numerous chemical components have been found to be preferentially adsorbed to the surface of such particles (see Section 2.7). Under most atmospheric conditions submicrometre size particles (< 1 μm) contain significant amounts of water and, hence, it has been suggested that gas-particle interactions involve a gas-liquid phase (U.S. NAS 1979; Lodge et al. 1981). Consequently, dry surface gas-particle chemistry for atmospheric aerosols is thought to be insignificant. The effects of surface properties on other atmospheric phenomena, including particle coagulation, formation of clouds and fog, electrostatic charging, etc. are discussed in later sections of this document.

2.5 PARTICLE FORMATION

Most of the fine particles present in the atmosphere originate from various condensation processes of gases and vapors. Fine particles are formed in or near sources or in the atmosphere in the nuclei size mode by various nucleation processes and grow in size by coagulation (particle interaction) and heterogeneous nucleation (gas-particle interaction).

Two types of nucleation reactions are important when considering the generation of fine particles: 1) condensation of hot, supersaturated vapor via homogeneous nucleation (eg. metallic fumes, condensation of low vapor pressure oils and other low pressure vapors formed by combustion) and 2) condensation of cold, supersaturated vapor via homogeneous and heterogeneous nucleation (e.g. photochemical smog formed by reactions of hydrocarbons with nitrogen oxides and sulfuric acid droplets and sulfate particles formed by oxidation of sulfur dioxide). It has been estimated that fine particle formation via nucleation processes ranges from 2 particles.$cm^{-3}.h^{-1}$ in clean atmospheres to 6×10^6 particles.$cm^{-3}.h^{-1}$ in thermal power-plant plumes (Whitby 1978).

Once formed, fine particles undergo extensive heterogeneous nucleation and homogeneous and heterogeneous coagulation. Particle coagulation reduces the number concentration of submicrometre particles formed by nucleation processes. Homogeneous coagulation (interaction between like-sized particles) is believed to be important in or near fine particle sources. Most aerosols from various sources and in the ambient atmosphere are rarely sufficiently monodispersed according to particle size to undergo extensive homogeneous coagulation. Instead, heterogeneous coagulation (interaction of particles of different sizes) is thought to be significant in such circumstances. The heterogeneous coagulation coefficient may be one or two orders of magnitude greater than the homogeneous coagulation coefficient. For example, the rate at which 0.1 μm particles coagulate with 0.2 μm particles has a coefficient of approximately 3×10^{-8} compared with 10^{-9} for 0.1 μm particles undergoing homogeneous coagulation (U.S. NAS 1979).

The dynamics of fine particle growth usually prevent such particles from becoming larger than approximately 1.0 μm (Hidy and Brock 1970; Storebo 1974). Most particles larger than approximately 1.0 μm are produced via mechanical processes (e.g. natural aerosols from wind-blown dust and sea spray; man-made aerosols from grinding of coal and cement). In general, such particles do not undergo significant gas-particle and particle-particle interactions in the atmosphere.

2.6 PARTICLE TRANSPORT AND REMOVAL

Once airborne, fine particles behave much like gases and vapors in the atmosphere and are dispersed via eddy diffusion and advection. Particles are removed from the atmosphere by both dry and wet deposition.

Particles contacting the ground or other solid surfaces may be deposited. Small particles (0.1-0.2 μm) are usually deposited by diffusion processes. The deposition of larger particles is determined by aerodynamic processes such as impaction; however, in the absence of precipitation, the relative inefficiency of dry deposition processes permits transport of fine particles over long distances. Sedimentation is not expected to play a significant role in the removal of most fine particles from the atmosphere but is of importance for particles larger than approximately 1.0 μm.

Fine particles may also be removed from the atmosphere by such wet deposition processes as rain out (i.e. particles serve as cloud condensation nuclei or are captured in the formation of cloud droplets; see Section 5.2) and wash out (i.e. particles removed by falling raindrops and snowflakes). The reader is referred to Appendix IV for a detailed discussion of the mechanisms of aerosol scavenging. The topic of dry deposition of particles is not treated in this document and the interested reader is referred to several reports in the literature (cf. Slinn 1977; Slinn 1978; McMahon and Denison 1979; Fowler 1980; Hicks 1980; Sehmel 1980; Whelpdale 1982).

Coarse particles, which are usually emitted close to the surface, are removed from the atmosphere before being transported long distances. High concentrations of airborne coarse particles (> 25 μm) are observed near their source or during conditions such as dust storms (Hagen and Woodruff 1973). However, in some circumstances convective transport of coarse particles can result in significant concentrations of these particles far removed from their sources. For example, natural coarse particles can be injected high into the troposphere over deserts and be transported long distances (Prospero and Bonatti 1969; Jaenicke _et al_. 1971; Bryson 1972).

2.7 CHEMICAL COMPOSITION

A distinction may be made between fine and coarse particles concerning not only their formation, transport and removal, but also their chemical composition. Studies of the dependency of chemical composition on particle size are too numerous to mention here and the interested reader is referred to several reviews (Lee 1972; Natusch *et al.* 1974; Natusch and Wallace 1974; Patterson and Wagman 1977; Lodge *et al.* 1981).

Most chemical constituents are usually found in either the fine or coarse particle modes, although there may be some overlap between modes. In general, particle mass in the fine particle mode (0.1-2.0 μm) is composed of sulfate, nitrate, ammonium, lead, bromine, elemental carbon and condensed organic matter. Although their relative amounts differ depending upon sampling location, etc., the sum of their individual masses approximate the total mass of the fine particle mode.

Sulfate and its associated cations have been found to be the predominant species in the fine particle mode, usually contributing at least 50% of the total fine particle mass (Tanner *et al.* 1979; Stevens *et al.* 1980; Pierson *et al.* 1980a; Macias *et al.* 1980; Leaderer and Stolwijk 1980). Ammonium ion was found to be highly correlated (r = 0.92 - 0.94) with sulfate ion in the fine particle mode (Tanner *et al.* 1979) and it was found that the concentrations of SO_4^{2-}, H^+ and NH_4^+ could be statistically represented almost entirely as $(NH_4)_x H_y SO_4$ (x+y=2) (Pierson *et al.* 1980b).

The relative proportions of constituents in the fine particle mass may differ dramatically depending upon such factors as sampling location, time of year, etc. For example, Stevens *et al.* (1980) found that sulfate and its associated cations represented 61% whereas elemental and organic carbon represented only 5 and 10% respectively, of the fine particle mass of samples collected in the forest of Smokey Mountain National Park near Knoxville, Tennessee in September 1978. On the other hand, Countess *et al.* (1981) found that 61% of the fine particle mass of samples collected near Denver, Colorado was made up of organic and elemental carbon (33% organic and 28% elemental) while only 30% of the mass was comprised of sulfate, nitrate and ammonium ions.

Although few good measurements have been made, the role of water in atmospheric particles is significant, especially when considering visibility impairment (see Chapter 4) and cloud formation (see Section 5.2). Relative humidity has a significant effect on particle size. Countess *et al.* (1981) found that high relative humidities, which cause hygroscopic particles to grow, resulted in an increase in particle size with respect to several chemical species. For example, the MMAD (mass medium aerodynamic diameter) of SO_4^{2-}-, NO_3^-- and NH_4^+-containing particles increased approximately 50% (0.27 to 0.42 μm) when the relative humidity increased from 40% to 70%. In addition, the MMAD of particles containing organic and elemental carbon increased approximately 20% for the same increment in relative humidity.

Minor contributions to the fine particle mass are made by soil-related elements, lead compounds and certain trace species (Stevens et al. 1978). Aluminum, calcium, iron, and silicon were found to be minor constituents of the New York summer aerosol (Stevens et al. 1980).

Particles in the coarse particle size model (> 2 μm) are predominately entrained dust raised by natural winds and road traffic (Lodge et al. 1981). The composition of particles collected in areas removed from specific sources approximates the mean composition of the earth's crust. Macias et al. (1980) found that aluminum, calcium and iron were present predominantly in the coarse particle mode whereas sulfur and titanium were present predominantly in the fine particle mode. Silicon and potassium had substantial concentrations in both modes. The relative contributions of other trace constituents are usually highly variable depending upon geographical and meteorological conditions.

2.7.1 ARTIFACT FORMATION DURING SAMPLING

The measurement of NH_4^+, SO_4^{2-} and NO_3^- mass using standard filtration techniques (e.g. high volume sampling with glass fiber filters) has been questioned by numerous researchers. Ammonia may interact with previously collected nitrate particles, yielding erroneously high ammonium ion concentrations. Pierson et al. (1980b) found that SO_4^{2-} was directly related to filter alkalinity, relative humidity and SO_2 concentration. Nitrate artifacts were also attributed to filter alkalinity. Wirtz and Wendt (1981) found that artifact sulfate and nitrate concentrations averaged 2.0 $\mu g.m^{-3}$ (0-10.9 $\mu g.m^{-3}$) and 8.3 $\mu g.m^{-3}$ (0-25.8 $\mu g.m^{-3}$), respectively. They attributed the sulfate produced to the adsorption of sulfur- and nitrogen-containing gases (e.g. SO_2, NO_2, HNO_3, etc.) with subsequent conversion on the collection filters to sulfates and nitrates. Stevens et al. (1980) found 0.7-2.2 $\mu g.m^{-3}$ of sulfate and 0.3-1.1 $\mu g.m^{-3}$ of carbon were due to artifact formation. Negative errors resulting from the volatilization of nitrate as gaseous HNO_3 (Appel et al. 1981) as well as liberation of gaseous HNO_3 upon reaction of nitrate with strong acids (e.g. H_2SO_4) already collected in the filter media (Pierson et al. 1980b; Appel et al. 1981) have been reported.

In addition, total suspended particulate (TSP) sampling methodology employing high volume sampling has been found to contain errors due to the passive loading of windblown particles during nonsampling periods. For example, Sweitzer (1980), using standard sampling techniques and gravimetric analysis, found a positive error of 16-17%. Ninety percent of the particles passively collected had diameters > 10 μm with some as large as 60 μm.

3.0 SOURCES AND EMISSIONS

3.1 INTRODUCTION

As discussed previously, particles may enter the atmosphere as a result of the activities of both man and nature. Sources of atmospheric particles may be grouped into two general categories: 1) direct sources, which refer to particles emitted in a gas stream and 2) indirect or fugitive sources, which refer to particles emitted without first passing through a stack or duct which directs and controls their flow. The following discussion focuses on the sources of atmospheric particles and draws upon the currently available information from various inventory studies to derive an understanding of the relative importance of various sources of particles to the total atmospheric particle burden.

3.2 GLOBAL PERSPECTIVE

To establish a perspective on the particle burden in the atmosphere, one must first examine the sources of particle emissions on a global scale. It is useful to distinguish between man-made and natural emissions of both primary and secondary particles (for terminology see Section 2-1 and Appendix I).

Global estimates have been made by a number of authors and show reasonably good agreement (Table 3-1) (Hidy and Brock 1971; Peterson and Junge 1971; SMIC 1971). Based on these data it can be seen that global emissions of particles are composed of about 7-19% from man-made sources and about 81-93% from natural sources. Man-made emissions consist of approximately 5-41% primary particles and 59-95% secondary particles. Peterson and Junge (1971) estimated that of the total man-made primary and secondary emissions, about 22% and 92% respectively, were < 5 μm. On a global basis, natural emissions are made up of 48-73% primary particles and 27-52% secondary particles. Again, using the data of Peterson and Junge (1971) about 49% of natural primary particle emissions and about 82% of natural secondary particle emissions are < 5 μm.

3.3 CANADA AND THE UNITED STATES

3.3.1 NATURAL SOURCES AND EMISSIONS

Particles emitted to the atmosphere may be divided into several categories depending upon origin, particle size characteristics and chemical composition. They are derived from soil, combustion, sea spray, vegetation and volcanic action.

Table 3-1. Estimated global production of particles from natural and man-made sources (10^9 kg.a^{-1}).

Source	After Peterson and Junge (1971) all sizes	After Peterson and Junge (1971) < 5 μm	After Hidy and Brock (1971) all sizes	After SMIC (1971) < 20 μm
1. Natural Primary				
Sea salt	1000	500	1095	300
Windblown dust	500	250	7-365	100-500
Volcanic emissions	-	25	4	25-150
Meteoric debris	10	0	0.02-0.2	-
Forest fires	25	5	146	3-150
Total	1535	780	1252-1610	428-1100
2. Natural Secondary				
Converted sulfates	420	335	36.5-36.8	130-200
Converted nitrates	75	60	600-620	140-700
Converted hydrocarbons	75	75	182-1095	75-200
Total	570	470	819-1752	345-1100
3. Man-Made Primary				
Industrial processes	56.4	12.4		
Stationary fuel combustion	43.4	9.6		
Solid waste incineration	2.4	0.4		
Transportation	2.2	1.8		
Miscellaneous	28.8	5.4		
Total	133.2	29.6	36.8-110	10-90
4. Man-Made Secondary				
Converted sulfates	220	200	109.5	130-200
Converted nitrates	40	35	23	30-35
Converted hydrocarbons	15	15	27	15-90
Total	275	250	159.5	175-325
Total Natural	2105	1250	2071-3362	773-2200
Total Man-Made	408	280	196-270	185-415
Grand Total	2513	1530	2267-3632	958-2615

The following discussion focuses on size and chemical composition of naturally occurring particles. Estimated emissions of these particles are presented later.

3.3.1.1 Particle Size and Chemical Composition

The size distribution of soil-derived aerosols is approximately bimodal (i.e. when particle volume is compared to particle size), the modes being 1-10 μm and 50 μm (Gillette 1980). On a mass basis, Winchester et al. (1979) found that over 90% were > 1 μm diameter. Soil-derived particles are primarily composed of seven major elements (silicon, aluminum, iron, sodium, potassium, calcium and magnesium); these elements occur in approximately the same proportions as in the earth's crustal material (Miller et al. 1972). Rahn (1976) and Sadasivan (1978) reported the principal elements to be Al, Fe, Ti, Si, Co, Sc along with numerous rare earth elements. The organic component of soil-derived particles is variable but usually constitutes only a small percentage of the particle mass (Corn 1976).

As regards natural combustion sources, there are three types of large-scale fires that may emit particles to the atmosphere: 1) wildfires (i.e. uncontrolled burning), 2) prescribed burning in natural areas and 3) agricultural burning. There is considerable variation in size and composition of particles produced by forest fires depending upon the type of combustion, type of material consumed, location of sampling, etc. However, in general, particles generated in temperate forest fires are composed of benzene-soluble organic matter (50%), elemental carbon (40%) and minerals (10%) (Ryan and McMahon 1976). Forest fires produce particles predominately in the range of 0.1 to 1 μm, although the absolute range can be much larger (i.e. 0.01-200 μm) (Corn 1976). Approximately 80% of the mass of particles from forest fires were < 1 μm, with the average size being 0.1 μm (Vines 1971). Radke et al. (1978) reported that approximately 94% of the mass was < 2.5 μm.

Sea spray particles are generated at the surface of the ocean by the action of wind, primarily via a process whereby air bubbles become entrained and rise to burst at the surface. At the point of emission, droplet size varies typically from 2 to 80 μm. Taback et al. (1979) have classified their size range according to the following mass distribution: > 10 μm, 24%; 3-10 μm, 54%; 1-3 μm, 20%; < 1 μm, 2%. Particles < 2.5 μm constitute approximately 15% of the annual sea-salt mass flux (Duce and Woodcock 1971; Meszaros and Vissy 1974). Depending upon the relative humidity, evaporation may reduce droplet size by a factor of 2 or more (Williamson 1973). Sea spray particles are composed mainly of water along with dissolved and suspended materials, primarily sodium chloride (Williamson 1973). Small amounts of potassium, calcium, magnesium, organic compounds, sulfates and carbonates are also present.

Vegetation-derived particles may be emitted via 1) the release of pollen and spores and 2) the release of volatile organic compounds that subsequently form particles. The size of pollen and spores typically ranges from 10 to 50 μm and 5 to 10 μm, respectively (Corn 1976). Although emissions of volatile organic compounds from vegetation are substantial (Went 1960), the portion of vapor converted to particles is not yet known. Isoprene derivatives are believed to make up the majority of organic compounds in these emissions. Some organic compounds are at least partially oxidized, resulting in haze over forested regions (Went 1960; Went et al. 1967). Trace metals are minor components of vegetation-derived particles, and are associated mostly with particles > 5 μm (Beauford et al. 1975; 1977).

With regard to volcanic-derived particles, it was established that, on a mass basis, 96% of the particles emitted during the 1976 eruption of the St. Augustine volcano in Alaska ranged from 0.01-66 μm while only 4% were in the range 0.01 to 5 μm (Stith et al. 1978). Depending upon the type of volcano and nature of the emission, particle size ranges between 0.02 and 100 μm. Fruchter et al. (1980) found that approximately 98% of the total mass of particles emitted from the Mount St. Helens eruption of May 18, 1980 was accounted for by particles > 3.5 μm. Volanic-derived particles are usually highly variable in chemical composition. Particles emitted during the St. Augustine eruptions were composed primarily of silicon, aluminum, magnesium, calcium and iron (Stith et al. 1978). Trace amounts of potassium, titanium, sulfur, nickel and chromium were also observed. Samples of ash from the Mount St. Helen's eruption contained silicon, aluminum, iron, calcium, sodium, magnesium, potassium, titanium, phosphorous and manganese. Trace amounts of sulfur, chlorine, strontium, barium, vanadium, zirconium and zinc were also detected (Fruchter et al. 1980).

3.3.1.2 Estimated Emissions

On a global basis, at least three-quarters of the total particle mass emitted to the atmosphere originates from natural sources. Emissions of natural primary particles have been estimated for Canadian terrestrial and marine regions (Environment Canada 1981a) and appear in Tables 3-2 and 3-3 respectively. Since these estimates were frequently calculated from a limited data base, they should be considered as order-of-magnitude approximations. On a nationwide basis, approximately 748 x 10^9 kg.a^{-1} of primary particles are emitted to the atmosphere from natural sources, of which 42% and 58% are derived from terrestrial and marine sources, respectively. With respect to terrestrial sources, soil-derived particles contribute the largest portion of the mass of primary particles emitted to the atmosphere; an estimated annual production rate is 304 x 10^9 kg. Most soil-derived particle emissions originate from grassland-agricultural biomass, primarily as a result of cultivation. Emission estimates from forest and brush fires as well as from plants (pollen and spores) are 732 x 10^6 kg.a^{-1} and 9.5 x 10^9

Table 3-2. Estimated Canadian annual terrestrial emissions of primary natural particles (kg x $10^6 \cdot a^{-1}$) (from Environment Canada 1981a).

Province/ Territory	Emission Source (Biome)[α]	Area (km²)	Soil-Derived Particles		Combustion Particles		Pollen and Spores		Total	
			Fine[β]	Coarse	Fine[β]	Coarse	Fine[β]	Coarse	Fine[β]	Coarse
Newfoundland	Tundra	22985	11.49	218.36	Nil	Nil	Nil	.69	11.49	219.05
	Boreal F.[γ]	2356[illegible]	Nil	Nil	7.21	.80	Nil	221.53	7.21	222.33
	Boreal B.[δ]	98124	Nil	Nil	12.03	1.34	Nil	161.85	12.03	163.19
		356790	11.49	218.36	19.24	2.14	Nil	384.07	30.73	604.57
Prince Edward Island	G.L.-Acad.[ε]	5660	.85	16.13	.83	.09	Nil	22.64	1.68	38.86
Nova Scotia	G.L.-Acad.	51277	7.69	146.16	7.58	.84	Nil	205.12	15.27	352.12
New Brunswick	G.L.-Acad.	70015	10.50	199.55	10.27	1.14	Nil	280.06	20.77	480.75
Quebec	Tundra	211215	105.61	2006.54	Nil	Nil	Nil	6.34	105.61	2012.88
	Boreal B.	391305	Nil	Nil	11.88	1.32	Nil	364.02	11.88	365.34
	Boreal F.	476777	Nil	Nil	58.85	6.54	Nil	793.36	58.85	799.90
	G.L.-Acad.	121264	18.19	345.61	17.83	1.98	Nil	485.02	36.02	832.61
	Grass-Ag.[ζ]	30718	59.46	1128.56	.083	.0090	Nil	57.04	59.54	1185.61
		1231279	183.26	3480.71	88.64	9.85	Nil	1705.78	271.90	5196.34
Ontario	Boreal B.	248396	Nil	Nil	7.60	.84	Nil	233.50	7.60	234.34
	Boreal F.	410432	Nil	Nil	50.24	5.58	Nil	677.22	50.24	682.80
	G.L.-Acad.	146487	21.97	417.50	21.56	2.40	Nil	585.93	43.53	1005.83
	Grass-Ag.	62224	118.47	2250.89	.18	.02	Nil	120.38	118.65	2371.29
		867539	140.44	2668.39	79.58	8.84	Nil	1617.03	220.02	4294.26
Manitoba	Boreal B.	184788	Nil	Nil	10.81	1.20	Nil	173.70	10.81	174.90
	Boreal F.	257589	Nil	Nil	60.26	6.69	Nil	425.02	60.26	431.71
	Aspen P.[η]	44287	675.38	12832.20	5.18	0.58	Nil	83.27	680.56	12916.05
	G.L.-Acad.	4763	.71	13.58	.23	.020	Nil	19.05	.94	32.65
	Grass-Ag.	17803	600.85	11416.19	.040	.010	Nil	18.88	600.89	11435.08
		509230	1276.94	24261.97	76.52	8.50	Nil	719.92	1353.46	24990.39
Saskatchewan	Boreal B.	47163	Nil	Nil	2.75	.31	Nil	44.33	2.75	44.64
	Boreal F.	264334	Nil	Nil	61.78	6.86	Nil	436.15	61.78	443.01
	Aspen P.	75205	1142.30	21703.76	8.81	.98	Nil	141.41	1151.11	21846.15
	Grass-Ag.	153208	5250.83	99765.69	.42	.050	Nil	162.41	5251.25	99928.15
		539910	6393.13	121469.45	73.76	8.20	Nil	784.30	6466.89	122261.95
Alberta	Tundra	2650	1.33	25.18	Nil	Nil	Nil	.080	1.33	25.26
	Boreal B.	2393	Nil	Nil	.14	.010	Nil	2.25	.14	2.26
	Boreal F.	407217	Nil	Nil	95.13	10.57	Nil	671.91	95.13	682.48
	Aspen P.	72821	1110.52	21099.91	8.52	0.95	Nil	136.90	1119.04	21237.76
	Coastal-Mt.[θ]	43629	2.18	41.44	Nil	Nil	Nil	71.99	2.18	113.43
	Grass-Ag.	89657	3025.92	57492.57	.25	.030	Nil	95.02	3026.17	57587.62
		618367	4139.95	78659.10	104.04	11.56	Nil	978.15	4243.99	79648.81
Northwest Territories & Yukon	Tundra	2292034	1146.02	21774.42	Nil	Nil	Nil	64.33	1146.02	21838.75
	Boreal B.	812633	Nil	Nil	47.48	5.28	Nil	763.87	47.48	769.15
	Boreal F.	461437	Nil	Nil	107.78	11.98	Nil	761.37	107.78	773.35
		3566104	1146.02	21774.42	155.26	17.26	Nil	1589.57	1301.28	23381.25
British Columbia	Tundra	147060	73.53	1397.07	Nil	Nil	Nil	4.41	73.53	1401.48
	Boreal F.	195027	Nil	Nil	14.74	1.64	Nil	321.80	14.74	323.44
	Coastal-Mt.	488841	2.44	464.88	28.60	3.18	Nil	806.58	31.04	1274.64
	Grass-Ag.	52505	1772.07	33669.26	.14	.020	Nil	55.67	1772.21	33724.95
		883433	1848.04	35531.21	43.48	4.84	Nil	1188.46	1891.52	36724.51
National Totals			15158.31	288425.45	659.20	73.26	Nil	9475.10	15817.51	297973.81
% of Total			4.83	91.92	.21	.023	Nil	3.02	5.04	94.97

[α] Biome - a major ecological community (such as boreal forest or grassland).

[β] Fine - fine particle (< 2.5 μm diameter).

[γ] Boreal F. - boreal forest.

[δ] Boreal B. - boreal forest - barrens.

[ε] G.L.-Acad. - Great Lakes - Acadian forest.

[ζ] Grass-Ag. - grassland - agriculture.

[η] Aspen P. - aspen parkland.

[θ] Coastal-Mt. - coastal and mountain forests.

Table 3-3. Estimated annual emissions of salts from Canadian marine environments (kg x $10^6.a^{-1}$) (Environment Canada 1981a).

Marine Zone	Area (km^2)	Emissions	
		Fine	Coarse
Arctic	2962200	28881	163662
Pacific (north)	41875	3172	17975
Pacific (south)	114375	9007	51040
Atlantic (north)	111250	5090	28842
Atlantic (south)	375650	18876	106966
		65026	368485

$kg.a^{-1}$, respectively. Fine (< 2.5 μm) and coarse particle emissions accounted for approximately 5 and 95% respectively, of the total terrestrial mass emission rate of 314 x 10^9 $kg.a^{-1}$. Of the total marine mass emission rate, 434 x 10^9 $kg.a^{-1}$, fine and coarse particles constituted 15 and 85%, respectively.

Natural sources of particles (primary and secondary) in the United States contribute approximately 84 x 10^9 $kg.a^{-1}$ to the total atmospheric particle burden (U.S. EPA 1981). The total amount consists of: 1) terrestrial dust emissions, 57 x 10^9 $kg.a^{-1}$ (Vandergrift 1971); 2) sea spray, 5.5 x 10^9 $kg.a^{-1}$ (U.S. EPA 1981); 3) vegetative emissions, 20 x 10^9 $kg.a^{-1}$ (U.S. EPA 1981); and 4) wildfires, 0.5 to 0.7 x 10^9 $kg.a^{-1}$ (Robinson and Robbins 1971; Yamate 1973). It must be emphasized that estimates of total emissions of primary particles for Canada and the United States are not directly comparable since the United States estimates do not include emissions from agricultural tilling, entrained dust from cropland, entrained dust from paved and unpaved roads, etc. Such emission estimates are discussed under nonindustrial indirect emissions (see Section 3.3.2.2). Volcanic activity contributes variable amounts. The average global volcanic emission rate is estimated at 3.6 x 10^9 $kg.a^{-1}$ (Robinson and Robbins 1971). The 1976 eruption of the St. Augustine volcano in Alaska generated approximately 7 x 10^9 kg of particles (Stith et al. 1978).

3.3.2 MAN-MADE SOURCES AND EMISSIONS

Particles are emitted into the atmosphere either directly or indirectly (fugitive) as a result of a large number of man's activities. These include: industrial processes, fuel combustion, transportation, solid waste incineration and various miscellaneous activities such as forest fires, slash burning, fertilizer application, etc. (see Table 3-6 for a description of source categories).

3.3.2.1 Particle Size and Chemical Composition

Although extensive data exist on the chemical composition of total particulate matter from man-made sources, relatively less information is available on the chemical composition of specific size fractions of particles.

Both size distribution and chemical composition of particles are highly variable as a result of the influence of several factors such as source type, operating conditions, general maintenance, cleanliness, type of emission control equipment, etc. In general, size and chemical composition of emitted particles reflect the materials used and the activity concerned (see for example Table 3-4 and 3-5). It is important

Table 3-4. Summary of size distributions and chemical composition of particles emitted from various sources (from Taback 1979).

No.	Source	Particle Size Distribution Wt % > 10µm	3-10µm	1-3µm	< 1µm	Primary Chemical Species (Composite Wt %)	Confidence Level^a
1	Industrial boiler (crude & resid.)	13	9	12	66	$SO_4^=$ (44), C (23), Fe(3)	II
2	Industrial boiler (#2 fuel oil)	2	1	1	96	$SO_4^=$ (25), C (15), NO_3^- (4)	III
3	IC engines (diesel fuel)	4	2	2	92	$SO_4^=$ (15), Ca (5), C (4)	IV
4	IC engines (gas fuel)	0.6	0.2	0.4	99	$SO_4^=$ (45), C (20), Cl (7)	III
5	Wood waste (hog fuel) boiler	0.3	5	21	74	C (30), Si (10), $SO_4^=$ (3), Cl(2)	II
6	Utility boilers (resid., 0.25%S)	3	4	8	85	$SO_4^=$ (28), C (22), Ca (10), Ni (5)	II
7	Rice dryer	89	2	1	8	C (12), Si (10)	III
8	Coffee/carob roasting	38	1	1	60	C (28)	III
9	Steel heat treating, salt quench	4	8	14	74	$SO_4^=$ (32), Cl (30), Fe (9)	III
10	Steel abrasive blasting	14	6	6	74	Al_2O_3 (80), Fe (15), Ti (3)	IV
11	Aluminum foundry	5	4	5	86	$SO_4^=$ (16), C (13), Cl (11), Fe (6), Ca (3)	III
12	Steel sintering plant	3	1	1	95	Cl (28), K (19), $SO_3^=$ (19), Fe (14), Pb (10), C (10), Cr (13), Cu (2)	III
13	Steel open hearth furnace	2	4	7	89	$SO_4^=$ (40), C (20), Fe (11), K (5), Cr (2)	III
14	Gypsum calcining	12	32	34	22	$SO_4^=$ (55), Ca (12), C (2)	III
15	Brick mfg., grinding & screening	44	4	4	48	Si (27), Fe (2), K (1)	III
16	Cement production	8	24	34	34	$SO_4^=$ (25), Ca (20), C (12), Si (10)	II
17	Glass furnace	2	1	2	95	$SO_4^=$ (58), C (12), Se (4), K (3), As (2)	II

Table 3-4. (Cont'd)

No.	Source	Particle Size Distribution Wt %				Primary Chemical Species (Composite Wt %)	Confidence Level[a]
		> 10 μm	3-10 μm	1-3 μm	< 1 μm		
18	Fiberglass forming	0.6	0.2	0.2	99	C (30), Cl (15)	III
19	Asphalt roofing	2	3	4	91	C (24), $SO_4^=$ (22), Ce (12), Ca (3), Fe (2), Co (2)	IV
20	Asphalt concrete batch plant	60	6	4	30	SiO_2(84), C(5), Ca(5), Fe(3), $SO_4^=$(2)	III
21	Paint booth (waterborne)	32	5	5	58	C (50), Ti (3), $SO_4^=$ (2)	III
22	Paint booth (solvent base)	5	2	3	90	C (55), Ti (3), $SO_4^=$ (2)	IV
23	Boric acid manufacturing	10	0.5	0.5	89	HBO_3 (98), $SO_4^=$ (2)	III
24	Chemical fertilizer (urea) mfg.	4	1	1	94	C (33), Cl (11), $SO_4^=$ (5)	III
25	Wood operations - resawing	60	11	9	20	C (42)	III
26	Wood operations - sanding	8	3	3	86	C (41)	III
27	Petroleum - heaters	4	2	2	91	$SO_4^=$ (47), C(7), Ca(5), Co(2)	III
28	Petroleum - FCC CO boiler	39	4	16	41	$SO_4^=$ (30), Si (10), C (2), Ce (1)	III
29	Feed & Grain operations	71	27	2	0	C (30), Si (15)	IV
30	Limestone kilns	70	17	6	7	C(40), Ca(30), Se (10), Fe (2)	III
31	Basic oxygen furnace	0	0	5	95	$SO_4^=$ (40), C(20), Fe(11), K(5), Cr(2)	V
32	Electric arc furnace	17	20	18	45	$SO_4^=$ (40), C(20), Fe(11), K(5), Cr(2)	V
33	Rock crusher	90	7	2	1	Si (40)	IV
34	Rock screening	50	30	18	2	Si (40)	IV
35	Structural fires	2	5	13	80	C(30), Si(10), K(5), Fe(2), Cl(2), Ca(1)	V
36	Residential nat. gas combustion	0	0	0	100	C (50), $SO_3^=$ (20)	IV

Table 3-4. (Cont'd)

No.	Source	Particle Size Distribution Wt % > 10 µm	3-10 µm	1-3 µm	< 1 µm	Primary Chemical Species (Composite Wt %)	Confidence Level[α]
37	Fireplaces	38	14	12	36	C(30), Si(10), K(5), Ca(5), Fe(4)	IV
38	Automobile tire dust	60	5	15	20	C (87), Zn (2)	III
39	Cigarette smoke	0	0	0	100	C (85)	II
40	Sea salt	25	55	18	2	Cl (55), Na (31), Mg (4), Ca(1)	III
41	Automobile brake lining dust	0	0	0	100	Asbestos (80), C (16)	IV
42	Livestock dust	25	13	16	46	Si(20), Al(8), Fe(3), Ca(2), K(2), C (2)	III
43	Unpaved road	54	16	12	18	Si(20), Al(8), Fe(31), Ca(2), K(2)	III
44	Construction & road building dust	43	20	17	20	Si (20), Al (8), Fe(3), Ca(2), K (2)	IV
45	Agricultural burning	0	2	8	90	C(30), Si(10), K(5), Fe(2), Cl(2), Ca(1)	IV
46	Forest fires	2	5	13	80	C(30), Si(10), K(5), Fe(2), Cl(2), Ca(1)	IV
47	Landfill operations	45	15	12	28	Si(20), Al(8), Fe(3), K(2), Ca(2)	III
48	Agricultural tilling	36	22	17	25	Si(20), Al(8), Fe(3), K(2), Cd(2)	III
49	Industrial boiler (nat. gas fuel)	0	0	0	100	C(50), $SO_3^=$ (20)	II

[α] Confidence Level.

I. Based on a composite of many tests so that the data are highly representative.

II. Based on a moderate number of tests or questionnaires which indicate that the data are reasonably representative.

III. Based on data which seems reasonable and should be more or less representative.

IV. Based on little data; not sufficient to be representative.

V. Results are highly judgmental and could differ significantly from source to source.

Table 3-5. Size distribution of primary particles emitted from various sources identified in the Canada nationwide inventory (from Environment Canada 1982).

Source Category	Particle size range (% of total) <2.5 µm	2.5-15 µm	>15 µm
1. Industrial Processes			
Iron and steel production	51.1	21.9	27.0
Iron ore mining and beneficiation	12.6	21.0	66.4
Pyrrhotite Roasting	94.4	1.9	3.7
Coal industry	16.6	17.1	66.3
Metallurgical coke manufacture	21.3	25.5	53.2
Primary aluminum production	96.6	1.8	1.6
Primary Cu and Ni production (including refining)	67.3	21.0	11.7
Primary Pb and Zn production	56.0	30.9	13.1
Ferroalloy manufacture	98.0	2.0	-
Abrasives manufacture	90.0	10.0	-
Ferrous foundries	43.3	24.2	32.5
Asbestos production	25.0	59.9	15.1
Cement manufacture	33.0	54.5	12.5
Asphalt production	75.0	15.0	10.0
Lime manufacture	58.9	27.2	13.9
Gypsum processing	47.3	50.6	2.1
Nepheline syenite processing	80.9	16.7	2.4
Silica processing	11.7	35.3	53.0
Stone processing	15.2	28.1	56.7
Sand and gravel processing	14.0	46.0	40.0
Mining and rock quarrying	10.6	20.6	68.8
Kraft pulping	67.7	16.5	15.8
Sulphite pulping	92.2	1.2	6.6
Potash processing	46.8	40.6	12.6
Phosphate rock processing	10.7	19.9	69.4
Phosphate fertilizer manufacture	10.4	12.9	76.7
Elemental phosphorus production	48.6	34.8	16.6
Nitrate fertilizer manufacture	50.0	32.8	17.2
Grain handling and milling	44.6	49.5	5.9

Table 3-5. (Cont'd)

Source Category	Particle size range (% of total) < 2.5 μm	 2.5-15 μm	 > 15 μm
Clay products manufacture	28.4	41.0	30.6
Petroleum refining	75.2	15.0	9.8
Natural gas processing	95.0	5.0	-
Tar sands operations	75.0	20.0	5.0
Glass manufacture	98.0	2.0	-
Concrete batching	50.0	38.0	12.0
Magnesium production	68.0	32.0	-
Carbon black	100.0	-	-
Salt prod.	50.0	30.0	20.0
2. Fuel Combustion/Stationary Sources			
Utility power generation[a]	43.6	29.5	26.9
Industrial fuel combustion			
Natural gas	95.0	5.0	-
Propane	95.0	5.0	-
Butane	95.5	4.5	-
Light oil	50.0	45.2	4.8
Heavy oil	50.0	45.1	4.9
Stove oil	70.0	25.2	4.8
Coal	10.0	50.0	40.0
Commercial Fuel Combustion			
Natural gas	95.0	5.0	-
Light oil	50.0	45.2	4.8
Heavy oil	50.0	45.1	4.9
Stove oil	70.0	25.2	4.8
Coal	10.0	50.0	40.0
Residential Fuel Combustion			
Natural gas	95.0	5.0	-
Propane	95.0	5.0	-
Butane	95.5	4.5	-
Light oil	50.0	45.2	4.8
Heavy oil	50.0	45.1	4.9

Table 3-5. (Cont'd)

Source Category	Particle size range (% of total)		
	<2.5 μm	2.5-15 μm	>15 μm
Stove oil	70.0	25.2	4.8
Coal	10.0	50.0	40.0
Fuelwood Combustion	89.9	9.0	1.1
3. Transportation			
Gasoline-powered motor vehicles	100.0	-	-
Railroads	73.8	10.8	15.4
Marine	27.3	41.9	30.8
Aircraft	100.0	-	-
Off-road use of gasoline	100.0	-	-
Diesel-powered engines	100.0	-	-
Tire wear	23.5	9.6	66.9
4. Solid Waste Incineration			
Municipal incineration	67.8	20.8	11.4
Industrial and commercial incineration	10.1	20.1	69.8
Sewage sludge incineration	65.3	11.9	22.8
Wigwam burners	84.3	10.3	15.4
5. Miscellaneous			
Fertilizer application	-	5.0	95.0
Pesticide manufacturing and application	-	-	100.0
Forest fires	90.0	9.1	0.9
Structural fires	90.0	8.8	1.2
Slash burning	90.0	9.2	0.8
Cigarette smoking	100.0	-	-

[α] Due to significant variations in control equipment used, processes, etc. the particle size distribution for this source has been combined for all fuels.

Table 3-6. Estimated Canadian annual emissions of man-made primary particles, 1976 (kg x $10^3.a^{-1}$) (from Environment Canada 1981b).

Source Category	Newfoundland	Prince Edward Island	Nova Scotia	New Brunswick	Quebec	Ontario	Manitoba	Saskatchewan	Alberta	British Columbia	North West Territories and Yukon	Total
1. Industrial Processes												
Iron and steel production	-	-	17785	-	8784	19320	383	1693	307	264	-	48536
Iron ore mining and beneficiation	142268	-	-	-	110396	73301	-	-	-	3749	-	329714
Pyrrhotite roasting	-	-	-	-	-	3185	-	-	-	250	-	3435
Coal industry	-	-	128	231	1	451	1403	1639	3042	55251	-	62146
Metallurgical coke manufacture	-	-	669	-	280	5700	-	138	-	526	-	7313
Primary aluminum production	-	-	-	-	14483	-	-	-	-	2360	-	16843
Primary copper and nickel production	-	-	-	-	11446	12926	12736	-	-	-	-	37108
Primary lead and zinc production	-	-	-	233	188	97	-	-	-	589	-	1107
Copper and nickel refining	-	-	-	-	45	2928	24	-	-	-	-	2997
Ferroalloy manufacture	-	-	-	-	25000	55	-	-	-	-	-	25055
Abrasives manufacture	-	-	-	-	3498	4507	-	-	-	-	-	8005
Ferrous foundries	4	9	149	446	3648	4290	659	28	623	490	-	10346
Asbestos production	7277	-	-	-	63014	2198	-	-	-	5759	8455	86703
Cement manufacture	834	-	2509	356	56423	1598	2008	1133	2814	791	-	68466
Asphalt production	985	1199	1913	2883	12281	6487	2573	3590	1250	4115	28	37304
Lime manufacture	-	-	-	1568	11164	9316	1624	-	1810	678	-	26160
Gypsum processing	230	-	152	276	3160	4390	546	330	988	2566	-	12638
Nepheline syenite processing	-	-	-	-	-	415	-	-	-	-	-	415
Fluorspar processing	80	-	-	-	-	-	-	-	-	-	-	80
Silica processing	15	-	13	-	465	619	366	64	73	13	-	1628
Stone processing	111	-	502	1034	12296	8654	458	-	140	824	-	24019
Sand and gravel processing	248	39	420	284	3858	3440	806	431	1226	1705	-	12457
Mining and rock quarrying	5581	-	3152	1539	66982	6468	599	4695	939	29688	3898	123541
Sulfate (kraft) pulping	338	-	3251	8830	19064	12523	850	3553	3043	46169	-	97621
Sulfite pulping	-	-	337	-	388	231	-	-	-	-	-	956

Table 3-6. (Cont'd)

Source Category	Newfoundland	Prince Edward Island	Nova Scotia	New Brunswick	Quebec	Ontario	Manitoba	Saskatchewan	Alberta	British Columbia	North West Territories and Yukon	Total
Sulfuric acid production	-	-	-	-	-	-	-	-	-	-	-	-
Nitric acid production	-	-	-	-	-	-	-	-	-	-	-	-
Potash processing	-	-	-	-	-	-	-	20207	-	-	-	20207
Phosphate rock processing	555	-	-	669	558	916	-	-	1222	226	-	4146
Phosphate fertilizer manufacture	-	-	-	265	252	729	202	-	2020	599	-	4067
Elemental phosphorus production	3534	-	-	-	5023	-	-	-	-	-	-	8557
Nitrate fertilizer manufacture	-	-	-	-	370	1461	362	-	1458	-	-	3651
Grain handling	-	-	372	222	8370	9962	4774	13155	8140	4247	-	49242
Grain milling	-	-	94	-	1528	2093	676	537	864	-	-	5792
Clay products manufacture	71	-	583	195	2991	7654	42	445	996	514	-	13491
Crude oil production	-	-	-	-	-	-	-	-	-	-	-	-
Petroleum refining	559*	-	1182	-	3812	3073	241	551	2078	1233	-	12729
Natural gas processing	-	-	-	-	-	-	-	-	-	-	-	-
Tar sands operations	-	-	-	-	-	-	-	-	14370	-	-	14370
Glass manufacture	-	-	-	28	310	833	-	-	36	71	-	1278
Concrete batching	5	5	8	7	106	176	11	31	61	45	-	455
Magnesium production	-	-	-	-	-	251	-	-	-	-	-	251
Phosphoric acid production	-	-	-	-	67	-	-	-	-	-	-	67
Carbon black	-	-	-	-	-	10	-	-	-	-	-	10
Salt production	-	-	1365	-	-	6786	59	611	650	-	-	9471
Subtotal	162695	1252	34584	19066	450251	217043	31402	52831	48150	162722	12382	1192378
2. Fuel Combustion/ Stationary Sources												
Utility power generation	498	463	20816	6781	282	7518	4534	37593	108244	197	234	187160
Residential fuel combustion	143	47	781	296	3164	2418	193	268	1464	510	9	9293
Industrial fuel combustion	1927	19	2142	4569	22476	17089	3161	1017	2399	4983	75	59857
Commercial fuel combustion	228	46	651	431	4894	2053	166	59	381	488	20	9417

Table 3-6. (Cont'd)

Source Category	Newfoundland	Prince Edward Island	Nova Scotia	New Brunswick	Quebec	Ontario	Manitoba	Saskatchewan	Alberta	British Columbia	North West Territories and Yukon	Total
Fuelwood combustion	972	384	1919	1791	16629	8314	1535	2047	1100	256	281	35228
Subtotal	3768	959	26309	13868	47445	37392	9589	40984	113588	6434	619	300955
3. Transportation												
Gasoline-powered motor vehicles	759	250	1463	1229	10255	15488	2372	3202	5144	5977	142	46281
Railroads	95	73	129	338	1284	2282	2228	395	471	1044	11	8350
Marine	207	4	82	45	200	172	2	-	-	335	1	1048
Aircraft	15	2	12	14	90	121	28	14	55	67	20	438
Off-road use of gasoline	23	12	52	45	100	616	181	590	596	152	7	2374
Diesel-powered engines	277	46	488	382	2713	3158	615	1215	1917	2020	313	13144
Tire wear	39	13	79	65	590	894	126	152	266	322	6	2552
Subtotal	1415	400	2305	2118	15232	22731	5552	5568	8449	9917	500	74187
4. Solid Waste Incineration												
Municipal	-	-	744	-	2681	2664	1687	124	-	65	-	7965
Industrial and commercial	21	6	43	33	332	517	56	42	94	137	3	1284
Sewage sludge	-	-	-	-	-	146	-	4	-	17	-	167
Wigwam burners	68	19	298	517	3854	1865	153	310	808	16860	7	24759
Subtotal	89	25	1085	550	6867	5192	1896	480	902	17079	10	34175
5. Miscellaneous												
Fertilizer application	11	118	73	128	866	2138	831	640	1298	152	-	6255
Pesticide manufacture and application	-	22	8	17	70	424	572	1091	745	27	-	2976
Gasoline and diesel handling	-	-	-	-	-	-	-	-	-	-	-	-
Dry cleaning	-	-	-	-	-	-	-	-	-	-	-	-
Application of surface coatings	-	-	-	-	-	-	-	-	-	-	-	-
Forest fires	63639	38	5680	1495	18446	176251	41494	29473	7276	18447	225007	587246
Structural fires	42	53	191	109	1497	2089	650	260	691	660	27	6269
Slash burning	1256	89	1852	4010	15576	9580	935	1539	3015	37263	67	75182
Cigarette smoking	105	22	155	127	1166	1546	191	173	344	462	12	4303
Subtotal	65053	342	7959	5886	37621	192028	44673	33176	13369	57011	225113	682231
Total	233020	2978	72242	41488	557416	474386	93112	133039	184458	253163	238624	2283925

* This figure includes the total from New Brunswick.

to note that the particle size and chemical composition data presented in these tables usually represent overall source categories; hence, not all of the different processes associated with one general source would have the same emission characteristics. In addition, the data presented in Table 3-4 refer to the south coast of California, U.S.A. and may not be typical of other locations in the United States or locations in Canada.

One of the factors having a significant effect upon particle size and chemical composition is the degree of emission control activity. Taback (1979), for example, reported that various emission control devices helped reduce the total particle mass loading in California's South Coast Air Basin by at least 95% over uncontrolled emissions. Discounting particles generated by mineral processing (i.e. rock crushing, sand and gravel operations, brick and ceramic manufacturing), 85% of the particle emissions from controlled sources had particle sizes < 10 μm.

With regard to fuel combustion, 77 to 97% of the particles (based on number) emitted from large oil-burning units of steam-powered thermal power generating stations are less than 2 μm in diameter (Environment Canada 1980). Coal-fired units also generate different amounts of particles. The percent by weight of particles < 10 μm in size, emitted from the following types of furnaces, was found to be: 10% for spreader/stoker-fired furnaces, 30% for pulverized fuel-fired furnaces and 76% for cyclone furnaces. In general, the efficiency of particle removal of most types of collection equipment varies inversely with particle size, so that the overall removal efficiency may be high on a particle mass basis but may be considerably lower on a particle number basis (Environment Canada 1980).

Emissions from oil-fired power plants often contain large amounts of carbon, as well as aluminum, calcium, iron, magnesium, nickel, sodium, silicon and vanadium found in the residual oil ash. Particle emissions from coal-fired power plants are composed primarily of silicates, aluminum oxides, sulfates and carbon, and may also include a large number of trace elements (e.g. vanadium, mercury, radioactive elements). Significant amounts of metals, such as magnesium, aluminum and manganese may also be present in particle emissions.

Another source of particle emissions is transportation. Particles from engine-related motor vehicle emissions are usually < 1 μm. Catalyst-equipped motor vehicles burning unleaded gasoline emit particles with mass median diameters (MMDs) of approximately 0.05 μm (Groblicki 1976) while vehicles burning leaded gasoline emit particles with MMDs of 0.25 μm (Moran et al. 1971). Diesel particle emissions have MMDs of 0.2 μm (Dolan and Kittleson 1979). Approximately 80% of the particles generated from tire wear are > 1 μm whereas 100% of the particles emitted from brake lining wear are < 1 μm (Taback 1979).

Engine-related particle emissions are composed primarily of lead halides, sulfates and carbonaceous material (Bradow et al. 1979). Diesel particles include traces of iron, copper, calcium and zinc along with carbon, lead, organic matter and sulfates (Lee and Duffield 1979). Particles from tire wear consist mainly of carbon while particles from brake lining wear are composed mainly of asbestos and carbon (Taback 1979).

In recent years, increasing emphasis has been placed on the characterization of particles emitted from indirect or fugitive sources; both industrial and nonindustrial. Industrial fugitive emissions may be divided into 1) dust emissions which result from wind erosion of storage piles and unpaved plant roads and from entrained dust due to vehicular traffic over paved roads and 2) process emissions which result from industry-related operations such as material handling, loading, unloading and transfer operations. Conventional sources that are not properly controlled and equipment that is not properly maintained may also contribute to fugitive emissions. For any given industry there are probably a large number of fugitive emission sources, although in terms of total particle emissions, only a few of these sources would be of significance.

Drehmel et al. (1979) examined mining and smelting operations in the United States and found that direct and indirect emissions contributed 35 and 65% respectively, to the total mass of particles emitted. Process fugitive emissions from the two primary sources, coke ovens and electric arc furnaces, contained particles that were primarily < 15 μm, a significant portion of which was < 5 μm. Open source fugitive emissions were generally characterized by particles > 15 μm with the exception of emissions from vehicular traffic over paved roads. Sources of preoperational fugitive emissions near a coal cleaning plant, at the site of an Appalachian generating station in the United States, were found to be coal storage and waste coal piles; approximately 44% of the particles collected were < 1 μm (Ambrose et al. 1977). The generally dirty surfaces of the plant grounds together with vehicular traffic around the plant were also significant sources of particles. A literature review of fugitive emissions from coal-fired power plants was conducted by Currier and Neal (1979). Emission factors were gathered for a number of processes and it was speculated that vehicular traffic accounted for 40% of the total fugitive emissions associated with coal storage. The authors also rated the emission factors as to their validity (i.e. whether the emission factor was based on reliable supporting data) and found that the work of Cowherd et al. (1974) and Cowherd and Hendricks (1977; 1978) had the highest validity for the greatest number of sources examined. Details of the Cowherd et al. (1974) and Cowherd and Hendricks (1977; 1978) methodology, and those parameters which significantly affect fugitive emission rates, are detailed in Appendix II.

Fugitive emissions were investigated in Allegheny County, Pennsylvania by Kirshner et al. (1979), who concluded that 67 to 76% of the measured total suspended particulate matter from a plant site was due to emission from roads and storage areas. For a given monitoring station, 42% of the total suspended particulate matter was due to emissions from nearby roads. Depending upon local meteorological conditions, 41-99% of the mass of the collected particulate matter was < 15 μm in size.

Emissions of particles from nonindustrial fugitive sources can, in certain circumstances, have a significant effect upon overall size distribution and chemical composition of atmospheric aerosols. Although little information is available, emissions from the sources are dependent upon such factors as material properties (e.g. moisture content), mechanism of generation (e.g. vehicular traffic) and meteorological conditions (e.g. wind speed, precipitation). Taback (1979) found that dust from unpaved roads, agricultural tilling, road building and construction was composed mainly of silicon, phosphorus, aluminum, iron, calcium and potassium. The majority of the particle mass resided in particles > 1 μm.

Emissions from agricultural and slash burning, composed of primarily fine particles (< 2 μm), were characterized by an enhanced concentration of potassium relative to soil-derived elements (Lyons et al. 1979).

3.3.2.2 Estimated Emissions

Fluxes of primary particles to the atmosphere from direct man-made sources have been estimated for both Canada and the United States. Although some differences exist in the designation of source categories, it is useful to compare estimated emissions on a North American scale.

Emissions of particles from man-made sources in Canada total 2,283 x 10^6 kg.a^{-1}, based on 1976 data (Table 3-6) (Environment Canada 1981b). This total consists of: industrial processes - 1,192 x 10^6 kg. a^{-1}; fuel combustion (stationary sources) - 301 x 10^6 kg.a^{-1}; transportation - 74 x 10^6 kg.a^{-1}; solid waste incineration - 34 x 10^6 kg.a^{-1} and miscellaneous sources - 682 x 10^6 kg.a^{-1}. Based on preliminary data for 1978, industrial processes in Canada account for 1,439 x 10^6 kg.a^{-1} of a total of 2,434 x 10^6 kg.a^{-1} from all recorded sources (Environment Canada 1982). The major difference between the 1976 and 1978 emission inventories is that only in the development of the 1978 estimates have fugitive emissions from industrial sources been considered. For those industrial sectors where fugitive emissions have been estimated, approximately 27% of the total emissions were fugitive.

Under the industrial process category, iron ore mining and beneficiation together with mining and rock quarrying were the two single largest emitters of particles in Canada, contributing 28 and 10%, respectively to the nationwide industrial process emission total for

1976. Preliminary estimates for 1978 indicate that the same two sources contribute 19 and 13% respectively to the nationwide total. It should be noted that of the 38 industrial source categories listed by Environment Canada, 21 emit at least 50% of their total particle mass loading as particles < 2.5 μm diameter.

Using 1978 data, industrial emissions of particles in the United States totalled 6,190 x 10^6 kg.a^{-1} (Table 3-7); source categories identified as metals and mineral products contributed 25 and 54% respectively, of this total (U.S. EPA 1980a).

Utility power generation contributed 62% (187 x 10^6 kg.a^{-1}) of the Canadian nationwide fuel combustion (stationary sources) particle emissions for 1976 (Table 3-6). Residential, industrial and commercial fuel combustion accounted for 26% while fuelwood combustion accounted for 12% of this total. Based on preliminary 1978 data, fuel combustion sources accounted for particle mass emissions of 275 x 10^6 kg.a^{-1}, of which utility power generation contributed approximately 57% (Environment Canada 1982). Fugitive emissions accounted for approximately 6% of the total emissions from utility power generation. In comparison, United States emissions for fuel combustion (stationary sources) totalled 3,770 x 10^6 kg.a^{-1} in 1978 (Table 3-8), with utility power generation accounting for 66% and residential, industrial and commercial combustion accounting for 34%.

Gasoline-powered automobiles contributed 62% of the total Canadian nationwide emissions of transportation-derived particles while diesel-powered engines contributed 18% (Table 3-6). Tire wear accounted for 3% while other forms of transportation accounted for 17% of the national totals. In comparison, engine-related particle emissions in the United States were estimated to be 1.3 x 10^9 kg.a^{-1} (U.S. EPA 1980b) of which approximately 75% were related to highway vehicles.

Total Canadian emissions of particles from solid waste incinerators (34 x 10^6 kg.a^{-1}) in 1976 consisted of emissions from wigwam burners (used to dispose of sawdust) (72%) and from municipal, industrial and commercial and sewage sludge incineration (28%). Solid waste incineration in the United States generated 500 x 10^6 kg.a^{-1} (U.S. EPA 1980a).

Particle emissions from forest fires in Canada in 1976 were classified under man-made sources and estimated at 587 x 10^6 kg.a^{-1}. Under Environment Canada's miscellaneous source category (Table 3-6) forest fires and slash burning were the two primary sources of particles in a nationwide basis for 1976, accounting for 86 and 11% respectively, of the miscellaneous total.

Although the estimated emissions of particles from direct sources, as discussed above, are based on a relatively extensive data base, very little information is available for indirect or fugitive

Table 3-7. Estimated United States emissions of primary particles from industrial processes, 1978 (U.S. EPA 1980a).

Source Category	Emissions (10^6 kg.a^{-1})
1. Metals	
Iron and steel	830
Primary smelting	480
Iron foundries	140
Other	120
Total	1570
2. Mineral Products	
Cement	780
Asphalt	150
Lime	150
Crushed rock	1340
Other	910
Total	3330
3. Petroleum	
Refining	70
Natural Gas production	-
Total	70
4. Chemicals	
Sulfuric acid	-
Other	190
Total	190
5. Other	
Grain processing	730
Pulp and Paper	240
Other	60
Total	1030
Total	6190

Table 3-8. Estimated United States emissions of primary particles from fuel combustion (stationary sources), 1978 (U.S. EPA 1980a).

Source Category	Emissions (10^6 kg.a^{-1})
1. Utility	
Coal	2350
Oil	140
Gas	10
Total	2500
2. Residential	
Coal	20
Oil	20
Gas	30
Total	70
3. Industrial	
Coal	700
Oil	90
Gas	40
Other (wood, bark waste)	280
Total	1110
4. Commercial/Institutional	
Coal	20
Oil	60
Gas	10
Total	90
Total	3770

sources. Uncontrolled industrial fugitive particle emissions for the United States are estimated to total 3,370 x 10^6 $kg.a^{-1}$ (Table 3-9) (U.S. EPA 1981). Mineral products, food and agricultural (grain elevators) and primary metals account for the majority (99%) of these emissions.

Preliminary emission estimates have been made in the 1978 inventory for several sectors considered as nonindustrial fugitive sources. These sources include: unpaved and paved roads, agricultural tilling, agricultural wind erosion, construction sites and mine tailings. Total emissions from these sources are approximately 40 x 10^9 $kg.a^{-1}$, of which construction activity and unpaved .oads contribute 44 and 40% of the total, respectively. Due to the magnitude of their emissions, these sources have been excluded from the nationwide totals so as not to dwarf the other emission estimates (Environment Canada 1982). Of the two United States studies available on nonindustrial fugitive sources (Cooper et al. 1979 and U.S. EPA 1980b) total emissions vary substantially from a high of 369 x 10^9 $kg.a^{-1}$ to a low of 112 x 10^9 $kg.a^{-1}$ for the United States. The major disparity between the two estimates arises from estimated emissions derived for unpaved roads: estimated emissions are 290 x 10^9 $kg.a^{-1}$ and 35 x 10^9 $kg.a^{-1}$ from the reports of Cooper et al. (1979) and U.S. EPA (1980b) respectively.

Table 3-9. Estimated emissions of primary particles from uncontrolled industrial fugitive sources, 1978 (U.S. EPA 1981).

Source Category	Emissions (10^6 kg.a^{-1})	Particle Size	Major Components
1. Mineral Products			
Crushed rock extraction, surface coal mining	730	10-50% < 10 μm; 1-2 < 1 μm	same as parent material
Portland cement	700	10-15% < 10 μm	limestone, clay, shale, gypsum, iron-bearing and siliceous materials
Asphalt concrete	100	50-70% < 4 μm	sand, crushed stone, limestone, hydrated lime
Lime manufacture	50	45-70% < 5 μm	limestone, lime
Concrete batching	30	10-20% < 5 μm	cement dust
Total	1610		
2. Food and Agriculture			
Grain elevators	1250	1% < 10 μm	grain dust
3. Primary Metals			
Coke, iron, steel	250	coke 15-26% < 2 μm iron 1-10% < 5 μm steel 50% < 5 μm	polycyclic organic matter, coal dust, coke dust, iron oxide dust, graphite, metal fume (iron oxide)
Foundries	125	50% < 15 μm	metal oxide fume (silicon and iron) carbonaceous fume
Aluminum	60	50-90% < 10 μm	fluorides, alumina, carbon dust, condensed hydrocarbons, tars
Copper	40	10-50% < 5 μm	copper, iron, silicon, silicon oxide, metal fume (oxides of As, Pb, Zn, Cu, Cd)
Lead	15	10-90% < 5 μm	metal fume (oxides of Pb, Cd, Zn, Sb)
Total	490		
4. Secondary Metals	10	80-100% < 5 μm	metal oxides (Al, Cu, Pd, Sn, Zn), oxides of other metals, $AlCl_3$, NH_4Cl, NaCl, $ZnCl_2$, fluorides, carbonaceous matter
5. Wood Products	10	40-90% < 10 μm	sawdust
Total	3370		

4.0 EFFECTS ON OPTICAL PROPERTIES OF THE ATMOSPHERE

4.1 INTRODUCTION

Aerosols have a unique property among all atmospheric pollutants in that they can be sensed with the naked eye. This characteristic, which results in reduced visibility as atmospheric aerosol loading increases, can be regarded along with the climatic effects caused by subsequent radiative energy reductions as the primary optical effect of atmospheric aerosols. The effect of aerosols on climatic conditions will be considered in Chapter 6 while this chapter will concern itself with reductions in visibility due to aerosols and with the scientific criteria useful in the assessment of environmental quality as influenced by such optical changes.

The study of the optical effects of aerosols hinges on an understanding of the nature of light scattering by particles. Several texts are devoted to this subject (Deirmendjian 1969; Kerker 1969; Van de Hulst 1957). The following section describes briefly some of the considerations in light scattering and a later section draws upon this development to relate atmospheric parameters such as meteorological visibility, turbidity, etc. to more fundamental light scattering quantities. Appendix III provides an explanation of the Mie Theory of light scattering.

4.2 SCATTERING OF LIGHT BY AEROSOLS

There are basically five factors determining the amount of light scattered by a single particle: 1) the wavelength of light, λ; 2) the radius of the particle, a; 3) the shape of the particle; 4) its real and imaginary indices of refraction, n_R and n_I; and 5) the angles through which the light is scattered. The Mie Theory (1908) completely solves the problem of scattering by spherical particles. More recent research has tried to extend the theory (with varying degrees of success) to nonspherical particles (Zerull 1976; Mugnai and Wiscombe 1980). For small particle sizes, where the particle radius $a < \lambda/2\pi$, Rayleigh or molecular light scattering predominates and a relatively simple analytical solution for scattered intensity is possible.

Some predominant features are noted in the Mie theory results. Light is most effectively scattered by particles whose radius is approximately equal to λ. For visible wavelengths (i.e. between 400 and 700 nanometers) submicron particles (< 1 μm) in the fine or accumulation mode of the particle size distribution scatter light more effectively than larger particles. Figure 4-1 shows the scattering efficiency, Q_{sca}, as a function of particle radius for a single nonabsorbing particle ($n_R = 1.33$; $\lambda = 500$ nm). The actual amount of light scattered is proportional to the scattering cross section (see Appendix III) which

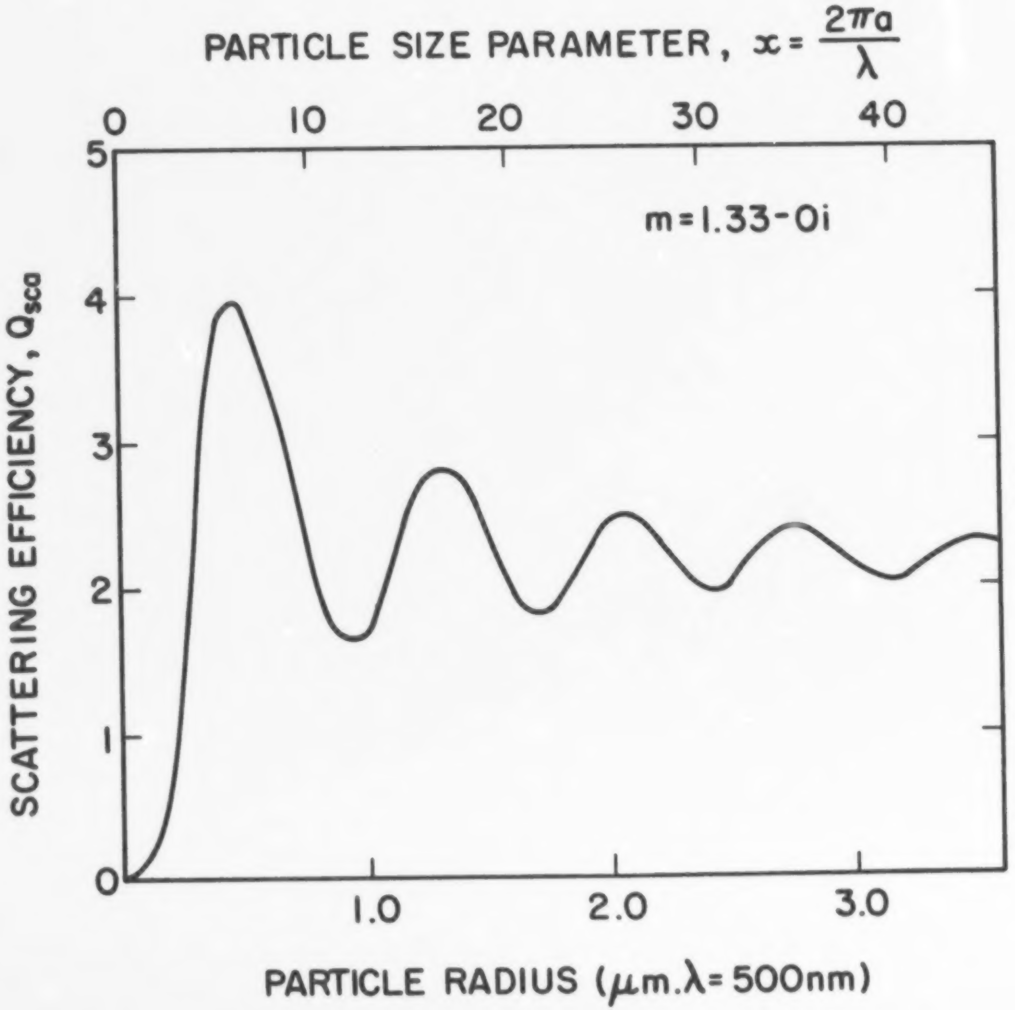

Figure 4-1. Scattering efficiency as a function of particle size for a single nonabsorbing particle (m is the real part of the complex index of refraction).

is the product of Q_{sca} and the particle cross-sectional area. This means that on a single particle basis, larger particles scatter more light but not as efficiently as smaller particles. When the particles have a nonzero imaginary index of refraction they absorb light and the total amount of energy removed from an incident light beam is greater than for scattering alone. Such increased attenuation of the light wave is termed extinction and is the sum of scattering and absorption.

For an aerosol (i.e. a dispersion of many particles of differing sizes in air), one must extend the Mie theory to integrate over the number of particles in each increment of particle size. Such approaches are not difficult given the size distribution of the aerosol. However many physical measurements of aerosols involve the mass distribution as a function of particle size; hence, some assumption is necessary about the mean particle density to infer the number distribution. It is apparent from Figure 4-1 that for particle size parameter $x = \frac{2\pi a}{\lambda}$ larger than about 10, the efficiency of light scattering oscillates about a value of 2. This means that for large particles the scattering cross section of a particle is roughly twice its area. The aerosol extinction efficiency is then the integral over the size parameter, x, of the product of the number of particles at a given x and the single particle scattering efficiency (see Appendix III). This integral is denoted by the volume extinction coefficient, b_{ext}. Similarly, the volume scattering coefficient is termed b_{scat} and the volume absorption coefficient, b_{abs}.

Observed mass distributions of aerosols have shown multimodal structure with a peak in the submicron accumulation mode and a second or series of peaks in the coarse particle modes (for further details see Chapter 2). Since the number distribution is related to the mass distribution by the cube of the radius of the particles and scattering is related only to the square of the radius for large particles, the net result of scattering from multimodal mass distributions of particles is that the submicron accumulation mode strongly dominates visible light scattering. This is shown in Figure 4-2 where the volume scattering coefficient per unit volume of particles is plotted against the particle size. The unit volume of particles is the total fraction of space occupied by the particles per unit volume of space (i.e. concentration by volume). If the particles are of uniform specific gravity, this is equal to the mass concentration divided by the specific gravity.

Humidity plays an important role in this process since most particles are hygroscopic to some degree and form nuclei for condensation of water droplets at high relative humidity. Tuomi (1975) has developed relationships for the growth of particle size as a function of relative humidity and has shown that when the relative humidity rises from 40% to 80% the particle size will increase 40%. In addition, the imaginary index of refraction (of a particle having a real index of refraction of 1.6) will decrease from 1.57 to 1.44 because of the absorbed water. This combination of factors can result in a near

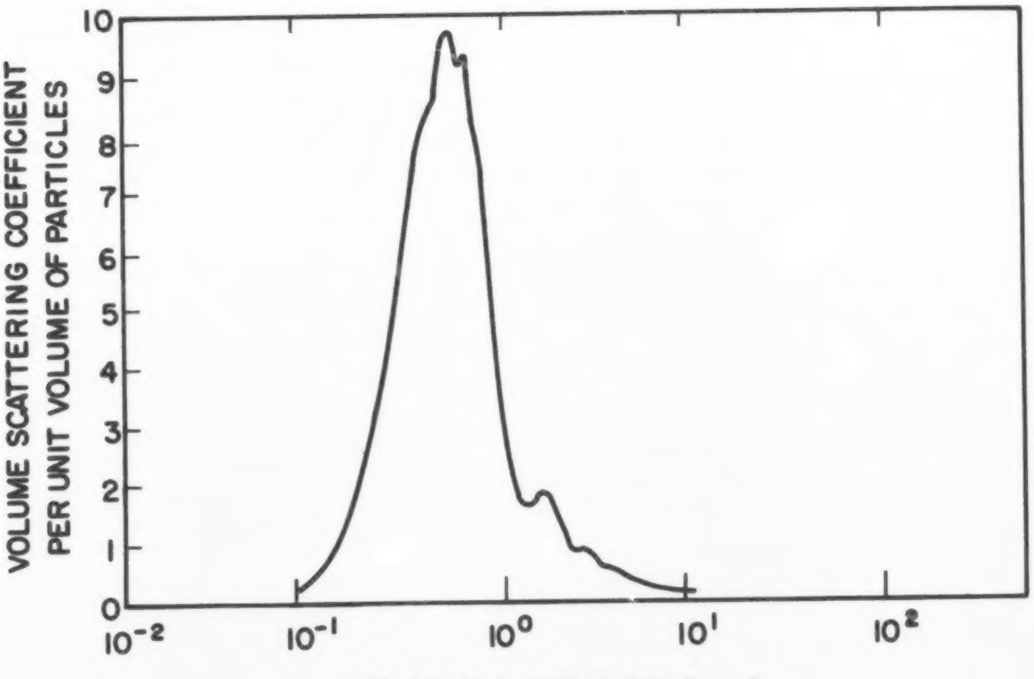

Figure 4-2. Volume scattering coefficient per unit volume of particles $\eta = 1.55-0.02\,i$; $\lambda = 0.55$ μm (from Waggoner and Weiss 1980).

doubling of the extinction coefficient due to a power law size distribution (where $N(r) \alpha r^{-3.5}$) (Figure 4-3).

The influence of absorption within the particles is demonstrated in Figure 4-4 where the fraction of extinction contributed by absorption as a function of particle size parameter is seen to rise as the imaginary index of refraction increases. It is now believed (Hansen et al. 1979; Weiss et al. 1979; Rosen et al. 1980) that the largest contributor to aerosol absorption in urban areas is carbon soot (which for comparison to Figure 4-4 has an imaginary index of refraction ~ 2.0). Perhaps as much as 50 percent of aerosol extinction in cities may be due to absorption.

In such discussions, it is generally assumed that the imaginary index of refraction is constant over the wavelength range of the light scattered. This may not be true if the aerosol has a strong spectral absorption band. Water vapor, for example, has several strong absorption features in the near infrared. Nitrogen dioxide can cause brown coloration of the sky by absorbing light in the 400-500 nm region of the spectrum. Brown plumes often seemingly appear from nowhere at distances two to ten kilometers from coal-fired electrical generating facilities when the emitted nitrous oxide plume is oxidized to NO_2 by ozone in the troposphere (Melo 1977). In general, however, sky coloration, horizon brightening, optical effects such as haloes around the sun and moon, sun pillars, sun dogs, etc. are due to the scattering of light by particles and gases within the atmosphere rather than by absorptive effects.

4.3 MEASURES OF VISIBILITY AND ATMOSPHERIC TURBIDITY

In the introduction, it was stated that reduced visibility is one of the primary perceived effects of atmospheric aerosols. In many cases such a reduction is either an indicator of poor air quality or an aesthetic nuisance. Visibility is, however, a reliable measure of atmospheric particle mass loading under certain constrained conditions. In addition, the prevention of significant deterioration of visibility has been included in U.S. law (U.S. Congress 1977). For marine and air navigation, restriction of visibility itself may constitute a safety hazard.

A heterogeneous aerosol mass with loading, M ($\mu g.m^{-3}$), will give rise to a volume scattering coefficient, $b_{scat}(m^{-1})$, which is the sum of scattering by aerosols in the air plus the background molecular light scattering by air itself. If the aerosol is nonabsorbing, the volume extinction coefficient of the aerosol mass equals the volume scattering coefficient. The meteorological criteria for visibility, or determination of the visual range of an observer at ground level, has been defined as the Meteorological Optical Range (MOR) and is "the length of the path in the atmosphere required to reduce the luminous

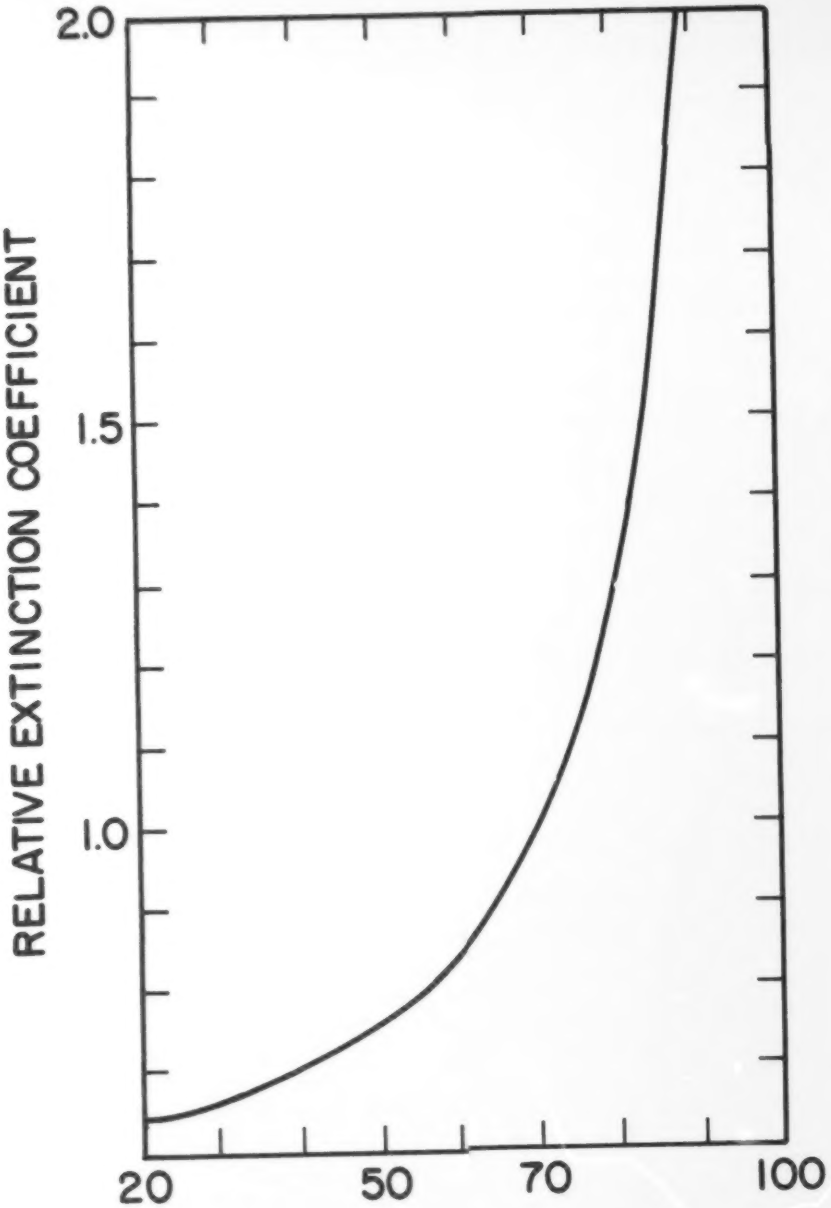

Figure 4-3. Computed relative extinction coefficient as a function of relative humidity at a power law exponent of $\nu = 3.5$ (from Tuomi 1975).

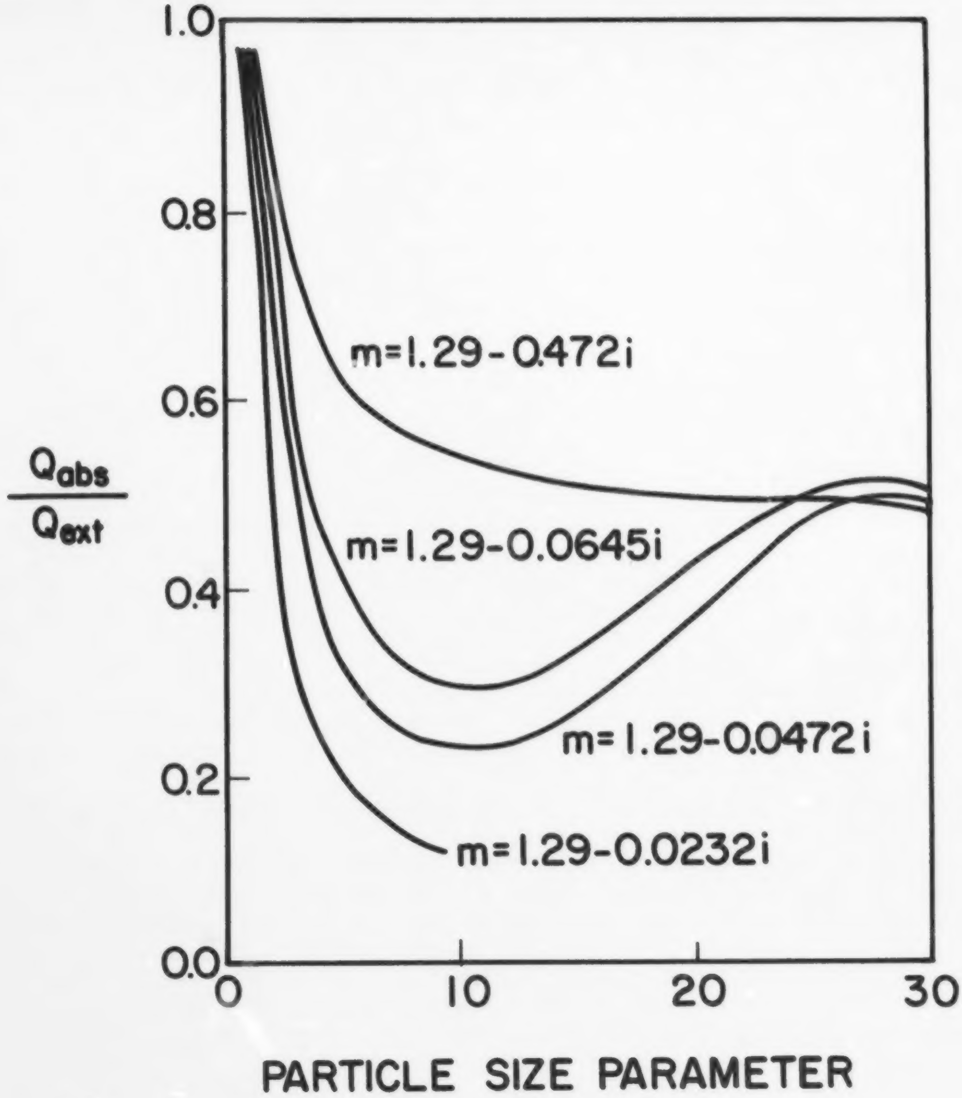

Figure 4-4. Fraction of extinction efficiency contributed by absorption as a function of particle size parameter (after Kerker 1969).

flux in a collimated beam from an incandescent lamp at a color temperature of 2700°K to 0.05 of its original value" (WMO 1971).

This definition avoids the problem of subjectivity of human observers (e.g. differences in day or night human observations of visibility). With such a definition it is possible to determine that the MOR is related to the volume extinction coefficient of an aerosol mass by:

$$\text{MOR} = \frac{3.0}{b_{ext}} \qquad (4\text{-}1)$$

This criteria is slightly different from that developed by Koschmieder (1924) who used 0.02 as the contrast threshold for human observers at 550 nm wavelength and obtained the commonly quoted result (see Appendix III).

$$V = \frac{3.91}{b_{ext}} \qquad (4\text{-}2)$$

where V is visibility.

The difference between equations (4-1) and (4-2) is important if visibility is to be used as a measure of air quality. Numerous studies of urban and regionally polluted air masses show that a strong correlation exists between aerosol mass loadings, M, and the scattering coefficient of the aerosol (Charlson _et al_. 1967; Samuels _et al_. 1973; Waggoner _et al_. 1976). Charlson _et al_. (1969) suggest the relationship

$$M/b_{scat} = 0.38 \text{ g.m}^{-2} \qquad (4\text{-}3)$$

when b_{scat} is measured with an integrating nephelometer in urban areas (see Appendix III). In a more recent study using a dichotomous sampler/integrating nephelometer combination, Waggoner and Weiss (1980) showed that for over 200 samples from pristine, residential, industrial and rural areas in the western United States, the ratio of dry particle mass in the fine particle fraction of diameter < 3 µm to b_{scat} is 0.32 g.m^{-2} with a correlation coefficient of greater than 0.95. The relatively high correlation of b_{scat} to M suggests the use of the above equations as a means of relating observed visibility to atmospheric particle loading:

$$M = \frac{1.25 \times 10^3}{V} \; (\mu\text{g.m}^{-3}) \qquad (4\text{-}4)$$

(it is assumed that the aerosol is nonabsorbing, that the 0.02 contrast threshold is used and that the relative humidity is $< 70\%$). It should be noted that the subjective concerns which are obvious in the visual determination of meteorological visibility are compounded by the uncertainties in the above M/b_{scat} ratio and thus could not be recommended as anything other than a rough indicator of atmospheric particle mass loadings. Use of filter media and gravimetric analysis are still standard measurement techniques for atmospheric particle mass loadings and for measurements of air quality.

Meteorological Optical Range, which is obtained on a horizontal path, is only one measure of light transmission in aerosol laden air. The depletion of direct solar radiation by an air mass is measurable using sunphotometers (see Appendix III) and the World Meteorological Organization has standardized turbidity measurements by specifying the use of Eppley Sunphotometers (Flowers et al. 1969). The decadic turbidity coefficient, B, is related to b_{ext} by (Schuepp 1949):

$$B = (\log_e 10)^{-1} \lambda^{-\alpha} b_{ext} \qquad (4\text{-}5)$$

where λ is in micrometres and α is the Angstrom exponent (Angstrom 1929) of the turbidity coefficient (see Appendix III). Worldwide turbidity measurements provide information on the geographical distribution of aerosols.

4.4 AEROSOL GEOGRAPHICAL DISTRIBUTION AND TRENDS IN HAZINESS

Evidence has mounted in recent years to show that decreased visibility associated with increased aerosol loadings has become an intercontinental problem. Work on the effects of reduced visibility, correlations between visibility and aerosol content and chemical characterization and dispersion of urban aerosol masses, has given rise to a significant body of data regarding urban and local scale haze climatologies (Patterson and Wagman 1977; Stevens et al. 1978; Ensor et al. 1972). Such studies have shown that coarse particle sizes may be extremely important on the local scale and that multimodal size distributions are commonly observed (Whitby et al. 1976). Such multimodal size distributions are primarily responsible for making the relationship between aerosol mass concentration and light scattering (or visibility reduction) site-specific and nonuniform.

Urban visibility degradation has been a problem which has plagued industrialized areas for centuries. Of more current concern is the apparently widespread dispersion of anthropogenic aerosols on a worldwide basis and the concurrent visibility reduction in pristine areas. Evidence of extensive ($> 10^5$ km^2) hazy air masses over land and sea have been observed from satellites on visible imagery (Lyons and Pease 1973). Such concern has prompted the United States to use visibility protection in pristine areas, such as national parks, as a criteria for the prevention of significant deterioration (PSD) of the environment. The Clean Air Act Amendments of 1977 (U.S. Congress 1977) provide for a Class I status to be placed on areas in the U.S. where any deterioration of air quality from present values is deemed significant. There are no similar visibility-related particle standards for Canada.

While prevailing visibility can be used to study regional changes in haziness and atmospheric particle loading, a somewhat cruder haze index is all that has been used to analyze such trends in Canada

(Munn 1973; Inhaber 1976; Vickers and Munn 1977). The haze index measures the frequency of occurrence of haze as: the cumulative total of hours during prevailing visibilities in the range 1 to 10 miles, which is recorded over an arbitrarily chosen period of constant duration from regular observations made at about 250 meteorological stations of the Atmospheric Environment Service. Three indices were computed that included: 1) all classes of visibilities in the 1 to 10 mile range; 2) classes with no precipitation, and 3) those occurring only at relative humidities less than 70%. In light of the demonstrated sensitivity of b_{scat} to relative humidity (Figure 4-3) it is clear that the latter form of the haze index will be more sensitive to changes in the loading in the fine particle fraction of the mass concentration.

The haze index has been used to delineate a crude seasonal haze climatology for Canada. The values computed, which are strongly influenced by factors such as urban/rural location, local topography, and meteorological factors including occurrences of fog or precipitation, range from in excess of 1000 (hours per 6 months) near polluted cities such as Windsor to 10-100 in rural districts in the Provinces of eastern Canada to almost zero in the Prairies and Northern Canada. Of the three classes of index evaluated, the following discussion will be restricted to classes of visibility with relative humidity less than 70% (i.e. class 3).

Vickers and Munn (1977) analyzed Canadian haze index date for two seven-year periods from 1953-60 and 1967-74 during summer and winter. Maps of the occurrence of haze for the 1967-74 summer and winter periods are shown in Figures 4-5a and 4-5b, respectively. The values draw a pattern which reflects high pollutant levels in the populous eastern area of Canada and in Alberta and around Vancouver, British Columbia. For most of the nation the index is clearly too insensitive to properly study the occurrence of haze.

Temporal results over this period (Munn 1973; Inhaber 1976) show that the haze index has increased consistently since 1953 for most areas in Canada except southern Ontario. Inhaber's results were normalized by major city population to show that the haze index did not increase as fast as the population.

Husar *et al.* (1979) has presented a similar study using five-year average extinction coefficients in the U.S. These results (Figure 4-6) show dramatically increasing haziness for spring, summer and fall months (Quarters 2, 3 and 4) throughout the eastern U.S. and a moderate increase during winter months (Quarter 1). The increase in the mean and limits of the eastern U.S. summer average extinction coefficients are plotted in Figure 4-7.

A similar study has been conducted using visibilities from Canadian meteorological observing stations. A conclusion drawn by the Atmospheric Environment Service is that, for the range of visibilities

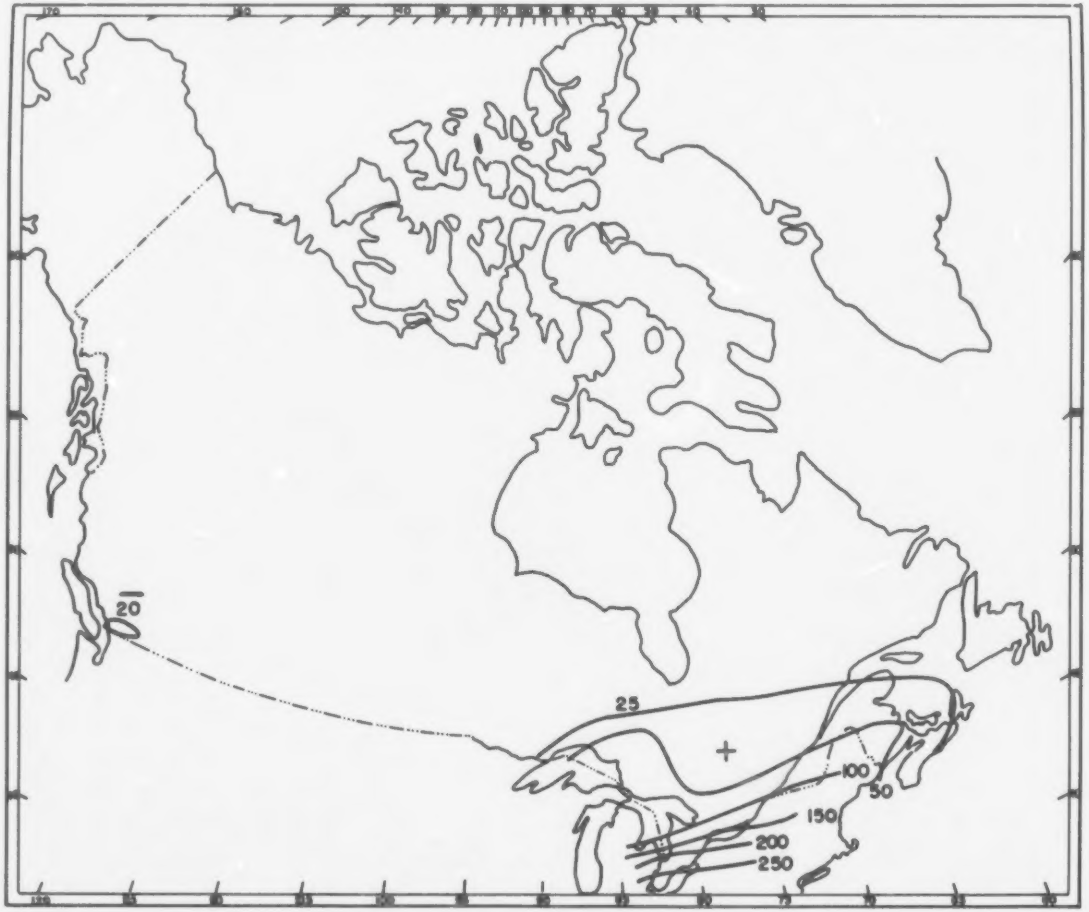
25
+
100
50
150
200
250
-
20

Figure 4-5a. Canadian haze index for the summer months, 1967-1974. "+" denotes areas which show increasing haze over the 20-year period and "-" indicates those with decreasing haze.

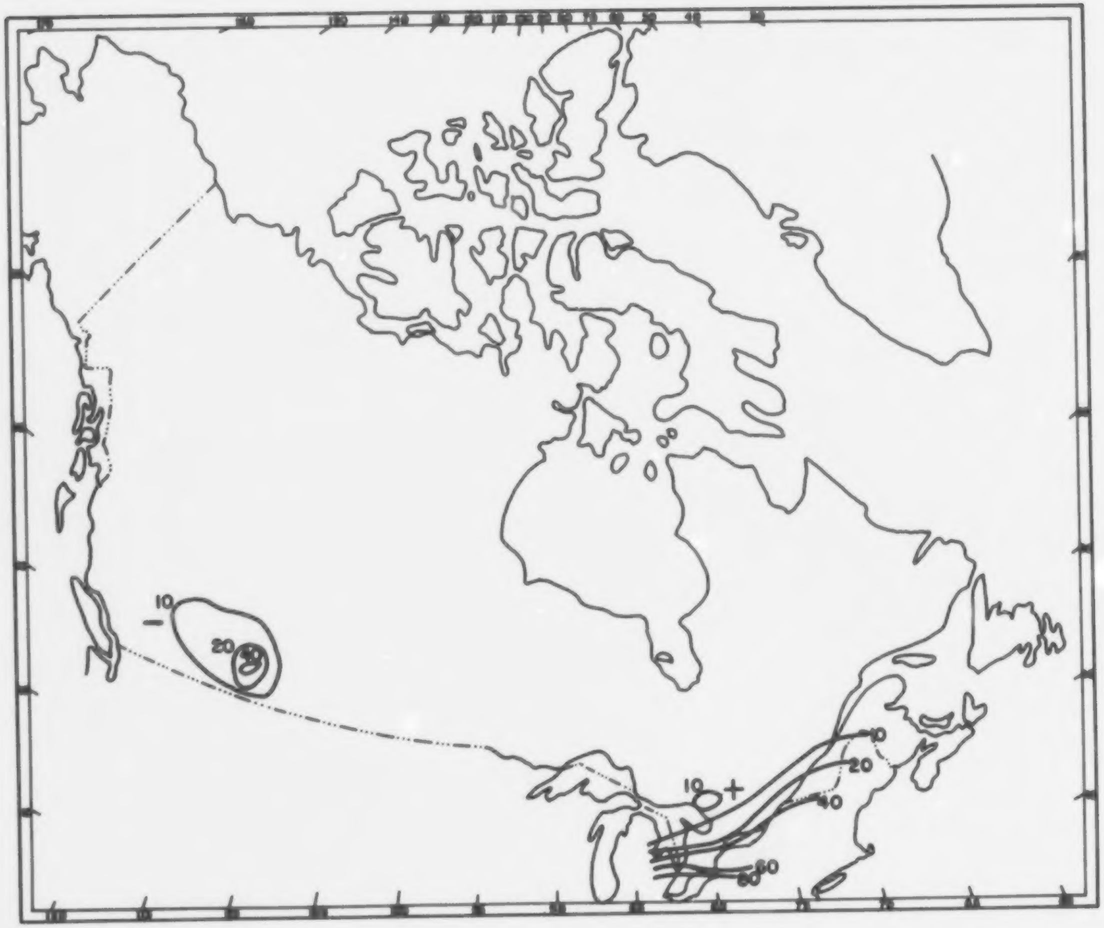
10
–
20
30
10
+
10
20
40
60
80

Figure 4-5b. Canadian haze index for the winter months, 1967-1974. "+" denotes areas which show increasing haze over the 20-year period and "-" indicates those with decreasing haze.

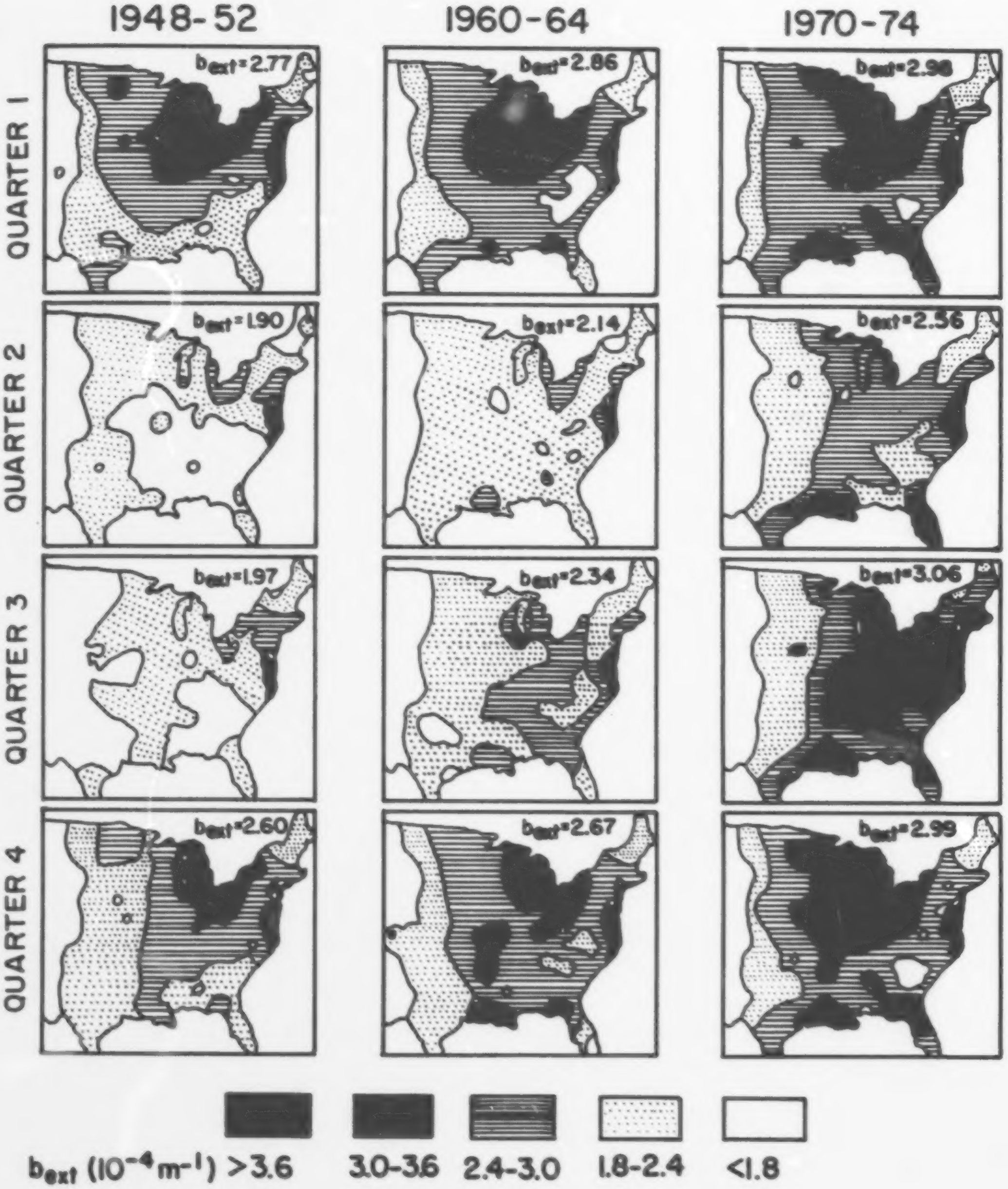
1948-52
1960-64
1970-74
QUARTER 1
QUARTER 2
QUARTER 3
QUARTER 4
b_{ext}=2.77
b_{ext}=2.86
b_{ext}=2.98
b_{ext}=1.90
b_{ext}=2.14
b_{ext}=2.56
b_{ext}=1.97
b_{ext}=2.34
b_{ext}=3.06
b_{ext}=2.60
b_{ext}=2.67
b_{ext}=2.99
b_{ext} (10^{-4} m^{-1}) >3.6 3.0-3.6 2.4-3.0 1.8-2.4 <1.8
vis(km) <10.6 10.6-12.9 12.9-16.1 16.1-21.4 >21.4

Figure 4-6. Spatial distribution of 5-year average extinction coefficients for the eastern United States (from Husar et al. 1979).

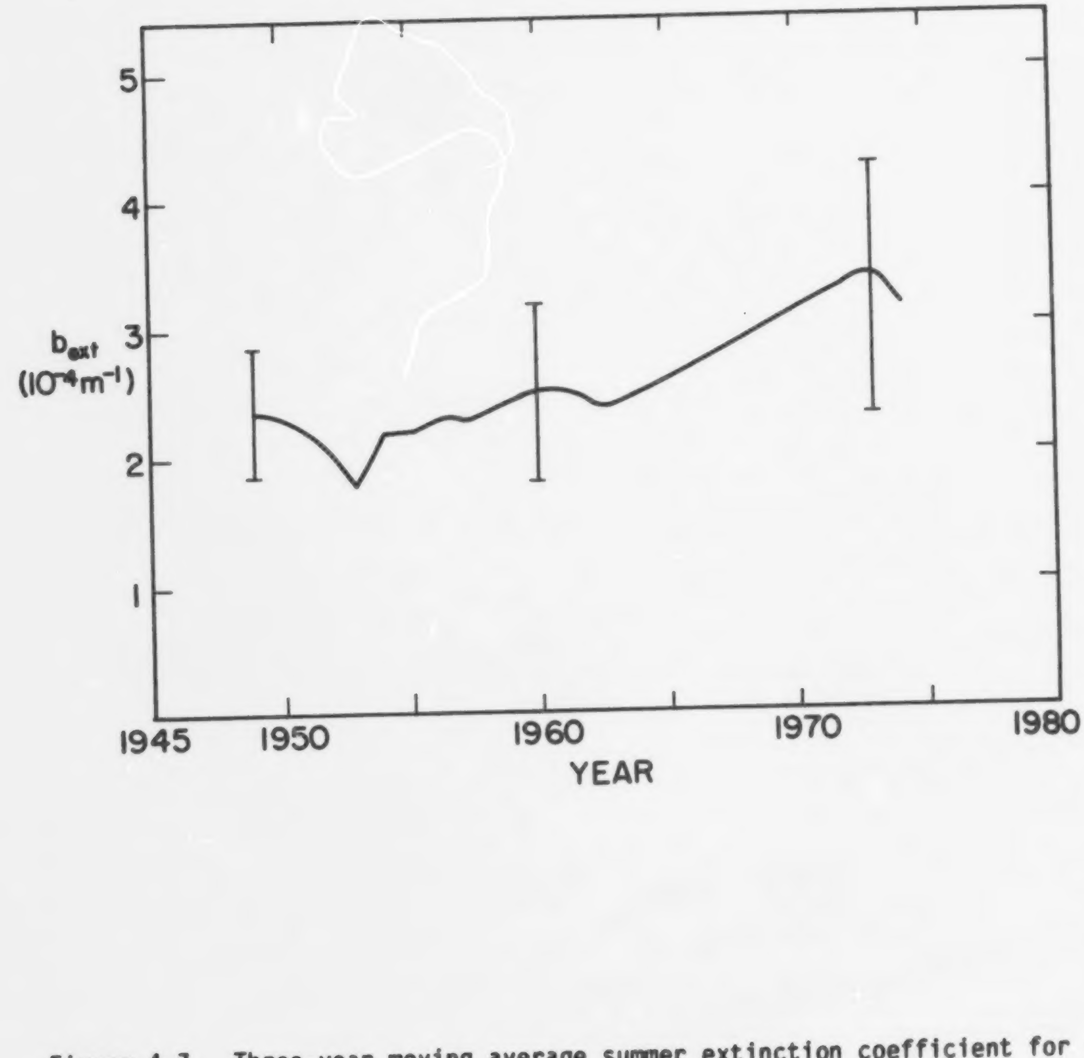

Figure 4-7. Three-year moving average summer extinction coefficient for the eastern United States (from Husar et al. 1979).

in Canada, the variability in the calculated extinction coefficients (as in Husar *et al.* 1979) is large enough to preclude drawing realistic contours of b_{ext} for Canada. The data from the U.S. study should be viewed with the caveat that the quality of the U.S. data is subject to a similar degree of variability as that of the Canadian data.

As part of its contribution to the World Meteorological Organization Background Air Pollution Monitoring Network (BAPMoN) (WMO 1978a), the Atmospheric Environment Service, Environment Canada, instituted routine measurements of the atmospheric turbidity coefficient, B, at selected locations in Canada (Table 4-1 and Figure 4-8).

The observations were made using the Eppley Sunphotometer, as described by Flowers *et al.* (1969). The data were corrected for altitude variations in the Rayleigh scattering factor and for ozone absorption at the nominal wavelength of 500 nm. The mean monthly values over the period 1974-1979 for selected stations are shown in Figure 4-9. All the stations exhibited a winter minimum in turbidity and a spring-to-summer maximum. The secondary peak in the Puntzi Mountain - Kelowna data set is questionable because of the smaller amount of data available. The ratio between minimum and maximum turbidities lay in the range of 2 - 4 and agreed with that found by Flowers *et al.* (1969) for the U.S. The western sites showed generally lower turbidities than those for eastern Canada and reflected similarly as the haze index, the different anthropogenic contributions to the aerosol loading throughout Canada. The winter minimum is felt to reflect the lessening of local and regional scale aerosol sources during months when there is snowcover and a dominance of air masses of northerly origin.

The national average value for the wavelength exponent (α) of 1.31 is very close to Angstrom's (1929) value of 1.3. A decadic turbidity coefficient of 0.08 at 500 nm is reasonably representative of a national average value. Ozone levels during the same period are out of phase with the turbidity results and probably do not interfere with the turbidity values reported.

Figure 4-10 shows the trend in annual turbidity for five stations during the years 1975-1979. The percentage difference from the five-year station mean is plotted for five stations. There is considerable scatter in the results which makes interpretation of an increase in turbidity in Canada tenuous. Long-term increases in turbidity at widely separated sites such as Washington, D.C.; Davos, Switzerland; and Jerusalem, Israel (Joseph and Manes 1971) indicate such temporal increases in turbidity in Canada might be expected.

Observations of widespread transport of aerosols, such as presented above, have given rise to the initiation of international programs designed to study sources and routes of aerosol transport to remote background locations. The United States operates Geophysical Monitoring for Climatic Change (GMCC) stations at Mauna Loa (Hawaii),

Table 4-1. Turbidity parameters observed at Canadian BAPMoN sites.

STATION	RECORD	B (500 nm) 1975	1976	1977	1978	1979	AVERAGE
Puntzi Mtn.[α]	May 75/Jan 77	0.051	0.040	0.044	0.059	0.070	0.053
Kelowna, B.C.	May 77/Dec 79						
Edson, Alta.	Apr 75/Dec 79	0.063	0.052	0.047	0.063	0.055	0.056
Wynyard, Sask.	Jan 75/Dec 79	0.090	0.086	0.089	0.096	0.105	0.093
Armstrong, Ont.[α]	Jan 75/Jan 77	0.094	0.099	0.104	0.114	0.091	0.100
Pickle Lake, Ontario	Feb 77/Nov 79						
Mount Forest, Ontario	Apr 75/Aug 79	0.071	0.080	0.089	0.087	0.107	0.087
Maniwaki, Que.	May 75/Dec 79	0.085	0.073	-	0.072	0.077	0.077
Sable Is., N.S.	May 75/Aug 79	0.099	0.109	-	0.094	0.086	0.097

[α] Stations were moved to a second site on the dates indicated.

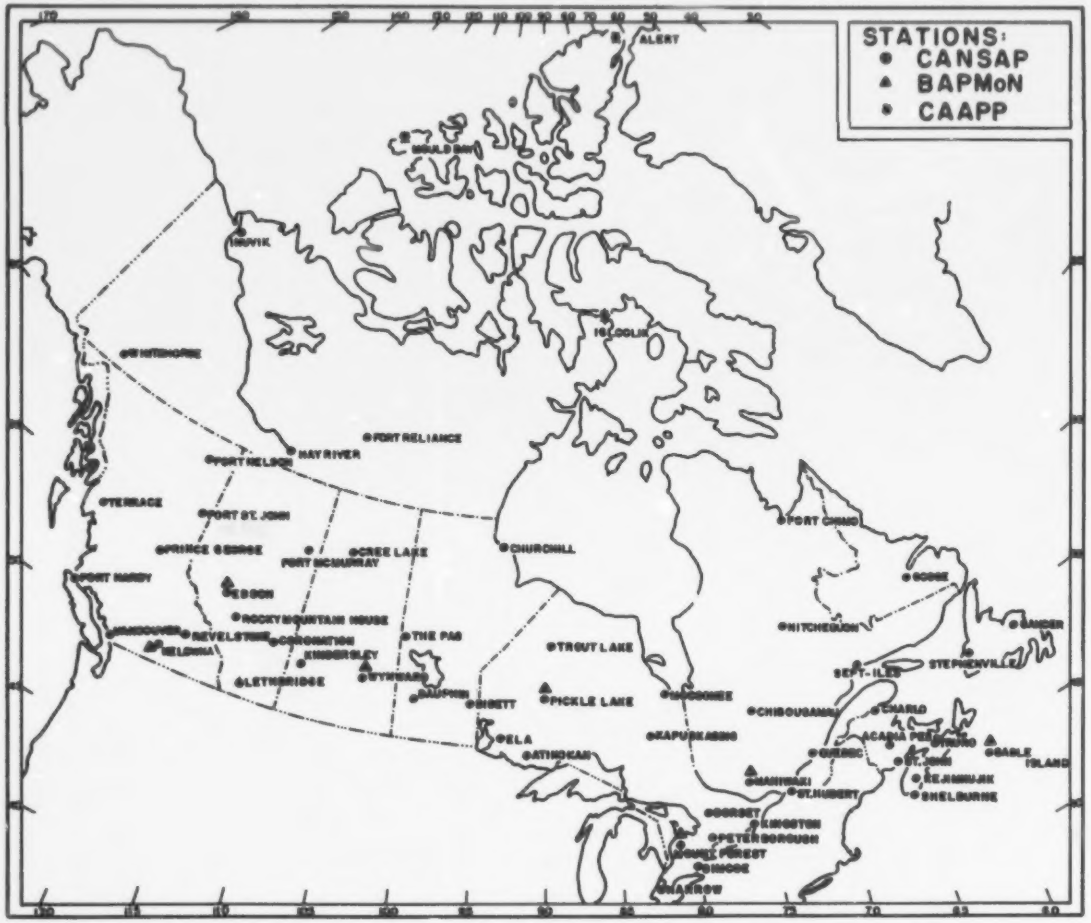
STATIONS:
● CANSAP
▲ BAPMoN
• CAAPP
ALERT
IGLOOLIK
INUVIK
WHITEHORSE
FORT RELIANCE
HAY RIVER
FORT NELSON
TERRACE
FORT ST. JOHN
PRINCE GEORGE
FORT MCMURRAY
CREE LAKE
CHURCHILL
PORT HARDY
EDSON
ROCKY MOUNTAIN HOUSE
VANCOUVER
REVELSTOKE
CORONATION
KELOWNA
KINDERSLEY
WYNYARD
THE PAS
LETHBRIDGE
DAUPHIN
BISSETT
ELA
ATIKOKAN
TROUT LAKE
PICKLE LAKE
MOOSONEE
KAPUSKASING
FORT CHIMO
GOOSE
SCHEFFERVILLE
GANDER
STEPHENVILLE
SEPT-ILES
CHIBOUGAMAU
CHARLO
ACADIA PEAT
QUEBEC
SABLE ISLAND
ST. JOHN
KEJIMKUJIK
SHELBURNE
MANIWAKI
ST. HUBERT
DORSET
KINGSTON
PETERBOROUGH
MOUNT FOREST
SIMCOE
HARROW
170
140
130
120
110
100
90
80
70
60
50
40
30
20
65
75
85
95
105
115
125

Figure 4-8. Geographic distribution of CANSAP, BAPMoN and CAAPP stations in Canada, 1981.

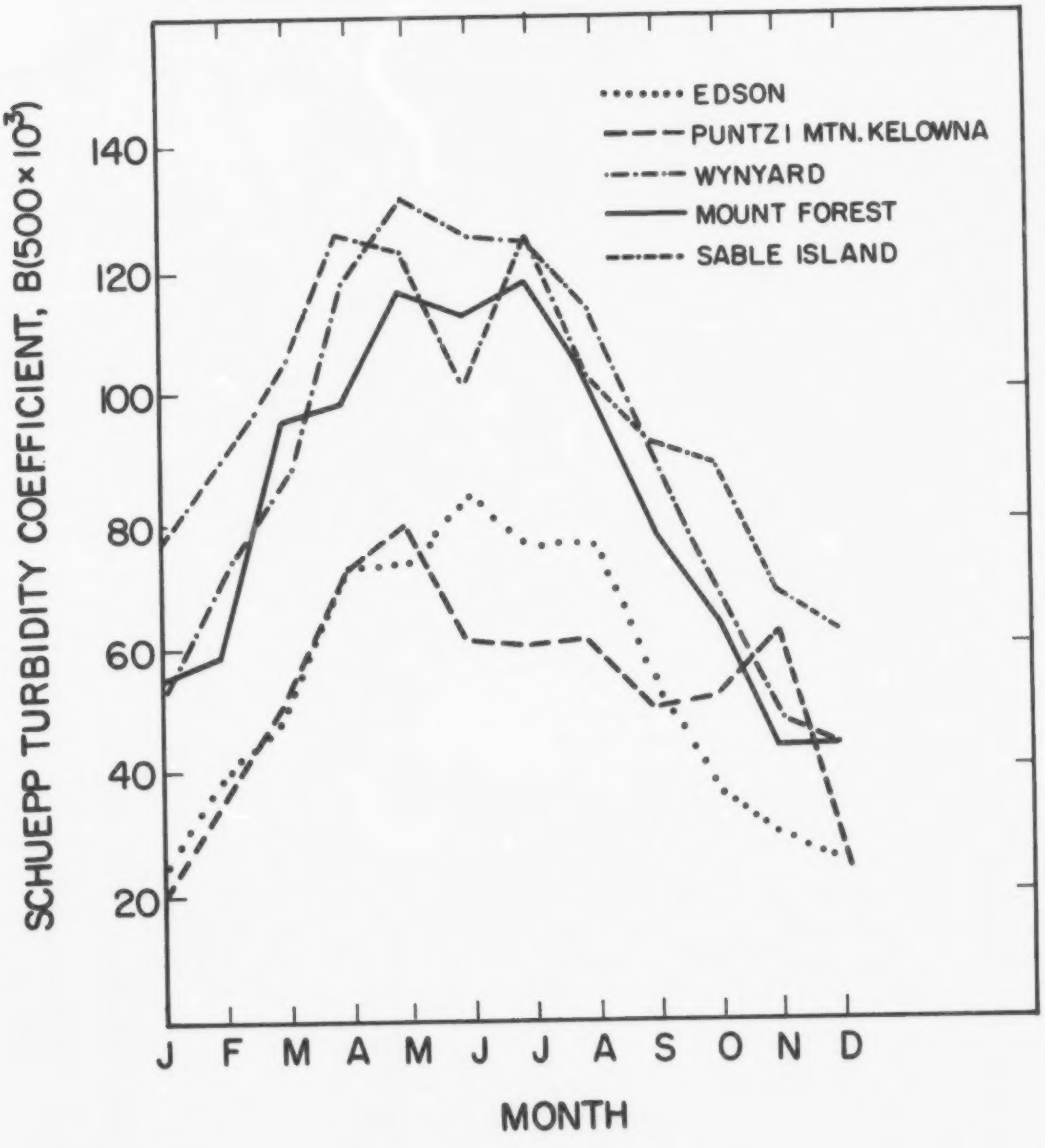

Figure 4-9. Mean monthly atmospheric turbidity coefficients over the period 1974-1979 for selected Canadian locations.

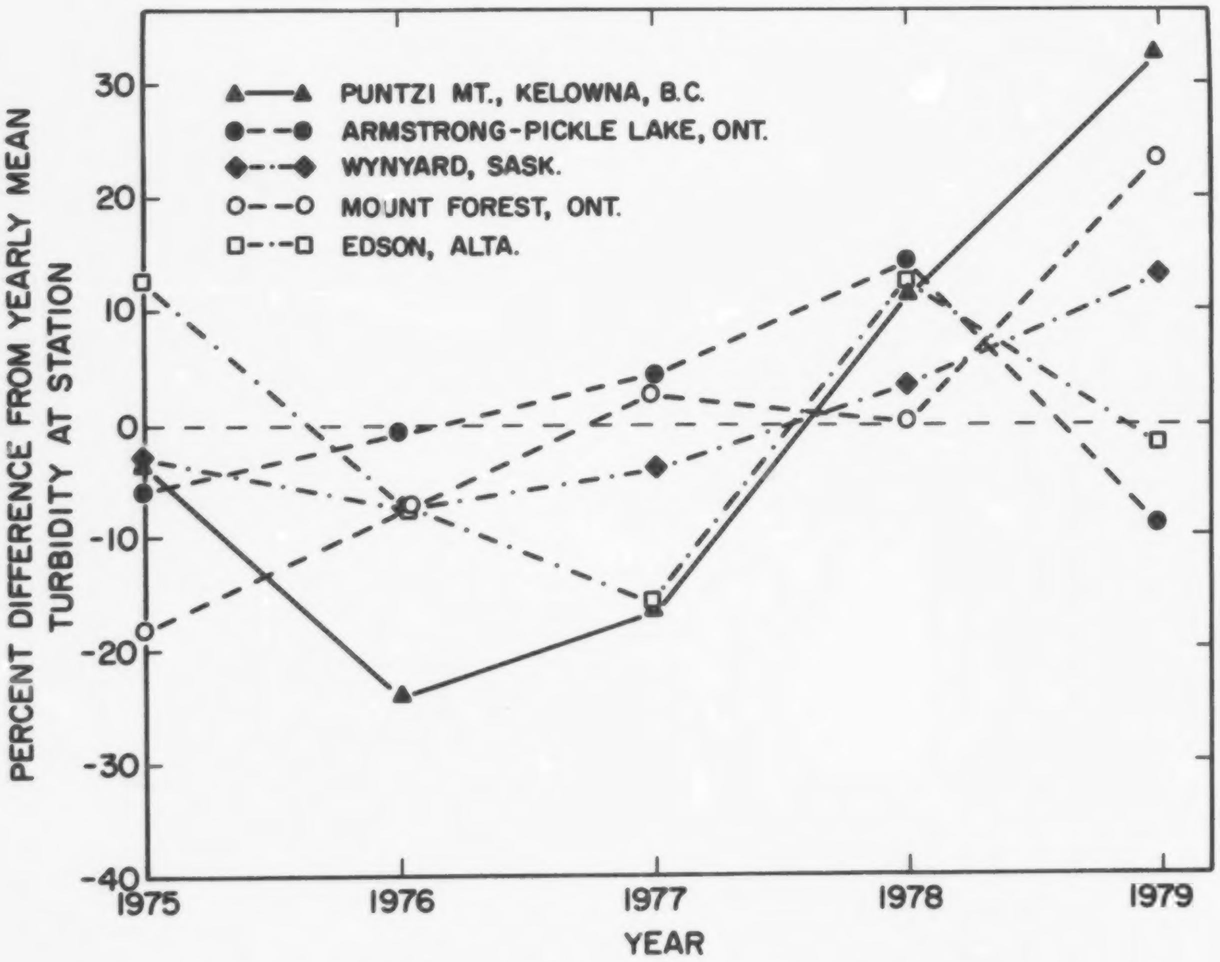

Figure 4-10. Trend in annual turbidity for five Canadian stations during the years 1975-1979.

American Samoa, the South Pole, and Barrow (Alaska). The latter station forms part of the International Arctic Pollution Network. Nephelometer data from the Canadian stations in that network at Mould Bay and Igloolik, N.W.T. (see Figure 4-8) are shown in Figure 4-11 (Barrie et al. 1981). An annual peak in light scattering from February through April is apparent and reflects what has been termed arctic haze (Rahn and McCaffrey 1979). This enhancement of spring haziness over the summer clear period is eightfold. A number of studies in industrialized areas have shown a high correlation between sulfate-bearing aerosols, which are largely man-made, and the light scattering coefficient of the aerosol (Waggoner et al. 1976; Anlauf et al. 1980). Figure 4-12 shows the correlation between b_{scat} seen by an integrating nephelometer and surface high-volume sampler measurements of excess sulfate (i.e. with the oceanic component removed) taken by the Canadian Arctic Air Pollution Program (CAAPP) (Barrie et al. 1981). It is clear that anthropogenic sulfates are affecting the Canadian arctic and it is estimated that such sulfates are about 30% of the aerosol burden in the arctic with the remainder thought to be carbonaceous material (soot) and windblown dust.

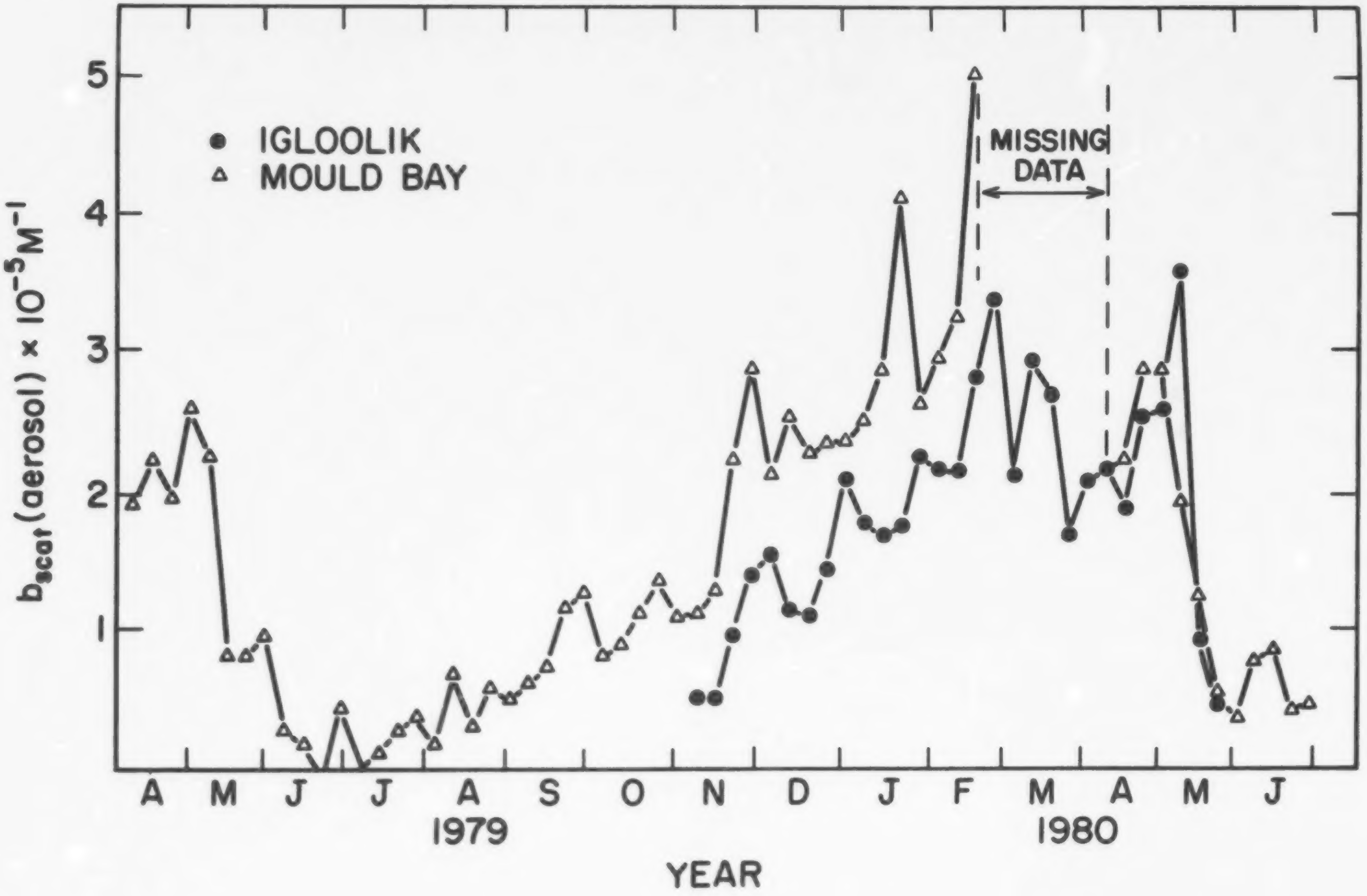

Figure 4-11. Nephelometer data from the Canadian Arctic Air Pollution Program (from Barrie et al. 1981).

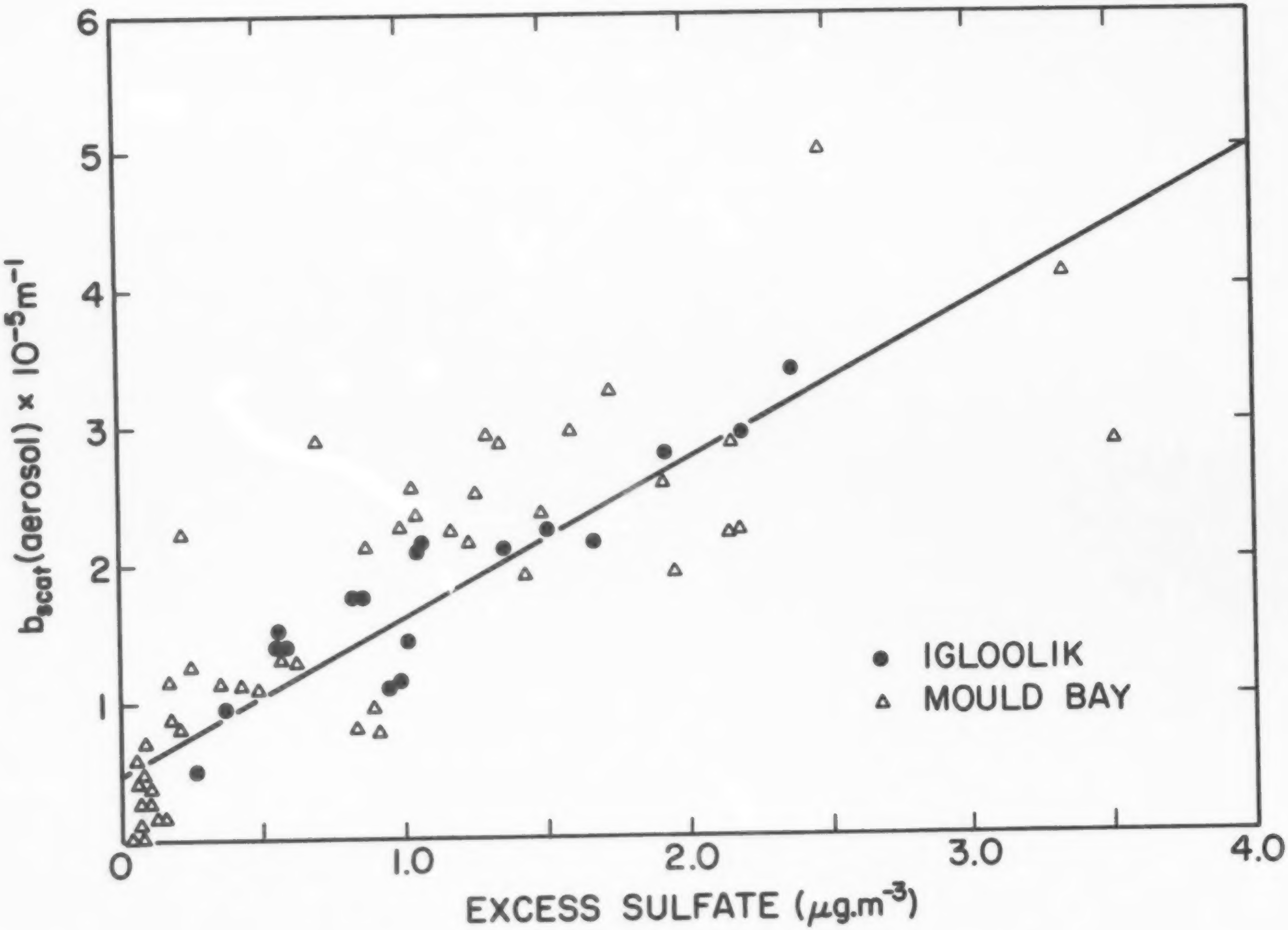

Figure 4-12. Aerosol light scattering in relation to excess sulfate levels for two stations in the Canadian Arctic.

5.0 EFFECTS ON CLOUDS, FOG, PRECIPITATION AND ATMOSPHERIC ELECTRICITY

5.1 INTRODUCTION

The effects of atmospheric particles extend beyond those effects, previously discussed, on the optical properties of the atmosphere. In addition, the formation of atmospheric clouds and fogs are influenced by atmospheric particles. Precipitation quantity and chemical composition are affected both temporally and spatially. Atmospheric particles also play an important role in the modification of atmospheric electricity.

5.2 EFFECTS ON CLOUDS, FOG AND PRECIPITATION

Virtually all atmospheric cloud and fog particles are formed by heterogeneous nucleation which is stimulated by cloud condensation nuclei (CCN) and ice nuclei (IN) (see Appendix IV.2.1). Without CCN, cloud droplets would form only if relative humidity with respect to water was greater than 200%. Similarly, any atmospheric ice nucleated at temperatures warmer than -40°C requires the presence of IN. The sensitivity of cloud and fog formation to small man-made changes in aerosol composition or concentration is not yet fully understood. Some of the known and theoretically postulated effects of aerosols on clouds and fogs are given below along with methods of measuring the particles involved.

5.2.1 PERTINENT PARTICLE MEASUREMENTS

5.2.1.1 Cloud Condensation Nuclei (CCN)

The concentration of CCN in an air parcel is a function of the ambient saturation with respect to water. Figure 5-1 illustrates a typical example of this relationship for continental and maritime air masses. Under normal circumstances, the CCN concentration is approximately 100-500 cm^{-3} at a relative humidity of 101%, with the particles being typically <1 μm in diameter (Fletcher 1962).

The most common CCN technique (Fletcher 1962) uses a thermal diffusion chamber with upper and lower wetted plates held at a constant temperature difference. The temperature and vapor pressure gradients within the chamber are accurately controlled and within the measurement section a known relative humidity can be maintained. The nuclei are thus activated and the droplets grow to optically detectable sizes within this chamber. The particles can be counted visually using a microscope, with photographic techniques, or with electronic detection

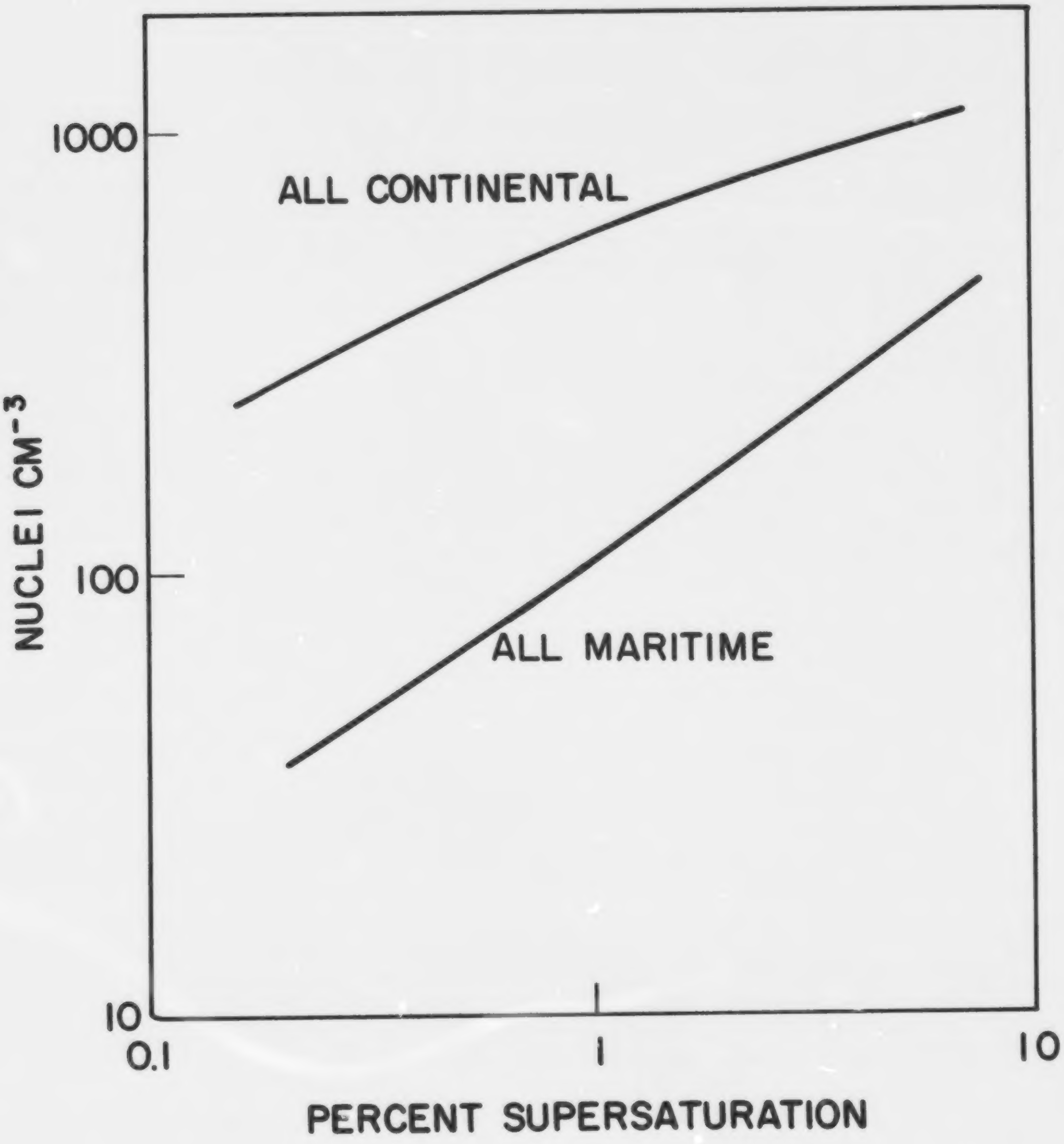

Figure 5-1. Median concentration of cloud condensation nuclei (CCN) as a function of supersaturation over water for observations over land and the oceans (from Twomey and Wojciechowski 1969).

of a beam of light scattered from droplets in the measurement section. One problem with such a counter has always been the inability to sense small concentrations of CCN (< 10 cm^{-3}) at low supersaturations ($< 0.2\%$) (Alofs 1978). Such CCN can be very important in the formation of hazes, light fogs or precipitation particles.

5.2.1.2 Ice Nuclei (IN)

Ice nuclei can be activated in four different modes: 1) by deposition or sublimation of vapor onto ice, 2) by condensation-freezing whereby a thin layer of water condensing on the nucleus is frozen, 3) by contact with the surface of a droplet and, 4) by interactions while immersed inside a water droplet. The physical process and/or the probability of activation is different for each of these four modes. Consequently, it has been very difficult to measure the concentration of natural ice nuclei. Refrigerated cloud chambers in which the IN are activated, and aerosol impaction onto filters with later filter processing at a controlled temperature and supersaturation, are two commonly used measurement techniques. However, there is no standard method (e.g. Mason 1971) and comparisons between different instruments have not yielded consistent results (Grant 1971; Vali 1976).

It is generally accepted that there exists one nucleus per litre effective at -20°C, with the concentration increasing by a factor of 10 for each 3 to 5°C drop in temperature (Fletcher 1962). Huffman (1973) has suggested that, instead of temperature, supersaturation with respect to ice is the critical parameter. IN concentrations around the world are generally similar (Bigg and Stevenson 1970) although local sources such as cities may affect these concentrations. Because ice nuclei form only a small fraction of the total aerosol ($1:10^7$), it is very difficult to determine their chemical composition (Mason 1971). The nuclei are non-hygroscopic although they may be attached to hygroscopic particles. Depending on their mode and temperature of activation, the nuclei may be formed only by a few molecules and may be as large as several μm (Fletcher 1962).

5.2.2 THEORETICALLY PREDICTED EFFECTS

5.2.2.1 Warm Rain Processes

Clouds form as air rises, cools, and water condenses out around the available CCN. The stability of the atmosphere and large scale meteorological processes determine whether the clouds thus formed are stratiform or cumuliform in character. Generally deeper clouds such as nimbostratus, cumulonimbus, or embedded convective cells in stratiform clouds, will produce precipitation.

Precipitation can be formed through either a warm rain or a cold rain process (Figure 5-2). In the warm rain process, no ice is required and the droplets formed around the CCN grow by condensation at a rate primarily controlled by the supersaturation with respect to water. These drops then begin to coalesce until they reach a size whereby they can fall through the sustaining updraft and reach cloud base as precipitation. The warm rain process involving condensation and coalescence takes a considerable time to form drizzle-size drops (15-30 min) (Leighton and Rogers 1974). Most rain in the tropical areas probably is produced by this process in the available deep and long lasting clouds. Theoretical calculations show that droplet growth is quicker if the available liquid water is distributed over fewer CCN condensation sites such as in a maritime air mass (Figure 5-1), or if the initial droplet size spectrum is broadened by a few CCN which react sooner at a lower supersaturation (Mason 1971).

5.2.2.2 Cold Rain Processes

The cold rain, or Bergeron-Findeisen, process can form precipitation sized particles much more quickly than the warm rain process. Basically, ice crystals activated from IN in supercooled clouds grow by deposition faster than similarly sized water droplets because of the higher supersaturation with respect to ice than with respect to water. The ice particles then begin to fall and accrete the surrounding droplets. At high ice particle concentrations, ice crystal aggregation is also an important process. The ice particles can either grow as snowflakes, graupel or hail if the cloud updrafts; liquid water contents and crystal concentrations are suitable for such an ice formation mechanism. If the air below cloud base is above 0°C, the snowflakes will melt and fall as rain, but some graupel and hail might be large enough to reach ground level in solid form.

Under certain conditions, not clearly understood, one IN can produce many ice particles through an ice multiplication process (Mossop 1976). It is generally thought that one ice crystal per litre is suffient to begin an effective cold rain process. However, because of the many unknowns in the ice nucleation process, the numerous growth rates of ice crystal habits (e.g. needles, dendrites, etc.), and the ice multiplication, crystal drop accretion, and crystal aggregation processes, numerical models cannot accurately predict the concentration of IN required for the most efficient rain-forming process.

Table 5-1 summarizes measurements made in Canadian summer cumuli near Yellowknife and Thunder Bay and shows that both warm and cold rain processes can occur in Canada (Schemenauer and Isaac 1980). Typical cloud droplet and ice particle concentrations near the summit of these clouds were $500.cm^{-3}$ and $< 0.1.L^{-1}$, respectively. Cloud top temperatures had to be as cold as -14°C before there was a 50% probability of detecting ice particles in concentrations $> 0.1.L^{-1}$. Table 5-1

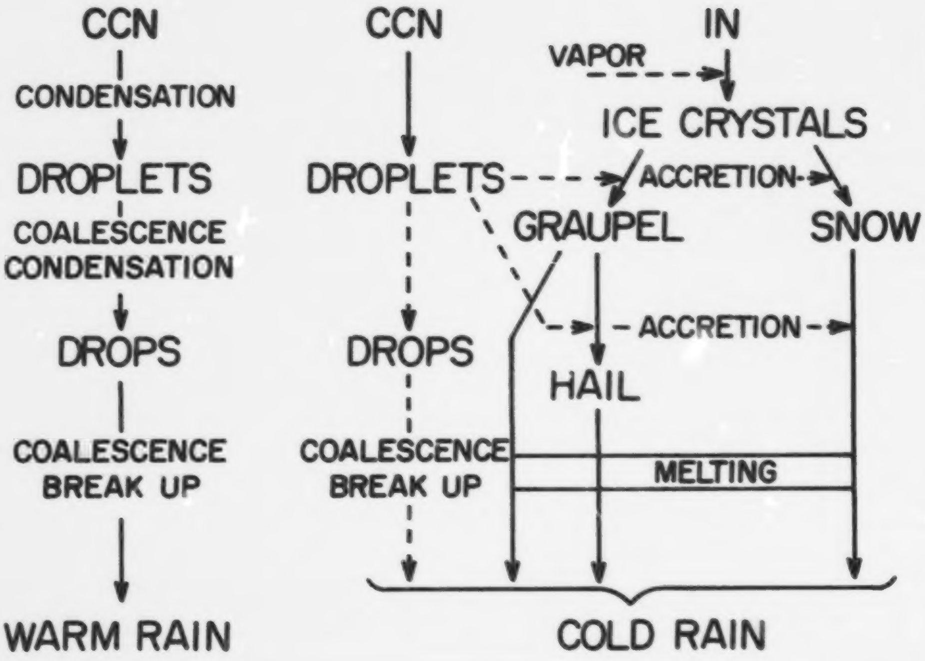
CCN
CONDENSATION
DROPLETS
COALESCENCE
CONDENSATION
DROPS
COALESCENCE
BREAK UP
WARM RAIN
CCN
IN
VAPOR
ICE CRYSTALS
DROPLETS
ACCRETION
GRAUPEL
SNOW
ACCRETION
DROPS
HAIL
COALESCENCE
BREAK UP
MELTING
COLD RAIN

Figure 5-2. Schematic diagram showing the evolution of warm and cold rain, starting from cloud condensation nuclei (CCN) and ice nuclei (IN) (from List 1979).

Table 5-1. The appearance of rain in 87 summer cumulus clouds in 1976, 1977 and 1978 taken from observations made near Yellowknife, N.W.T. and Thunder Bay, Ontario[α].

	Ice	Water
Rain	10	7
No rain	10	60

[α] The columns indicate whether the clouds contained some ice or were all water. For Yellowknife cumuli the median cloud top and base heights were generally at 4400 m (-9°C) and 2300 m (+3°C) respectively. For the Thunder Bay clouds the median cloud top and base heights were approximately 5000 m (-9°C) and 1800 m (+12°C) respectively. (after Schemenauer and Isaac, 1980).

suggests that the cold rain process is more efficient in summer cumuli since 50% of the clouds containing ice precipitated, versus 10% of the all water clouds. However, little is known about other cloud types. Interactions between the warm and cold rain processes may be important but further research needs to be performed on this topic.

5.2.2.3 Warm, Supercooled and Ice Fogs

Even at low relative humidities (< 70%), condensation will begin on active CCN. As the relative humidity increases to 90%, the initial haze droplets can grow to become fog droplets with a resulting decrease in visibility (Petterssen 1958). At temperatures warmer than 0°C, a warm fog forms; at temperatures colder than 0°C, if few ice nuclei are present, a supercooled fog can develop. Thick "London type" fogs or smogs can be generated at relative humidities much less than 100% if there is a high concentration of hygroscopic particles which serve as efficient CCN.

The visibility in the fog will depend upon the concentration and size of the resulting droplets. For example, a clean maritime air mass with few CCN can generate a fog with a low concentration of large drops and greater visibility than a city fog with a high concentration of small drops.

Ice fogs can form at cold temperatures (< -20°C), when there are sufficient quantities of ice nuclei and water vapor available. Several investigators (Hage 1972; Lawford et al. 1974) have correlated the frequency of ice fog occurrence with the release of water vapor into the atmosphere by the burning of fossil fuels.

5.2.3 OBSERVED EFFECTS

5.2.3.1 Planned Weather Modification

Many methods are used today in scientific experiments and operational programs designed to modify the weather. Almost all attempt to modify or stimulate the warm and cold rain process in clouds or fogs. For example, efficient CCN such as NaCl particles can be added to otherwise relatively stable clouds to accelerate the growth of a few drops and begin a warm rain process. For cold rain modification, IN in the form of AgI particles or other ice nucleants are injected into clouds in order to rapidly create large ice crystals which can grow to precipitation sizes. Dry ice pellets or similar coolants are often released into clouds, causing homogeneous nucleation of ice crystals.

In most cases, an attempt is made to generate greater numbers of large drops or ice crystals in order to increase the rain or snow producing efficiency of the cloud. In addition, fogs or thin layer clouds can be made to dissipate because most of the cloud water is transferred to a few large particles which fall to lower levels. To suppress hail formation, ice crystals are generated which provide competition for the available water and thus reduce the size of hail particles formed inside the cloud. For hurricane modification, the ice nucleant is placed inside some clouds and the latent heat released during the formation of ice crystals is thought to change the dynamics of the cloud system.

The scientific literature contains sufficient evidence to indicate that warm and cold fog dispersal, and the modification of stratus, orographic, and isolated cumulus clouds are feasible under some circumstances. However, only a few experiments which attempt to increase rainfall over a large area have demonstrated successful results when evaluated by statistical techniques (WMO 1978b; Gagin and Neuman 1976; Woodley et al. 1976). Snowfall augmentation performed in the U.S. Rockies (Grant 1974) had withstood statistical verification; however, some of these positive results have recently been questioned (Rangno 1979). Some Canadian weather modification experiments have been described by Godson et al. (1966), Isaac et al. (1979) and Goyer and Renick (1979).

5.2.3.2 Inadvertent Weather Modification

There is little doubt that cities, some industries, and natural phenomena such as volcanoes and forest fires generate large quantities of particles (see Chapter 3). Volcanoes and industries are known to produce efficient ice nuclei (Pruppacher and Klett 1978) which could affect precipitation processes. It has also been postulated that urban aerosols and sugar cane fires can alter cloud reflectivity (Bodhaine 1979) and this ultimately might change the earth's climate (see Chapter 6).

As discussed previously, the addition of CCN and IN to a cloud may alter its microphysical structure; such a change may either increase or decrease the probability of precipitation. Despite the existence of a large quantity of data on the anthropogenic generation of weather-modifying nuclei the causal relationships between sources and altered precipitation have not yet been fully established.

Landsberg (1956) found precipitation increases of 5-15% downwind of several large urban areas. The La Porte, Indiana, weather anomaly was investigated by Changnon (1968) who found that La Porte experienced increases of 31% in precipitation, 38% in frequency of thunderstorm days and 246% in frequency of hailstorm days between 1951 and 1965. Changnon suggested that a possible cause of this precipitation anomaly was the emission of CCN, IN, water vapor and heat from the heavy industry complex in Chicago, Illinois, 48 km east of La Porte. Since the publication of Changnon's original paper, numerous studies have attempted to either substantiate (Changnon 1975, Hidore 1971a, 1971b) or disprove (Holzman and Thom 1970, Holzman 1971; Pittock 1977) the suggested causal relationships. Other studies suggest that the La Porte anomaly was not a unique situation. Historical records were examined for several American urban areas of differing size, type and climate (Changnon 1969; Huff and Changnon 1973). The six largest cities investigated all experienced warm season rainfall increases of 9-17% as well as increases in frequency of thunderstorm days (13-41%) and hailstorm days (90-450%). It was suggested that this precipitation enhancement was related to city size, industrial nuclei generation and urban thermal effects.

Warner (1968), analyzing 60 years of rainfall data in Australia, found a decrease in rainfall of approximately 25% during sugar cane harvesting. He hypothesized that through their activity as CCN, the small particles generated during cane burning resulted in an increase in concentration and subsequent reduction in size of cloud droplets, thereby hindering the coalescence processes necessary for rain formation. Although producing significant quantities of CCN, water vapor and heat, steelworks in Australia were found not to increase rainfall more than 5% (Ogden 1969).

Increases in mean annual precipitation in excess of 30% adjacent to or downwind from large industrial sources of CCN in Washington State were observed by Hobbs et al. (1970). The authors suggested that the increased precipitation was a consequence of the emission of CCN from sources such as pulp and paper mills. Such mills also emit significant quantities of heat and water vapor. In a later study, Eagan et al. (1974) found that large numbers of both submicron and large (> 30 μm) particles were emitted from pulp and paper mills in Washington State. This observation tended to confirm Hobb's et al. (1970) suggestion that the emissions from the pulp and paper mills were probably responsible for the elevated precipitation. However, Pittock (1977) suggested that natural changes in general circulation, locally enhanced by topography, largely accounted for these changes in precipitation.

Intensive investigations in the St. Louis, Missouri-Illinois, area (METROMEX study) (Semonin 1974; Schickedanz 1974; Huff and Vogel 1978; Vogel and Huff 1978) lead to the general conclusion that urban areas do enhance rainfall. This enhancement was greater (30-35%) than that associated with topographic effects (9-14%). In addition, thunderstorm day frequency data showed an urban-related increase of 20%. The urban-related increase in precipitation was the result of the intensification of existing precipitation systems rather than the initiation of individual storms (Semonin 1974; Huff and Vogel 1978; Gatz 1979). Schickedanz (1974) analyzed the size and intensity of rain cells in the area of St. Louis and found a 176-262% increase in average rainfall volume. There was a threefold increase in concentration of CCN measured downwind with clouds containing both small and large particles (Semonin 1974). It was suggested that the large cloud particles which formed on giant condensation nuclei were present in sufficient quantities to alter cloud precipitation processes. Although urban-induced rainfall increases have been observed in the above studies, no single cause for such enhancement has yet been identified. Gatz (1979) reported that there were weak correlations between rainfall enhancement and suspended particulate matter in certain areas of St. Louis filtering sites; however, an aerosol involvement in the urban rainfall anomaly could not be firmly established.

Powe (1969) found a pronounced precipitation maximum near the city of Montreal. Precipitation figures given by Hare and Thomas (1979) show that the downtown rain gauge sites of Montreal and Toronto received more annual precipitation than the airport sites located in the upwind western edges of both cities. However, it is difficult to prove whether these precipitation anomalies are due to the city heat island, to local terrain influences or to urban aerosols.

5.3 EFFECTS ON ATMOSPHERIC ELECTRICITY

Electrical processes are constantly taking place in the lower atmosphere and may be generally divided into two types: 1) intense electrification accompanying local storms and 2) fair-weather electrical activity dispersed worldwide, which is produced by electrified storms, cosmic rays and radioactive gases and particles.

The classical concept of atmospheric electricity envisages the earth and the ionosphere as the two conductors of a spherical capacitor separated by an imperfectly insulating atmosphere. The electric field, E, in the atmosphere near the earth's surface is given by:

$$E = \frac{I}{\lambda} = \frac{V}{R\lambda} \qquad (5\text{-}1)$$

where I is the air-earth current density, λ is the total electrical conductivity, V is the ionospheric potential and R is the columnar resistance. The columnar resistance, by definition is given by:

$$R = \int \frac{dh}{\lambda(h)} \qquad (5\text{-}2)$$

where h is the altitude. The electrical conductivity (λ) is influenced by the presence of particles in the atmosphere.

The atmosphere contains both positive and negative ions which consist of gas molecules, molecular clusters, and finely divided particles. The distribution of such particles in air of high nuclei content is illustrated in Figure 5-3. Although, three distinct kinds of

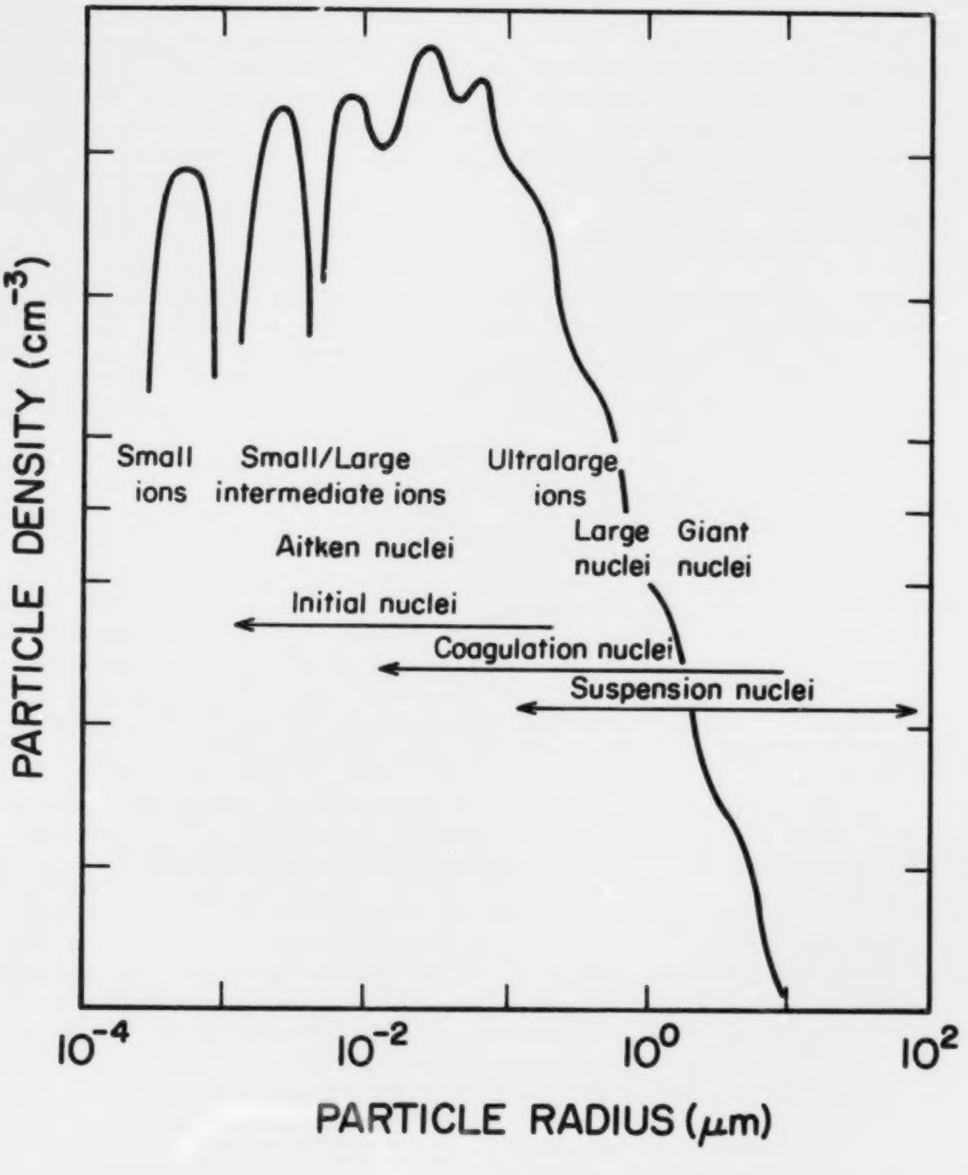

Figure 5-3. Distribution of particles, in relation to particle size, in air of high nuclei content (from Israël 1971).

ions (small, large and intermediate) have been observed, the usual practice in atmospheric electricity research is to divide the ions into two categories: 1) small ions having mobilities of 1-2 $cm^2.volt^{-1}.s^{-1}$ and 2) large ions (intermediate ions included) having mobilities about 0.1 to 0.001 times as great. Apart from the difference in mobility of small and large ions, another important difference is the nature of these two ions. A small ion, usually consisting of a group of molecules, exists only as long as its charge, since the charge itself is the mechanism by which the molecules congregate. On the other hand, a large ion can be detected as an uncharged nucleus when it loses its charge. This is also true for intermediate ions and is the reason why they are classified as large rather than small ions.

The formation and nature of small ions have been extensively investigated (e.g. Huertas and Fontan 1977; Mohnen 1977). The constituent formula for positive ions is believed to be $H_3O^+.(H_2O)_n$. Negative ion chemistry is not yet understood, although likely formulas are $O^-_2.(H_2O)_n$ and $CO^-_4.(H_2O)n$.

The ionic equation for small ions (e.g. positive ions) is:

$$\frac{dn_+}{dt} = q - \alpha n_+ n_- - o_{12} n_+ N_- - o_{10} n_+ Z \qquad (5\text{-}3)$$

where q is the rate of production; α is the recombination coefficient; o_{12} is the recombination coefficient of positive small ions with large negative ions; o_{10} is the recombination coefficient of positive small ions with uncharged nuclei; n_+ is the small positive ion concentration; n_- is the small negative ion concentration; N_- is the large negative ion concentration; and Z is the uncharged nuclei concentration.

At equilibrium, the ionic equation (Eq. 5-3) becomes zero and there is a balance between small negative and positive ion concentration and large negative and positive ion concentration. Hence,

$$q = \alpha n^2 + \beta n Z \qquad (5\text{-}4)$$

where β is the attachment coefficient; n is the small ion concentration; and N is the large ion concentration. The attachment coefficient is dependent upon the radius of a neutral particle (Hoppel 1977). Typical values for β are 0.58×10^{-12} $m^3.s^{-1}$ for particles of radius 0.02 μm and 8.2×10^{-12} $m^3.s^{-1}$ for particles of radius 0.2 μm.

The relationship between electrical conductivity (λ) and small ion concentration (n) is given by:

$$\lambda = enk \qquad (5\text{-}5)$$

where e is the electric charge and k is the small ion mobility.

The small ion concentration (n) is dependent upon the uncharged nuclei concentration (Z). Hence electrical conductivity (λ) will be influenced by changes in uncharged nuclei concentration. Near the earth's surface, the electric field (E) is inversely proportional to the electrical conductivity. At higher altitudes, changes in the electrical conductivity will result in changes to the columnar resistance (R) and the air-earth current density (I).

Over the oceans, ionizing radiation produces approximately 2 ion pairs.$cm^{-3}.s^{-1}$ and a resulting small ion concentration and electrical conductivity near sea level of approximately 1000 ions.cm^{-3} and 2.5×10^{-14} $ohms^{-1}.m^{-1}$, respectively (Cobb 1973). The residence time of the small ions thus generated is governed by removal via recombination with oppositely charged small ions and attachment to large charged and neutral particles. These particles provide relatively immobile surfaces for the diffusional attachment of highly mobile small ions, thereby leading to a subsequent reduction in the electrical conductivity.

The fair-weather electric field at the earth's surface fluctuates somewhat spatially and temporally, largely as a result of local variations in atmospheric electrical conductivity. In remote areas, the electric field has a diurnal cycle independent of position or local time which is quite similar to the diurnal cycle of global thunderstorm activity (Chalmers 1967). Mauchly (1923) found that the electrical conductivity at sea level had a variation of the order of 30% of its mean value with a single maximum in the afternoon. Alternatively, the diurnal variation of the electric field over land usually contains an early morning minimum, a morning maximum, a daytime minimum and an evening maximum (Rose 1937). This variation is considered to be made up of local effects superimposed upon the global variation observed in remote oceanic areas.

The effects of man-made aerosols on atmospheric electricity are not well known, although there are some studies which examine both continental and global effects as well as local and urban effects. Measurements of electrical conductivity have been carried out since the early part of this century in remote regions as well as in areas experiencing elevated particle loadings (Sagalyn 1958; Gunn 1964; Cobb and Wells 1970; Misaki and Takeuti 1970; Cobb 1973; Hogan et al. 1973). The atmosphere above most of the oceans appears to be maintaining a relatively constant electrical conductivity, indicating a relatively fixed particle loading. However, there are several significant exceptions (Figure 5-4), including the pathways of aerosols extending eastward from the United States into the North Altantic, eastward from Japan into the North Pacific and southward from Asia into the North Indian Ocean (Cobb 1973). The electrical conductivity has remained relatively constant in remote regions of the South Pacific since 1900, whereas it has decreased at least 20% in the North Atlantic (Cobb and Wells 1970). The majority (15%) of this reduction has occurred since 1929.

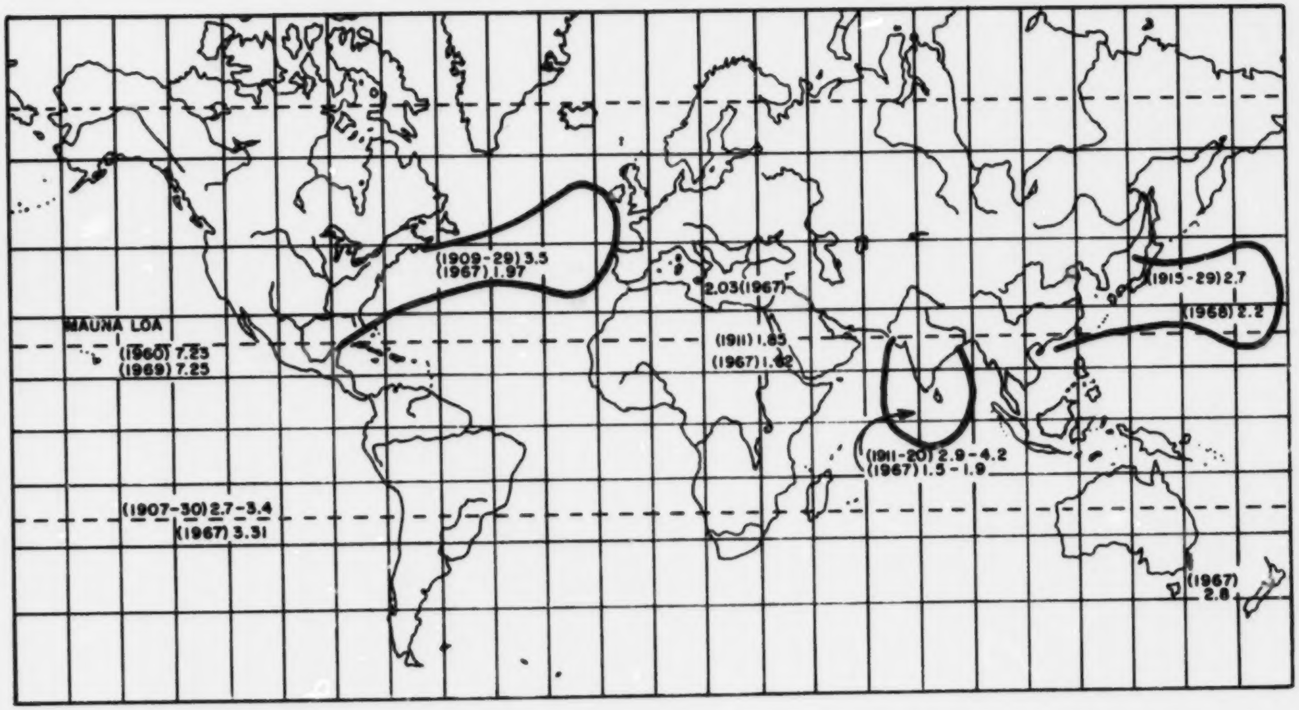
MAUNA LOA
(1960) 7.25
(1969) 7.25
(1909-29) 3.5
(1967) 1.97
2.03(1967)
(1911) 1.85
(1967) 1.62
(1911-20) 2.9-4.2
(1967) 1.5-1.9
(1915-29) 2.7
(1968) 2.2
(1907-30) 2.7-3.4
(1967) 3.31
(1967)
2.8

Figure 5-4. Worldwide oceanic measurements of atmospheric conductivity. Conductivity units are ohms^{-1}.m^{-1} x 10^{14}. Areas bounded by heavy contours show regions of decrease in atmospheric conductivity (from Cobb 1973).

Electrical conductivity over the oceans was found to vary with distance from land; it decreased upon approaching the coast (Misaki and Takeuti 1970).

Historical trends in continental or global electrical conductivity have been complicated since 1945 by the production of man-made radioactive aerosols. The net effect of radioactive contamination is to make the atmosphere more conductive (i.e. increase electrical conductivity) (Cobb and Wells 1970). Boeck (1976) indicated that ^{85}Kr, a radioactive, chemically inert gas, may be produced and released in quantities sufficient to create atmospheric ions at rates comparable to the present natural ion production near the tropical ocean surface. Calculations, based on a simple model of the global atmospheric electric circuit, indicate an increase of 43% in the electrical conductivity and a decrease of 10% in the columnar resistance (R) of clean oceanic air in the next 50 years.

In areas of elevated aerosol loadings, such as in certain domestic, urban and industrial settings, atmospheric electrical conductivity is usually much lower than over the oceans. More than 50 years ago, Whipple (1929) reported at Kew, England, a close resemblance in the diurnal variation of electrical potential gradient and dust content of air. Sapsford (1937) found that in Samoa there was a significant difference in the diurnal variation of potential gradient between weekdays and Sunday, due to the cooking habits of the local inhabitants.

In general, the atmospheric electric field in an urban area shows a local-time diurnal variation with double maxima, one in the morning and the second in the afternoon. Chalmers (1967) attributed this variation to the effects of particles produced by human activities in populated areas. Similar results were reported by Israel (1973), Anderson (1977) and Ogawa and Huzita (1979).

In Canada, few studies have been reported on the effects of particles on atmospheric electricity. Rose (1937) found that the potential gradient in and near Ottawa, Ontario, was influenced by particles emanating from the city and by local meteorological conditions. Bhartendu (1971) examined weekly variations in potential gradient, electrical conductivity and air-earth current density at Toronto, Ontario, for the effects of local pollution. In addition, Bhartendu (1974) indicated that the diurnal variation in potential gradient at Toronto and other stations could be due to vertical motion of aerosols.

The consequences of altering atmospheric electricity by changing aerosol loading are unknown. Vonnegut (1973) and Boeck (1976) mentioned possible effects on thunderstorm activity. Boeck (1976) also speculated on changes in the coalescence of cloud droplets and the formation of sulfate particles by gas-to-particle conversions involving air ions. Brock and Marlow (1975) reported that such processes as particle coagulation, dry deposition and deposition in the human respiratory system could be affected by changes in atmospheric electricity.

6.0 EFFECTS ON CLIMATE

6.1 INTRODUCTION

If atmospheric processes are systematically influenced by aerosols, both weather (the instantaneous state of the atmosphere) and climate (the long-term average of weather) can be modified. Climate will be considered as the mean thermal state of the earth-atmosphere system. Limiting climate to the thermal regime reflects the main emphasis in climate-aerosol studies to date. Most have sought, in response to increasing amounts of atmospheric aerosols, to estimate the quantitative change in surface temperature or whether the change was positive or negative.

Following the pioneering studies of Budyko (1969) and Sellers (1969) the possibility of significant climatic modifications arising from aerosols because of volcanic activity or the activities of man has been recognized (SCEP 1970; SMIC 1971). Both Budyko and Sellers have shown that surface temperature is remarkably sensitive to very small changes in solar irradiance, such that a complete glaciation of the planet would result from a reduction of 1.5-2% in the solar constant. Such a reduction could be produced by an increase in atmospheric aerosol loading without changes in either solar output or the Earth's orbit around the Sun. This alarming result gave some support to Bryson's (1968) view that the observed decrease in northern hemisphere surface temperatures since the 1940's has been due to an increase in aerosol loading. These studies motivated attempts in the 1970's to determine the relationships between aerosol loading and climate. The more salient relationships that have been investigated in recent years will be discussed in this chapter. Climate variation and models pertinent to understanding aerosol effects will be considered first.

6.2 CLIMATE VARIATION AND MODELS

Over the last 20,000 years, the most radical change in temperature relative to today's values occurred during the Wisconsin glaciation. Surface temperatures were then about 5°K lower than at present (Bryson 1974). During the last 1000 years, for extended periods, temperatures have been about 1°K below those of the present, especially during the Little Ice Age (1550-1850 AD). This resulted in reduced crop yields in northern Europe causing widespread famine (Bryson 1974). Pollack et al. (1976a) argued that if a 1°K reduction in temperature could cause such distress, a temperature depression of 0.3-0.5°K may be very important. This is of the order of the temperature decrease in the northern hemisphere since the 1940's which Bryson and Dittberner (1976) and Budyko (1977) have attributed to an increase in aerosol loading. Such an interpretation, however, must be accepted cautiously. Surface temperature has fluctuated significantly before the advent of anthropogenic aerosols and at times of volcanic quiescence. Such fluctuations may not have been due to any deterministic external cause, but to the nonlinearities in the earth-atmosphere system (Lorenz 1976). Spatial gaps in networks of observing stations and high frequency weather fluctuations also limit the ability to detect small climatic signals, especially over decadal periods (Geisler 1977).

To date it cannot be claimed irrefutably that changes in aerosol amounts have had observable effects upon world surface temperatures. Mass and Schneider (1977) found only a weak volcanic aerosol 'signal' in a statistical analysis of surface temperature data. Without measured responses, climate models have to be used to gain insight into possible influences of aerosols on climate. If it is assumed that the aerosol loading of the troposphere will increase in proportion to world population and industrialization (Kellogg et al. 1975), and that the loading of the stratosphere may increase suddenly with future outbreaks of major volcanic activity, attempts should be made to predict possible climatic consequences.

On an annual basis the amount of infrared radiation emitted to space by the planet equals the amount of absorbed solar radiation. This state of radiative equilibrium applies to the stratosphere but not to the troposphere and the planetary surface. On an annual and globally-averaged basis the surface has a positive radiation balance while the balance for the troposphere is negative. This establishes convective energy exchange between the surface and the troposphere. The atmosphere is virtually transparent to solar radiation but largely opaque to infrared wavelengths, thus reducing the loss to space of radiation emitted by the surface. This is called the greenhouse effect. As a consequence of Sun-Earth geometry and the tilt of the earth's axis, the planetary system is heated unequally, thereby producing temperature gradients between the tropics and poles. These initiate convectional circulation cells which are disrupted by the rotation effects of the earth to produce the broad features of the general circulation. The energy budget at any latitude involves energy transport by atmosphere and ocean in addition to radiative and convective exchanges. Surface topographic variations and differences between land and water further increase complexity of climate on regional scales. The increasing complexity from the planetary to the regional scale requires a hierarchy of models ranging from simple zero-dimensional energy balance statements to three-dimensional general circulation models. Studies of aerosol effects on temperature have been restricted mainly to zero- and one-dimensional models.

6.2.1 GLOBAL SCALE MODELS

6.2.1.1 Planetary Energy Balance

Over periods of at least one year the earth is in radiative equilibrium such that:

$$(\beta/4)\ (1-\alpha) - F = 0 \tag{6-1}$$

where β is the solar constant (~1360 $W.m^{-2}$), α the planetary albedo (~0.3), $F = \sigma\ T_e{}^4$ where T_e is the effective radiating temperature, or equilibrium temperature of the earth, and σ, the Stefan-Boltzmann constant. Equation (6-1) has been used in stratospheric studies by Harshvardhan and Cess (1976) and Herman et al. (1976).

An increase in atmospheric aerosol content, due either to natural or anthropogenic emissions, has the potential for modifying the global energy balance through influences on the planetary albedo or the greenhouse effect. If q is a measure of the amount of aerosol in an atmospheric column, the sensitivity of surface temperature to a change in q can be obtained by differentiating equation (6-1) (Ramanathan and Coakley 1978). This yields:

$$\frac{dT_s}{dq} = - \frac{[\delta F/\delta q + (\beta/4)\delta\alpha/\delta q]}{[\delta F/\delta T_s + (\beta/4)\delta\alpha/\delta T_s]} \tag{6-2}$$

which indicates that the sensitivity of surface temperature to aerosol change involves not only the respective sensitivities of the infrared loss to space and the planetary albedo to aerosol loading, but also the thermal infrared feedback ($\delta F/\delta T_s$) and the albedo feedback ($\delta\alpha/\delta T_s$) parameters. Recently, Dickinson (1979) estimated that $\delta F/\delta T_s = 2 \pm 0.4$ $W.m^{-2}.°K^{-1}$ and $(\beta/4)\delta\alpha/\delta T_s = -0.5 \pm 0.3$ $W.m^{-2}.°K^{-1}$. The denominator in equation (6-2) becomes 1.5 ± 0.5 $W.m^{-2}.°K^{-1}$, indicating an uncertainty by a factor of two in assessing surface temperature response to a change in aerosol content, or in any atmospheric constituent.

6.2.1.2 Radiative Convective Model

For an annually and horizontally steady state atmosphere, atmospheric divergence and storage can be neglected and the thermodynamic energy equation reduces to:

$$Q_S(z) + Q_T(z) + Q_C(z) = 0 \tag{6-3}$$

where Q_S is the net solar radiative flux, Q_T the net infrared flux and Q_C the convective flux; each is a function of height z. Equation (6-1) is the boundary condition. Radiative convective models assume that the radiative equilibrium is maintained in the stratosphere and that convection maintains a critical lapse rate, usually set at -6.5 $°K.km^{-1}$ in the troposphere. For modelling purposes, the atmosphere is divided into layers. Starting with an arbitrary temperature profile, the radiative equilibrium equation is solved for each layer. The radiative heating rate is calculated and then used to determine a new temperature profile.

If a temperature difference between two adjacent layers exceeds a critical value it is set equal to that value. In this way convective adjustment is made. Calculations are repeated until the criteria for thermal equilibrium are satisfied (Manabe and Strickler 1964); 1) radiative equilibrium exists at the top of the atmosphere and wherever the lapse rate is subcritical; 2) surface radiation balance equals the net radiative cooling of the whole atmosphere; and 3) further calculations produce insignificant changes in the temperature profile. It should be noted that feedback mechanisms are neglected. This model has been used in aerosol studies by Reck (1974a, 1974b, 1975), Wang and Domoto (1974), Hansen et al. (1978) and Reck and Hummel (1981).

6.2.1.3 Surface Energy Balance Model

On an annual basis, the energy balance for the planetary, or hemispherical, surface can be stated as:

$$\varepsilon_s \delta T_s / \delta t = R_s - H - E \qquad (6\text{-}4)$$

where ε_s is the heat capacity of the substrate, R_s the surface radiation balance (absorbed solar plus net infrared radiation) and H and E the sensible and latent heat fluxes, respectively, from the surface. Bryson and Dittberner (1976) parameterized terms on the right hand side such that equation (6-4) could be solved for surface temperature. Aerosol effects were incorporated through empirical solar radiation transmission coefficients. They applied this parameterization to estimate northern hemisphere surface temperature from the late nineteenth century to the present.

6.2.2 REGIONAL MODELS

Because tropospheric aerosols show greater spatial variation than their stratospheric counterparts, their regional climatic effects are of primary interest. The earth atmosphere system is very complex on this scale. Energy storage and divergence terms must be treated. In principle, General Circulation Models (GCMs) are well suited for this purpose. These solve the thermodynamic energy equation along with the equations of motion, continuity, state and radiative transfer for all points in a three dimensional grid and for some desired time interval from an initial state. Currently, these models are primitive, with significant processes ignored or parameterized crudely. In the future, they may be the main numerical tools for simulating regional climate and for studying effects of perturbations in atmospheric contaminants. Effects of increases in atmospheric carbon dioxide have already been studied with a GCM (Manabe and Wetherald 1975; Gates et al. 1980) but no attempts have yet been made to determine possible thermal effects of increases in aerosol loading.

Three types of climate models have been used regionally. The first, the Budyko-Sellers model, extends the global energy balance model to incorporate latitudinal variations (Budyko 1969; Sellers 1969). Surface temperature (T_s) is made a function only of latitude (ϕ) and all model parameters are functions of temperature:

$$S(\phi)\,[1 - \alpha_p(\phi,\, T_s)] - F(\phi,\, T_s) - E(\phi,\, T_s) = \varepsilon T_s/\delta t \qquad (6\text{-}5)$$

where $S(\phi)$ is the extraterrestrial solar radiation, $\alpha_p(\phi,\, T_s)$ the zonal planetary albedo, $F(\phi,\, T_s)$ the zonal emission of infrared radiation to space, $E(\phi,\, T_s)$ the energy transport due to sensible, latent and potential energy in the atmosphere and heat by the oceans and ε is the heat capacity of the system. Budyko and Sellers assumed equilibrium, hence setting the storage term equal to zero. Both models were extensibely parameterized to fit the present climate. Aerosol effects were incorporated by decreasing solar radiation by differing amounts. The Sellers model was extended (Sellers 1973) to incorporate land and water effects, and a more formal treatment of winds and radiation transfer was attempted.

The second type of model is either global or regional, and specifies only the ability of an aerosol layer to warm or cool the earth-atmosphere system. The models of Schneider (1971) and Mitchell (1971) come under this category. Schneider considered the effect upon planetary albedo of introducing an aerosol layer above an existing reflecting system. If the aerosol layer has a transmittance t, backscatterance b, absorptance a for solar radiation, and reflectance of the underlying system A_o, the planetary albedo with multiple reflections considered is obtained from the infinite series (Figure 6-1):

$$\alpha = b + A_o t^2 + bA_o^2 t^2 + b^2 A_o^3 t^2 + \ldots \qquad (6\text{-}6)$$

as

$$\alpha = b + \frac{A_o t^2}{1 - A_o b} \qquad (6\text{-}7)$$

The difference between α and A_o is the basis for determining the heating or cooling of the aerosol layer. Although Schneider applied equation (6-6) to the earth as a whole, Joseph and Wolfson (1975) have applied it regionally.

Mitchell's model considers the effect of aerosol loading on the energy balance in determining the sign of temperature change near the surface. Warming or cooling occurs if the actual ratio of absorption to backscatter is greater or less than the critical value of the ratio for which the addition of aerosol has no thermal effect. The critical ratio was defined as:

$$(a/b)_{crit} = C(1 - A_s)\,(1 - A_s k)/[D(1 + A_s) - C(1 - A_s)] \qquad (6\text{-}8)$$

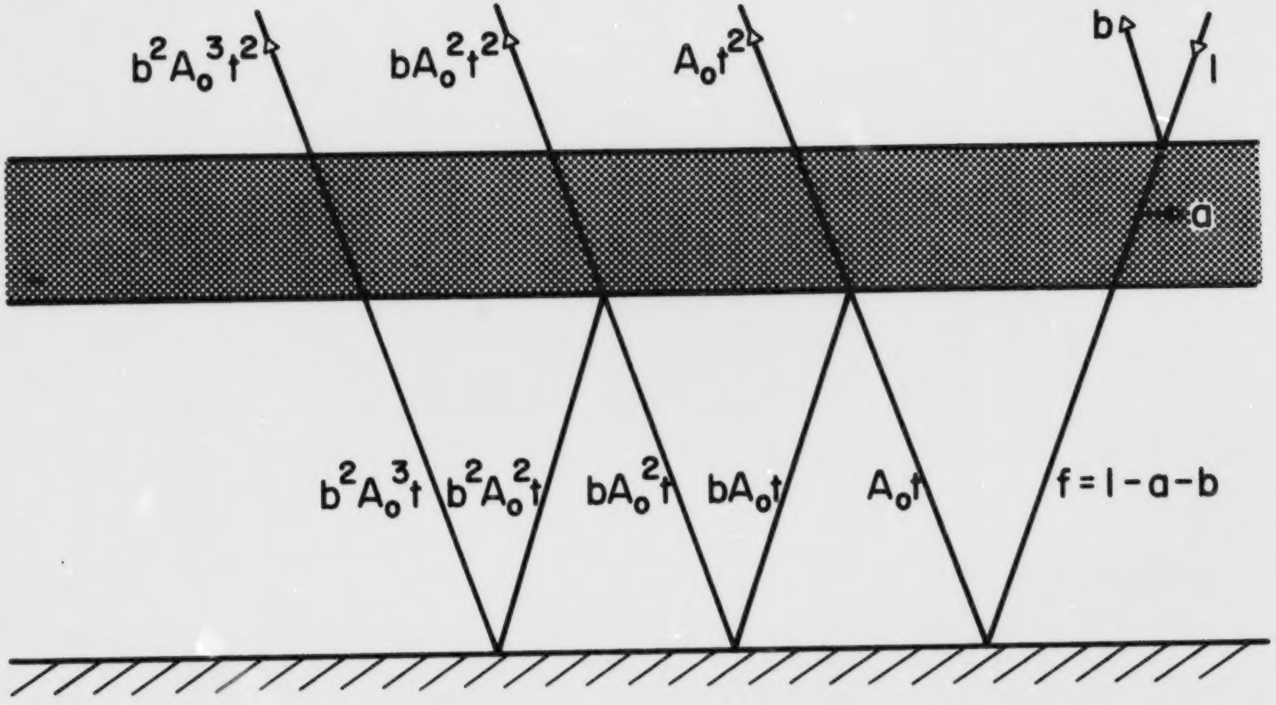
$b^2A_o^3t^2$
$bA_o^2t^2$
A_ot^2
b
I
a
$b^2A_o^3t$
$b^2A_o^2t$
bA_o^2t
bA_ot
A_ot
f = I - a - b

Figure 6-1. Schematic diagram showing multiple reflections between the ground and an aerosol layer.

in which $C = H/(H + E)$ at the surface, D is the fraction of the total aerosol which is convectively in contact with the ground, A_s is the surface albedo and k is a proportionality factor applied to b to determine aerosol backscatter for radiation reflected from the ground.

Boundary-layer models constitute the third type of regional model. Several models have been used to examine aerosol effects on urban climates (Atwater 1971; Bergstrom and Viskanta 1973; Ackerman 1977; Viskanta et al. 1977). Atwater determined aerosol effects on the energy budget using a simple, empirical radiative transfer model while the other studies used one- or two-dimensional time-dependent models with detailed spectral radiative transfer calculations.

Radiation is of primary importance in climate models. One-dimensional, latitudinal models have employed empirical relationships to evaluate both solar and infrared fluxes (Budyko 1969; Sellers 1969; Bryson and Dittberner 1976) whereas models which consider variation with height in the atmosphere solve the equation of radiative transfer.

6.3 RADIATIVE TRANSFER

Optical properties of individual spherical particles and polydispersions can be computed readily from the Mie theory for the case of single particle scattering (Appendix III.0). It is usually assumed that infrared effects are negligible. For the same aerosol, solar optical depths are at least an order of magnitude larger than those for infrared wavelengths. Coakley and Grams (1976) indicate two exceptions: 1) extinction efficiencies for both visible and infrared radiation may be of the same order of magnitude for large particles and 2) very small particles which absorb strongly in the infrared, but not in the visible, may have infrared extinction efficiencies which are much larger than values for solar radiation. Since the atmosphere is virtually black for infrared wavelengths smaller than 8 μm and larger than 14 μm, the effect of aerosols is restricted mainly to the atmospheric window (8-14 μm).

Greater emphasis has been placed upon solar radiation effects of aerosols. Multiple scattering, which may be significant in aerosol layers, increases attenuation by increasing path length through the atmosphere. To treat multiple scattering, the equation of radiative transfer must be solved. For the spectral intensity I_λ of radiation, wavelength λ, along a ray of direction μ passing through an absorbing, emitting and scattering medium at height z, this can be stated as:

$$\mu\, dI_\lambda(\tau,\mu)/d\tau = (1 - \omega_0)B_\lambda(\tau) - I_\lambda(\tau,\mu) + \frac{\omega_0}{2}\int_{-1}^{1} P(\tau,\mu,\mu')I_\lambda(\tau,\mu')d\mu' \qquad (6\text{-}9)$$

Here, B_λ is the Planck function; $P(\tau,\mu,\mu')$ the scattering phase function specifying the intensity scattered from the direction μ' into the direction μ; and τ and ω_0 are the spectral optical depth and spectral single scattering albedo defined as:

$$d\tau = P(z)\ [K_\lambda(z) + \sigma_\lambda(z)]dz \tag{6-10}$$

and

$$\omega_0 = \sigma_\lambda(z)/[K_\lambda(z) + \sigma_\lambda(z)] \tag{6-11}$$

where $P(z)$ is atmospheric density, and $K_\lambda(z)$ and $\sigma_\lambda(z)$ the mass absorption and scattering coefficient, respectively. The single scattering albedo, which specifies the scattering fraction of attenuation, depends on the imaginary part of the complex index of refraction.

With appropriate boundary conditions for the problem to be tackled, the transfer equation can be solved in several ways. Equation (6-9) is easily integrated for direct beam solar radiation since both the Planck function and phase function terms can be neglected. The integration leads to Beer's law (Appendix III.0), equation (III-24). However, equations for diffuse radiation, both solar and infrared, cannot be as simply treated. If aerosol scattering of infrared radiation can be neglected, the phase function term in Equation (6-9) is ignored and the resulting first order differential equation can be solved analytically. If scattering of infrared radiation by aerosols is important the full integro-differential equation must be treated, as is always the case for scattered solar radiation. Methods of solution have been discussed extensively (e.g. Paltridge and Platt 1976; Lenoble 1977; Lenoble 1980). The phase function presents the main difficulty in solving equation (6-9). In aerosol studies two approaches have been principally used: 1) the phase function can be replaced with a Legendre series expansion where the coefficients must be determined a priori from Mie theory calculations for a particular aerosol-containing atmosphere (Bergstrom and Viskanta 1973; Braslau and Dave 1973a, 1973b) or 2) use of the two stream approximation (Rasool and Schneider 1971; Sellers 1973; Reck 1974a, 1974b; Chylek and Coakley 1974, 1975; Wang and Domoto 1974) which assumes isotropic upwelling and downwelling intensities. This is the most common approach in climate studies. Both approaches reduce equation (6-9) to a system of linear differential equations which are solved by standard methods. Spectral values of τ, ω_0 and a number of Legendre coefficients are required for the aerosol species under consideration together with similar data for Rayleigh scattering, scattering by clouds and absorption by gases. Uncertainty in these values for aerosols probably leads to greater error in calculated intensities and fluxes than the approximations involved in the mathematical solutions of equation (6-9).

6.4 RADIATIVE AND THERMAL EFFECTS OF AEROSOLS

The stratosphere and the troposphere will be discussed separately since the regimes are different. The stratosphere is relatively dry and cloud-free with little vertical mixing. Aerosols from penetrating volcanic plumes are usually present in larger concentrations in the stratosphere than in the troposphere. Minimum residence time for volcanic aerosols is typically about one year. Without strong convective links with the troposphere radiational effects are the dominant influence on the thermal regime of both troposphere and surface. The troposphere contains most of the atmosphere's moisture and cloud and all of its weather. It is well mixed with significant scavenging and sedimentation of atmospheric particles. Aerosol residence times are therefore smaller than for the stratosphere and range from a few days to a few weeks, depending on particle sizes and entrainment height. Tropospheric aerosols originate both from natural nonvolcanic sources and from anthropogenic sources (see Chapter 3).

6.4.1 CLIMATIC EFFECTS OF STRATOSPHERIC AEROSOLS

A major concentration of large ($r > 0.1$ μm), optically active sulphate particles occurs in the Junge layer at heights between 16 and 23 km. Concentrations increase after volcanic eruptions because of the injection of silicates and sulfurous gases. In the first months following an eruption, silicate particles are dominant. Within a year they are replaced by sulfates from gas-to-particle conversion (Baldwin et al. 1976). The effects upon aerosol concentrations of the Agung and Fuego eruptions in 1963 and 1974 respectively, have been observed. Both lidar and balloon-borne counter measurements showed a progressive decrease in concentrations in the interval between the two volcanic eruptions (Russell and Hake 1977). However, particles are present in the stratosphere even in the absence of volcanic activity. Carbonyl sulfide (CSO), a combustion product of fossil fuel burning, is a possible source for these particles (Crutzen 1976). It is inert in the troposphere and can diffuse into the stratosphere, where it is photolyzed, thus releasing SO_2 which is eventually converted into sulfate.

Toon and Pollack (1976) considered the stratospheric aerosol to consist of sulfuric acid particles (a liquid mixture of 75% H_2SO_4 and 25% water) which fit a zero-order logarithmic distribution function. However, Gras and Michael (1979) pointed out that this distribution was fitted to impactor data solely and does not fit their combined impactor-light scatter distributions overall. Recently, Russell et al. (1981) have collected stratospheric aerosol data to produce height dependent aerosol size and refractive index information.

Values for the real and imaginary parts of the refractive index are not well known. Pinnick et al. (1976) suggested that the real part lies between 1.4 and 1.5 with the imaginary part being < 0.05, while Russell et al. (1981) consider these to be between 1.33 to 1.52 and < 0.0005, respectively.

Because the aerosol layer is optically thin ($\tau << 1$) the single scattering assumption has been used in most radiative transfer studies. Pinnick *et al.* (1976) determined the maximum value of τ to be 0.01.

All climate models have considered the effects of an increase in aerosol loading on solar radiation while Harshvardhan and Cess (1976), Pollack *et al.* (1976b); Coakley and Grams (1976) and Harshvardhan (1979) have also included the effects on infrared radiation.

In the shortwave portion of the spectrum, absorption and backscatter by an aerosol layer will change the planetary albedo by an amount $\Delta\alpha$ and thereby decrease the solar radiation reaching the underlying system. Following Russell and Hake (1977) this decrease can be expressed as a fraction of the solar constant $\Delta\beta/\rho$. Cadle and Grams (1975) evaluated $\Delta\alpha$ from equation (6-6) in the form:

$$\Delta\alpha = \alpha - A_0 = b + \frac{A_0 t^2}{1-A_0 b} - A_0 \qquad (6\text{-}12)$$

and $\Delta\rho/\beta$ from:

$$\Delta\beta/\rho = -b(1 - A_0) - a \qquad (6\text{-}13)$$

In the optically thin limit (Chylek and Coakley 1974):

$$\Delta\alpha = 2\omega_0\, b\tau \qquad (6\text{-}14)$$

which can be readily evaluated from Mie theory calculations. Russell and Hake (1977) have tabulated values of $\Delta\alpha$ and $\Delta\rho/\rho$ for four models (Table 6-1). For all four, an increase in aerosol loading increases planetary albedo and decreases the amount of solar radiation reaching the troposphere. Both parameters are proportional to the change in optical depth. The weaker dependence of $\Delta\alpha$ and $\Delta\rho/\rho$ upon $\Delta\tau$ for the Pollack *et al.* (1976b) model may arise from the full treatment of multiple scattering, using the doubling method, which would result in greater absorption by the aerosol.

Herman *et al.* (1976) examined seasonal and latitudinal changes in planetary albedo and equilibrium temperature for the northern hemisphere which might result from an injection of a 75% H_2SO_4 aerosol into the stratosphere. Assuming a log-normal distribution for the particles, an aerosol optical depth of 0.03 at $\lambda = 0.5$ μm and very little absorption (the imaginary part of the refractive index $n_i = 0$ for $0.4 < \lambda < 1.25$ μm, and $n_i < 3 \times 10^{-3}$ for $1.5 < \lambda < 2.5$ μm), the radiative transfer equation was solved to obtain albedo values. These were compared with similar calculations made without the presence of the aerosol. The largest increases (> 1.4%) in planetary albedo were obtained in polar regions, with uniform increases of < 0.3% south of 40°N for most of the year. Harshvardhan (1979) obtained similar results.

Table 6-1. Change in planetary albedo $\Delta\alpha$ and effective reduction in solar constant $\Delta\beta/\beta$ due to a change in optical depth $\Delta\tau$ (after Russell and Hake 1977).

	$\Delta\alpha$	$\Delta\beta/\beta$
Cadle and Grams (1975)	$0.17 \pm 0.07\ \Delta\tau$	$-0.25 \pm 0.11\Delta\tau$
Pollack _et al._ (1976b)*	$0.08\ \Delta\tau$	$-0.14\ \Delta\tau$
Pinnick _et al._ (1976)	$0.2\ \Delta\tau$	$-0.28\ \Delta\tau$
Harshvardhan and Cess (1976)	$0.19\ \Delta\tau$	$-0.26\ \Delta\tau$

* This is the only model which incorporates multiple scattering effects.

Aerosol effects on infrared radiation have been shown implicitly by Harshvardhan and Cess (1976) and Pollack et al. (1976a) as surface temperature changes due to a perturbation in stratospheric aerosols. From an energy balance study of a stratospheric aerosol layer, Harshvardhan and Cess (1976) determined the effect on surface temperature. Their model showed surface cooling as a result of an increase in stratospheric aerosol loading (Figure 6-2a). The infrared opacity of the aerosol had a slight compensating effect. The calculated surface temperature responses refer to a steady state and do not indicate a response to an increase in optical depth due to an isolated volcanic explosion. Sustained volcanic activity would be required to produce steady state conditions. The temperature response of the stratosphere to an increase in optical depth after a volcanic explosion is rapid and large. Newell (1970) found a temperature increase of 6°K at 20 km immediately after the Agung eruption. Harshvardhan and Cess (1976) obtained this value from their model by using the 8-fold increase in optical depth observed in the southern hemisphere for one year after the Agung eruption (Volz 1970).

Pollack et al. (1976b) calculated values of the infrared loss to space, F, for a given optical depth perturbation using a range of surface temperatures. The surface temperature which yielded the value of F needed to balance equation (6-1) was interpolated from these. The U.S. Standard Atmosphere (1965) was used as the starting point. Upon changing surface temperature, the temperature profile of the whole atmosphere was changed to preserve constant lapse rates. Changes in surface temperature due to aerosol perturbation were determined by comparing surface temperatures computed in this way with the value obtained for an unperturbed reference atmosphere. Figures 6-2a and 6-2b show temperature change as a function of $\Delta\tau$ for a constant relative humidity profile (A) when both solar and infrared effects are considered. Similar to the results of Harshvardhan and Cess (1976), aerosols were found to cool the surface. The aerosol effect on infrared radiation reduced the magnitude of the cooling by 40%. Latitudinal and seasonal changes in equilibrium temperatures ΔT_e due to the effect of aerosols have been examined by Herman et al. (1976) and Harshvardhan (1979). Herman et al. (1976) calculated ΔT_e from the aerosol perturbation on the albedo of an atmospheric column. Using equation 6-1 and assuming radiative equilibrium for the column:

$$\Delta T_e = \frac{-\,S_o \Delta\alpha}{4\varepsilon\sigma T_e{}^{-3}} \qquad (6\text{-}15)$$

where S_o is the extraterrestrial radiation of a given latitude, $\Delta\alpha$ the latitudinal perturbation in albedo, ε the effective emissivity of an atmospheric column (0.9), σ the Stefan-Boltzmann constant and T the mean temperature of the column. For $\Delta\tau = 0.03$, maximum cooling occurs in polar areas (> 0.5°K) but for most of the hemisphere south of 50°N values are < 0.25°K. Herman et al. (1976) emphasized that polar areas also undergo greater temperature variation during periods of climate change than do other latitudes. These calculations refer only to solar radiation; infrared radiation, feedbacks, convective adjustment and dynamic effects have been neglected.

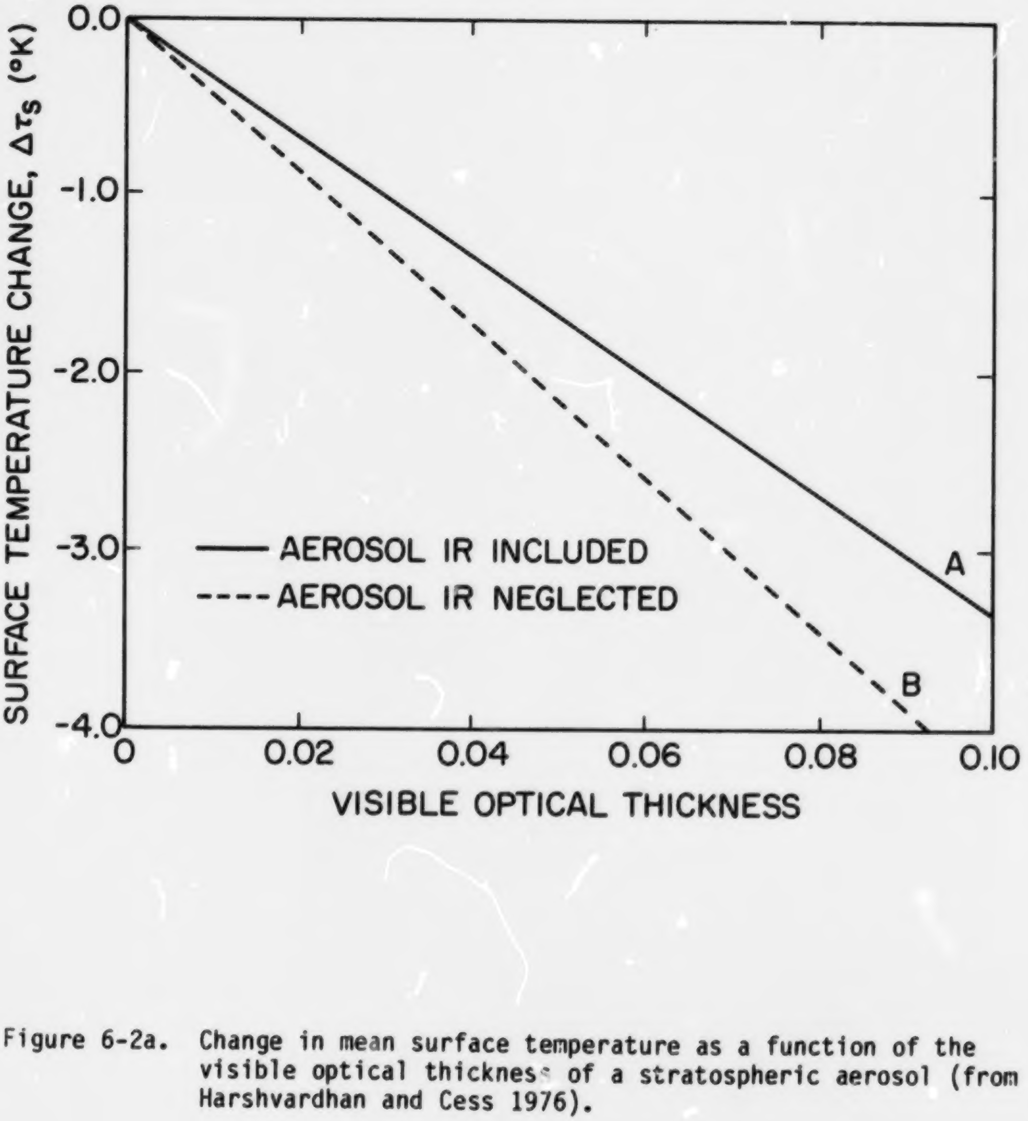

Figure 6-2a. Change in mean surface temperature as a function of the visible optical thickness of a stratospheric aerosol (from Harshvardhan and Cess 1976).

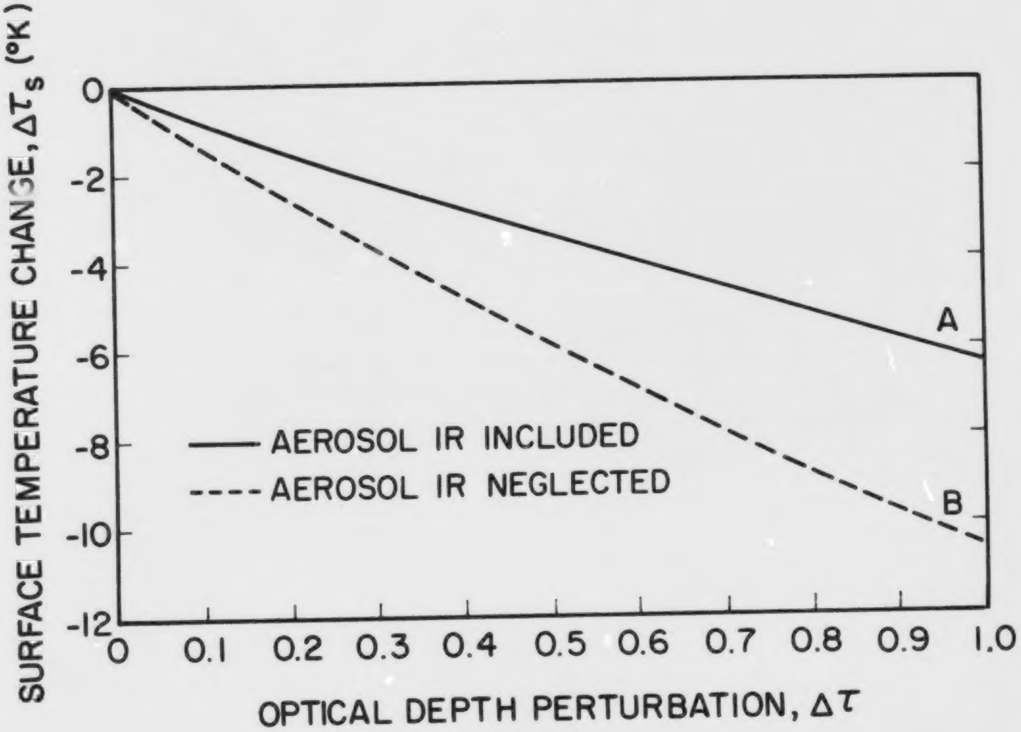

Figure 6-2b. Change in mean surface temperature as a function of optical depth perturbation of sulfuric acid droplets and aerosols (from Pollack et al. 1976b).

Harshvardhan (1979) combined longwave radiation calculations based on the procedures used by Harshvardhan and Cess (1976) to determine the sum of the aerosol effects on solar and infrared radiation, (i.e. $S(\phi)\Delta\alpha\ (\phi) + \Delta F(\phi)$) for the addition of an aerosol layer of $\tau_{vis} = 0.1$). Values range from +2.5 $W.m^{-2}$ in the tropics for all seasons to +9 $W.m^{-2}$ in polar regions, but are so small that they lie within the uncertainty of monthly radiation balance values determined from satellite data.

Harshvardhan (1979) determined ΔT_e from:

$$\Delta T_e = \frac{S_0\ \Delta\alpha\ (\phi) + \Delta F(\phi)}{4\sigma T_e^3} \qquad (6\text{-}16)$$

where T_e is calculated from emitted infrared data obtained by satellites (Ellis and Vonder Haar 1976). With the exception of polar regions, (Figure 6-3), in the polar night aerosols reduce the effective radiative temperature at all latitudes in all seasons. Between the latitudes of 50°N and 50°S the cooling does not exceed 1°K. Poleward values decline to -3°K. Small positive values of ΔT_e occur in the polar night. Hence, in spring and fall there is a marked change in the equator-to-pole thermal gradient, which could change atmospheric dynamics and lead to significant climatic consequences.

The climatic effects of perturbation in stratospheric aerosols due to vehicles and volcanic explosions have received considerable attention. Pollack et al. (1976a) considered a threshold surface temperature change of 0.1°K as climatically significant. They determined likely optical depth perturbations due to supersonic transports (SSTs) and space shuttles. The effect of space shuttles in the foreseeable future was found to be negligible ($\Delta\tau = 3.3 \times 10^{-5}$) but by the year 2000 the number of SSTs may be sufficient to increase optical depths by 1-3 x 10^{-3}, which could produce a temperature change close to the threshold value. In general, however, the climatic effect of vehicles is unlikely to be significant in the foreseeable future.

Effects of volcanic aerosols are much more significant. Hansen et al. (1978) computed the atmospheric temperature change after the Agung eruption using a radiative convective model to calculate the average tropospheric temperature change globally and in the tropical belt between 30°N and 30°S. From actual observations of optical depth changes, calculations were made for both pure silicate and 75% H_2SO_4 aerosols. They calculated the unperturbed atmospheric profile using the Toon and Pollack (1976) model. An active mixed ocean layer of 70-100 m accommodated the effect of ocean heat storage. For two years after the eruption, model calculations showed tropospheric temperature decreases of up to 0.5°K and maximum stratospheric warming of 5°K for sulfates and of 13°K for silicates.

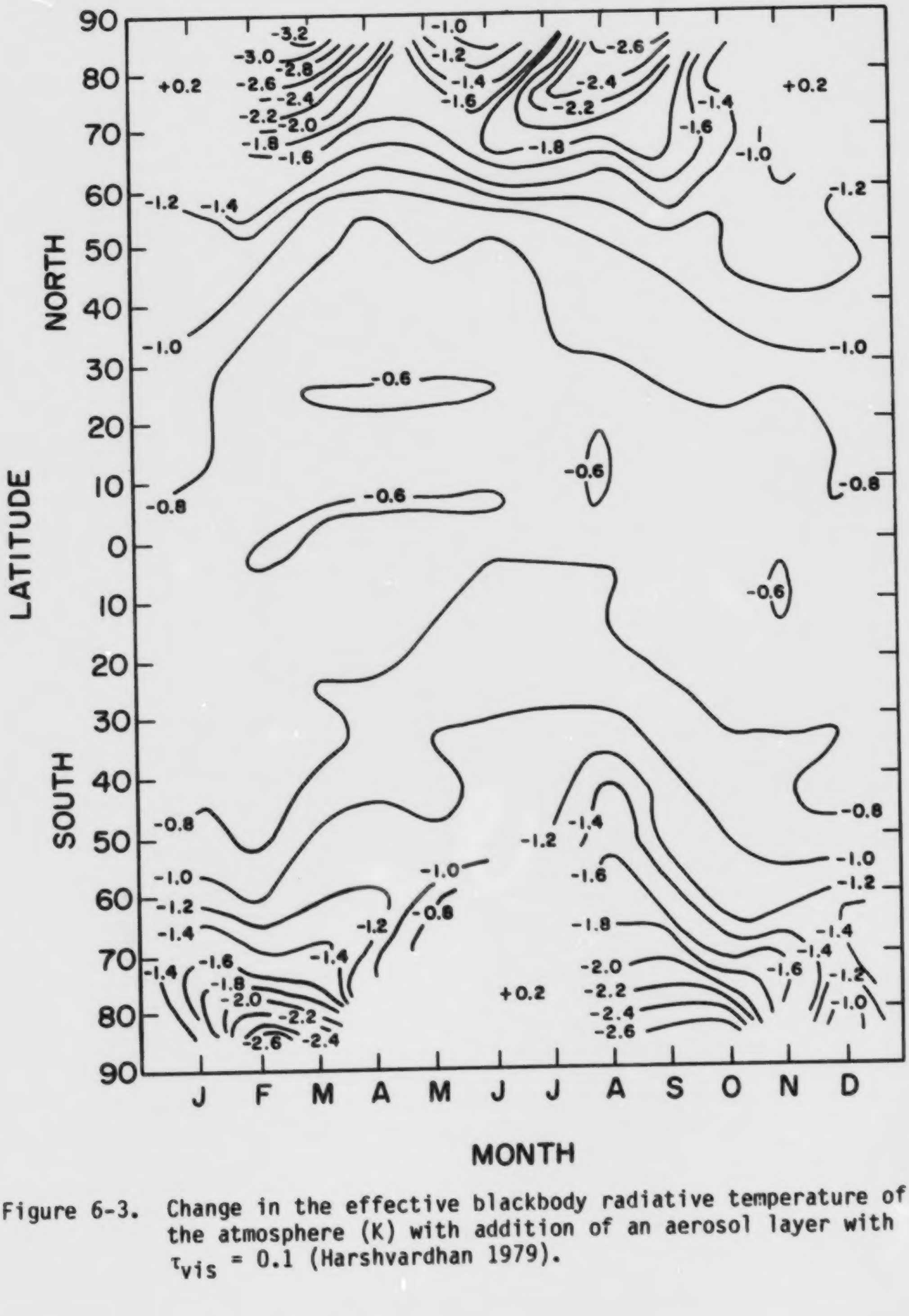

Figure 6-3. Change in the effective blackbody radiative temperature of the atmosphere (K) with addition of an aerosol layer with τ_{vis} = 0.1 (Harshvardhan 1979).

Russell and Hake (1977) applied the results of Table 6-1 to determine climatic effects of the Fuego eruption. Unperturbed and perturbed values of 0.005 and 0.030 were used for visible optical depth. The models of Cadle and Grams (1975), Pinnick et al. (1976) and Harshvardhan and Cess (1976) indicated a 1.5% increase in planetary albedo and a 0.7% reduction in the radiation reaching the troposphere. Values from the model of Pollack et al. (1975) are about half of these. This may be due to greater absorption achieved by full multiple scattering calculations. Pollack et al. (1975, 1976a, 1976b) and Baldwin et al. (1976) have considered the effect of volcanic explosions on climatic change during the last century with variations of $\Delta\tau$ obtained from measurements (direct beam radiation and transmitted starlight) or, as in the case of the Little Ice Age, estimated from Lamb's (1970) dust veil index. The constructed picture of $\Delta\tau$ (Figure 6-4a) is well correlated with volcanic events, as expected. Figure 6-4b indicates that ΔT values of this magnitude for a sulfuric acid aerosol could produce temperature decreases of about 1°K. This decline suggests that significant climatic change can result from volcanic activity. Pollack et al. (1976b) constructed a model temperature time series for the period since 1860, which considered the cumulative effect of a sequence of volcanic events. Decadal averages of $\Delta\tau$ were used to determine temperature changes. The results of Manabe and Wetherald (1967) were used to incorporate temperature change (warming) due to increasing carbon dioxide content of the atmosphere. The results, together with the mean temperature of the northern hemisphere from 1860 to 1970 (Figure 6-4b) show that the decrease in volcanic activity between the late 19th century and 1960 produced a larger increase in temperature than the observed increase in atmospheric CO_2 content. They considered that the two effects together accounted for much of the observed temperature increase until 1940. The downward trend in temperature after 1940 is not so readily accounted for. Apparently, changes in the level of volcanic activity between 1940 and the present are uncertain. However, increased activity in the 1960s may have contributed to the observed temperature trend.

Longer term climatic significance of volcanic aerosols has also been examined. Ice cores from Antarctica and Greenland contain bands with a large number of volcanic particles. In Antarctica, changes in the oxygen isotope 18 to 16 ratios for the cores provided estimates of temperature change. These have clearly shown that lower temperatures were associated with the environment when the bands were formed. Temperature changes during the second half of the Wisconsin ice age are well correlated with the volcanic particles in the ice cover; cooler periods correspond to increased volcanic activity and warmer periods to relative quiescence. Ice cores have not shown changes in volcanic particle content at the start of the Wisconsin period, however, which indicates that volcanic activity did not initiate the ice age.

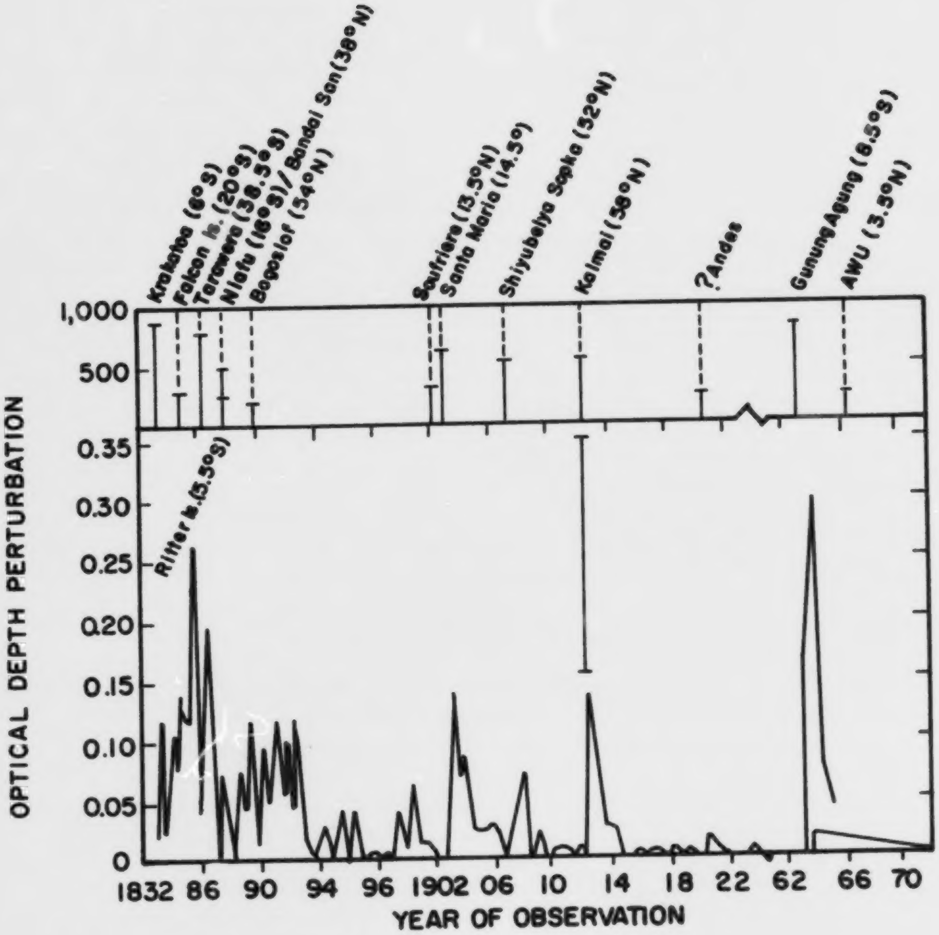

Figure 6-4a. Optical depth perturbations of the atmosphere at a wavelength of 550 nm as a function of time and volcanic explosion that Lamb (1970) has judged to have injected significant quantities of particles into the stratosphere (from Pollack et al. 1976b).

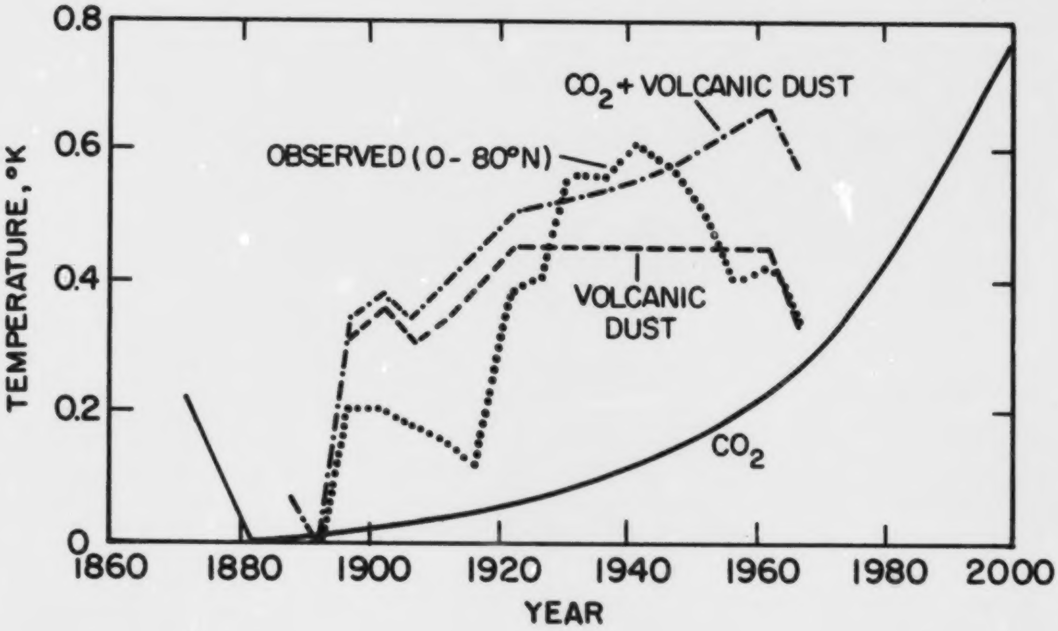

Figure 6-4b. Comparison between the observed temperature change for the northern hemisphere over the last century and those expected from changes in the level of volcanic activity and carbon dioxide content of the atmosphere (Pollack et al. 1975).

6.4.2 CLIMATIC EFFECTS OF TROPOSPHERIC AEROSOLS

It is harder to generalize about aerosol effects on climate in the troposphere than in the stratosphere. Both concentrations and optical properties are much more variable spatially and temporally. There is some evidence that overall concentrations of tropospheric aerosols have increased over the last several decades. This is based upon observed decreases in direct beam solar radiation (e.g. Budyko 1969; Joseph et al. 1973). Although increases in aerosol loading can be reasonably anticipated for urban areas, the absence of an increase at the Mauna Loa Observatory (Dyer 1974) casts doubt on the certainty of a global increase. Anthropogenic aerosols could be responsible for increases in aerosol loading in the northern hemisphere while the concentration in the southern hemisphere has remained stable (Whelpdale and Munn 1976). Global increases are assumed in the climate models of Budyko (1969), Sellers (1969, 1973) and Bryson and Dittberner (1976), and are implicitly assumed in radiative convective models.

During the 1960s climatic effects of aerosols were synonymous with effects on solar radiation. Surface cooling was generally assumed to be the result of an increase in aerosol loading (Bryson 1968) since aerosols were regarded only as scatterers; their effects on infrared radiation were not considered. The 1970s witnessed a shift from this position to a realization that aerosols might absorb solar radiation in significant amounts, causing warming, and that effects on infrared radiation could be significant. Undoubtedly, this shift has been partly due to an increase in our knowledge of atmospheric particles, but also to the widespread application of Mie scattering calculations, which have shown that changes in the imaginary part of the complex refractive index have significant effects on the radiation budget. Most recently, there has been a realization (Twomey 1977; Grassl 1979) that aerosols may have a significant effect on the reflective properties of clouds since they may increase the number of condensation nuclei significantly (see Section 5.2).

In view of the spatial variation of tropospheric aerosols the following discussion will place greatest emphasis on studies which are applicable to regions. Charlson and Pilat (1969) were first to show that if aerosols absorbed solar radiation, tropospheric warming could be significant and that Bryson's view of general cooling by aerosols should be treated cautiously. Mitchell (1971) extended the analysis to consider surface and atmospheric heating with a full treatment of the surface energy balance. From equation (6-8), he established that the critical ratio of aerosol absorption to backscatter, which would result in neither warming nor cooling with an increase in aerosol concentration, would be:

$$(a/b)_{crit} = (1-A)^2/2A \qquad (6\text{-}17)$$

for an aerosol in convective contact with a dry surface. Ensor et al. (1971) also extended the work of Charlson and Pilat (1969) but arrived at a different value for the ratio:

$$(a/b)_{crit} = (1-A)/A \qquad (6\text{-}18)$$

In both cases the ratio is dependent only on surface albedo and was derived by assuming an optically thin aerosol layer. Two separate analyses have since confirmed equation (6-17). Chylek and Coakley (1974) derived equation (6-17) by solving the radiative transfer equation using the two-stream approximation whereas Joseph and Wolfson (1975) derived it directly from equation (6-7):

$$\alpha - A_s = b + \frac{A_s t^2}{1-A_s b} - A_s = 0 \qquad (6\text{-}19)$$

so that

$$(a/b)_{crit} = \frac{(1-A_s)^2 + 2A_s a}{A_s(2-a)} \qquad (6\text{-}20)$$

where a is the aerosol asborptance. In this form the ratio is independent of optical depth. For an optically thin aerosol (case of weak extinction), $a \rightarrow 0$, equation (6-17) is obtained. For strong extinction ($a \rightarrow 1$):

$$(a/b)_{crit} = (1+A_s^2)/A_s \qquad (6\text{-}21)$$

Hence,

$$\frac{(1-A)^2}{2A} < \left(\frac{a}{b}\right)_{crit} < \frac{1 + A^2}{A} \qquad (6\text{-}22)$$

Curves for the weak and strong extinction cases are plotted in Figure 6-5a, together with actual ratios of absorption to backscatter obtained by measurement. These curves represent mainly temperate locations, and were calculated from measured values of spectrally integrated global G and diffuse D irradiances and theoretical values of the same irradiances for an aerosol-free atmosphere by a procedure established by Robinson (1962). Following Joseph and Wolfson (1975):

$$(a/b) = (f/b)\,(\delta G/\delta D) - 1 \qquad (6\text{-}23)$$

where f is the forward scatter and:

$$\delta G = \delta G \text{ (clear)} - \delta G \text{ (measured)} \qquad (6\text{-}24)$$

$$\delta G = \delta D \text{ (measured)} - \delta D \text{ (clear)} \qquad (6\text{-}25)$$

Here, (clear) refers to calculated values for an aerosol-free atmosphere. Values of f/b were taken from Robinson (1962). Data for Hamilton, Ontario, for summer months are included (Rouse and Bello 1979;

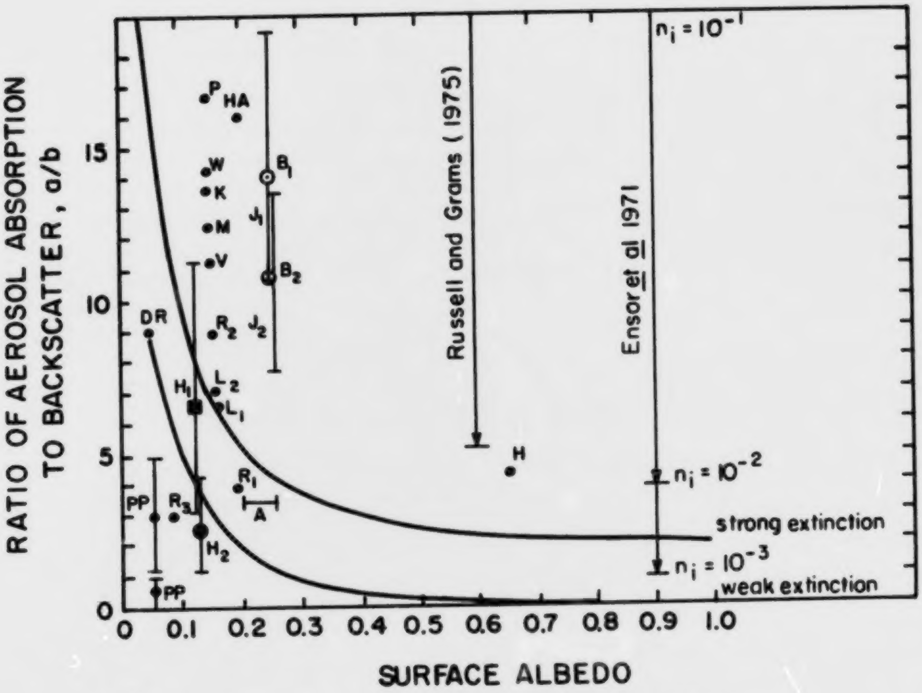

A	Arizona, U.S.A. (Idso 1972) - arid desert
B_1	Bet-Dagan normal clear days-arid+urban
B_2	Bet-Dagan khamsinic clear days-desert
H	Halley Bay-desert-background
HA	Waldram, 1945-(Robinson 1962)-urban
J_1	Jerusalem normal clear days-arid+urban
J_2	Jersusalem Khamsinic clear days-desert
K	Kew-urban
L_1	Lerwick (Robinson 1962)-maritime background
L_2	Lerwick (Forbes and Hamilton 1969)-maritime background
M	Malta-arid
P	Pretoria-arid+urban
PP	Australia (Paltridge and Platt 1973) arid+agricultural
R_1	South England (Robinson 1962)-urban
R_2	Robinson 1966 (hazy day)-urban
R_3	English Channel (Robinson 1962)-urban
V	Vienna-urban
W	Windhoek-arid+urban
DR	West-Indies (Drummond and Robinson 1974)-maritime-desert
H_1	Hamilton, Ontario (Rouse and Bello 1979)-urban
H_2	Hamilton, Ontario (Davies 1982)-urban

Figure 6-5a. Influence of aerosol absorption to backscatter ratio (a/b) on the shortwave radiation balance as a function of surface albedo (except for the data from Hamilton, Ontario, references appear in Joseph and Wolfson 1975).

Davies (1982)). Values of a/b were determined by Rouse and Bello from aircraft measurements of upwelling and downwelling global irradiance. Davies applied Robinson's analyses using surface measurements of direct and global radiation and a numerical model for calculating theoretical irradiances in clear atmospheres. Also included are ranges of a/b from Ensor *et al.* (1971) and Russell and Grams (1975), obtained from Mie theory calculations.

Most of the actual values of a/b in Figure 6-5a exceed the critical values for both weak and strong extinction and therefore the aerosols warm the system. Surface warming will occur, however, only if the aerosol layer is in convective contact with the ground. Otherwise, the surface cools, since aerosols reduce the amount of solar radiation received at the ground. Russell and Grams (1975) emphasized this point and indicated that it serves to reconcile the warming implied by the data in Figure 6-5a with the cooling effect of aerosols that is postulated by Bryson (1974).

Joseph and Wolfson (1975) emphasized the significance of abrupt changes in surface albedo beneath an air column with constant aerosol amounts and optical properties. Upon passing from land to ocean the warming effect of an aerosol layer would change to a cooling effect. In the Canadian context it would seem that over snow cover, aerosols should generally have a warming effect irrespective of the optical properties of the aerosol. On the east coast of North America and in the vicinity of the unfrozen Great Lakes, extreme differences in albedo between snow-covered land and open water could be expected to reverse the effect of aerosols from warming to cooling. These possibilities and their effects on the surface energy balance have not been investigated in North America. Joseph and Wolfson (1975) recommend that high priority should be given to studies of aerosol transport along land/ocean boundaries.

The derivation of $(a/b)_{crit}$ implies that A can be the albedo of the surface or of a portion of the earth-atmosphere system below an aerosol layer. Weare *et al.* (1975) have examined the effect of changing the position of the aerosol layer with respect to clouds. They considered three cloud-aerosol relationships: 1) (D1) aerosol above the cloud; 2) (D2) aerosol below the cloud; and 3) (D3) a uniform mixture of cloud and aerosol. Cloud is considered as a single, continuous, uniform layer. The case D1 yields $(a/b)_{crit}$ values which are the same as those given by equation (6-17). For the case of aerosol between the cloud and the surface, which occurs typically in the troposphere:

$$A_{D2} = b_c + \frac{A_o t_c^2}{1-Ab_c} \qquad (6\text{-}26)$$

or

$$A_{D2} = \frac{b_c \; t_c{}^2 \; [t_a{}^2 A_s + b_a \; (1-b_a A_s)]}{(1-b_a A_s(1-b_c b_a) - b_c A_s t_a{}^2)} \qquad (6\text{-}27)$$

where A_0 is given by equation (6-7), b_c and t_c are the reflectivity and transmissivity of the cloud, and b_a and t_a their aerosol counterparts. Figure 6-5b(i) shows the results for constant surface albedo (0.12) and variable cloud optical depth and Figure 6-5b(ii) those for variable surface albedo and constant cloud optical depth (τ=2). In the first case, the most noticeable feature is the constant value of $(a/b)_{crit}$ for D3 which is larger than values for D1 or D2. In the second case, D2 values are larger than those for D1 and D3 but they vary with surface albedo. These results indicate that if an aerosol is located below the cloud, its absorption must be greater, thereby producing a warming effect. This applies to all surfaces except snow.

Kellogg *et al.* (1975) recognized that simple models neglected not only cloud, *but* also the effect of atmospheric gases on the scattering and absorption of radiation. They reevaluated $(a/b)_{crit}$ using the Lacis and Hansen (1974) parameterization of absorption and scattering of radiation by gases and clouds and used a global average two-stream approximation for an optically-thin aerosol to compute the effect of aerosols (Chylek and Coakley 1975). Inclusion of these effects did not produce any substantial departures in the values of $(a/b)_{crit}$ from those given by equation (6-18) (Figure 6-5c). Their analysis was further extended to include aerosol effects on infrared radiation. These should contribute to surface warming since an aerosol reduces radiation loss from the system and increases the downward infrared flux to the surface. To include infrared radiation effects, $(a/b)_{crit}$ was redefined as the ratio "for which no change in the surface temperature occurs with an increase in the aerosol concentration". The revised critical ratio was obtained by balancing the decrease in the net infrared flux with the decrease in net solar flux at the top of the troposphere. The effect of incorporating changes in infrared radiation is illustrated in Figure 6-5c. Values of $(a/b)_{crit}$ are reduced substantially over surfaces with an albedo of less than 0.3. The relationship between a/b and albedo is not fixed when infrared effects are included, since it must vary with changing aerosol properties.

Kellogg *et al.* (1975) found that the introduction of an aerosol layer with *an imaginary* part of the complex refractive index of 0.01 for the visible spectrum and 1.0 for the infrared, produced surface cooling for a surface albedo < 0.36 (critical surface albedo). Warming occurs at larger albedo values. However, anthropogenic aerosols may have a larger imaginary refractive index which could reduce the critical surface albedo. Much of the data plotted in Figure 6-5a suggests a critical albedo value of about 0.1 with an imaginary refractive index $n_i > 10^{-2}$. Kellogg *et al.* (1975) also found that the critical surface albedo is 0.08 for *an imaginary* refractive index of 0.1. Warming by aerosols may be significant over northern hemisphere land areas where the greatest concentration of anthropogenic aerosols occur. The

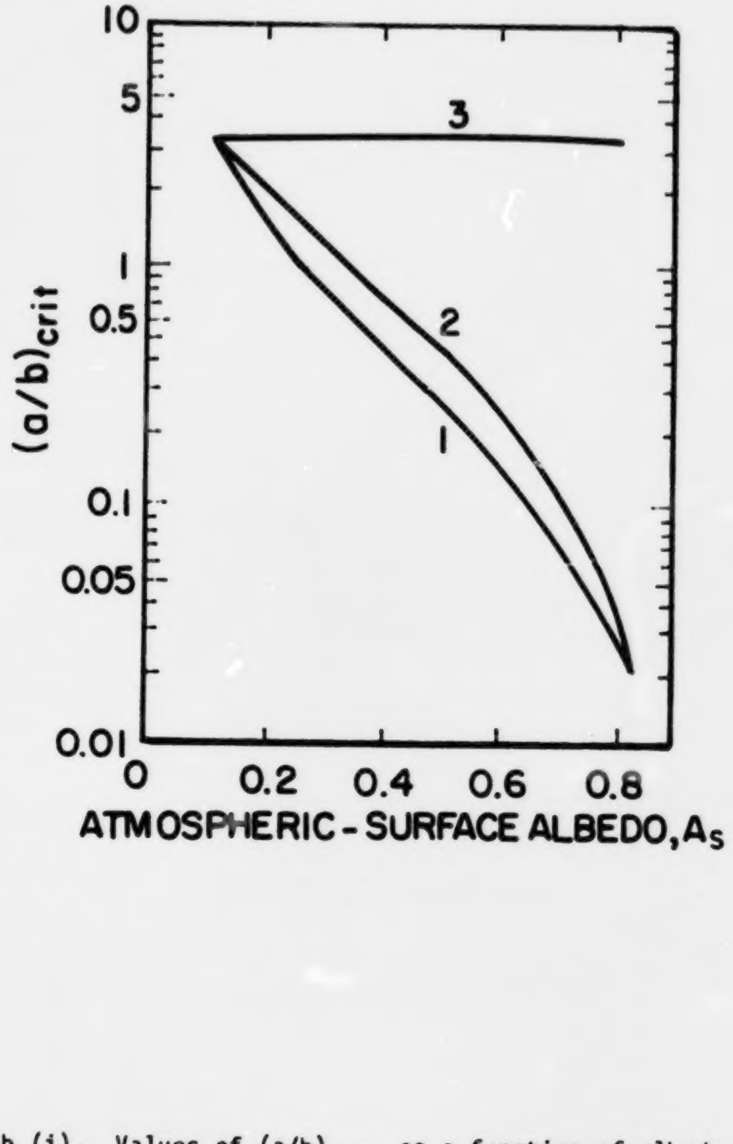

Figure 6-5b (i). Values of $(a/b)_{crit}$ as a function of albedo with three distributions of aerosol; 1) above the cloud, 2) between the cloud and the surface and 3) well mixed. Surface reflectivity is 0.12 with variable cloud optical depth.

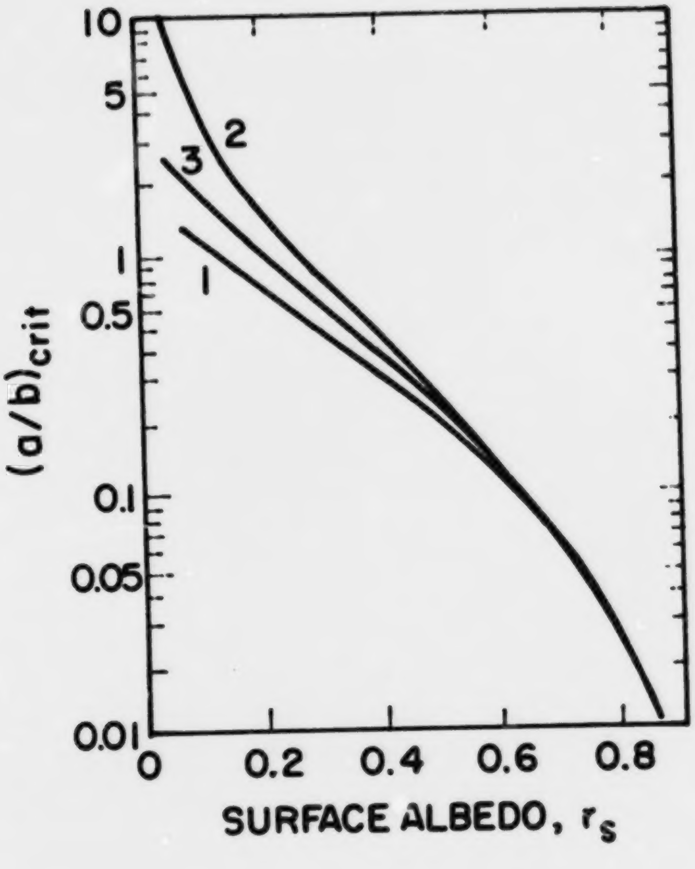

Figure 6-5b (ii). Values of $(a/b)_{crit}$ as a function of albedo with three distributions of aerosol; 1) above the cloud, 2) between the cloud and the surface and 3) well mixed. Cloud optical depth is fixed at 2.0.

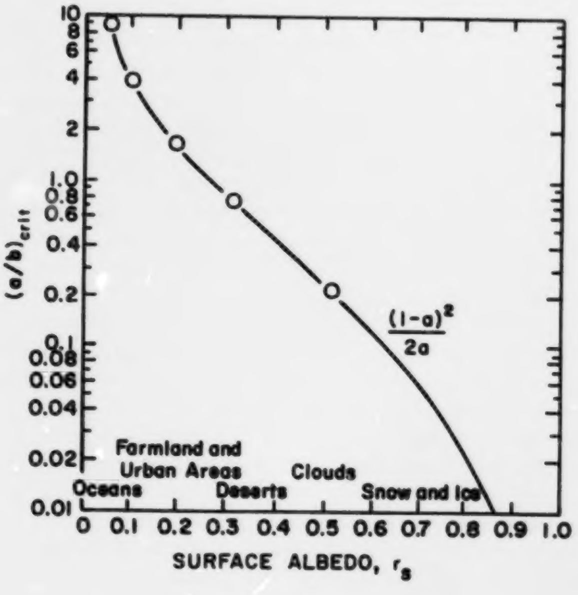

Figure 6-5c. Values of $(a/b)_{crit}$ as a function of surface albedo. The open circles represent results which would include absorption and scattering of radiation by gases and clouds. The curve represents results for both solar and infrared effects combined.

absorptive property of aerosols is the most crucial property that must be established quantitatively on both regional and global scales before the climatic impact of aerosols can be demonstrated. Yamamoto and Tanaka (1972) demonstrated the critical nature of n_i for both planetary albedo and surface temperature change. Their detailed radiative transfer calculations together with Budyko's (1969) global climate model showed that values of n_i between 0.05 and 0.1 are threshold values. Planetary albedo decreases and surface temperature increases for larger values. The significance of n_i is also emphasized in the radiative transfer work of Eschelbach (1973), Bergstrom and Viskanta (1973), Braslau and Dave (1973a, 1973b), Moriyama (1978), and Blanchet and Leighton (1981).

The uncertainty of the effect of aerosols on surface temperature is apparent in equation (6-2). The sign of $\delta F/\delta q$ is negative because an increase in aerosol loading decreases the infrared loss at the top of the troposphere. As Ramanathan and Coakley (1978) point out, the absorptive and reflective properties of the aerosol and the planetary albedo before the addition of aerosol determine the sign of $\delta\alpha/\delta T_s$. This second term is usually larger than the first in radiative transfer calculations (e.g. Wang and Domoto 1974) so that the sign of the surface temperature change is determined by the sign of $\delta\alpha/\delta T_s$. Revised ideas concerning n_i may modify predictions of surface temperature change.

Since both concentrations and optical properties of tropospheric aerosols are uncertain, their effects on large-scale climate remain unknown. It seems likely that anthropogenic aerosols over land areas will reduce the surface cooling effect of an increase in silicate or sulfate content of the stratosphere. In this respect, these aerosols may reinforce the carbon dioxide greenhouse effect. The energy balance models of Budyko (1969), Sellers (1969, 1973) and Bryson and Dittberner (1976) ignore this possibility. Aerosols are a cooling mechanism in these models. At the present state of knowledge we can conclude only that either warming due to aerosol is extremely small and can be neglected in such simple models or that the models are so heavily tuned to present-day climate (e.g. Budyko and Sellers) or to recent climate fluctuations (Bryson and Dittberner) that warming effects have gone unrecognized but have been inadvertently parameterized.

Results of the radiative-convective models of Wang and Domoto (1974) and Reck (1974a, 1974b, 1975) have shown that aerosols will heat the earth-atmosphere system for surface albedo values greater than 0.3 and 0.6 respectively. Both showed systematic surface temperature decreases. There are difficulties with results from these studies, however (Ramanathan and Coakley 1978). Light haze, in the Wang and Domoto model, decreased surface temperature by 2 K° whereas their heat balance data used in equation (6-2) indicated a surface warming, while Reck's values of $(a/b)_{crit}$ were significantly larger than those given by equation (6-17). Further studies with radiative convective models may clarify these discrepancies (Reck and Hummel 1981).

Generalizations from boundary layer models are difficult to make (Viskanta *et al.* 1977) because of differences in meteorological conditions, concentration and radiative properties of aerosols and surface parameters. The dynamic model of Viskanta *et al.* (1977) showed that aerosols could play a major role in urban radiative regimes. Attenuation of solar radiation by aerosols (18%) agrees with estimates from measurements at Hamilton, Ontario (Rouse *et al.* 1973). Although aerosols increased incoming infrared radiation at the ground, those were substantially smaller than the 11% increases reported by Rouse *et al.* (1973). In general, the model produced a net warming of the system since the decrease in absorbed solar radiation by the ground was offset by increased solar radiation absorption in the system. This result agrees with the warming effect implied by much of the data in Figure 6-5a. Although these models are sensitive, through radiative transfer, to amounts and properties of aerosols, surface temperature changes are also sensitive to turbulent exchanges of sensible and latent heat, which, in turn, are dependent on atmospheric turbulence. Understanding aerosol effects on thermal regimes of cities and regions requires improvements in the models and input data, together with reliable measurements of radiation and energy exchange for real situations.

APPENDIX I.0 GLOSSARY

AERODYNAMIC PARTICLE DIAMETER: the diameter of a hypothetical sphere of unit density (1 g.cm^3) having the same terminal velocity as the particle in question.

DEPOSITION: removal of pollutants from the atmosphere by contact with and retention on the ground or ground supported protrusions.

ENTRAINMENT/SUSPENSION: the taking up into the atmosphere of particulate matter from a surface by the forces of wind or machinery.

POLLUTANT ARTIFACT: substance present within a collected air pollutant sample which was not present in the atmosphere but formed by a reaction of one collected pollutant with another or with the sample collection medium.

RE-ENTRAINMENT/RESUSPENSION: entrainment/suspension of particulate matter which was originally deposited from the atmosphere onto an exposed surface.

STOKES PARTICLE DIAMETER: the diameter of a hypothetical sphere having the same density and terminal settling velocity as the particle in question.

TOTAL SUSPENDED PARTICULATE: airborne particulate that is captured from ambient air as it is drawn into a standard high-volume sampler.

WIND EROSION: entrainment of particulate matter from an exposed surface into the atmosphere by the forces of wind.

APPENDIX II.0 EMISSION FACTORS FOR FUGITIVE EMISSIONS OF PARTICLES

II.1 PARAMETERS

At least six different parameters have been found to substantially affect fugitive emission rates: 1) soil type, 2) windspeed, 3) surface moisture, 4) precipitation, 5) vegetation cover, 6) traffic activity across the surface. The following discussion of these parameters is based on a report by Jutze and Axetell (1976).

1. Soil Type

Two different characteristics of soil are most important in determining emission rates: 1) soil structure, or its resistance to breakdown into its component particles; and 2) soil texture, or the site distribution of the individual component particles.

The standard measure of dust losses from soil surfaces is the erodibility index, e, in units of tons.$acre^{-1}.a^{-1}$. This index estimates the relative erodibility of different soil surfaces, not the actual quantities erodible under field conditions. The erodibility indices for different soil textures are shown in Table II-1. The erodibility index estimates the relative soil loss for different soil types, but does not adequately account for the greatly varying percentages of that total soil loss which are in the suspended particle size range and thus available to become airborne. Movement of larger soil particles near the ground is referred to as saltation or surface creep.

Figure II-1 gives comparable particle size ranges for different soil types and movements. The size limits shown are approximate as they depend on particle density, shape and surface forces as well as on particle size. The normal crusting characteristics of the soils are considered in their erodibility indices. Surface treatment with chemicals, compaction or controlled watering can enhance natural crusting and a well crusted soil surface loses dust at a rate of about one-sixth that of the same soil in a noncrusted state. Soils undergo seasonal changes in their erodibility as a result of biological activities, alternate wetting and drying, and freezing and thawing. These actions decrease erodibility in the winter and increase erodibility in the summer.

2. Wind Speed

Wind speed affects emission rates primarily from the wind erosion sources such as cleared land and agricultural fields. The rate of soil movement is a function of surface wind speed after it attains

Table II-1. Erodibility and average percent by weight of suspended particles for different soil types.

Soil Texture	Erodibility Index (tons.acre^{-1}.a^{-1})[α]	Aggregates < 0.05 mm, (percent by weight)[β]
Sand	220[δ]	0.9
Loamy sand	134	1.0
Sandy loam	86	2.1
Clay	86	0.8
Silty clay	86	0.8
Loam	56	0.6
Sandy clay loam	56	4.1[γ]
Sandy clay	56	1.0[γ]
Silty loam	47	4.1
Clay loam	47	2.5[γ]
Silty clay loam	38	4.1
Silt	38	0.8[γ]

[α] Source: Craig, D.G. and Turelle, J.W. Guide for wind erosion control on cropland in the great plains states. U.S Department of Agriculture, Soil Conservation Service. July 1964. Table 1.

[β] Source: Chepil, W.S. Soil conditions that influence wind erosion. U.S. Department of Agriculture, Agricultural Research Service and Kansas Agricultural Experiment Station, Washington, D.C. Technical Bulletin Number 1185. June 1958. Table 1.

[γ] Estimated from most similar soil types.

[δ] For conversion to metric units see Appendix II-3.

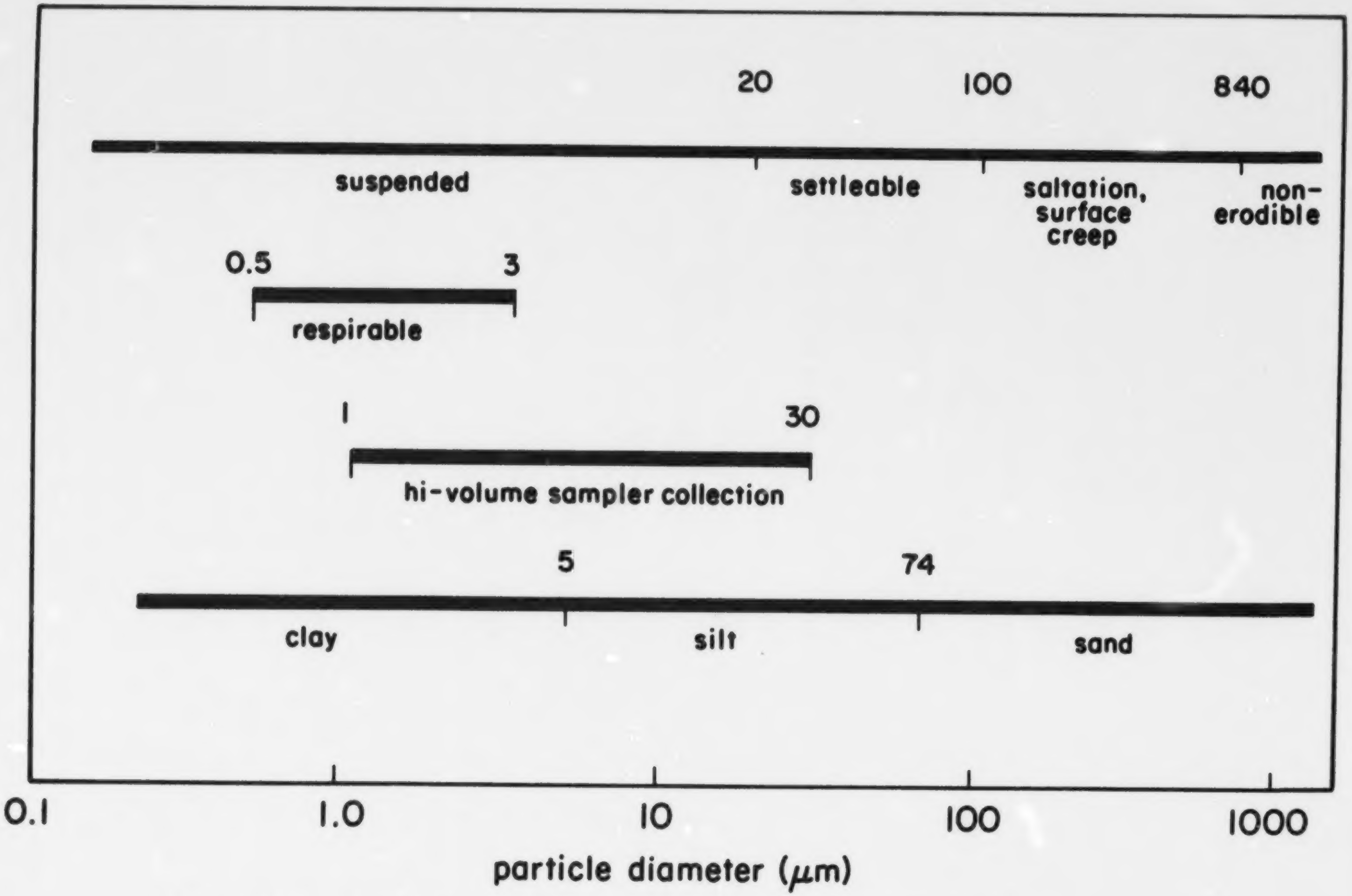

Figure II-1. Particle size ranges for soil types and soil movements (from Jutze and Axetell 1976).

some minimum or threshold speed necessary to initiate movement. Clearly, some allowance must be made for the aerodynamic effects of the surface being considered.

There is a high resistance of fine dust particles to erosion by wind partially because of cohesion but mainly because the particles are too small to protrude above a laminar and viscous layer of air close to the surface of the ground. Fine dust is lifted mainly by impacts of larger grains or other mechanical action.

Turbulence is as important as average velocity in lifting and transporting soil and so the gustiness and variation in speed are also factors affecting emissions.

3. Surface Moisture

For any surface moisture content above air-dried moisture content, a distinct decrease in erodibility is observed. Soil movement is reduced only slightly by the first moisture, but decreases more rapidly with additional moisture. At a moisture content approximately corresponding to the permanent wilting point for vegetation, soil loss is completely arrested.

The approximate percentage of water required to eliminate loss for various soil types is: dune sand (1%), sandy loam (4%), silty loam (11%) and silty clay (21%). Average surface moisture content of soils is not routinely measured. Instead, Thornthwaite's (1931) Precipitation-Evaporation (PE) Index, calculated from the sum of 12 monthly ratios of measured precipitation to measured evapotranspiration, is used as an indicator. Empirical data show that soil loss varies inversely as the square of the PE index. PE values do not give meaningful monthly climatic factors because of the large variations in monthly rainfall. Also, the PE index is not precise enough to evaluate soil moisture conditions for periods as short as one month. Only average soil moisture for a season or the entire year should be considered in the surface moisture function as a means of adjusting the locally applicable emission factor to reflect emission rates with normal retained moisture.

4. Precipitation

As long as the soil surface is noticeably moist, it will not generate airborne particles, even with traffic or surface activity. Analyses near fugitive dust sources on days with rain and no rain showed that hi-vol readings on rainy days are generally about half of those on nonrain days. These hi-vol measurements include some contribution from point sources, conventional area sources and background sources, as well as fugitive sources, so that the 50% reduction appeared to be from a large reduction in fugitive sources and rain out. On an annual or seasonal basis, the current assumption of no fugitive emissions on days with rain seems to be reasonable.

5. Vegetative Cover

Ground cover primarily reduces wind losses by: 1) absorbing some of the drag at the surface and decreasing the wind speed locally, and 2) acting as a soil binder. The initial ground cover on a field usually provides more protection than additional increments of vegetation.

The amount of vegetation is expressed in $lb.acre^{-1}$ of air-dried residue. For ground cover more than 250 $lb.acre^{-1}$, additional vegetation reduces soil loss approximately linearly. A ground cover of 1000 to 2000 $lb.acre^{-1}$ is required to eliminate soil loss. The amount of vegetation changes seasonally. Deciduous trees and bushes are reported to lose 20% to 40% of their effectiveness when they are defoliated in the winter. Hence, a usable estimate of average seasonal variations due to vegetation might be a 20% increase from annual emission rates during winter and a 20% reduction during summer for sources with ground cover.

6. Traffic Activity Across the Surface

Traffic movement over unpaved surfaces causes dust to be thrown into the air at contact points between the vehicle and the surface, or pulled into the air by the vehicles' wake. Also, traffic may break the protective surface crusts and leave the soil more susceptible to subsequent wind erosion. The fugitive dust emitted by traffic movement is related to the amount of traffic and its average speed. Most studies show that emission rates increase with higher vehicle speeds throughout the normal operating range of the vehicles. Within the accuracy of the measurements, the emission factor used should be a linear function of vehicle speed.

II.2 EMISSION FACTOR EQUATIONS[α]

Emission factor equations based on the best available data and methodology are detailed in this section. They will cover the following source types: 1) unpaved roads, 2) paved roads, 3) aggregate storage piles, 4) open area wind erosion, 5) heavy construction, and 6) agricultural tilling.

1. Unpaved Roads (Cowherd and Hendricks 1978)

$$E_{UR} = 5.9 \left(\frac{S}{12}\right) \left(\frac{V}{30}\right) \left(\frac{W}{3}\right)^{0.8} \left(\frac{d}{365}\right) \qquad \text{(II-1)}$$

where E_{UR} = pounds per vehicle-mile travelled,

[α] For conversions to metric units see Appendix II-3.

S = silt content of road surface material in % (that is, that passing through a 200 mesh screen),

V = average vehicle speed in miles per hour,

W = vehicle weight in tons, and

d = number of dry days per year.

The silt content (S) can be approximated by using a value of 12% for gravel roads or by using the silt content of the area parent soil for dirt roads if no on-site measurements are available. The number of dry days per year can be estimated from Figure II-2 which is plot of the mean annual number of days with 0.01 inches or more of rainfall (w) by using the following relationship:

$$d = (365 - w) \qquad \text{(II-2)}$$

Equation (II-1) is valid for vehicle speeds between 30 and 50 miles.h^{-1}, and gives a particle size distribution of 60% < 30 μm and 40% > 30 μm by weight.

Some discussion is presented in Ochsner et al. (1979) that suggests that a factor accounting for the degree of mechanical disturbance of the roadbed can be included by adding the term (number of wheels/4)$^{0.5}$ to equation (II-1). In most cases of mining and industrial operations, this has the effect of adding 20% to the emissions since large off-road trucks generally have six or more wheels. Various control strategies can be applied to reduce emissions from unpaved roads that result in various levels of control efficiency. Table II-2 lists some control methods and efficiencies.

2. Paved Roads (Cowherd and Hendricks 1978)

$$E_{PR} = 0.45 \left(\frac{S}{10}\right) \left(\frac{L}{5000}\right) \left(\frac{W}{3}\right)^{0.8} \qquad \text{(II-3)}$$

where E_{PR} = pounds per vehicle-mile travelled,

S = silt content of the surface dust in %,

L = surface dust loading on the travelled portion of the road in pounds per mile, and

W = vehicle weight in tons.

The most efficient control method for reducing emissions from paved roads is street-washing. No data are available but the correlation factor for the number of wheels is also probably applicable in this case.

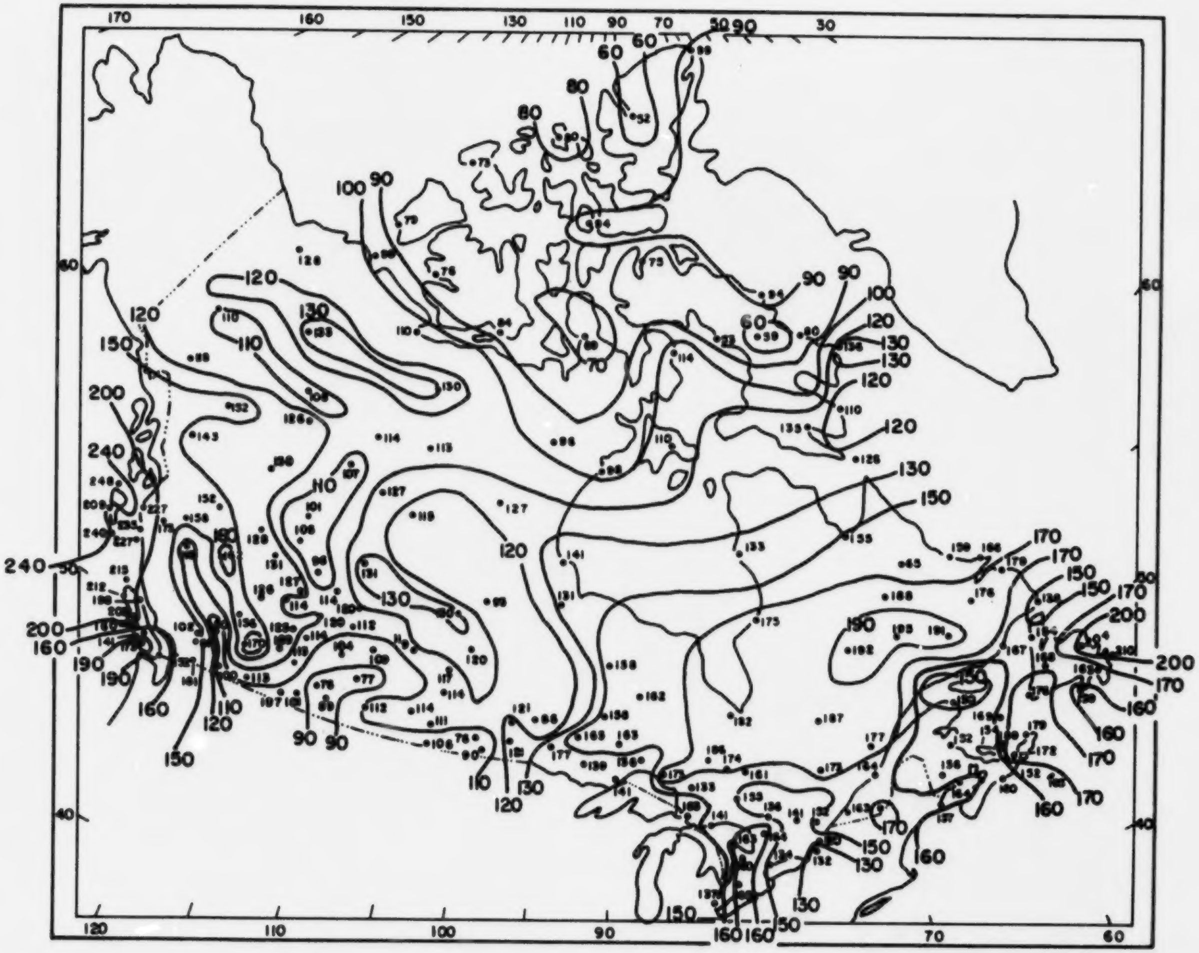
170
160
150
130
110
90
70
50
30
120
110
100
90
70
60
60
40
60
40
60
60
80
80
90
100
90
90
100
120
130
130
120
120
130
150
170
170
150
150
170
200
200
170
160
160
170
160
170
170
150
130
130
150
160
160
150
130
120
120
110
130
120
110
130
110
120
150
200
240
240
200
160
190
190
160
110
120
150
90
90
190
60
70
120

Figure II-2. Mean annual number of days with 0.01 inches or more of rainfall (w) for Canada (1941-1970).

Table II-2. Various control strategies used to reduce emissions from unpaved roads.

Control Method		Control Efficiency
Paving		85%
Treating with surface penetrating chemicals		50%
Working soil stabilizing chemicals into roadbed		50%
Speed control	> 40 miles/hour	0%
	30 miles/hour	25%
	20 miles/hour	65%
	15 miles/hour	85%

3. Aggregate Storage Piles (Cowherd and Hendricks 1978)

a) Conveyor Load-in (continuous)

$$E_{CLI} = 0.0018\ (\frac{S}{5})\ (\frac{U}{5}) /\ (\frac{M}{2})^2 \qquad \text{(II-4)}$$

where E_{CLI} = emission rate in pounds per ton of material put through storage,

S = silt content of the aggregate in %,

U = mean wind speed in miles per hour, and

M = moisture content of the aggregate in %.

Cowherd and Hendricks suggest that the free-fall height will influence the emission rate. Limited testing by Lovblad and Grennfelt (1977) confirms this but an equation modification has not been made. The most effective control is to limit the free fall using telescoping chutes or stacking conveyors.

b) Batch Load-in/out

$$E_{BLI} = 0.0018\ (\frac{S}{5})\ (\frac{U}{5})\ /\ \left[(\frac{M}{2})^2\ (\frac{Y}{6})\right] \qquad \text{(II-5)}$$

where E_{BLI} = emission rate in pounds per ton of material put through storage,

S = silt content of aggregate in %,

U = mean wind speed in miles per hour,

M = moisture content of the aggregate in %, and

Y = dumping device capacity in cubic yards.

c) Storage Pile Wind Erosion

$$E_{SPWE} = 0.05\ (\frac{S}{1.5})(\frac{d}{235})(\frac{f}{15})(\frac{D}{90}) \qquad \text{(II-6)}$$

where E_{SPWE} = emission rate in pounds per ton of material put through storage,

S = silt content of aggregate in %,

d = number of dry days per year,

f = percentage of the time that wind speed exceeds 12 miles per hour, and

D = length of time (duration) that the material stays in storage in days.

Cowherd and Hendricks (1978) state that this equation provides for aerodynamic effects of the pile by assuming that the emissions are reduced to correspond to an average wind speed of half the pile top wind speed in the emission zone. The only control measures available are spraying with water or a sealant, and compaction.

d) Storage Pile Maintenance and Traffic (Cowherd and Hendricks 1978)

$$E_{SPMT} = 0.10\ K\ (\frac{S}{1.5})(\frac{d}{235}) \qquad \text{(II-7)}$$

where E_{SPMT} = emission rate in pounds per ton of material put through storage,

K = activity factor,

S = silt content of the aggregate in %, and

d = number of dry days per year.

The activity factor (K) is related to the intensity of the materials handling activity and no guidance is provided for its calculation. For the worst case, assume K = 1.

4. Open Area Wind Erosion (Cowherd *et al*. 1979)

$$E_{OA} = 3400\ (\frac{e}{50})(\frac{S}{15})(\frac{f}{25})\ C\ /\ (\frac{PE}{50})^2 \qquad \text{(II-8)}$$

where E_{OA} = emission rate in pounds per acre per year of exposed land,

e = soil erodibility or potential annual soil loss rate for a wide, unsheltered, isolated field with a bare, smooth surface in tons per acre per year,

S = silt content of eroding surface in %,

f = percentage of the time that wind velocity measured one foot above the surface exceeds the nominal wind erosion threshold value of 12 miles per hour,

C = fractional value reflecting the reduction of wind erosion due to vegetative cover (bare soil = 1.0), and

PE = Thornthwaite's Precipitation-Evaporation Index.

Soil erodibility can be estimated from Table II-1.

From data given in Jutze and Axetell (1976), the vegetative cover parameter can be estimated from the assumed linear relationship given in Figure II-3. Typical values for common field crops are presented in Table II-3. Thornthwaite's Precipitation-Evaporation Index (PE) is a measure of the annual or seasonal surface moisture function and is used to adjust emission rates reflecting normal retained moisture. Using the method outlined in Thornthwaite (1931), Figure II-4 gives the annual PE index for Canada.

5. Heavy Construction

In the area of heavy construction, data are not sufficient to derive the specific dependence of dust emissions on the various contributing parameters. U.S. EPA (1975) gives an emission rate for apartment and construction projects as: 1.2 tons.acre^{-1} of construction per month of activity. This assumes a medium activity level, moderate silt content (approx. 30%) and a semiarid climate (PE approximately 50). Twice daily watering of the complete area of activity will reduce emission by up to 50%.

The equations given by emissions from open areas (equation II-8), unpaved roads (equation II-1) and storage piles (equations II-5 and II-6) can be used to give estimates for heavy construction activity.

6. Agricultural Tilling (Evans and Cooper 1980)

$$E_{AT} = 1.1\ TS\left(\frac{V}{5.5}\right) / \left(\frac{PE}{50}\right)^2 \qquad (II\text{-}9)$$

where E_{AT} = emission rate in pounds per acre,

T = number of tillings.a^{-1},

S = silt content of agricultural soil (%),

PE = Thornthwaite's Precipitation Evaporation Index,

V = implement speed (mph)

This yields a total emission rate and tests show that the particle size distribution by weight is as follows: < 2 μm (35%), 2-30 (45%), > 30 μm (20%) (Mathtech Inc. 1980).

Evans and Cooper (1980) suggest that irrigation water can be converted to an equivalent rainfall for use in the PE equation. Mathtech Inc. (1980) advances the following argument. To develop an emissions model based on short-term precipitation and temperature data,

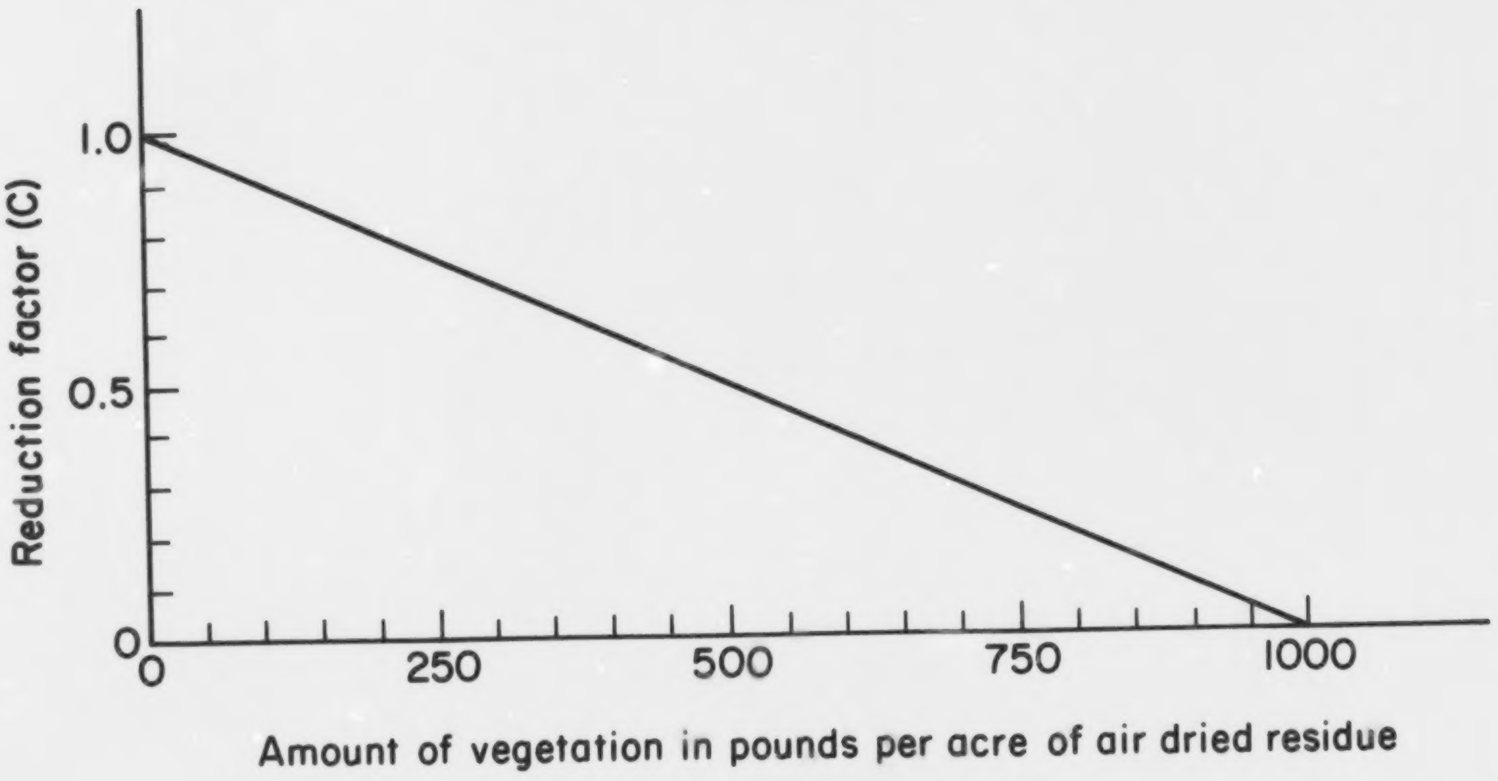

Figure II-3. Reduction factor (C) for wind erosion over vegetative cover (adapted from Jutze and Axetell 1976).

Table II-3. Values of equivalent vegetative cover for common field crops (from Jutze and Axetell 1976).

Crop	V ($lb.acre^{-1}$)
Alfalfa	3000
Barley	1100
Beans	250
Corn	500
Cotton	250
Grain hays	1250
Oats	1250
Peanuts	250
Potatoes	400
Rice	1000
Rye	1250
Safflower	1500
Sorghum	900
Soybeans	250
Sugar beets	100
Vegetables	100
Wheat	1350

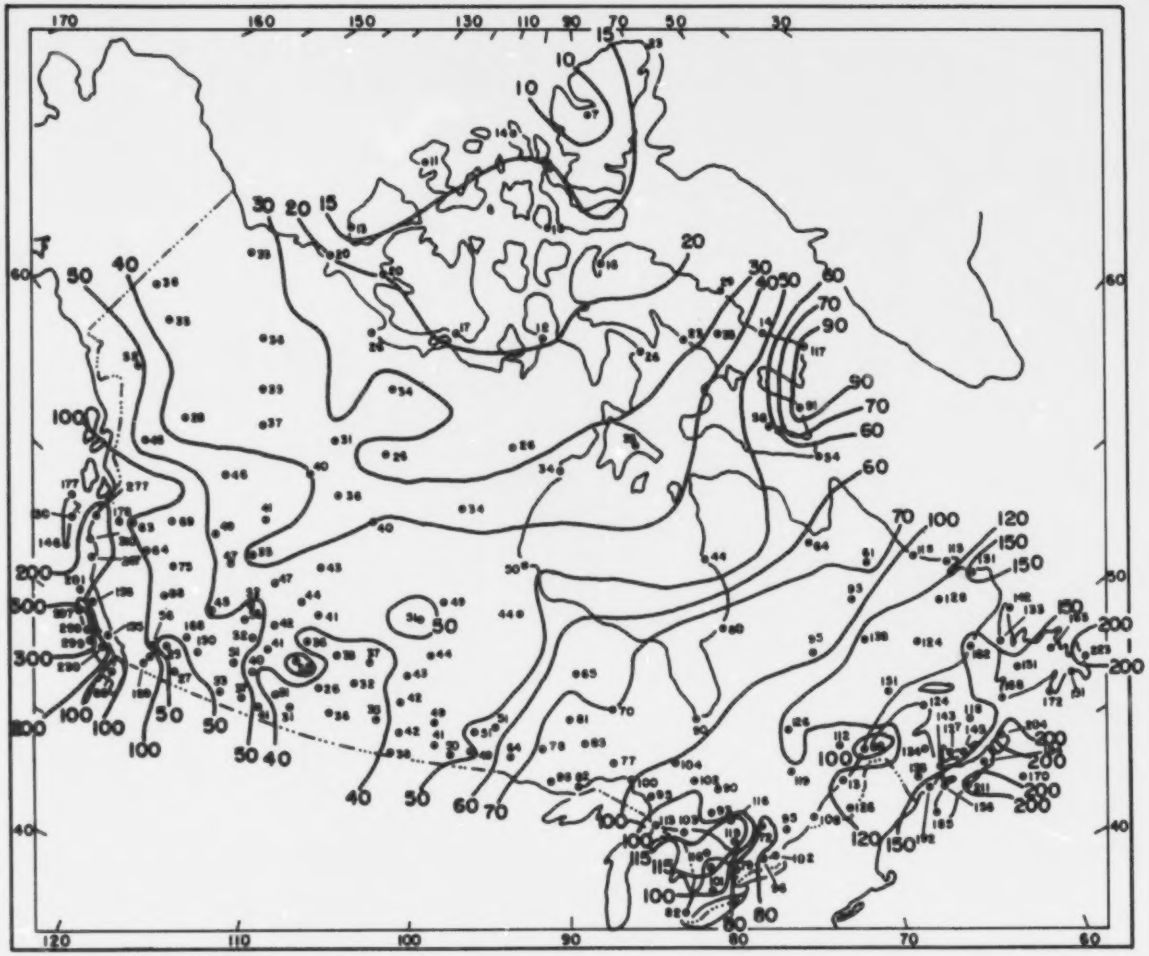
170
160
150
130
110
90
70
50
30
120
110
100
90
80
70
60
60
50
40
10
15
20
30
40
50
60
70
80
90
100
115
120
150
200
300

Figure II-4. Thornthwaite's Annual Precipitation-Evaporation Index for Canada (1941-1970).

consider the equation

$$pe = \left[\left(\frac{720}{t}\right)\left(\frac{P_t}{T - 10}\right)\right]^{10/7} (115 \times 12) \qquad \text{(II-10)}$$

where P_t = inches of precipitation during 5 hours,

$\frac{720}{t}$ = scale-up factor to equate P_t to monthly precipitation

T = average temperatue (°F) during t hours.

The pe is a short-term P/E ratio. The formulas which can be used to estimate emissions during the eight-hour sampling periods for field measurements are:

$$E = \frac{K}{pe^2} \text{ if } pe > 10; \qquad \text{(II-11)}$$

$$E = \frac{K}{100} \text{ if } pe < 10 \qquad \text{(II-12)}$$

The lower limit of 10 for the pe index was taken from the minimum value of Thornthwaite's PE indices for the continental United States. When pe < 10 occurs, no soil moisture is assumed.

To calculate pe, it is reasonable to use a value of t equal to the number of hours since the last period of precipitation. Thus, $1/pe^2$ will be zero during precipitation and will decrease to 0.01 as t increases. A similar formula can be applied to the watering of roads. Suppose K gallons of water are applied to an area of X square inches; this is equivalent to 231 K/X inches of rainfall. This value should be added to P to obtain total precipitation on a road.

To a certain extent, the above definition of an hourly PE index is unsatisfactory. If emissions are calculated over each hour for a year, the calculated annual emissions will not equal those given by using an annual PE index.

II.3 CONVERSION FACTORS

As the preceeding section was developed in English units, the following conversion factors are given for the metric system:

1 pound = 0.454 kilogram

1 foot = 0.305 metre

1 mile = 1.61 kilometres

1 acre = 0.00405 square kilometre

1 short ton = 0.907 metric tonne

1 mile/hour = 0.447 metre/second

1 cubic foot/minute = 1.70 cubic metres/hour

1 pound/acre = 0.112 gram/square metre

APPENDIX III.0 OPTICAL PROPERTIES OF AEROSOLS AND MEASUREMENT TECHNIQUES

III.1 PARAMETERIZATION

It is convenient to parameterize the particle size by the nondimensional parameter

$$x = 2\pi a/\lambda \qquad \text{(III-1)}$$

where λ is the wavelength of light, a is the particle radius and

$$\lambda = c/\nu \qquad \text{(III-2)}$$

where ν is the frequency of light and c is the speed of light.

A second important optical parameter is the complex index of refraction:

$$m(x) = n_R(x) - n_I(x) \qquad \text{(III-3)}$$

where n_R and n_I are the real and imaginary indices of refraction, respectively. The absorption coefficient of the particle is given by:

$$\alpha = 4\pi n_I/\lambda \qquad \text{(III-4)}$$

Equation III-3 has been written as a function of x since there is considerable evidence that the index of refraction of real particles is dependent on their size as well as on the wavelength of light. However, the composition of particles as a function of particle size is an area of current research and analytical solutions for light scattering are currently available where the indices of refraction are independent of both particle size and wavelength.

A third set of parameters deal with the scattering geometry of the interaction of a photon with the particle (Figure III-1). The polar angle θ becomes the primary angular factor in scattering of light from aerosols while the angle ϕ is of importance in determining the degree of scattering from the two polarization states of the incoming radiation. These polarization components for a linearly polarized input photon would be i_1 and i_2 for the scattered radiation components perpendicular and parallel to the input photon polarization.

III.2 SOLUTIONS FOR LIGHT SCATTERING BY SPHERICAL PARICLES (Mie 1908)

Analytical solutions for the amount of light scattered by spherical dielectric particles were derived by Mie. Subsequent contributions to the theory have been primarily concerned with the application

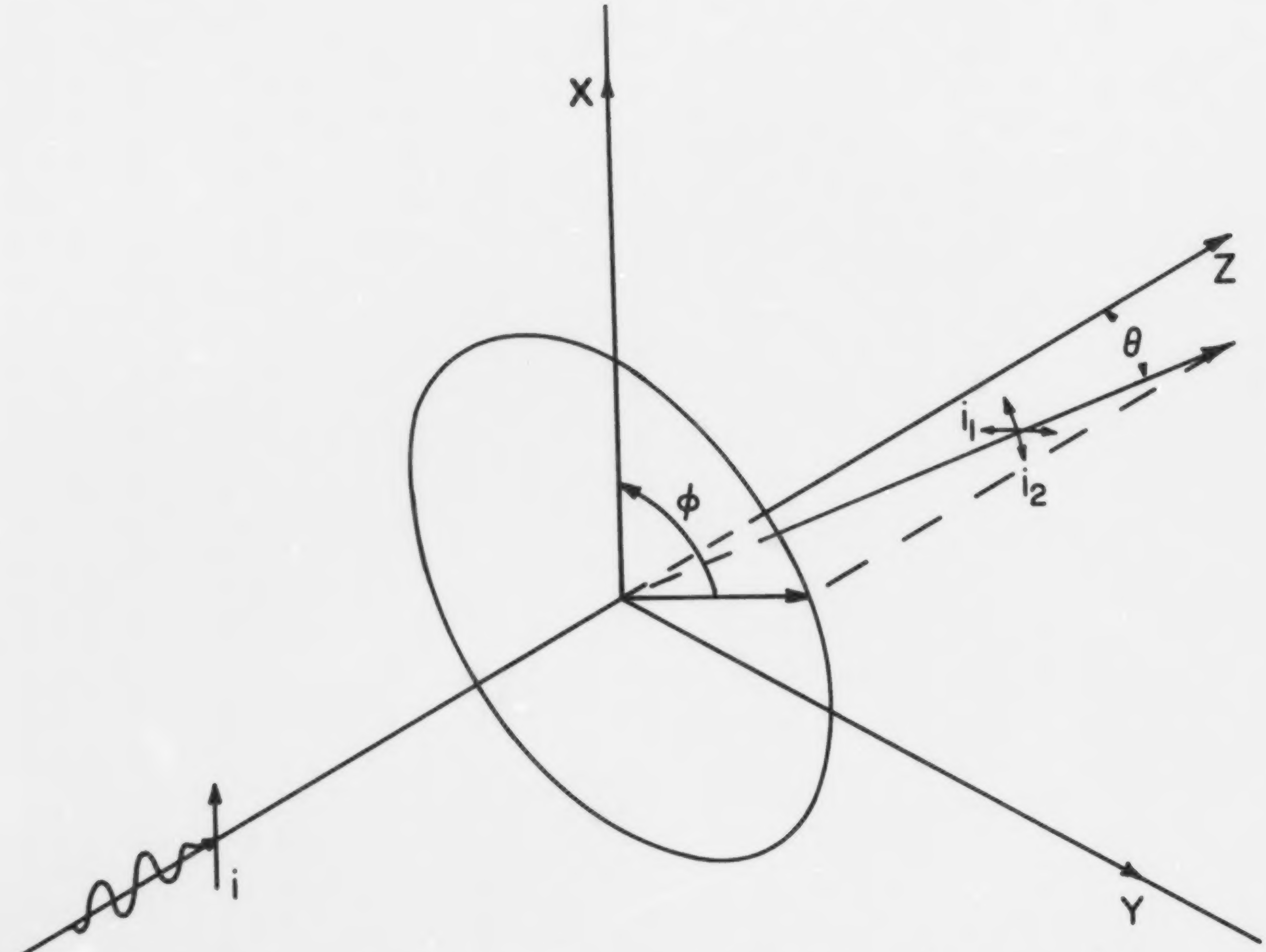
X
Z
θ
ϕ
i_1
i_2
i
Y

Figure III-1. Scattering geometry for the interaction of a photon with a particle.

of numerical techniques and algorithms, so that computers could most efficiently process the complex functions involved in the theory. The nomenclature used in the appendix follows Van de Hulst (1957) and Kerker (1969). The scattered intensity functions of the input radiation field of unit irradiance are:

$$i_1 = \left| \sum_{n=1}^{\infty} \frac{2n+1}{n(n+1)} \left(a_n \pi_n (\cos\theta) + b_n \tau_n (\cos\theta)\right) \right|^2 \qquad \text{(III-5)}$$

and

$$i_2 = \left| \sum_{n=1}^{\infty} \frac{2n+1}{n(n+1)} \left(a_n \tau_n (\cos\theta) + b_n \pi_n (\cos\theta)\right) \right|^2 \qquad \text{(III-6)}$$

where the coefficients a_n, b_n are products of Ricatti - Bessel functions whose arguments are functions of x, m and the coefficients τ_n and π_n are given by:

$$\tau_n (\cos\theta) = \frac{1}{\sin\theta} P_n^{(1)} (\cos\theta) \qquad \text{(III-7)}$$

$$\pi_n (\cos\theta) = \frac{d}{d\theta} P_n^{(1)} (\cos\theta) \qquad \text{(III-8)}$$

where P_n are the nth Legendre polynomials. It is appropriate for many applications to integrate these solutions over all scattering angles, θ, and to talk of total efficiencies for extinction. Extinction denotes the amount of radiation removed from the incident wave from processes of scattering and absorption. The extinction efficiency is:

$$Q_{ext} = C_{ext}/\pi a^2 = \left(\frac{2}{x^2}\right) \sum_{n=1}^{\infty} (2n+1) \operatorname{Re} (a_n + b_n) \qquad \text{(III-9)}$$

where C_{ext} is the extinction cross section. The scattering efficiency is:

$$Q_{sca} = C_{sca}/\pi a^2 = \left(\frac{2}{x^2}\right) \sum_{n=1}^{\infty} (2n+1) \left(|a_n|^2 + |b_n|^2\right) \qquad \text{(III-10)}$$

and

$$Q_{ext} = Q_{sca} + Q_{abs} = \frac{1}{\pi a^2} \left(C_{sca} + C_{abs}\right) \qquad \text{(III-11)}$$

The details of numerical solutions to these equations are not appropriate here and the reader is referred to the literature (Dave 1968, 1970; Deirmendjian 1969). Extensive catalogues of the numerical solutions for various particle size distributions and indices of refraction are available (Kerker 1969; Van de Hulst 1957; Deirmendjian 1969).

Figure III-2 shows the scattering efficiency as function of θ for a specific index of refraction and size parameter. Devices, such as the polar nephelometer, are designed to exploit these scattering signatures to characterize particle distributions. In general, however, instrumentation has been designed to minimize response to these strong

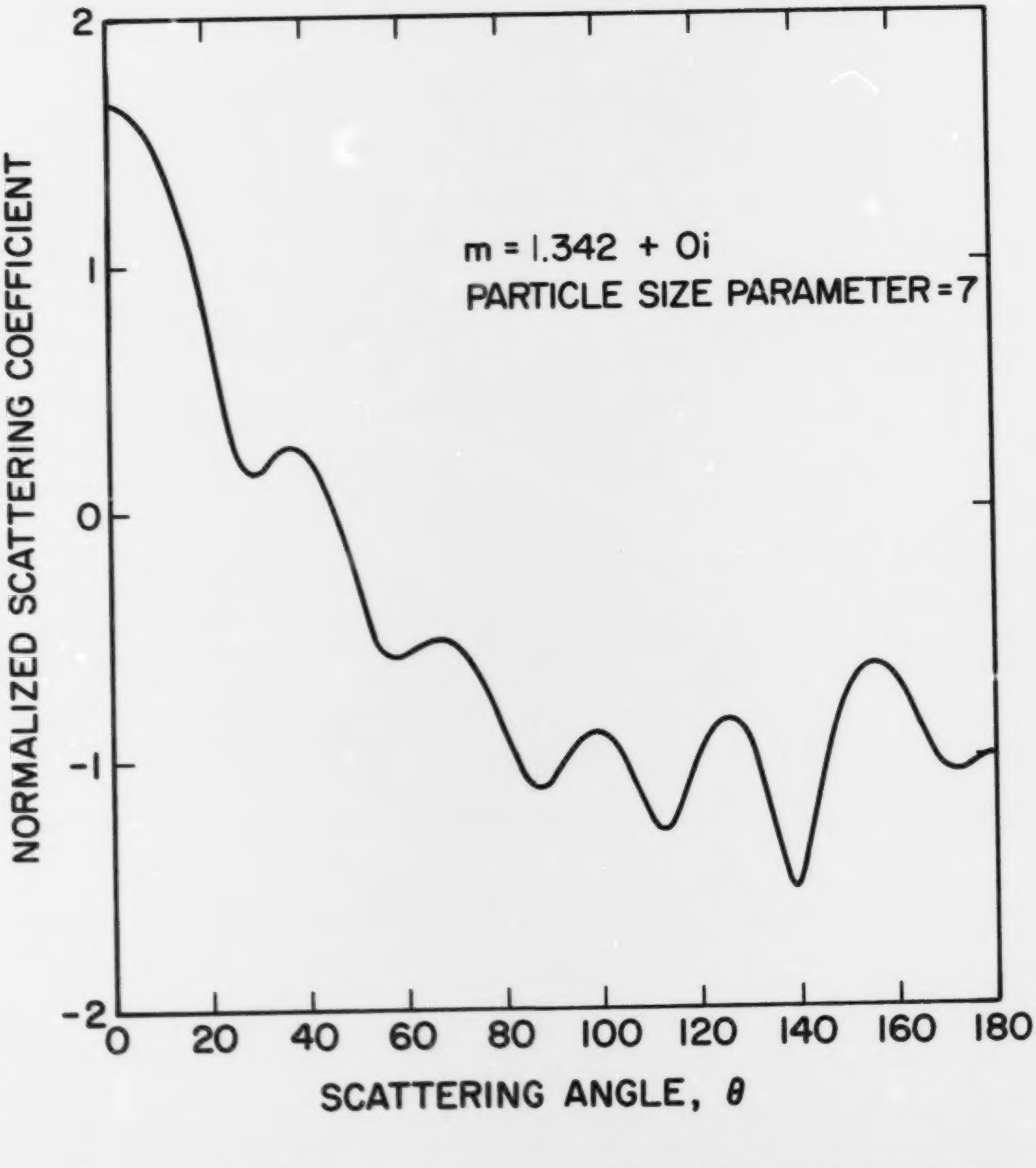

Figure III-2. Scattering efficiency as a function of scattering angle. Scattering efficiency normalized by the factor $(4/Q_{sca} \cdot x^2)$.

scattering function variations. The total extinction for monochromatic radiation of wavelength, λ, of a volume of particles with density $N = \int_0^\infty n(a)da$, where $n(a)$ is the particle number per unit radius is:

$$b_{ext}(\lambda, m) = \int_0^\infty C_{ext}(x, m)dn(a) \qquad \text{(III-12)}$$

$$= \int_0^\infty \pi a^2\, Q_{ext} dn(a) \qquad \text{(III-13)}$$

and similarly

$$b_{sca}\,(\lambda, m) = \int_0^\infty C_{sca}\,(x, m)dn(a) \qquad \text{(III-14)}$$

$$= \int_0^\infty \pi a^2\, Q_{sca}\,(x,m)dn(a) \qquad \text{(III-15)}$$

When a white light or non-monochromatic extinction coefficient is needed (cf. for visibility calculations) one must separately integrate over radius and wavelength in equations (III-13) and (III-15). This integration over wavelength has the attractive advantage of smoothing the features of Q_{ext} (which otherwise makes linear instrumental response to optical properties of the aerosols improbable).

III.3 THE RELATIONSHIP OF THE EXTINCTION COEFFICIENT TO VISIBILITY

The Beer-Bouguer-Lambert law of extinction applied to the luminance of a target L(0) gives the apparent luminance L(D) at a distance D from the target:

$$L(D) = L(0)\, \exp \left[- \int_0^D \sigma(R)dR \right] + L_A \qquad \text{(III-16)}$$

The additional "airlight" term L_A is the total luminance introduced into the line of sight from observer to target by atmospheric scattering of light from extraneous sources, e.g. sunlight (see Figure III-3). $\sigma(R)$ is the volume extinction coefficient and equals b_{ext} (eq. III-12).

By definition:

$$C = (L_T - L_B)/L_B \qquad \text{(III-17)}$$

where C is the luminance contrast ratio of the target luminance L_T and background luminance L_B. Substitution of this definition into equation (III-16) gives an expression for the propagation of the luminance contrast ratio:

$$C(D) = C(0)\, \exp \left[- \int_0^D \sigma(R)dR \right] L_B(0)/L_B(D) \qquad \text{(III-18)}$$

Koschmieder's model assumption of horizontal uniformity allows the integral to be replaced by the product σD. Horizontal uniformity

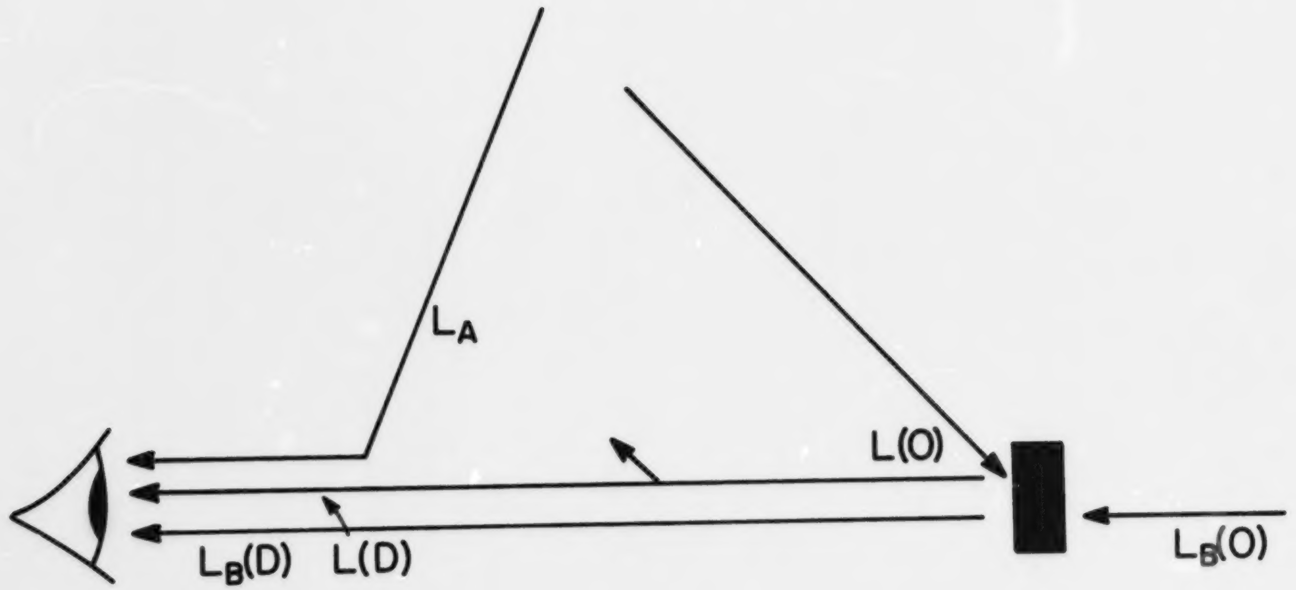

Figure III-3. Contributions to luminosity seen by an observer. L_B is background luminance, L is target luminance and L_A is "airlight" luminance.

of illumination implies $L_B(D) = L_B(0)$ (i.e. the background horizon luminance is constant). A black target is also assumed and gives $C(0) = -1$.

Equation (4-18) becomes:

$$C(D) = -\exp(-\sigma D) \qquad \text{(III-19)}$$

Therefore if the luminance contrast ratio of a target at distance D is equal to the luminance constrast threshold (ε) of the observer, then this target is just detectable and the visibility (V) is defined as that distance.

From equation (III-19) Koschmieder's Law is:

$$\varepsilon = + \exp(-\sigma V) \qquad \text{(III-20)}$$

where the minus sign is absorbed by the appropriate definition of ε. Koschmieder assumed a value of $\varepsilon = 0.02$ for which we have the simple relationship between visibility and extinction:

$$V = 3.91/\sigma \qquad \text{(III-21)}$$

Allard's Law was formulated in 1876. It considers the loss of illumination from a point source of light due to the $1/R^2$ factor and extinction:

$$E(D) = I\ D^{-2} \exp(-\sigma D) \qquad \text{(III-22)}$$

where E is the illumination at a distance D from a source of intensity I. As for Koschmieder's model the atmosphere is assumed planar with uniform extinction coefficient in each layer.

If the illumination from a point source at distance D equals the illumination threshold (E_t) of the observer, then the source is just detectable, and the visibility (V) is defined as that distance.

From equation (III-22) Allard's Law is:

$$E_t = I\ V^{-2} \exp(-\sigma V) \qquad \text{(III-23)}$$

This equation is usually applied when the ambient illumination is low and the inherent contrast of nonluminous targets against the sky approaches zero. At such times artificial sources of light become the predominant visibility targets. Their distance from the observer compared to their dimensions allows them to be considered point sources.

Several sources of inaccuracies arise in the determination of visibility through the extinction coefficient. The atmosphere is seldom uniform over the spatial scale of typical visibilities. Thus large errors in estimating visibility from Koschmieder's or Allard's Laws can arise when point samples of σ are assumed representative of the entire field of view of an observer. However, this is a necessary assumption with present day commercial sensors since it is impractical to measure σ over more than few hundred metres of path length or in more than one direction.

If there are extraneous sources of luminance entering the line of sight such as scattered sunlight from a fog, the apparent contrast ratio may be "washed out". Quantitatively this effect is represented by the term $L_B(0)/L_B(D)$ in equation (III-18) when the background luminance at the point of observation $L_B(D)$ greatly exceeds its value measured at the target $L_B(0)$. This implies that "airlight" term L_A in equation (III-16) is significant. Extreme cases of such "white out" conditions can greatly reduce contrast and therefore the visibility.

Another factor is that Koschmieder's and Allard's Laws deal only with the physical processes which affect visibility and do not fully account for the complex physiological processes of the human visual system. The luminance contrast threshold ε is not a constant but is dependent on such factors as the adaption luminance of the retina, the dimensions and color of the target, the time available for searching for the target and the physical and psychological condition of the observer. For identical experimental conditions there are variances amongst observers.

The illumination threshold is an even stronger function of adaptation luminance and this fact must be taken into account if Allard's Law is to be applied to visibility calculations such as runway visual range.

Koschmieder's Law gives the distance at which a target can just be detected but in many applications recognition is also necessary. This requires more definition in the image, making the recognition distance less than the detection distance.

A final consideration in the determination of visibility is the problem of slant visual range versus horizontal visibility. Because the atmosphere is not only nonuniform in a horizontal plane but also vertically, horizontal visibility parameters such as prevailing visibility and runway visual range may not adequately represent the pilot's actual visibility along the approach glide path called the slant visual range (SVR).

While a measure of RVR (runway visual range) is necessary to determine the pilot's visibility once on the runway, an accurate slant visual range measurement on the glide path is needed to determine if visual contact with the runway will occur before the aircraft has reached its minimum altitude for ground contact (decision height).

III.4 TURBIDITY PARAMETERS

In an atmosphere which contains no water vapor or other absorbers and has no haze or dust, the depletion of solar radiation is mainly by molecular or by Rayleigh scattering with a scattering coefficient having a λ^{-4} wavelength dependence. Linke and Boda (1922) referred the extinction coefficient in an actual turbid atmosphere to this basic scattering effect and defined a Turbidity Factor (T) which was an indicator of how many atmospheres of pure air would produce the same total depletion of direct solar radiation as measured by an instrument sensitive to all wavelengths. Since the Rayleigh scattering coefficient is dependent on wavelength, the mean extinction coefficient becomes a function of the airmass and hence T is not constant even when the atmospheric turbidity remains constant.

Using the Beer-Lambert Law, one can derive an expression for the attenuation through the whole atmosphere of the form:

$$I\ (\lambda) = I_0(\lambda)\exp(-m\tau(\lambda)) \qquad \text{(III-24)}$$

where I_0 is the normal incident radiation intensity at the top of the earth's atmosphere, m is the air mass (the secant of the solar zenith angle), and $\tau(\lambda)$ is the optical thickness for an air mass of unity. The optical thickness can be partitioned to account for Rayleigh scattering ($\tau_R(\lambda)$), gaseous absorption ($\tau_g(\lambda)$) and aerosol scattering ($\tau_A(\lambda)$) giving:

$$\tau(\lambda) = \tau_R(\lambda) + \tau_g(\lambda) + \tau_A(\lambda) \qquad \text{(III-25)}$$

The gaseous absorption term ($\tau_g(\lambda)$) is normally used only for an ozone correction. Angstrom (1929) approximated ($\tau_A(\lambda)$) using an expression of the form:

$$\tau_A(\lambda) = \beta\ \lambda^{-\alpha} \qquad \text{(III-26)}$$

for wavelengths near one micron where β is referred to as the turbidity coefficient and α is called the wavelength exponent. Substitution of (III-25) and (III-26) into (III-21) and introducing a factor S to account for the variations in the earth-sun distance gives:

$$I(\lambda) = \frac{I_0\ (\lambda)}{S} \exp\left[- m\ (\tau_R + \tau_g + \beta\lambda^{-\alpha})\right] \qquad \text{(III-27)}$$

Schuepp (1949) proposed a similar expression:

$$I(\lambda) = \frac{I_0\ (\lambda)}{S}\ .10^{-m\ (\tau_R + \tau_g + \beta\lambda^{-\alpha})} \qquad \text{(III-28)}$$

for wavelengths near 0.5 μm where β is referred to as the Decadic turbidity coefficient.

The formulated approximations for aerosol scattering in both equations (III-27) and (III-28) are valid over the wavelengths from 0.5 to 3.5 μm and for Junge-type (power law) size distributions of aerosols which follow the form:

$$dn = Cr^{-(\alpha+3)}dr \qquad \text{(III-29)}$$

where r is the particle radius and n is the number of particles per unit volume per unit radius interval. This is a reasonable approximation for some types of continental aerosols but not for other forms such as marine aerosols. For this reason it would be preferable to simplify the Schuepp and Angstrom formulations and use only the aerosol optical thickness as a measure of atmospheric turbidity. Thus equation (III-28) could be solved for the aerosol optical thickness to yield:

$$\tau_A(\lambda) = \frac{1}{m} \log_{10} \frac{S \cdot I(\lambda)}{I_o(\lambda)} - \tau_g(\lambda) - \frac{p}{p_o} \tau_R (\lambda) \qquad \text{(III-30)}$$

where the Rayleigh scattering terms have been modified by the ratio of the standard atmospheric pressure at the point of observation (p) and the mean sea level pressure (p_o) to allow for changes in τ_R arising from differences in elevation.

For astronomical purposes, an extinction coefficient k, has been used (Roosen _et al_. 1973) based on the formulation:

$$\frac{I(m)}{I_o} = 10^{\frac{k}{-2.5} \cdot m} \qquad \text{(III-31)}$$

where k is given in units of stellar magnitudes per unit airmass.

III.5 METHODS OF MEASUREMENT

An excellent compendium on visibility instrumentation as well as other visibility related matters is given by Douglas and Booker (1977). In this section, a brief overview on instrumentation, which yields visibility and turbidity related parameters, will be described.

A transmissometer is a telephotometer for measuring the transmittance of the atmosphere over a fixed baseline. Transmittance is defined as the ratio of received to projected illumination over a specified distance. Extinction of light from a focussed source is due to scattering or absorption by the particulate matter in the beam. Koschmieder's and Allard's Laws can be rewritten in terms of transmittance:

$$\varepsilon = T^{V/B} \qquad \text{(III-32)}$$

$$E_T = (I\ T^{V/B})/V^2 \qquad \text{(III-33)}$$

where T is the transmittance over a baseline B, the other constants having been defined in Section III.3. These equations form the basis for the "Day" and "Night" runway visual range (RVR) equations.

Douglas and Young (1945) designed a transmissometer for the United States National Bureau of Standards. The instrument is calibrated against meteorological observations of V to determine a value of $\varepsilon = 0.055$. E_t was defined for the RVR nighttime use as 2.0 mile-candles. This instrument and these values have been used operationally in North America to measure RVR for the past 30 years. Similar instruments are used in other countries.

The advantage of transmissometers over other visibility sensors such as scattering function meters is that they measure an atmospheric parameter that is directly related to visibility through equations (III-20) and (III-23). However they have some disadvantages in practical operation. Their installation is costly because the projector and receiver require stable concrete bases. Frequent maintenance is necessary to assure alignment of receiver and projector optics and adjustment of lamp intensities. Also calibration is difficult except on very clear days when the transmittance is assumed to be 100%.

The accuracy of visibility measurements by transmissometers is nonlinear over the range of transmittance because of the exponential nature of equation (III-32). Assuming T can be measured to 1%, which is demanding in practice, then visibility is accurate to 10% over a range from ½ to 20 times the baseline length. This limits the measurement range of a 250-foot-baseline[α] transmissometer from about 0.02 to 1 mile, which is suitable for RVR but not other applications.

For these reasons, a new generation of visibility sensor has been developed in the past 20 years. These instruments measure the angular scattering function of the atmosphere in a small volume near the sensor. For this parameter to be a unique measure of the atmospheric extinction two assumptions are necessary. First there is to be no absorption, i.e. all extinction is due to scattering alone. At visual wavelengths this is usually the case, but in industrially polluted air, this assumption may lead to an underestimation of the extinction coefficient by as much as a factor of 3.

Secondly, it is assumed that the total scattering coefficient will be a unique function of scattering at a particular angle or range of angles for all types of particles. The Mie theory indicates that in general this is not the case. There are however certain scattering angles less dependent on variations in the particle size to wavelength ratio (equation III-1) than others.

For practical reasons, the first commercial sensors of this type were backscatter meters because the projector and receiver optics

---

[α] For conversions to metric units see Appendix II-3.

were most easily configured in a single housing. The monitoring volume may extend several hundred feet, but under reduced visibilities the majority of the sensed light is from a much smaller range.

Forward scatter meters were developed to take advantage of the constancy of the angular scattering to total scattering ratio over limited angular ranges in the near forward direction. The geometric configuration of these sensors usually limits their monitoring volume to a much smaller region than backscatter sensors. However, unless the sensor restricts the free circulation of the atmosphere or changes the characteristics of the particles, these smaller volumes seem just as representative of the observers' field of view as those of backscatter devices.

A third type of scattering function meter is the integrating nephelometer. The geometry of the field of view of the detector relative to the illumination of the scattering volume permits viewing from 7° to 170° of the optic axis. This integration over a large range of scattering angles gives rise to the name of the device and theoretically should remove intensity fluctuations due to the τ and π functions (equations III-5 to III-8). In practice, because of the large dynamic range in intensity as a function of angle (see Figure III-2), forward and backward directions are still predominant in the measured scattered intensity. These devices have demonstrated reasonable linearity with particulate mass loadings in the atmosphere (Charlson et al. 1967). A criticism of these devices is that they do not respond accurately in measuring visibility during precipitation events. A model analysis of the use of nephelometers for obtaining visibility has been carried out by Harrison (1979).

A polar nephelometer is a device which measures the scattering function (Figure III-2) directly. The result can be inverted (with varying degrees of success) to give the size distribution of the aerosol or integrated to give $b_{scat} = b_{ext}$ (by assumption), from which a visibility might be derived. These devices, however, are presently more suited to laboratory work and are not commercially available for atmospheric aerosol measurement.

A final device which has some relevance to visibility measurements is the Slant Visual Range LIDAR. A LIDAR, which is the laser analogue of a microwave radar, fires a pulse of light. From its time of flight to a target and return, and from the strength of the returned signal, a particle concentration as a function of distance can be determined. The LIDAR signal is governed by the equation:

$$P(R) = P_c A_r^e \exp\left(-2\int_0^R \sigma(r)dr\right) \beta_\pi (R)\ell/R^2 \qquad \text{(III-34)}$$

where

$P(R)$ = power returned from range R

P_0 = power transmitted

A_r^e = effective receiver area (including beam overlap function)

$\beta_\pi(R)$ = backscattering cross section at range $R(m^{-1})$

$\sigma(R)$ = $b_{ext}(R)$ = extinction cross section (m^{-1})

and ℓ = LIDAR pulse length (m).

From this equation it can be seen that the value of SVR can be determined in similar fashion to equation (III-20) by:

$$\varepsilon = \exp\left[-\int_0^V \sigma(r)dr\right] = \left[\frac{P(V)\ V^2}{P_0 A_r{}^e \ell \beta_\pi(V)}\right]^{\frac{1}{2}} \qquad \text{(III-35)}$$

Several problems are associated with this detemination of SVR. The first is that the parameters on the right hand side of equation (III-35) depend on V and so the equation must be solved iteratively until the $\varepsilon = 0.05$ criteria is satisfied. Secondly, the LIDAR should operate at 500 nanometers to approximate human visual peak sensitivity. This wavelength, however, implies eye safety hazards for a high power LIDAR system firing up the aircraft approach path and one must move to non-visual wavelengths for eye safety. Finally, the parameter $\beta_\pi(R)$ is itself unknown and unless an assumption is made about the ratio of $\beta_\pi(R)/\sigma(R)$, the solution for the atmospheric extinction is impossible. Despite these difficulties, the measurement of SVR is considered to be of enough importance to warrant further research. For example it should not be expected that a point measure of the backscatter function in a radiation fog would necessarily agree well with a human observation of prevailing visibility because of spatial nonrepresentativeness. Experiments involving such comparisons by the Atmospheric Environment Service of the Department of the Environment indicate that a point measurement of the atmosphere will at best agree within a factor of 2 with prevailing visibility with 99% confidence (Sheppard 1978).

Other conclusions from that work can be summarized here. Backscatter metre calibrations in terms of prevailing visibility are more dependent on the particle type than on forward scatter. For the same extinction coefficient the backscatter in rain can be only half of that in snow. This is particularly important in applications where the obstruction to vision type may not be known, such as an automated weather station. For the same atmospheric conditions an observer may see further at night than in the day depending on the intensity of the lights used as visibility targets. At Toronto International Airport this difference was approximately a factor of 2 for visibilities around 1 mile.

APPENDIX IV.0 AEROSOL SCAVENGING

IV.1 INTRODUCTION

The interaction between particles and precipitation may lead to the removal of the particles from the atmosphere and their concentration in the precipitation. Such removal can occur in both natural precipitation and in the artificial precipitation of spray droplet scrubbers, although we will confine our attention to the former. In discussing these interactions, the terminology proposed by Slinn (1977a) will be used. "Scavenging" is the general term used to describe the removal of particles or gases from the atmosphere by processes connected with clouds or the precipitating hydrometeors which fall from them. This term may be modified by appropriate adjectives which describe the location of the scavenging (e.g. in-cloud or below-cloud scavenging), the type of precipitation (e.g. snow or rain scavenging), the type of pollutant (e.g. particle or gas scavenging), or the scavenging mechanism (e.g. inertial or nucleation scavenging). When describing the type of precipitation doing the scavenging an abbreviation is frequently used. Thus for example, "rain scavenging" can be contracted to "rain out". The more general term, "precipitation scavenging", which refers to scavenging by any type of precipitating hydrometeor, can be contracted to "wash out".

Figure IV-1 illustrates how precipitation scavenging fits into the overall material balance of particles or gases in a region. In this appendix particle scavenging is examined. A thorough and recent survey of the extensive scavenging literature undertaken from a Canadian point of view is to be found in the work of Denison et al. (1979). A more accessible summary of parts of this report has been given by McMahon and Denison (1979). The proceedings of the 1974 Conference on Precipitation Scavenging are also a good source of information in the field (Semonin and Beadle 1977). As a source of more recent information, the U.S. National Technical Information Service publishes an annually updated bibliography with abstracts, on the subject of gas and particle wash out (Brown 1979). Finally, for a sound and comprehensible review of scavenging, the report by Slinn (1977b) is useful.

IV.2 SCAVENGING MECHANISMS

Many of the mechanisms discussed here apply generally to the process of particle scavenging, whatever the nature of the collector and collected particles. These mechanisms will be described in the context of a rigid spherical water drop of diameter D, interacting with a rigid spherical particle of diameter d. Deviations from these assumptions, while possibly important, have received limited attention. For example, the details of snow mechanisms are poorly understood, although the basic physics is no doubt similar to that outlined below.

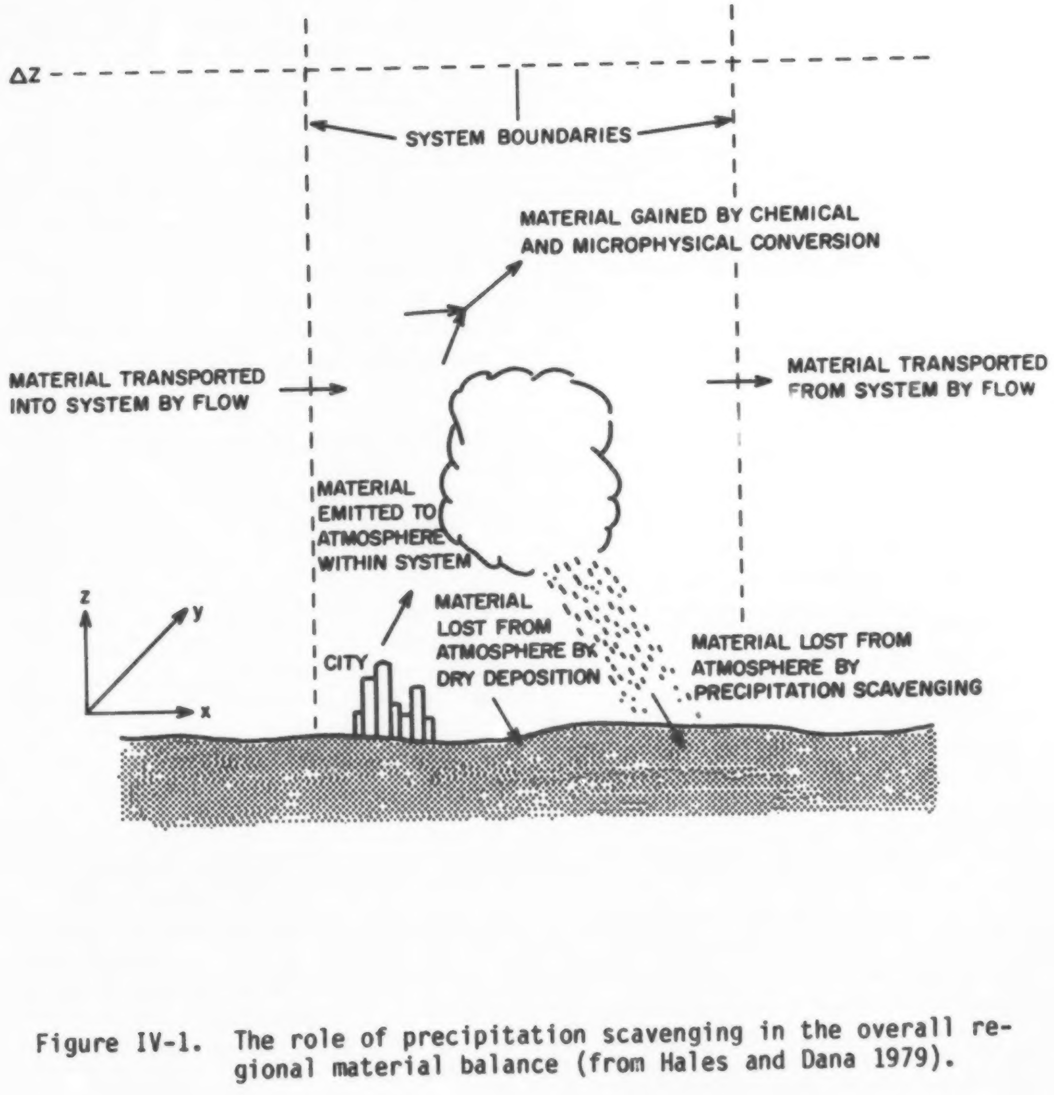
ΔZ
SYSTEM BOUNDARIES
MATERIAL GAINED BY CHEMICAL AND MICROPHYSICAL CONVERSION
MATERIAL TRANSPORTED INTO SYSTEM BY FLOW
MATERIAL TRANSPORTED FROM SYSTEM BY FLOW
MATERIAL EMITTED TO ATMOSPHERE WITHIN SYSTEM
z
y
x
CITY
MATERIAL LOST FROM ATMOSPHERE BY DRY DEPOSITION
MATERIAL LOST FROM ATMOSPHERE BY PRECIPITATION SCAVENGING

Figure IV-1. The role of precipitation scavenging in the overall regional material balance (from Hales and Dana 1979).

The water drop may be thought of as sweeping out a cylindrical volume of air with an effective diameter D+d. Of the total number of particles of diameter d with centers in this volume, the fraction which actually collides with the water drop is called the collision efficiency of the drop, η (D,d). The principal objective of most theoretical developments in this field has been to determine this collision efficiency. Some workers prefer to consider a related parameter known as the coagulation coefficient or collection kernel, defined according to:

$$K(D,d) = \frac{\pi}{4} (D+d)^2 (v(D) - v(d))\ \eta(D,d) \qquad \text{(IV-1)}$$

where v(D) and v(d) are respectively, the unperturbed fallspeeds of the drop and particle, and K is the effective collision volume swept out by the water drop in unit time. The water drop may be thought of as colliding in unit time with all particles of size d whose centers lie within this volume.

A collision may not necessarily mean capture of the particle because of the possibility of bouncing or disruption of the water drop. Consequently, the fraction of colliding particles which actually adhere to the water drop is known as the retention efficiency (or coalescence efficiency if the aerosol particle is also a liquid droplet). The product of the collision and retention efficiencies is called the collection efficiency. Very little work has been undertaken to estimate retention efficiencies of aerosol particles colliding with water drops. Certain experiments, however, indicate a value close to unity, and this is the figure which is generally adopted. Thus the collection and collision efficiencies are usually taken to be equal.

Several mechanisms have been suggested to explain how an aerosol particle may collide with a water drop. These are described below. Davenport and Peters (1978) have developed equations which have been used for estimating the collision efficiency of each process. Certain of these processes (e.g. Brownian diffusion) are essentially independent of the chemical composition of the particle and depend principally on its size. Others (e.g. nucleation scavenging) depend critically on the particle's chemical composition.

IV.2.1 NUCLEATION SCAVENGING

The process whereby certain aerosol particles give rise to the formation of water droplets in slightly supersaturated air is known as the nucleation of condensation. These particles are called cloud condensation nuclei (see Section 5.2). Particles which are hygroscopic and soluble in water can cause the formation of haze droplets even in subsaturated air. Certain particles may also encourage adsorption of water vapor which, at sufficiently low temperatures, is transformed into ice. These are known as deposition ice nuclei. Clearly both can lead to the removal of particles from the atmosphere through their incorporation into embryo cloud droplets and ice crystals. This may in fact be the most important process for the removal of particles in the accumulation size range (0.1 μm < d < 1 μm).

IV.2.2 BROWNIAN OR CONVECTIVE DIFFUSION SCAVENGING

Brownian motion is the term applied to the irregular motion ("random walk") of particles in response to their thermal bombardment by gas molecules. If the water drop is stationary with respect to the air, the Brownian motion of the particles alone will give rise to collisions. This process is termed Brownian diffusion because it can be expressed in terms of a macroscopic diffusion coefficient for the particles. If the water drop is falling through the air, the Brownian diffusion process will be enhanced by the forced convection of particles past the drop in the airstream. This combined process of forced convection with Brownian diffusion is generally referred to as convective diffusion. The relative importance of the convective and diffusive contributions to the overall transport of particles is governed by the Péclet number, $\text{Pé} = v(D)D/\Delta$, where Δ is the particle diffusivity. The convective diffusion process is generally considered to be unimportant relative to other processes when d > 1 μm, but is thought to dominate the overall scavenging when d << 0.1 μm.

IV.2.3 TURBULENCE SCAVENGING

Velocity gradients in turbulent air may cause relative motion of the aerosol particle and the water drop, giving rise to the possibility of a collision. This is referred to as turbulent shear scavenging. A second mechanism involving turbulence is based on turbulent accelerations, which can also give rise to relative velocities between the particle and the drop. This is referred to as turbulent acceleration scavenging. Both of these mechanisms are enhanced by the convective particle flux, if the drop is falling with significant speed. No rigorous general treatment of this process exists, although Monte Carlo simulations have been performed to determine the effect of turbulence on collisions among cloud droplets. However, several plausible formulae for the collision efficiency have been derived on the basis of analogies with the theory of convective diffusion.

IV.2.4 THERMO- AND DIFFUSIOPHORETIC SCAVENGING

Thermophoresis is the name given to the diffusion of particles down the temperature gradient in a gas. Although it occurs with particles of all sizes, the explanation is simplest for small particles with a large Knudsen number $Kn = \lambda/d$ (λ is the mean free path of the gas molecules). The gas molecules hitting the warm side of such tiny particles deliver a greater net impulse than do those hitting the cool side. Thus the particle experiences a net force directed down the temperature gradient. This mechanism is of no consequence if the water drop is in thermal equilibrium with its environment. However, if it is evaporating (e.g. cloud droplets in an ice-saturated environment, or raindrops below the cloud), the direction of the temperature gradient is such as to enhance the diffusive flux of particles towards the drop. Conversely, if the drop is growing, the particle flux is diminished.

Diffusiophoresis refers to aerosol particle motion induced by concentration gradients in a gaseous mixture (e.g. water vapor in air). There are two aspects in this phenomenon. The first is analogous to thermophoresis. The tendency for water vapor and air molecules to migrate down their respective concentration gradients gives rise to forces on aerosol particles embedded within these gradients. The second effect is a continuum flow (Stefan flow) set up in the air, to compensate for the diffusive flux of air molecules. For example, if a drop is evaporating, water molecules will diffuse away from the drop and air molecules towards it. Because the air molecules do not "condense" on the drop, a compensating Stefan flow of air away from the drop is set up. The net effect is that diffusiophoresis tends to oppose thermophoresis if the water drop is growing or evaporating. Numerical calculations show that thermophoresis dominates if $d < 1$ μm. The two processes may be considered to behave essentially independently, although there is a coupling with Brownian motion.

IV.2.5 GRAVITATIONAL OR INERTIAL IMPACTION SCAVENGING

Because of the relative settling rates of the water drop and the particle in a gravitational field, collision between the two becomes possible. For low Reynolds number flow ($D < 20$ μm) around the drop, the particle trajectory may not deviate significantly from a streamline. Nevertheless, because of the finite size of the particle, a collision may still occur. This is known as the interception effect. At higher Reynolds numbers, the inertia of the particle will cause it to deviate from the streamline of the airflow, towards the drop, thereby giving rise to inertial impaction. Much of this type of capture will occur on the upstream (lower) hemisphere of the drop. However, if the drop has a standing vortex wake, the particle may be entrained into it and be captured on the downstream hemisphere. This is known as wake capture. It is not thought to be significant if the wake of the drop is turbulent. Although there is a continuous transition between interception and inertial impaction, the two processes are often treated independently.

IV.2.6 ELECTROSTATIC SCAVENGING

If the water drop and the aerosol particle are charged, there may be a significant modification to the capture rate. Similar charges will tend to inhibit collisions, while dissimilar charges will tend to encourage them. However,. it is not necessary for both the drop and particle to carry a net charge. Electrical effects may still occur even if only one is charged or if they are uncharged but polarized by an existing electric field within or below the cloud. Electrostatic scavenging is probably the least understood of the mechanisms which have so far been postulated. This is not because the fundamental force is poorly understood, but rather because electrical effects are hard to measure, and because the precise nature and role of electrical effects in precipitation processes are still controversial.

IV.2.7 COMBINING INDIVIDUAL SCAVENGING MECHANISMS

Although formulae exist for computing individual collision efficiencies for each scavenging mechanism, it is not apparent exactly how to combine these in order to calculate an overall collision efficiency. Should the mechanisms, for example, be thought of as acting simultaneously or sequentially? Are they independent or do they interfere with each other? Ideas for combining collision efficiencies have ranged from the use of probability theory for independent events, to taking the square root of the sum of the squares of the individual collision efficiencies. If the individual collision efficiencies are very small, however, a simple sum is probably as good as any of these more complicated procedures. In principle, a more rigorous way to combine the various scavenging mechanisms is the trajectory method (e.g. Grover et al. 1977). Using a computer model, the equation of motion of the particle relative to the drop is solved. The various forces are incorporated into this equation, and an overall collision efficiency is deduced from an analysis of the particle trajectories. The drawback to this approach is that it is usually very costly in terms of computer time, and that it is still not apparent precisely how to combine all of the relevant forces.

These limitations notwithstanding, most efforts which have been made to deduce total collision efficiencies by combining several (although not necessarily all) of the individual mechanisms, have found that the overall scavenging coefficient exhibits a broad minimum for aerosol particles in the accumulation size range ($0.1\ \mu m < d < 1\ \mu m$). This has come to be known as the "Greenfield gap" (after Greenfield 1957). It is the result of the fact that Brownian motion dominates the capture of the smallest particles while inertial impaction dominates the capture of the largest ones. Neither of these processes is particularly effective in the intermediate size range. Phoretic and electrostatic scavenging are believed to fill this minimum somewhat. It is also thought that nucleation may play an important role in the removal from the atmosphere of particles in the accumulation mode.

IV.3 INTEGRAL SCAVENGING EFFECTS

Assuming that the water drops act independently, the loss rate of aerosol particles per unit volume of air as a result of scavenging by an ensemble of water drops is given by:

$$\frac{\delta n(d,t)}{\delta t} = - n(d,t) \int_0^\infty K(D,d)N(D,t)dD \qquad \text{(IV-2)}$$

where N(D,t)dD is the number of water drops per unit volume in the size interval D to D+dD at time t; n(d,t) is the corresponding quantity for aerosol particles, and K(D,d) is the collective kernel for particles of diameter d by drops of diameter D, as defined by equation (IV-1). Although not explicitly stated in the equations, it should be pointed out that in general, N,n and K will be functions of spatial location. In practice, the integral in equation (IV-2) is normally replaced by a summation over the drop size distribution. The fractional depletion rate of the aerosol concentration by scavenging is called the "scavenging coefficient", $\Lambda(s^{-1})$, which according to equation (IV-2) is given by:

$$\Lambda(d,t) \equiv \int_0^\infty K(D,d)N(D,t)dD \qquad \text{(IV-3)}$$

Using the definition of Λ, equation (IV-2) may be integrated with respect to time to give:

$$n(d,t) = n(d,0)e^{-\int_0^t \Lambda(d,t)dt} \qquad \text{(IV-4)}$$

If the drop size distribution is invariant with time, so that Λ is a constant with time, then equation (IV-4) may be simplified still further to yield:

$$n(d,t) = n(d,0)e^{-\Lambda(d)t} \qquad \text{(IV-5)}$$

Again it should be noted that the variables in this equation are normally functions of space as well as of time. However, in applying this equation, an atmospheric homogeneity assumption is frequently made in the horizontal and/or vertical axes.

Another parameter which is frequently used to describe the result of the overall scavenging process is the "scavenging ratio", S. This is defined as the ratio of the mixing ratio of the contaminant in the precipitation at the ground, to its mixing ratio in the column of air through which the precipitation will fall prior to the commencement of scavenging. It is a measure of the extent to which scavenging "concentrates" the contaminant. In practice, the mixing ratio in the air is measured at ground level. Making the homogeneity assumption in the vertical and the horizontal and assuming no sources or sinks (e.g. radioactive decay) of aerosol particles after the onset of scavenging, the scavenging ratio for below-cloud scavenging can be related to the scavenging coefficient by:

$$S(\tau) = \frac{\rho_a H(1-e^{-\Lambda\tau})}{\rho_w R\tau} \qquad \text{(IV-6)}$$

where H is the height of the cloud base (m), R is the rainfall rate ($m.s^{-1}$), τ its duration, and ρ_a and ρ_w are, respectively, the density of air and water. It should be noted that some authors define S as a concentration ratio, in which case the factor ρ_a/ρ_w is missing from its definition. According to the model of equation (IV-6), S is a function of the duration of the precipitation. For short durations, it is a maximum and almost independent of τ. It decreases as the duration increases, and finally diminishes as $1/\tau$ after essentially all the particles have been removed.

The value of $S(\tau)$ given by equation (IV-6) is determined by Λ, which in turn is a function of the particle diameter. In practice, S is usually determined as an integral value over a range of particle sizes. Equation (IV-6) can still be used to relate such a mean scavenging ratio to an "effective Λ". However, it should be borne in mind that this "effective Λ" is not necessarily the same as the mean value of Λ averaged over all particle sizes. Some authors have argued that the use of S can be deceptive if it is applied in an inappropriate context. S, as defined in equation (IV-6), is a measure of the volumetric removal of particles. However, in some applications (atmospheric chemistry, for example), it might be more meaningful to have a measure of the removal of particle surface area.

Still another quantity which is used to describe the overall effect of the scavenging process is the "removal rate", R*. This is defined as the ratio of the total particle mass deposited on unit area of the ground, to that originally airborne in an atmospheric column of unit cross section. For spatially homogeneous conditions, R* can be related to Λ by:

$$R^* = 1 - e^{-\Lambda\tau} \qquad \text{(IV-7)}$$

where once again it should be remembered that the R and Λ used in this equation are strictly functions of particle diameter. Nevertheless, integral values may be used in equation (IV-7) subject to a similar caveat to that mentioned above in connection with S.

Below-cloud scavenging is conceptually a very simple process if the spatial homogeneity assumption is made. It is essentially governed by the equations given above. In-cloud scavenging on the other hand is intrinsically a more complicated process. One reason for this difference is that horizontal convergence of air into the cloud base provides a continuing "source" of new particles. Thus the previous implicit assumption that the particle field is specified initially and then changes only because of scavenging, is no longer valid. Another reason is that the below-cloud scavenging process is envisaged in terms of a collector drop encountering and gathering up particles as it descends. Each such drop is assumed to maintain its identity during the fall. In-cloud scavenging, however, must be viewed as at least a two-stage process. In the first stage, aerosol particles with diameters less than about 1 μm are efficiently combined with cloud droplets or small ice crystals principally via nucleation, Brownian and turbulent diffusion, and phoretic scavenging. This process is very efficient because of the large surface area presented by these tiny hydrometeors. Subsequently in the second stage the cloud water is scavenged, primarily through inertial capture, by large precipitation particles (raindrops, snowflakes, graupel and hail). This process too is fairly efficient, although it is thought that it may represent the rate-limiting one for the overall scavenging. In view of the potential efficiency of in-cloud scavenging processes, it is now believed by at least some workers in the field that the direct removal of particles by wash out below cloud base is of secondary importance, having a significant effect on only the largest aerosol particles. Thus the overall removal rate of particles is thought to be governed by the frequency with which aerosol laden air is entrained into precipitating cloud water to rain. Aerosol particles remaining in cloud droplets will, of course, be returned to the atmosphere when the droplets evaporate, although chemical processes occurring in the droplets may change their size and chemical composition.

IV.4 LABORATORY MEASUREMENTS OF SCAVENGING

Relatively few laboratory experiments on the scavenging of particles performed under conditions relevant to the atmosphere have been undertaken (e.g., Lai *et al.* 1978; Wang and Pruppacher 1977; Knutson 1974). Because of the multiplicity of parameters which control the scavenging (drop size or snow crystal type and size, particle size and composition, electric charges, temperature, pressure and relative humidity), the experimental work which has been done, has covered only very limited ranges of conditions. Trying to compare the experimental results with theoretical models is also difficult, because frequently it is not known precisely what scavenging mechanisms are active in the experiments, and often certain parameters have to be assumed rather than measured (e.g. the charge on the particles). Nevertheless, recent experimental results do demonstrate at least a qualitative agreement with theory, and some authors claim a still higher level of agreement within the ranges of conditions considered. One of the principal qualitative results is that for a given particle size (in the accumulation mode) the collection efficiency for raindrops has a maximum at a diameter of about one millimetre. The explanation offered is that wake capture in the standing eddy behind a water drop is an important capture process. A drop of about 1 mm diameter is about the largest size which retains such a standing eddy. The experiments also show the "Greenfield gap", with a minimum in the collection efficiency for a given collector drop size, at a particle diameter of about 0.5 μm. The very few experiments which have been done involving the effects on scavenging of electrical charge on the collector drops, suggest that for normal rainfalls in the atmosphere the charge effect on wash out is probably small. However, this appears to be a very preliminary conclusion and it requires further testing and verification in the field. The situation with regard to ice scavenging is even less certain, although it appears that the "Greenfield gap" phenomenon does occur, and in about the same particle size range as for raindrops.

IV.5 THEORETICAL ESTIMATES AND FIELD MEASUREMENTS OF SCAVENGING

Equation (IV-3) expresses the fact that the scavenging coefficient is a function of both the particle size (through K(D,d)) and the drop size distribution (through K(D,d) and N(D,t)). Thus, in order to make valid estimates of Λ or comparisons between theory and experiment, both the drop spectrum and the particle spectrum should be measured. It is important to note in this connection that if the particles are hygroscopic, their size will be a function of relative humidity. Unfortunately, particle and precipitation size measurements are infrequently made with the result that comparisons among various measurements of integral (over particle and drop size) scavenging effects are not always meaningful. Nevertheless, some authors have made measurements of integral (overall drop sizes) values of Λ. These are summarized in Figure (IV-2).

Because Λ is a function of the drop size distribution, it seems reasonable that it should be related to the instantaneous rainfall rate, R, which is given by:

$$R(t) = \int_0^\infty \frac{\pi}{6} D^3 \, N(D,t) v(D) dD \qquad \text{(IV-8)}$$

By comparing equation (IV-8) with equation (IV-3), it can be seen that the relationship between R and Λ is not a unique one, and it will vary with the details of the drop size distribution. In general, therefore it will be a function of spatial location. Even the spatially averaged relation, however, will depend on the type of precipitation (convective, stratiform, etc.) and on the geographical location.

Nevertheless, in view of the many uncertainties in the rain scavenging problem, Slinn (1977b) suggests the approximate relation:

$$\Lambda(d,t) \approx \frac{R(t)}{D_m} \, o(D,d) \qquad \text{(IV-9)}$$

where D_m is the mass median diameter of the raindrops. This diameter is usually a function of rainfall rate. For example, for steady frontal rain, Slinn (1977b) gives:

$$D_m = 0.70 \, R^{\frac{1}{4}} \qquad \text{(IV-10)}$$

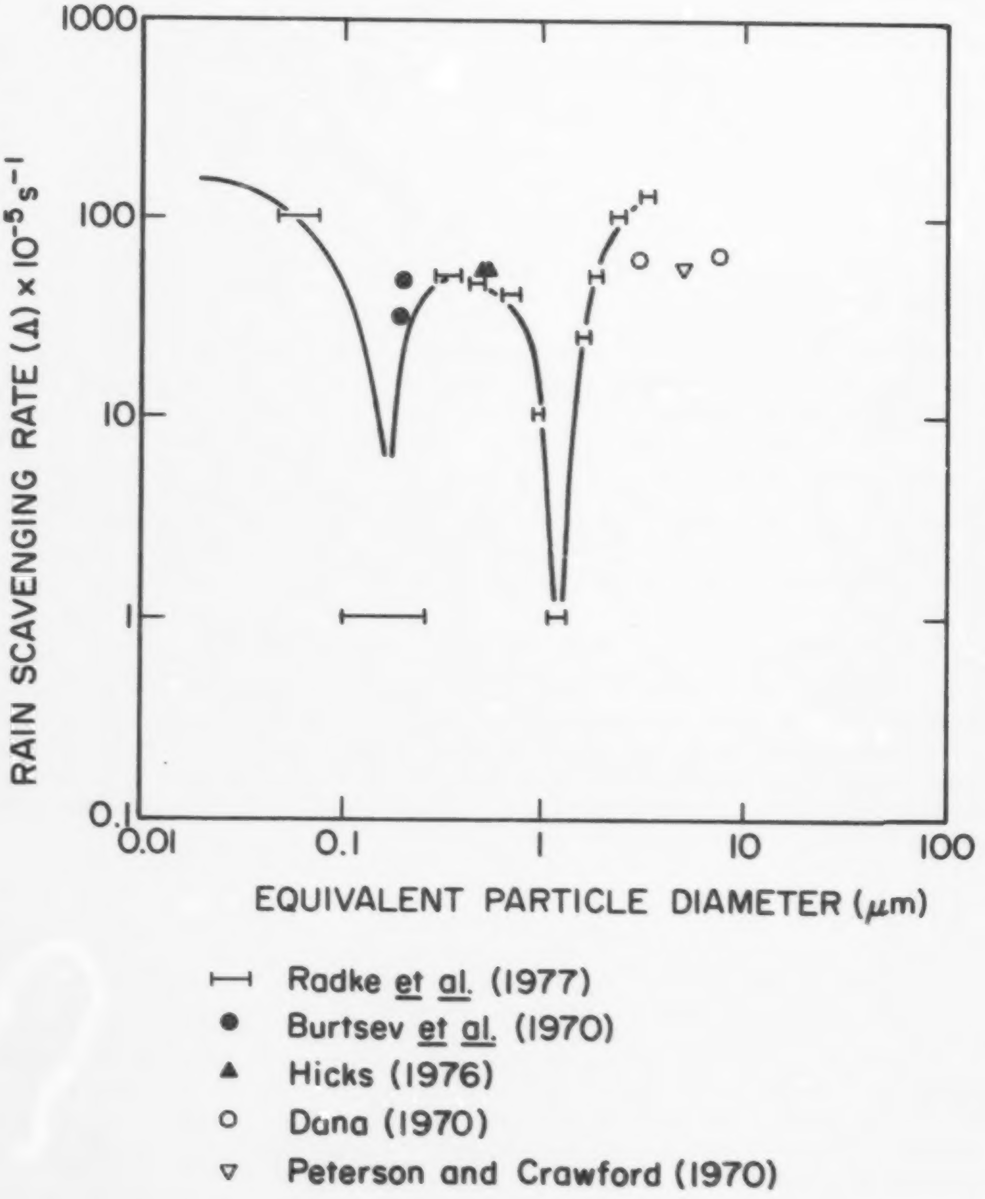

Figure IV-2. Relationship between the rain scavenging rate and particle size (figure and references are from Denison et al. 1979).

where D_m is expressed in mm and R in $mm.h^{-1}$. A comparison of the predictions of equations (IV-9) and (IV-10) with the very limited experimental data for in-cloud scavenging suggests a value for α of about 1/3. These approximations can also be used in conjunction with equation (IV-6) to obtain the following approximate relation for the scavenging ratio, S:

$$S \approx \frac{\rho_a nH}{\rho_w D_m} \qquad \text{(IV-11)}$$

A number of workers have undertaken field measurements of scavenging as a function of particle size, and some have made comparisons with theoretical estimates. Unfortunately, many of these reports are not in the open literature. Whitby (1975) measured aerosol size distributions at the ground before and during a rainfall (Figure IV-3) in Ft. Collins, Colorado. His results confirm qualitatively the existence of the Greenfield gap in the accumulation size range. Coarse and fine particles were efficiently removed by the rain but the concentration in the accumulation mode remained essentially unchanged. Davenport and Peters (1978) made similar but less detailed measurements of particle size spectra during three rainfalls in Lexington, Kentucky. Their measurements covered the range of 0.007 to 0.02 μm and 0.4 to 10 μm diameter. Unfortunately, only part of the accumulation mode was measured. They calculated wash out coefficients on the basis of their measurements to be in the range $2 \times 10^{-5}.s^{-1}$ to $1 \times 10^{-4}.s^{-1}$. These values did not vary greatly with particle size. Except for the 10 μm particles, very poor agreement was obtained with theoretical estimates of Λ based on the processes of inertial impaction, Brownian diffusion, thermo- and diffusiophoresis and electrostatic scavenging. The authors therefore make the disconcerting claim that these mechanisms cannot adequately explain their observations.

IV.6 SCAVENGING MODELS

An investigator who employs or devises a scavenging model must appreciate that the type of model to be used will depend on the purpose to which it is put. The investigator must, therefore, begin by answering questions such as: 1) Is it desirable to model a single scavenging episode or scavenging climatology? and 2) Is the model intended to be a predictive model, or is it designed to test the sensitivity of the scavenging process to various parameters? Those who make comparisons of observations and models should also bear these questions in mind, and ensure that the measurements are commensurate with the requirements of the model.

Denison et al. (1979) reviewed a number of available models, most of which fall into the episodic category. That is, they employ as an initial condition a specified spatial distribution of cloud droplets, aerosol particles, and raindrops or ice crystals, and, with the aid of

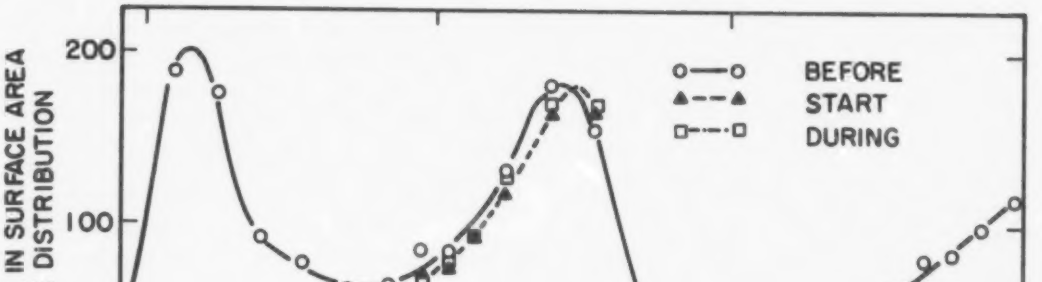

Figure IV-3. Surface area distribution of particles measured at ground level before, at the beginning of, and during a rain in Ft. Collins, Colorado (from Whitby 1975).

detailed microphysical equations (such as those developed by Davenport and Peters (1978)) follow the subsequent development of this system until the precipitation reaches the ground. Such models, while useful for making sensitivity tests, and perhaps for making comparisons with single point estimates of scavenging during a particular rainfall, suffer from a number of drawbacks. First, they are usually very costly in terms of computer time. Second, their practical validity is questionable since the existing models of this type frequently omit various scavenging mechanisms, and because the collision efficiencies for the mechanisms which are included may not be well determined. Third, they can rarely be applied in practice because they require the sorts of detailed initial conditions which present observation systems are unable to supply. The ultimate justification for this type of model, however, may be that such detailed calculations provide a theoretical basis, however shaky, for parameterizing the scavenging process in a simple way which can be incorporated into larger scale air pollution models (e.g. long-range transport models). Other workers, however, believe that this foundation is still too fragile or not sufficiently amenable to parameterization. They prefer to base their parameterizations on fairly elementary theoretical considerations, tempered by empirical evidence (cf. the approximations suggested by Slinn in Section IV.6).

This latter approach appears to be gaining in popularity as, with further study of the intricate details of the scavenging process, it becomes apparent that the removal rates are tending towards simple and rather obvious results. Slinn (1977b), for example, has summarized his view of the situation regarding long-range wet deposition in the following three points:

1. "For the large-scale problem, most wet removal of industrial pollutants occurs by in-cloud scavenging."
2. "In-cloud scavenging typically removes 10 to 90% of the pollutant ingested by the storm, depending on the efficiency with which the storm removes cloud water."
3. "The long-term wet removal space scale is dictated by the distance over which the material is transported, between its encounters with storms which efficiently remove their precipitation."

Thus mean residence times of aerosols in the atmosphere, subject to precipitation scavenging only, can be expected to be of the same order as the interval between significant efficient storms. For this reason, the statistics of precipitation systems, and their interaction with the statistics of the aerosol distribution, are likely to be very important (Rogers and Zawadzki 1979).

IV.7 SNOW SCAVENGING

Although the basic physical scavenging mechanisms are the same for snow as for rain, there will be differences in detail due to differences in the phase and the shape of the two types of precipitation. For example, inertial impaction is modified because of the possibility of particles passing "through" a snowflake, and because the characteristic size of the effective particle collectors (e.g. dendritic branches) is considerably smaller than that of the flake. This process has been called "filtration". Pitter (1977) has recently reviewed snow and ice scavenging. He points out that ice scavenging is not only important when the endproduct of the precipitation is snow (i.e. in winter). In fact, a substantial fraction of midlatitude, continental clouds probably involve the ice phase at some stage in their development.

Several studies have found that individual snow and ice particles are at least as efficient scavengers as raindrops since they have a larger surface area per unit mass, but it is difficult to present meaningful results in terms of overall cloud scavenging because of the present uncertainty of the nature and role of ice in clouds, and because of the growing feeling that it is the overall precipitation efficiency of the cloud system, and not just the individual collision efficiencies, which ultimately control the overall scavenging efficiency. Nevertheless, Slinn (1977b) has tentatively proposed an approximate equation for Λ for snow scavenging, which is similar to equation (IV-9). It is:

$$\Lambda_s(d,t) \approx 10^6 \frac{R(t)}{v^2} \eta_s(L,d) \qquad \text{(IV-12)}$$

where R(t) is the precipitation rate in $cm.h^{-1}$ (rainwater equivalent), L is a characteristic dimension of the ice particle, and v is its settling speed in $cm.s^{-1}$.

IV.8 PRECIPITATION CHEMISTRY

One of the main reasons why precipitation scavenging is of concern is the role that it plays in the chemistry of precipitation. After particles (or gases) have been scavenged from the atmosphere by drops, the fluid environment provides an ideal setting for various chemical reactions which may effectively remove certain chemical species from the atmosphere or change their size, even if the drops subsequently evaporate. In addition, because of the concentration of pollutants which scavenging brings about, these reactions may occur much more rapidly and efficiently in the precipitation than they could in the air. One of the principal concerns at present is the problem of acidic deposition and an understanding of particle scavenging is an essential step towards understanding this more general problem. However, the scope of the subject of precipitation chemistry is far too broad to survey in ths chapter. For further details on this topic consult NRCC 1981.

The multiplicity of chemical reactions and their dependence on the type and size of the particle is only beginning to be understood. The interested reader is referred for an overview of this area to Denison _et al._ (1979).

IV.9 INDIRECT EFFECTS OF PRECIPITATION MECHANISMS

Although the direct interaction of precipitation and particles by collision and capture is probably the most significant in terms of the removal of particles from the atmosphere, there may be other indirect interactions occurring as well. The winds associated with clouds and precipitation systems tend to stir up the planetary boundary layer, thereby causing a dilution of particles, which under quiescent conditions would tend to be concentrated close to the ground. This effect can give rise to an observed reduction in ground level concentration whether or not precipitation actually falls. It is an effect which must be borne in mind when making ground level measurements of natural aerosols, to compare with precipitation scavenging models. The inflow to cloud systems furthermore acts like a vacuum cleaner, removing particles from the mixed layer, and, unless the cloud precipitates, injecting them into higher levels of the troposphere or even into the stratosphere. Still stronger winds associated with thunderstorm inflow and outflow regions can stir up a great deal of surface dust and entrain it into the storm. In this way thunderstorms may act as a source as well as a sink of particles. Finally, clouds may have an effect on the fair weather electric field over substantial distances (see for example Section 5.3). To the extent that the electric field may affect the dry removal processes, precipitation systems may, paradoxically, play a role in dry deposition also.

REFERENCES

Ackerman, T.P. 1977. A model of the effect of aerosols on urban climates with particular applications to the Los Angeles Basin. J. Atmos. Sci. 34: 531-547.

Allard, E. 1876. Memoire sur l'intensité et la portée des phases. Dunod, Paris, France.

Alofs, D.J. 1978. Performance of a dual-range cloud nucleus counter. J. Appl. Meteorol. 17: 1286-1297.

Ambrose, D., Brown, D., Clark, R. 1977. Fugitive monitoring at a coal cleaning plant site. Presented at the 2nd Symposium on Fugitive Emissions: Measurement and Control, Houston, Texas. pp. 66-113.

Anderson, R.V. 1977. Atmospheric electricity in the real world. Useful application of observations which are perturbed by local effects. In Electrical processes in the atmosphere. Edited by D. Steinkopff Verlag. Darmstadt. pp. 1-17.

Angstrom, A. 1929. On the atmospheric transmission of sun radiation and on dust in the air. Geogr. Ann. Ser. A 11: 156-166.

Anlauf, K.A., Olson, M. and Wiebe, H.A. 1980. Atmospheric transport of particulate sulfate and ozone into the Toronto region and its correlation with visibility. 14th International Symposium on Atmospheric Pollution, Paris, France.

Appel, B.R., Tokiwa, Y. and Haik, M. 1981. Sampling of nitrates in ambient air. Atmos. Environ. 15: 283-289.

Atwater, M.A. 1971. Radiative effects of pollutants in the atmospheric boundary layer. J. Atmos. Sci. 28: 1367-1373.

Baldwin, B., Pollock, J.B., Summers, A. and Toon, O.B. 1976. Stratospheric aerosols and climatic change. Nature 263: 551-555.

Barrie, L.A., Hoff, R.M. and Daggupaty, S.M. 1981. The influence of mid-latitudinal pollution sources on haze in the Canadian Arctic. Atmos. Environ. 15: 1407-1419.

Beauford, W., Barber, J., Barringer, A.R. 1975. Heavy metal release from plants into the atmosphere. Nature 256: 35-37.

Beauford, W., Barber, J., Barringer, A.R. 1977. Release of particles containing metals from vegetation into the atmosphere. Science 195: 571-573.

Bergstrom, R.W. and Viskanta, R. 1973. Prediction of the solar radiant flux and heating rates in a polluted atmosphere. Tellus 25: 486-498.

Bhartendu, S. 1971. Atmospheric electricity measurements of Toronto. Atmosphere 9: 16-25.

Bhartendu, S. 1974. Electric potential gradient terdiurnal variation. J. Atmos. Terr. Phys. 36: 343-349.

Bigg, E.K. and Stevenson, C.M. 1970. Comparisons of concentrations of ice nuclei in different parts of the world. J. Rech. Atmos. 4: 41-58.

Blanchet, J.P. and Leighton, H.G. 1981. The influence of the refractive index and size spectrum on atmospheric heating due to aerosols. Contrib. Atmos. Phys. 54: 143-158.

Bodhaine, B.A. 1979. GMCC aerosol chemistry workshop: summary and recommendations. Bull. Am. Meteorol. Soc. 60: 1337-1339.

Boeck, W.L. 1976. Meteorological consequences of atmospheric krypton - 85. Science 193: 195-198.

Bradow, R.L., Black, F.M., Braddock, J.N., Hare, C.T., Ingalls, M. and Kawecki, J.M. 1979. Study of particle emissions from motor vehicles. A report to the United States Congress, U.S. Environmental Protection Agency, Research Triangle Park, North Carolina.

Braslau, N. and Dave, J.V. 1973a. Effect of aerosols on the transfer of solar energy through realistic model atmospheres. Part I: Non-absorbing aerosols. J. Appl. Meteorol. 12: 601-615.

Braslau, N. and Dave, J.V. 1973b. Effect of aerosols on the transfer of solar energy through realistic model atmospheres. Part II: Partly-absorbing aerosols. J. Appl. Meteorol. 12: 616-619.

Brock, J.R. and Marlow, M.H. 1975. Charged aerosol particles and air pollution. Environ. Lett. 10: 53-57.

Brown, R.J. 1979. Precipitation washout (a bibliography with abstracts). National Technical Information Service, Springfield, Virginia, NTIS/PS-79/0721.

Bryson, R.A. 1968. "All other factors being constant..." A reconciliation of several theories of climatic change. Weatherwise 21: 56-61.

Bryson, R.A. 1972. Climatic modification by air pollution. In Proceedings of the First International Conference on Environmental Future. Edited by N. Polunin. Macmillan Press, London. pp. 134-174.

Bryson, R.A. 1974. A perspective on climatic change. Science 184: 753-760.

Bryson, R.A. and Dittberner, G.J. 1976. A non-equilibrium model of hemispheric mean surface temperature. J. Atmos. Sci. 33: 2094-2105.

Budyko, M.I. 1969. The effect of solar radiation variations on the climate of the earth. Tellus 21: 611-619.

Budyko, M.I. 1977. On present-day climatic changes. Tellus 29: 193-204.

Cadle, R.D. and Grams, G.W. 1975. Stratospheric aerosol particles and their optical properties. Rev. Geophys. Space Phys. 13: 475-501.

Chalmers, J.A. 1967. Atmospheric electricity. 2nd ed. Pergamon Press, Toronto. 514 pp.

Changnon, S.A. 1968. The La Porte weather anomaly - fact or fiction? Bull. Am. Meteorol. Soc. 49: 4-11.

Changnon, S.A. 1969. Recent studies of urban effects on precipitation in the United States. Bull. Am. Meteorol. Soc. 50: 411-421.

Changnon, S.A. 1970. The La Porte precipitation anomaly. Bull. Am. Meteorol. Soc. 51: 337-342.

Charlson. R.J. and Pilat, M.J. 1969. Climate: The influence of aerosols. J. Appl. Meteorol. 3: 1001-1002.

Charlson, R.J., Horvath, H. and Pueschel, R.F. 1967. The direct measurement of atmospheric light scattering coefficient for studies of visibility and pollution. Atmos. Environ. 1: 469-478.

Charlson, R.J., Ahlquist, N.C., Selvidge, H. and MacCready, P.B. Jr. 1969. Monitoring of atmospheric aerosol parameters with the integrating nephelometer. J. Air Pollut. Control Assoc. 19: 937-942.

Chylek, P. and Coakley, J.A. 1974. Aerosols and climate. Science 183: 75-77.

Chylek, P. and Coakley, J.A. 1975. Manmade aerosols and the heating of the atmosphere over polar regions. In Climate of the Arctic. Edited by G. Weller and S.A. Bowling. University of Alaska. pp. 159-165.

Coakley, J.A. and Grams, G.W. 1976. Relative influence of visible and infrared optical properties of a stratospheric aerosol layer on the global climate. J. Appl. Meteorol. 15: 679-691.

Cobb, W.E. 1973. Oceanic aerosol levels deduced from measurements of the electrical conductivity of the atmosphere. J. Atmos. Sci. 35: 101-106.

Cobb, W.E. and Wells, H.J. 1970. The electrical conductivity of oceanic air and its correlation to global atmospheric pollution. J. Atmos. Sci. 27: 814-819.

Cooper, D.W., Sullivan, J.S., Quinn, M., Antonelli, R.C. and Schneider, M. 1979. Setting priorities for control of fugitive particulate emissions from open sources. U.S. Environmental Protection Agency, Washington, D.C. EPA-600/7-79-186.

Corn, M. 1976. Aerosols and the primary air pollutants - non-viable particles. Their occurrence, properties and effects. In Air pollution, Vol. I, 3rd ed. Edited by A.C. Stern. Academic Press, N.Y. pp. 77-168.

Countess, R.J., Cadle, S.H., Groblicki, P.J. and Wolff, G.T. 1981. Chemical analysis of size-segregated samples of Denver's ambient particulate. J. Air Pollut. Control Assoc. 31: 247-252.

Cowherd, C. and Hendricks, R.V. 1977. Fugitive emissions from integrated iron and steel plants - open dust sources. Paper 77-6.2 presented at the 70th Annual Meeting of the Air Pollution Control Association, Toronto, Ontario.

Cowherd, C. and Hendricks, R.V. 1978. Development of fugitive dust emission factors for industrial sources. Paper 78-55.4 presented at the 71st Annual Meeting of the Air Pollution Control Association, Houston, Texas.

Cowherd, C., Axetell, K., Guenther, C., and Jutze, G. 1974. Development of emission factors for fugitive dust sources. U.S. Environmental Protection Agency. EPA-450/3-74-037.

Cowherd, C., Cuscino, T. and Gillette, D.A. 1979. Development of emission factors for wind erosion of aggregate storage piles. Paper 79-11.1 presented at the 72nd Annual Meeting of the Air Pollution Control Association, Cincinnati, Ohio.

Crutzen, P.J. 1976. The possible importance of CSO for the sulfate layer of the stratosphere. Geophys. Res. Lett. 3: 73-76.

Currier, E.L. and Neal, B.D. 1979. Fugitive emissions from coal-fired power plants. Paper 79-11.4 presented at the 72nd Annual Meeting of the Air Pollution Control Association, Cincinnati, Ohio.

Dave, J.V. 1968. Subroutines for computing the parameters of the electromagnetic radiation by a sphere. Palo Alto, California. IBM Report 320-3237.

Dave, J.V. 1970. Coefficients of the Legendre and Fourier series for the scattering functions of spherical particles. Appl. Opt. 9: 1888-1896.

Davenport, H.M. and Peters, L.K. 1978. Field studies of atmospheric particulate concentration changes during precipitation. Atmos. Environ. 12: 997-1008.

Davies, J. 1982. Personal communication. McMaster University, Hamilton, Ontario.

Deirmendjian, D. 1969. Electromagnetic scattering on spherical polydispersions. American Elsevier Publ. Co., New York. Rand Corp. Report R-456-PR. 209 pp.

Denison, P.J., McMahon, T.A. and Kramer, J.R. 1979. Literature review on pollution deposition processes. Alberta Oil Sands Environmental Research Program, Report 50.

Dickinson, R.E. 1979. Climate change and climate modelling. Short course No. 440. Institute for Atmospheric Optics and Remote Sensing, Williamsburg, Virginia.

Dolan, D.F. and Kittleson, D.B. 1979. Roadway measurements of diesel exhaust aerosols. Detroit, Mich. SAE Paper No. 790492.

Douglas, C.A. and Booker, R.L. 1977. Visual range: concepts, instrumental determination and aviation applications. Federal Aviation Administration Report FAA-RD-77-8. Washington, D.C. 357 pp.

Douglas, C.A. and Young, L.L. 1945. Development of a transmissometer for determining visual range. FAA, Washington, D.C. CAA Tech. Dev. Report 47.

Drehmel D., Daugherty, D.P. and Gooding, C.H. 1979. State of control technology for industrial fugitive process particulate emission. RTP Internal Report.

Duce, R.A. and Woodcock, A.H. 1971. Difference in chemical composition of atmospheric sea salt particles produced in the surf zone and on the open sea in Hawaii. Tellus. 23: 427-435.

Dyer, A.J. 1974. The effect of volcanic eruptions on global turbidity and an attempt to detect long-term trends due to man. Q.J.R. Meteorol. Soc. 100: 563-571.

Eagan, R.C., Hobbs, P.V. and Radke, L.F. 1974. Particle emissions from a large kraft paper mill and their effects in the microstructure of warm clouds. J. Appl. Meteorol. 13: 535-552.

Ellis, J. and Vonder Haar, T.H. 1976. Zonal average earth radiation budget measurements from satellite for climate studies. Colorado State Univ. Atmos. Sci. Paper No. 240. 50 pp.

Ensor, D.S., Porch, W.M., Pilat, M.J. and Charlson, R.J. 1971. Influence of the atmospheric aerosol on albedo. J. Appl. Meteorol. 10: 1303-1306.

Ensor, D.S., Charlson, R.J., Ahlquist, N.C., Whitby, K.T., Husar, R.B. and Liu, B.Y.H. 1972. Multiwavelength nephelometer measurements in Los Angeles smog aerosol. I. Comparison of calculated and measured light scattering. J. Colloid Interface Sci. 39: 242-251.

Environment Canada. 1980. Air pollution emissions and control technology: Thermal power generation industry. Vol. 2. Particulate emissions from steam-powered stations. Air Pollution Control Directorate, Environmental Protection Service. EPS 3-AP-79-6.

Environment Canada. 1981a. National inventory of natural sources and emissions of primary particulates. Air Pollution Control Directorate, Environmental Protection Service. (Feb. 1981 Draft.) 115 pp.

Environment Canada. 1981b. A nationwide inventory of emissions of air contaminants. Air Pollution Control Directorate, Environmental Protection Service. EPS 3-AP-80-1. 183 pp.

Environment Canada. 1982. Personal communication from A. Sheffield. Air Pollution Control Directorate, Environmental Protection Service.

Eschelbach, G. 1973. Computations of the influence of aerosols on the atmospheric radiation balance in the visible spectrum. Contrib. Atmos. Phys. 46: 249-261.

Evans, J.S. and Cooper, D.W. 1980. An inventory of particulate emissions from open sources. J. Air Pollut. Control Assoc. 30: 1298-1303.

Fletcher, N.H. 1962. The physics of rain clouds. Cambridge University Press, Cambridge. 386 pp.

Flowers, E.C., McCormick, R.A. and Kurfis, K.R. 1969. Atmospheric turbidity over the United States, 1961-1966. J. Appl. Meteorol. 8: 955-962.

Fowler, D. 1980. Removal of sulfur and nitrogen compounds from the atmosphere in rain and by dry deposition. In Proceedings of the International Conference on Ecological Impact of Acid Precipitation, Norway. Edited by D. Drablos and A. Tollen.

Fruchter, J.S., Robertson, D.E., Evans, J.C., Olsen, K.B., Lepel, E.A., Laul, J.C., Abel, K.H., Sanders, R.W., Jackson, P.O., Wogman, N.S., Perkins, R.W., Van Tuyl, H.H., Beauchamp, R.H., Shade, J.W., Daniel, J.L., Erikson, R.L., Sehmel, G.A., Lee, R.N., Robinson, A.V., Moss, O.R., Briant, J.K. and Cannon, W.C. 1980. Mount St. Helens ash from the 18 May 1980 eruption: chemical, physical, mineralogical, and biological properties. Science 209: 1116-1125.

Gagin, A. and Neuman, J. 1976. The second Israeli cloud seeding experiment - the effect of seeding on varying cloud populations. Preprints 2nd WMO Conference on Weather Modification, Boulder, Colorado. pp. 195-204.

Gates, W.L., Cook, K.H. and Schlesinger, M.E. 1980. Simulation of the climatic effects of increased CO_2 with the OSU general circulation model with climatological sea-surface temperatures. Carbon Dioxide Research Progress Report NTIS DOE EV-0071. 79 pp.

Gatz, D.F. 1979. An investigation of pollutant source strength-rainfall relationships in St. Louis. J. Appl. Meteorol. 18: 1245-1251.

Geisler, J.E. 1977. Proceedings of the Workshop on Regional Climate and Stratospheric Change. NCAR, Boulder, Colorado. 81 pp.

Gillette, D. 1980. Major contributions of natural primary continental aerosols - source mechanisms. In Aerosols: Anthropogenic and natural sources and transport. Edited by T.J. Kneip and P.J. Lioy. Ann. N.Y. Acad. Sci. 338: 348-358.

Godson, W.L., Crozier, C.L. and Holland, J.D. 1966. An evaluation of silver iodide cloud seeding by aircraft in western Quebec, Canada, 1960-1963. J. Appl. Meteorol. 5: 500-512.

Goyer, G.G. and Renick, J.H. 1979. Results of hailstorm research and hail suppression operations in Alberta. Preprints 7th Conference on Weather Modification, Banff, Alberta. pp. J35-J36.

Grant, L.O. (Ed.) 1971. The 2nd International Workshop on Condensation and Ice Nuclei, Colorado State University. 149 pp.

Grant, L.O. 1974. Weather modifications for augmenting orographic precipitation. Where are we now? Where should we be going? Preprints 4th Conference on Weather Modification, Fort Lauderdale, Florida. pp. 408-413.

Gras, J.L. and Michael, C.G. 1979. Measurement of the stratospheric aerosol particle size distribution. J. Appl. Meteorol. 18: 855-860.

Grassl, H. 1979. Possible changes of planetary albedo due to aerosol particles. In Man's impact on climate. Edited by W. Bach, J. Panrath and W. Kellogg. Elsevier Scientific Publishing Co., New York. pp. 229-241.

Greenfield, S.M. 1957. Rain scavenging of radioactive particle material from the atmosphere. J. Meteorol. 14: 115-125.

Groblicki, P.J. 1976. General Motors sulfate dispersion experiment: Aerosol sizing measurements. General Motors Corporation GMR - 2127. Warren, Mich.

Grover, S.N., Pruppacher, H.R. and Hamielec, A.E. 1977. A numerical determination of the efficiency with which spherical aerosol particles collide with spherical water drops due to inertial impaction and phoretic and electrical forces. J. Atmos. Sci. 34: 1655-1663.

Gunn, R. 1964. The secular increase of the world-wide fine particle pollution. J. Atmos. Sci. 21: 168-181.

Hage, K.D. 1972. Urban growth effects on low-temperature fog in Edmonton. Boundary-Layer Meteorol. 2: 334-347.

Hagen, L.J. and Woodruff, N.P. 1973. Air pollution from duststorms in the Great Plains. Atmos. Environ. 7: 323-332.

Hales, J.M. and Dana, M.T. 1979. Precipitation scavenging of urban pollutants by convective storm systems. J. Appl. Meteorol. 18: 294-316.

Hansen, A.D.A., Rosen, H., Dod, R.L. and Novakov, T. 1979. Optical attenuation as a tracer for the primary component of the carbonaceous aerosol. In Proc. Carbonaceous Particles in the Atmosphere, March 20-22, 1978. Edited by T. Novakov. University of California, Berkeley, California. Lawrence Berkeley Laboratory Report LBL-9037.

Hansen, J.E., Wang, W.C. and Lacis, A.A. 1978. Mt. Agung eruption provides test of a global climate perturbation. Science 199: 1065-1068.

Hare, F.K. and Thomas, M.K. 1979. Climate Canada, 2nd ed. John Wiley and Sons, Toronto. 230 pp.

Harrison, A.W. 1979. Nephelometer estimates of visual range. Atmos. Environ. 13: 645-652.

Harshvardhan. 1979. Perturbation of the zonal radiation balance of a stratospheric aerosol layer. J. Atmos. Sci. 36: 1274-1285.

Harshvardhan and Cess, R.D. 1976. Stratospheric aerosols: Effect upon atmospheric temperature and global climate. Tellus 28: 1-10.

Herman, B.M., Browning, S.R. and Rabinoff, R. 1976. The change in earth atmosphere albedo and radiational equilibrium temperatures due to stratospheric pollution. J. Appl. Meteorol. 15: 1057-1067.

Hesketh, H.E. 1972. Understanding and controlling air pollution. Ann Arbor Science Publishers Inc., Ann Arbor, Michigan. 411 pp.

Hicks, B.B. 1980. On the dry deposition of acid particles to natural surfaces. In Polluted rain. Edited by T.Y. Toribara, M.W. Miller and P.E. Morrow. Plenum Press, New York. pp. 327-339.

Hidore, J.J. 1971a. The effects of accidental weather modification on the flow of the Kankakee River. Bull. Am. Meteorol. Soc. 52: 99-103.

Hidore, J.J. 1971b. More on the La Porte fallacy - Reply. Bull. Am. Meteorol. Soc. 52: 573-574.

Hidy, G.M. and Brock, J.R. 1970. The dynamics of aerocolloidal systems. Pergamon Press, Oxford. 379 pp.

Hidy, G.M. and Brock, J.R. 1971. An assessment of the global sources of tropospheric aerosols. In Proc. Second Clean Air Congress, Washington, D.C., Dec. 6-11, 1970. Edited by H.M. Englund and W.T. Beery. Academic Press, New York.

Hobbs, P.V., Radke, L.F. and Shumway, S.E. 1970. Cloud condensation nuclei from industrial sources and their apparent influences on precipitation in Washington State. J. Atmos. Sci. 27: 81-89.

Hogan, A.W., Mohnen, V.A. and Schaefer, V.J. 1973. Comments on "oceanic aerosol levels deduced from measurements of the electrical conductivity of the atmosphere". J. Atmos. Sci. 30: 1455-1460.

Holzman, B.G. 1971. More on the La Porte fallacy. Bull. Am. Meteorol. Soc. 52: 572-573.

Holzman, B.G. and Thom, H.C.S. 1970. The La Porte precipitation anomaly. Bull. Am. Meteorol. Soc. 51: 335-337.

Hoppel, W.A. 1977. Ion-aerosol attachment coefficients and the diffusional charging of aerosols. In Electrical processes in the atmosphere. Edited by D. Steinkopff Verlag. Darmstadt. pp. 60-69.

Huertas, M.I. and Fontan, J. 1977. Evolution of tropospheric ions. In Electrical processes in the atmosphere. Edited by D. Steinkopff Verlag. Darmstadt. pp. 45-51.

Huff, F.A. and Changnon, S.A. 1973. Precipitation modification by major urban areas. Bull. Am. Meteorol. Soc. 54: 1220-1232.

Huff, F.A. and Vogel, J.L. 1978. Urban topographic and diurnal effects on rainfall in the St. Louis region. J. Appl. Meteorol. 17: 565-577.

Huffman, P. 1973. Supersaturation spectra of AgI and natural ice nuclei. J. Appl. Meteorol. 12: 1080-1082.

Husar, R.B., Patterson, D.E., Holloway, J.M., Wilson, W.E. and Ellestad, T.G. 1979. Trends of eastern U.S. haziness since 1948. In Proc. Fourth Symposium on Atmospheric Turbulence, Diffusion and Air Pollution. American Meteorological Society, Reno, Nevada. pp. 249-256.

Inhaber, H. 1976. Changes in Canadian national visibility. Nature 260: 129-310.

Isaac, G.A., Schemenauer, R.S., Crozier, C.L., Strapp, J.W. and Chisholm, A.J. 1979. A physical evaluation of summer cumulus cloud seeding experiments near Yellowknife and Thunder Bay, Canada. Preprints 7th Conference on Weather Modification, Banff, Alberta. pp. 156-157.

Israël, H. 1971. Atmospheric electricity. Vol. 1. Fundamentals, conductivity, ions. Israel Program for Scientific Translations, Jerusalem. 317 pp.

Israël, H. 1973. Atmospheric electricity. Vol. 2. Fields, charges, currents. Israel Program for Scientific Translations, Jerusalem. 796 pp.

Jaenicke, R., Junge, C. and Kanter, H.J. 1971. Messungen der aerosol aerosolgrossenverteilung uber dem Atlantik. ρMeteorρ Forschungsergeb. Reihe B 7: 1-54.

Joseph, J.H. and Manes, A. 1971. Secular and seasonal variations of atmospheric turbidity at Jerusalem. J. Appl. Meteorol. 10: 453-462.

Joseph, J.H. and Wolfson, N. 1975. The ratio of absorption to backscatter of solar radiation by aerosols during khamsin conditions and effects on the radiation balance. J. Appl. Meteorol. 14: 1389-1396.

Joseph, J.H., Manes, A. and Ashbel, D. 1973. Desert aerosols transported by khamsinic depressions and their climatic effects. J. Appl. Meteorol. 12: 792-797.

Jutze, G.A. and Axetell, K. 1976. Factors influencing emissions from fugitive dust sources. Presented at the Symposium on Fugitive Emissions, Measurement and Control, Hartford, Conn. May 17-19. pp. 159-179.

Kellogg, W.W., Coakley, J.A. and Grams, G.W. 1975. Effect of anthropogenic aerosols on the global climate. In Proc. WMO/IAMAP Symposium on Long-term Climatic Fluctuations, Geneva, Switzerland. WMO Doc. No. 421. pp. 323-330.

Kerker, M. 1969. The scattering of light and other electromagnetic radiation. Academic Press, New York. 666 pp.

Kirshner, M., Roffman, A. and Norton, C.L. 1979. An assessment of nontraditional emission contributions to ambient air quality at selected monitoring stations in Alleghany County, Penn. Paper 79-11.5 presented at the 72nd Annual Meeting of the Air Pollution Control Association, Cincinnati, Ohio.

Knutson, E.O. 1974. Scavenging study of snow and ice crystals. IITRI Report No. C6105-28. Available as NTIS COO-578-28.

Koschmieder, H. 1924. Theorie der horizontalen sichtweite. Beitr. Phys. Freien. Atm. 12: 33-53, 171-181.

Lacis, A.A. and Hansen, J.E. 1974. A parameterization for the absorption of solar radiation in the earth's atmosphere. J. Atmos. Sci. 31: 118-133.

Lai, K.Y., Dayan, N. and Kerker, M. 1978. Scavenging of aerosol particles by a falling water drop. J. Atmos. Sci. 35: 674-682.

Lamb, H.H. 1970. Volcanic dust in the atmosphere: With a chronology and assessment of its meteorology significance. Philos. Trans. R. Soc. London Serv. A 266: 425-533.

Landsberg, H.E. 1956. The climate of towns. In Man's role in changing the face of the earth. Edited by W.L. Thomas. University of Chicago Press. pp. 584-606.

Lawford, R.G., Berry, M.O. and Savdie, I. 1974. Ice fog at arctic airports. 8th Annual Congress CMOS, York University, Toronto.

Leaderer, B.P. and Stolwijk, J.A.J. 1980. Optical properties of the urban aerosol and their relation to chemical composition. Ann. N.Y. Acad. Sci. 338: 70-85.

Lee, R.E. 1972. The size of suspended particulate matter in air. Science 178: 567-575.

Lee, R.E. and Duffield, F.V. 1979. Sources of environmentally important metals in the atmosphere. In Advances in chemistry, Series 172. Edited by T.H. Risby. American Chemical Society, Washington, D.C. pp. 146-171.

Leighton, H.G. and Rogers, R.R. 1974. Droplet growth by condensation and coalescence in a strong updraft. J. Atmos. Sci. 31: 271-279.

Lenoble, J. (Ed.) 1977. Standard procedures to compute atmospheric radiative transfer in a scattering atmosphere. NCAR, Boulder, Colorado. 125 pp.

Lenoble, J. (Ed.) 1980. Standard procedures to compute atmospheric radiative transfer in a scattering atmosphere. Vol. II. Part A. Review of methods for horizontally inhomogeneous atmospheres. Part B. Problems of scattering with gaseous absorption. IAMAP Radiation Commission, NCAR, Boulder, Colorado. 98 pp.

Linke, F. and Boda, K. 1922. Vorschlage zur berechnung des trubungsgrades der atmosphare aus den messungen der intensitat der sonnenstrahlung. Meteorol. Z. 39: 161-166.

List, R. 1979. The cloud physics dilemma. Riv. Ital. Geofis. Sci. Affini. 5: 131-138.

Lodge, J.P., Waggoner, A.P., Klodt, D.T. and Crain, C.N. 1981. Non-health effects of airborne particulate matter. Atmos. Environ. 15: 431-482.

Lorenz, E.N. 1976. Non-deterministic theories of climatic change. Quat. Res. (N.Y.) 6: 495-506.

Lovblad, G. and Grennfelt, P. 1977. Air pollution in conjunction with the handling and storage of coal. Institute for Water and Air Conservation Research, Göteberg, Sweden.

Lyons, W.A. and Pease, S.R.. 1973. Detection of particulate air pollution plumes from major point sources using ERTS-1 imagery. Bull. Am. Meteorol. Soc. 54: 1163-1170.

Lyons, C.E., Tombach, I., Eldred, R.A., Terraglio, F.P. and Core, J.E. 1979. Relating particulate matter sources and impacts in the Willamette Valley during field and slash burning. Paper 79-46.3 presented at the 72nd Annual Meeting of the Air Pollution Control Association, Cincinnati, Ohio.

Macias, E.S., Blumenthal, D.L., Anderson, J.J. and Cantrell, B.K. 1980. Size and composition of visibility-reducing aerosols in southwestern plumes. Ann. N.Y. Acad. Sci. 338: 233-257.

Manabe, S. and Strickler, R.F. 1964. Thermal equilibrium of the atmosphere with a convective adjustment. J. Atmos. Sci. 21: 361-385.

Manabe, S. and Wetherald, R.T. 1967. Thermal equilibrium in the atmosphere with a given distribution of relative humidity. J. Atmos. Sci. 24: 241-259.

Manabe, S. and Wetherald, R.T. 1975. Effects of doubling CO_2 concentration on climate of a general circulation model. J. Atmos. Sci. 32: 3-15.

Mason, B.J. 1971. The physics of clouds. Clarendon Press, Oxford. 671 pp.

Mass, C. and Schneider, S.H. 1977. Statistical evidence on the influence of sunspots and volcanic dust on long-term temperature records. J. Atmos. Sci. 34: 1995-2004.

Mathtech Inc. 1980. Fugitive dust from western surface coal mines. A report for IERL, U.S. NTIS. Cincinnati, Ohio. PB 80-221955.

Mauchly, S.J. 1923. On the diurnal variation of the potential gradient of atmospheric electricity. Terr. Magn. Atmos. Electr. 28: 61-82.

McMahon, T.A. and Denison, P.J. 1979. Empirical atmospheric deposition parameters - a survey. Atmos. Environ. 13: 571-585.

Melo, O.T. 1977. Nanticoke Generating Station brown plume study. Toronto, Ontario. Ontario Hydro Research Division Report No. 77-250-K.

Meszaros, A. and Vissy, K. 1974. Concentration, size distribution and chemical nature of atmospheric aerosol particles in remote oceanic areas. J. Aerosol Sci. 5: 101-109.

Mie, G. 1908. Contributions of optics to cloudy media, especially colloidal metal works. Ann. Phys. 25: 377-445.

Miller, M.S., Friedlander, S.K. and Hidy, G.M. 1972. A chemical element balance for the Pasadena aerosol. J. Colloid Interface Sci. 39: 165-176.

Misaki, M. and Takeuti, T. 1970. The extension of air pollution from land over ocean as revealed in the variation of atmospheric electric conductivity. J. Meteorol. Soc. Jpn. 48: 263-269.

Mitchell, J.M. 1971. The effect of atmospheric aerosols on climate with special reference to temperature near the earth's surface. J. Appl. Meteorol. 10: 703-714.

Mohnen, V.A. 1977. Formation, nature and mobility of ions of atmospheric importance. In Electrical processes in the atmosphere. Edited by D. Steinkopff Verlag. Darmstadt. pp. 1-17.

Moran, J.B., Manary, O.J., Fay, R.H. and Baldwin, M.J. 1971. Development of particle emission control techniques for spark-ignition engines. U.S. Environmental Protection Agency, Ann Arbor, Michigan. APTD-0949.

Moriyama, S. 1978. The radiative effect of atmospheric pollution: Latitudinally dependent radiation calculations including cloud contribution. Atmos. Environ. 12: 1875-1887.

Mossop, S.C. 1976. Production of secondary ice particles during the growth of graupel by riming. Q.J.R. Meteorol. Soc. 102: 45-57.

Mugnai, A. and Wiscombe, W.J. 1980. Scattering of radiation by moderately nonspherical particles. J. Atmos. Sci. 37: 1291-1307.

Munn, R.E. 1973. Secular increases in summer haziness in the Atlantic Provinces. Atmosphere 11: 156-161.

Natusch, D.F.S. and Wallace, J.R. 1974. Urban aerosol toxicity. The influence of particle size. Science 186: 695-699.

Natusch, D.F.S., Wallace, J.R. and Evans, C.A. 1974. Toxic trace elements. Preferential concentration in respirable particles. Science 183: 202-204.

Newell, R.E. 1970. Stratospheric temperature change from the Mt. Agung volcanic eruption of 1963. J. Atmos. Sci. 27: 977-978.

NRCC. 1981. Acidification in the Canadian aquatic environment: Scientific criteria for assessing the effects of acidic deposition on aquatic ecosystems. Associate Committee on Scientific Criteria for Environment Quality. National Research Council of Canada. NRCC No. 18475. 369 pp.

NRCC. 1982. Health effects of inhaled particles: Influence of particle size and shape. Associate Committee on Scientific Criteria for Environmental Quality. National Research Council of Canada. NRCC No. 18564. (In preparation)

Ochsner, J.C., Chalekode, P.K., Blackwood, T.R. 1979. Source assessment-transport of sand and gravel. A Report by Monsanto Research for U.S. Environmental Protection Agency, U.S. NTIS PB 78812BE.

Ogawa, T. and Huzita, A. 1979. Atmospheric electric-field measurements as a monitor of large-scale air pollution. J. Meteorol. Soc. Jpn. 57: 84-87.

Ogden, T.L. 1969. The effect of rainfall on large steelworks. J. Appl. Meteorol. 8: 585-591.

Paltridge, G.W. and Platt, C.M.R. 1976. Radiative processes in meteorology and climatology. Elsevier Scientific Publishing Co., New York. 318 pp.

Patterson, R.K. and Wagman, J. 1977. Mass and composition of an urban aerosol as a function of particle size for several visibility levels. J. Aerosol Sci. 8: 269-279.

Peterson, J.T. and Junge, C.E. 1971. Sources of particulate matter in the atmosphere. In Man's impact on the climate. Edited by W.H. Mathews, W.W. Kellogg and G.D. Robinson. MIT Press, Cambridge, Mass. pp. 310-320.

Petterssen, S. 1958. Introduction to meteorology. McGraw Hill, Toronto. 327 pp.

Pierson, W.R., Brachaczek, W.W., Truex, T.J., Butler, J.W. and Korniski, T.J. 1980a. Ambient sulfate measurements on Allegheny Mountain and the question of atmospheric sulfate in the northeastern United States. Ann. N.Y. Acad. Sci. 338: 145-173.

Pierson, W.R., Brachaczek, W.W., Korniski, T.J., Truex, T.J. and Butler, J.W. 1980b. Artifact formation of sulfate, nitrate and hydrogen ion on backup filters-Allegheny Mountain experiment. J. Air Pollut. Control. Assoc. 30: 30-34.

Pinnick, R.G., Rosen, J.M. and Hofmann, D.J. 1976. Stratospheric aerosol measurements III: optical model calculations. J. Atmos. Sci. 33: 304-314.

Pitter, R.L. 1977. Snow and ice scavenging. Report of Department of Environmental Technology, Oregon Graduate Center, Beaverton, Oregon. 101 pp. Available as UCRL 13759 (from NTIS).

Pittock, A.B. 1977. On the cases of local climatic anomalies, with special reference to precipitation in Washington State. J. Appl. Meteorol. 16: 223-230.

Pollack, J.B., Toon, O.B. and Sagan, C. 1975. The effect of volcanic activity on climate. *In* Proc. WMO/IAMAP Symposium on Long-term Climatic Fluctuations. Geneva, Switzerland. WMO Doc. No. 421. pp. 279-285.

Pollack, J.B., Toon, O.B., Summers, A., Van Camp, W. and Baldwin, B. 1976a. Estimates of the climatic impact of aerosols produced by space shuttles, SST's and other high flying aircraft. J. Appl. Meteorol. 15: 247-258.

Pollack, J.B., Toon, O.B., Sagan, C., Summers, A., Baldwin, B. and Van Camp, W. 1976b. Volcanic explosions and climatic change: A theoretical assessment. J. Geophys. Res. 81: 1071-1083.

Powe, N.N. 1969. The climate of Montreal. Dept. Transport. Climatological Studies No. 15. 51 pp.

Prospero, J.M. and Bonatti, E. 1969. Continental dust in the atmosphere of the eastern equatorial Pacific. J. Geophys. Res. 74: 3362-3371.

Pruppacher, H.R. and Klett, J.D. 1978. Microphysics of clouds and precipitation. Reidel Publishing Co., Boston. 714 pp.

Radke, L.F., Stith, J.L., Hegg, D.A. and Hobbs, P.V. 1978. Airborne studies of particles and gases from forest fires. J. Air Pollut. Control Assoc. 28: 30-34.

Rahn, K. 1976. Silicon and aluminum in atmospheric aerosols: crust-air fractionation. Atmos. Environ. 10: 597-601.

Rahn, K.A. and McCaffrey, R.J. 1979. Long range transport of pollution aerosol to the Arctic: a problem without borders. Sofia, Bulgaria. Proc. WMO Symp. Rep. 538: 25-36.

Ramanathan, V. and Coakley, J.A. 1978. Climate modeling through radiative-convective models. Rev. Geophys. Space Phys. 16: 465-489.

Rangno, A.L. 1979. A reanalysis of the Wolf Creek Pass cloud seeding experiment. J. Appl. Meteorol. 18: 579-605.

Rasool, S.I. and Schneider, S.H. 1971. Atmospheric carbon dioxide and aerosols: Effects of large increases on global climate. Science 173: 138-141.

Reck, R.A. 1974a. Aerosols in the atmosphere: Calculation of the critical absorption/backscatter ratio. Science 186: 1034-1036.

Reck, R.A. 1974b. Influence of surface albedo on the change in the atmospheric radiation balance due to aerosols. Atmos. Environ. 8: 823-833.

Reck, R.A. 1975. Influence of aerosol cloud height on the change in the atmospheric radiation balance due to aerosols. Atmos. Environ. 9: 89-99.

Reck, R.A. and Hummel, J.R. 1981. Influence of aerosol optical properties on surface temperature computed with a radiative-convective model. Atmos. Environ. 15: 1727-1731.

Robinson, E. and Robbins, R.C. 1971. Emissions, concentrations and fate of particulate atmospheric pollutants. Stanford Research Institute, Mendo Park, California.

Robinson, G.D. 1962. Absorption of solar radiation by atmospheric aerosol, as revealed by measurements at the ground. Arch. Met. Geophys. Bioklimatol. Ser. B. 12: 19-40.

Rogers, R.R. and Zawadzki, I.I. 1979. Rainfall statistics for application to plume rainbow models. Atmos. Environ. 13: 279-286.

Roosen, R.G., Angione, R.J. and Klemcke, C.J. 1973. Worldwide variations in atmospheric transmission: Baseline results from Smithsonian observations. Bull. Am. Meteorol. Soc. 54: 307-316.

Rose, D.C. 1937. The atmospheric potential gradient at Ottawa, Canada. Can. J. Res. 15: 119-148.

Rosen, H., Hansen, A.D.A., Dod, R.L. and Novakov, T. 1980. Soot in urban atmospheres: determination by an optical absorption technique. Science 208: 741-744.

Rouse, W.R. and Bello, R.L. 1979. Short-wave radiation balance in an urban aerosol layer. Atmosphere-Ocean 17: 2157-2168.

Rouse, W.R., Noad, D. and McCutcheon, J. 1973. Radiation, temperature and atmospheric emissivities in a polluted urban atmosphere at Hamilton, Ontario. J. Appl. Meteorol. 12: 788-807.

Russell, P.B. and Grams, G.W. 1975. Application of soil dust optical properties in analytical models of climate change. J. Appl. Meteorol. 14: 1037-1043.

Russell, P.B. and Hake, R.D. 1977. The post-Fuego stratospheric aerosol: Lidar measurements with radiative and thermal implications. J. Atmos. Sci. 34: 163-177.

Russell, P.B., Swissler, T.J., McCormick, M.P., Chu, W.P., Livingston, J.M. and Pepin, T.J. 1981. Satellite and correlative measurements of the stratospheric aerosol. I: An optical model for data conversions. J. Atmos. Sci. 38: 1279-1294.

Ryan, P.W. and McMahon, M. 1976. Some chemical and physical characteristics of emissions from forest fires. Paper 76-2.3 presented at the 69th Annual Meeting of the Air Pollution Control Association, Portland, Oregon, June 22-July 1, 1976.

Sadasivan, S. 1978. Trace elements in size-separated aerosols over sea. Atmos. Environ. 12: 1677-1683.

Sagalyn, R.C. 1958. The production and removal of small ions and charged nuclei over the Atlantic Ocean. In Recent advances in atmospheric electricity. Edited by L.G. Smith. Pergamon Press, Toronto. pp. 21-41.

Samuels, H.J., Twiss, S.A., Wong, E.W., Wong-Woo, H., Mueller, P.K., Magda, J.A and Taylor, G.S. 1973. Visibility, light scattering and mass concentration of particulate matter. California Air Research Board, Sacramento, California.

Sapsford, H.B. 1937. Influence of pollution on potential gradient at Apia. Terr. Magn. Atmos. Electr. 42: 153-158.

SCEP. 1970. Study of critical environmental problems. Man's impact on the global environment. Massachusetts Institute of Technology Press, Cambridge, Mass. 319 pp.

Schemenauer, R.S. and Isaac, G.A. 1980. Observations of cold and warm rain processes and their implications for cloud seeding in Canada. Preprints 3rd WMO Conference on Weather Modification, Clermont-Ferrand, France. pp. 77-84.

Schickedanz, P.T. 1974. Inadvertent rain modification as indicated by surface raincells. J. Appl. Meteorol. 13: 891-900.

Schneider, S.H. 1971. A comment on "Climate: the influence of aerosols". J. Appl. Meteorol. 10: 840-841.

Schuepp, W. 1949. Die bestimmung der komponenten der atmospharischen trubung aus actinometermessungen. Arch. Meteorol. Geophys. Bioklimatol. Ser. B. 1: 257-346.

Sehmel, G.A. 1980. Particle and gas dry deposition: a review. Atmos. Environ. 14: 983-1011.

Sellers, W.D. 1969. A global climatic model based on the energy balance of the earth-atmosphere system. J. Appl. Meteorol. 8: 392-400.

Sellers, W.D. 1973. A new global climatic model. J. Appl. Meteorol. 12: 241-254.

Semonin, R.G. 1974. Urban induced weather modification. In Earth environment and resources conference digest of technical papers. Louis Winner, New York. pp. 40-41.

Semonin, R.G. and Beadle, R.W. (Ed.) 1977. Precipitation scavenging. Proceedings of a Symposium held at Champaign, Illinois, 1974. ERDA Symposium Series.

Sheppard, B.E. 1978. Comparison of scattering function visibility sensors at Toronto International Airport, March 1973 to December 1975. Atmospheric Environment Service, Downsview, Ont. Instruments Branch Tech. Record TR4.

Slinn, W.G.N. 1977a. Precipitation scavenging terminology. In Precipitation scavenging. Edited by R.G. Semonin and R.W. Beadle. ERDA Symposium Series.

Slinn, W.G.N. 1977b. Some approximations for the wet and dry removal of particles and gases from the atmosphere. Water Air Soil Pollut. 7: 513-543.

Slinn, W.G.N. 1978. Parameterizations for resuspension and for wet and dry deposition of particles and gases for use in radiation dose calculations. Nucl. Saf. 19: 205-219.

SMIC. 1971. Study of man's impact on climate. Inadvertent climate modification. Massachusetts Institute of Technology Press, Cambridge, Mass. 308 pp.

Stevens, R.K., Dzubay, T.G., Russwurm, G. and Rickel, D. 1978. Sampling and analysis of atmospheric sulfates and related species. Atmos. Environ. 12: 55-68.

Stevens, R.K., Dzubay, T.G., Shaw, R.W., McClenny, W.A., Lewis, C.W. and Wilson, W.E. 1980. Characterization of the aerosols in the Great Smokey Mountains. Environ. Sci. Technol. 14: 1491-1498.

Stith, J.L., Hobbs, P.V. and Radke, L.F. 1978. Airborne particles and gas measurements in the emissions from six volcanoes. J. Geophys. Res. 83: 4009-4017.

Storebo, P.B. 1974. Formation of radiactivity size distributions in nuclear bomb debris. J. Aerosol Sci. 5: 555-577.

Sweitzer, T.A. 1980. Characterization of passively loaded particles on Hi-Vol samplers. J. Air Pollut. Control Assoc. 30: 1324-1325.

Taback, H.J. 1979. Fine particle emissions; size distribution and chemical composition. In Specialty Conference on Emission Factors and Inventories, Anaheim, California, Nov. 13-16, 1978. Edited by Air Pollution Control Directorate. pp. 61-73.

Taback, H.J., Brienza, A.R., Macko, J., Brunetz, N. 1979. Fine particle emissions for stationary and miscellaneous sources in the South Coast Air Basin. KVB Report 5806-783.

Tanner, R.L., Garber, R., Marlow, W., Leaderer, B.P. and Leyko, M.A. 1979. Chemical composition of sulfate as a function of particle size in New York summer aerosol. Ann. N.Y. Acad. Sci. 322: 99-113.

Thornthwaite, C.W. 1931. The climates of North America according to a new classification. Geogr. Rev. 21: 633-655.

Toon, O.B. and Pollack, J.B. 1976. A global average model of atmospheric aerosols for radiative transfer calculations. J. Appl. Meteorol. 15: 225-246.

Tuomi, T.J. 1975. The effect of relative humidity on Lidar backscatter and extinction by the atmospheric aerosol. Beitr. Phys. Atmos. 48: 159-167.

Twomey, S. 1977. Atmospheric aerosols. Elsevier Scientific Publishing Co., New York. 302 pp.

Twomey, S. and Wojciechowski, T.A. 1969. Observations of the geographical variation of cloud nuclei. J. Atmos. Sci. 26: 684-688.

UN-ECE. 1979. Fine particulate pollution. United Nations Economic Commissions for Europe. Pergamon Press, New York. 108 pp.

U.S. Congress. 1977. Clean air act amendments. Washington, D.C.

U.S. EPA. 1975. Compilation of air pollutant emission factors, 2nd ed. Environmental Protection Agency.

U.S. EPA. 1980a. National air pollutant emissions estimates, 1970-1978. Environmental Protection Agency, Research Triangle Park, North Carolina. EPA-450/4-80-002.

U.S. EPA. 1980b. National emissions report. Environmental Protection Agency, Research Triangle Park, North Carolina. EPA-450/4-80-005.

U.S. EPA. 1981. Air quality criteria for particulate matter and sulfur oxides. Volume II, Chapter 4, January 1981. Environmental Protection Agency. Draft No. 2.

US HEW. 1969. Air quality criteria for particulate matter. U.S. Department of Health, Education and Welfare. Washington, D.C. 211 pp.

US NAS. 1979. Airborne particles. National Academy of Sciences. University Park Press, Baltimore. 343 pp.

U.S. Standard Atmosphere. 1965. AFRCL Handbook of geophysics and space environments. Edited by S.L. Valley.

Vali, G. (Ed.) 1976. The 3rd International Workshop on Ice Nucleus Measurements. University of Wyoming Report. 187 pp.

Van de Hulst, H.C. 1957. Light scattering by small particles. John Wiley and Sons, New York. 470 pp.

Vandergrift, A.E. 1971. Particulate pollutant system study. A Report by Midwest Research Institute for U.S. Environmental Protection Agency. Report No. APTD-0743.

Vickers, G.G. and Munn, R.E. 1977. A Canadian haze climatology. Climatic Change 1: 97-103.

Vines, R.G. 1971. On the nature, properties and behaviour of bush-fire smoke. Commonwealth Scientific and Industrial Research Organization, Australia.

Viskanta, R., Bergstrom, R.W. and Johnson, R.O. 1977. Radiative transfer in a polluted urban planetary boundary layer. J. Atmos. Sci. 34: 1091-1103.

Vogel, J.L. and Huff, F.A. 1978. Relation between the St. Louis urban precipitation anomaly and synoptic weather factors. J. Appl. Meteorol. 17: 1141-1152.

Volz, F.E. 1970. Atmospheric turbidity after the Agung eruption in 1963 and size distribution of the volcanic aerosol. J. Geophys. Res. 75: 5185-5193.

Vonnegut, B. 1973. Electrical balance in the lower atmosphere. In Annual review of earth and planetary science. Vol. 1. Edited by F.A. Donath, F.G. Stehill and G.W. Wetherill. Annual Reviews Inc., Palo Alto, California. pp. 297-311.

Waggoner, A.P. and Weiss, R.E. 1980. Comparisons of fine particle mass creation and light scattering extinction in ambient aerosols. Atmos. Environ. 14: 623-626.

Waggoner, A.P., Vanderpol, A.J., Charlson, R.J., Larsen, S., Granat, L. and Tragardh, C. 1976. Sulphate-light scattering ratio as an index of the role of sulfur in tropospheric optics. Nature 261: 120-122.

Wang, P.K. and Pruppacher, H.R. 1977. An experimental determination of the efficiency with which aerosol particles are collected by water dropsd in subsaturated air. J. Atmos. Sci. 34: 1664-1669.

Wang, W.C. and Domoto, G.A. 1974. The radiative effect of aerosols in the earth's atmosphere. J. Appl. Meteorol. 13: 521-534.

Warner, J. 1968. A reduction in rainfall associated with smoke from sugarcane fires - an inadvertent weather modification? J. Appl. Meteorol. 7: 247-251.

Weare, B.C., Temple, R.L. and Snell, F.M. 1975. Aerosols and climate: Some further considerations. Science 134: 827-828.

Weiss, R.E., Waggoner, A.P., Charlson, R.J., Thorsell, D.L., Hall, J.S. and Riley, L.A. 1979. Studies of the optical, physical and chemical properties of light absorbing aerosols. In Proc: Carbonaceous particles in the atmosphere. March 20-22, 1978. Edited by T. Novakov. University of California, Berkeley, California. Lawrence Berkeley Laboratory Report LBL-9037. pp. 257-262.

Went, F.W. 1960. Organic matter in the atmosphere and its possible relation to petroleum formation. Proc. Natl. Acad. Sci. U.S.A. 46: 212-221.

Went, F.W., Slemmons, D.E., Mozingo, H.N. 1967. The organic nature of atmospheric condensation nuclei. Proc. Natl. Acad. Sci. U.S.A. 58: 69-74.

Whelpdale, D.M. 1982. Wet and dry deposition. In Chemistry of the unpolluted and polluted troposphere. Nato Advanced Study Institute. Corfu, Greece. October 1981.

Whelpdale, D.M. and Munn, R.E. 1976. Global sources, sinks and transport of air pollution. In Air pollution. Edited by A.C. Stern. Academic Press, New York. pp. 290-327.

Whipple, F.J.W. 1929. Potential gradient and atmospheric pollution - the influence of "summer time". Q.J.R. Meteorol. Soc. 55: 351-361.

Whitby, K.T. 1975. Modeling of the atmospheric aerosol particle size distributions. Sampling and analysis of atmospheric aerosols. University of Minnesota. Particle technology laboratory report No. 253.

Whitby, K.T. 1978. The physical characteristics of sulfur aerosols. Atmos. Environ. 12: 135-159.

Whitby, K.T., Kittelson, D.B., Cantrell, B.K., Barsic, N.J., Dolan, D.F., Tarvestad, L.D., Nieken, D.J., Wolf, J.L. and Wood, J.R. 1976. Aerosol size distributions and concentrations measured during the General Motors Proving Ground sulfate study. In The General Motors/EPA sulfate dispersions experiment. Edited by R.K. Stevens, P.J. Lamothe, W.E. Wilson, J.L. Durham and T.G. Dzubay. U.S. Enviromental Protection Agency, Research Triangle Park, North Carolina. EPA-600/3-76-035. pp. 29-80.

Williamson, S.J. 1973. Fundamentals of air pollution. Addison - Wesley, Reading, Mass. 472 pp.

Winchester, J.W., Ferek, R.J., Lawson, D.R., Pillotte, J.O., Thiemens, M.H. and Wangen, L.E. 1979. Comparison of aerosol sulfur and crustal element concentrations in particle size fractions from continental U.S. locations. Water Air Soil Pollut. 12: 431-440.

Wirtz, S. and Wendt, J.G. 1981. Artifact sulfate and nitrate formation at two sites in the South Coast Air Quality Management District and the California Air Resources Board. Environ. Sci. Technol. 15: 79-83.

WMO. 1971. Guide to meteorological instruments and observing practices, 4th ed. World Meteorological Organization, Geneva, Switzerland.

WMO. 1978a. International operations handbook for measurement of background atmospheric pollution. World Meteorological Organization. Report No. 491. 110 pp.

WMO. 1978b. PEP Design document. World Meteorological Organization. PEP Report No. 9.

Woodley, W.L., Simpson, J., Biondini, R. and Sambatoro, G. 1976. NOAA's Florida Area Cumulus Experiment (FACE) main rainfall results 1970-1975. Preprints 2nd WMO Conference on Weather Modification, Boulder, Colorado. pp. 151-158.

Yamamoto, G. and Tanaka, M. 1972. Increase of global albedo due to air pollution. J. Atmos. Sci. 29: 1405-1412.

Yamate, G. 1973. Development of emission factors for estimating atmospheric emissions from forest fires. U.S. Environmental Protection Agency, Research Triangle Park, North Carolina. EPA-450/3-73-009.

Zerull, R. 1976. Scattering measurements of dielectric and absorbing nonspherical particles. Beitr. Phys. Atmos. 49: 168-188.

PUBLICATIONS

of the
du

Environmental Secretariat
Secrétariat de l'environnement

NRCC Associate Committee on Scientific Criteria for Environmental Quality
CNRC-Comité associé sur les critères scientifiques concernant l'état de l'environnement

NRCC No. CNRC nº	
12678	Inventory of Pollution-Relevant Research in Canada. Interim Report, Vols. 1, 2. Etat de recherches sur la pollution au Canada. Rapport provisoire, Tomes 1, 2. 1972. 310 pp. $6.50.
14108	Inventory of Pollution-Relevant Research in Canada. Vols. 3, 4. Etat de recherches sur la pollution au Canada. Tomes 3, 4. 1975. 558 pp. $6.50.
12226	Environmental Fluoride (Special Report). 1971. 39 pp.
12226	Le fluor dans l'environnement. 1971. 41 pp.
13079	Detection and Inactivation of Enteroviruses in Water. 1973. 26 pp. $1.25.
13236	Détection et inactivation des entérovirus dans l'eau. 1973. 30 pp. $1.25.
13080	Problems and Selection of Topics for Compilation of Cause/Effect Data. 1973. 51 pp. $1.25.
13339	Problèmes et choix de thèmes en vue d'une compilation de données cause/effet. 1974. 45 pp. $1.25.
13501	The Effects of Pulp and Paper Wastes on Aquatic Life with Particular Attention to Fish and Bioassay Procedures for Assessment of Harmful Effects. 1973. 60 pp. $2.50.
13502	L'effet des déchets de pâtes et papier sur la vie aquatique. 1974. 75 pp. $2.50.
13566	A Criteria Digest on Radioactivity in the Environment. 1974. 53 pp. $1.50.
13567	Un résumé de critères sur la radioactivité dans l'environnement. 1974. 45 pp. $1.50.
13682	Lead in the Canadian Environment. 1973. 116 pp. $2.00.
13683	Le plomb dans l'environnement canadien. 1973. 130 pp. $2.00.
13684	Picloram: The Effects of Its Use as a Herbicide on Environmental Quality. 1974. 128 pp. $1.00.
13685	Piclorame: les effets de son utilisation comme herbicide sur l'état de l'environnement. 1974. 130 pp. $1.00.
13686	A Method of Monitoring Nationally for Possible Delayed Effects of Various Occupational Environments. 1974. 42 pp. $1.25.
13687	Une méthode de surveillance nationale des effets possibles, à long terme, du milieu professionnel sur la santé. 1974. 40 pp. $1.25.
13688	Environmental Cause/Effect Phenomena Relating to Technological Development in the Canadian Arctic. 1974. 125 pp. $2.00.
13689	Phénomènes environnementaux de cause à effet liés au progrès technique dans l'arctique. 1974. 128 pp. $2.00.
13690	The Application of the Phosphorus Loading Concept to Eutrophication Research. 1974. 42 pp. $1.25.
13691	Application du concept de la vitesse d'apport de phosphore par unité de surface à la recherche sur l'eutrophisation. 1974. 44 pp. $1.25.

Available through prepaid purchase orders from

En vente, moyennant commandes prepayées, au Service des

Publications, NRCC/CNRC
Ottawa, Ontario K1A 0R6

NRCC No. CNRC nº	
14094	Chlordane: Its Effects on Canadian Ecosystems and Its Chemistry. 1974. 189 pp. $1.00.
14095	Chlordane: ses effets sur les ecosystèmes canadiens et sa chimie. 1975. 192 pp. $1.00
14096	Photochemical Air Pollution: Formation, Transport and Effects. 1975. 224 pp. $2.50.
14097	La pollution photochimique de l'air: sa formation, son transport et ses effets. 1976. 203 pp. $2.50
14098	Endosulfan: Its Effects on Environmental Quality. 1975. 100 pp. $1.25.
14099	Endosulfan: ses effets sur l'état de l'environnement. 1976. 98 pp. $1.25.
14100	Waterborne Dissolved Oxygen Requirements and Criteria With Particular Emphasis on the Canadian Environment. 1975. 111 pp. $2.00.
14101	Exigences et critères relatifs à l'oxygène dissous dans l'eau, et leurs particularités à l'environnement canadien. 1976. 111 pp. $2.00.
14102	Methoxychlor: Its Effects on Environmental Quality. 1975. 164 pp. $2.00.
14103	Méthoxychlore: ses effets sur l'état de l'environnement. 1976. 161 pp. $2.00.
14104	Fenitrothion: The Effects of Its Use on Environmental Quality and Its Chemistry. 1975. 162 pp. $2.00.
14105	Fénitrothion: effets de son utilisation sur l'état de l'environnement, et sa chimie. 1976. 164 pp. $2.00.
14106	Arboviruses and Human Health in Canada. 1975. 35 pp. $1.25.
14107	Arbovirus pathogènes au Canada. 1976. 40 pp. $1.25.
14109	Waste Heat in the Aquatic Environment. 1975. 40 pp. $1.00.
14110	Pollution thermique de l'environnement aquatique. 1976. 68 pp. $1.00.
15015	Sulphur and Its Inorganic Derivatives in the Canadian Environment. 1977. 426 pp. $5.00.
15016	Le soufre et ses dérivés mineraux dans l'environnement canadien. 1978. 441 pp. $5.00.
15017	Effects of Chromium in the Canadian Environment. 1976. 168 pp. $2.00.
15018	Les effets du chrome dans l'environnement canadien. 1977. 162 pp. $2.00.
15019	The Effects of Alkali Halides in the Canadian Environment. 1977. 171 pp. $2.00.
15020	Les effets des halogénures alcalins dans l'environnement canadien. 1977. 171 pp. $2.00.
15021	The Effects of Petroleum Refinery Liquid Wastes on Aquatic Life, with Special Emphasis on the Canadian Environment. 1976. 77 pp. $2.00.
15022	Les effets des déchets liquides du raffinage du pétrole sur la vie aquatique, particulièrement dans l'environnement canadien. 1977. 86 pp. $2.00.
15023	NTA (Nitrilotriacetic Acid) - An Ecological Appraisal. 1976. 46 pp. $1.25.
15024	NTA (acide nitrilotriacétique) - une analyse écologique. 1977. 48 pp. $1.25.
15383	Effects of Noise on Man. 1976. 87 pp. $2.50.
15384	Les effets du bruit sur l'homme. 1977. 92 pp. $2.50.
15385	*Bacillus thuringiensis*: Its Effects on Environmental Quality. 1976. 133 pp. $2.00.
15386	*Bacillus thuringiensis*: ses effets sur l'état de l'environnement. 1977. 127 pp. $2.00.
15387	Medicare Data: Its Use in Defining the Effects of the Environment on Health. 1977. 164 pp. $2.50.
15388	Les statistiques de l'assurance-maladie et leur rôle dans la définition de l'influence de l'environnement sur la santé. 1978. 166 pp. $2.50.

NRCC No. CNRC nº	
15389	Fenitrothion: The Long Term Effects of Its Use in Forest Ecosystems - Current Status. 1977. 18 pp. $1.00.
16074	Fénitrothion: effets à long terme de son utilisation dans les écosystèmes forestiers - situation actuelle. 1977. 20 pp. $1.00.
15391	Effects of Arsenic in the Canadian Environment. 1978. 363 pp. $2.00.
15392	Les effets de l'arsenic sur l'environnement canadien. 1979. 415 pp. $2.00.
16073	Proceedings of a Symposium on Fenitrothion: The Long-Term Effects of Its Use in Forest Ecosystems. Comptes rendus du symposium sur le fénitrothion: les effets à long terme de son utilisation dans les écosystèmes forestiers. 1977. 628 pp. $10.00.
16075	Phenoxy Herbicides: Their Effects on Environmental Quality with Accompanying Scientific Criteria for 2,3,7,8-Tetrachlorodibenzo-*p*-Dioxin (TCDD). 1978. 440 pp. $2.00.
16076	Herbicides phénoxy - analyse de leurs effets sur l'état de l'environnement accompagnée de critères scientifiques à l'égard de la 2,3,7,8-tétrachlorodibenzo-*p*-dioxine (TCDD). 1979. 452 pp. $2.00.
16077	Polychlorinated Biphenyls: Biological Criteria for an Assessment of Their Effects on Environmental Quality. 1978. 172 pp. $2.00.
16078	Polychlorobiphényles: critères biologiques pour évaluer leurs effets sur l'état de l'environnement. 1979. 208 pp. $2.00.
16079	Ecotoxicology of Chlorpyrifos. 1978. 314 pp. $2.00.
16080	Ecotoxicologie du chlorpyrifos. 1979. 250 pp. $2.00.
16081	Environmental Fluoride 1977. 1978. 152 pp. $2.00.
16082	Le fluorure dans l'environnement, 1977. 1979. 175 pp. $2.00.
16446	Effects of Ultraviolet Radiation on Man. 1978. 90 pp. $2.00.
16447	Les effets du rayonnement ultraviolet sur l'homme. 1979. 91 pp. $2.00.
16448	The Biological Effects of Radio-frequency and Microwave Radiation. 1979. 244 pp. $5.00.
16449	Effets biologiques des radiofréquences et des micro-ondes. 1980. 244 pp. $5.00.
16450	The Aqueous Chlorination of Organic Compounds: Chemical Reactivity and Effects on Environmental Quality. 1978. 136 pp. $2.00.
16451	Chloration en milieu aqueux de composés organiques: réactivité chimique et effets sur l'état de l'environnement. 1979. 149 pp. $2.00.
16452	Effects of Asbestos in the Canadian Environment. 1979. 185 pp. $3.00.
16453	Les effets de l'amiante dans l'environnement au Canada. 1980. 202 pp. $3.00.
16454	Copper in the Aquatic Environment: Chemistry, Distribution, and Toxicology. 1979. 227 pp. $3.00.
16455	Le cuivre dans l'environnement aquatique: chimie, répartition et toxicologie. 1980. 249 pp. $3.00.
16736	Effects of Lead in the Environment - 1978. Quantitative Aspects. 1979. 779 pp. $5.00.
16737	Effets du plomb dans l'environnement - 1978. Aspects quantitatifs. 1980. 853 pp. $5.00
16738	Report of a Special Conference on Hearing Threshold Levels of "Isolated" Human Populations. Comptes rendus du symposium spécial sur les niveaux d'audition des populations humaines "isolées". 1978. 104 pp. $3.00.
16739	Effects of Mercury in the Canadian Environment. 1979. 290 pp. $3.00.
16742	Effets du mercure dans l'environnement au Canada. 1980. 292 pp. $3.00.

NRCC No. CNRC nº	
16740	Carbofuran: Criteria for Interpreting the Effects of Its Use on Environmental Quality. 1979. 191 pp. $2.00.
16741	Carbofurane: critères pour interpréter les effets de son utilisation sur l'état de l'environnement. 1980. 184 pp. $2.00.
16743	Effects of Cadmium in the Canadian Environment. 1979. 148 pp. $3.00.
16744	Les effets du cadmium dans l'environnement canadien. 1979. 150 pp. $3.00.
16745	Effects of Lead in the Canadian Environment - 1978. Executive Report. Effets du plomb dans l'environnement canadien - 1978. Rapport administratif. 1979. 24 pp. $1.00.
17581	Water Hardness, Human Health, and the Importance of Magnesium. 1979. 119 pp. $3.00.
17582	Dureté de l'eau, santé et importance du magnésium. 1980. 123 pp. $3.00.
17583	Phthalate Esters in the Aquatic Environment. 1980. 108 pp. $3.00.
17584	Esters phtaliques dans l'environnement aquatique. 1981. 110 pp. $3.00.
17585	Executive Reports: Effects of Chromium, Alkali Halides, Arsenic, Asbestos, Mercury, and Cadmium in the Canadian Environment. 80 pp. Rapports Administratifs: effets du chrome, des halogénures alcalins, de l'arsenic, de l'amiante, du mercure, et du cadmium sur l'environnement canadien. 92 pp. 1980. $3.00.
17586	A Case Study of a Spill of Industrial Chemicals - Polychlorinated Biphenyls and Chlorinated Benzenes. 1980. $5.00.
17587	Effects of Yellow Phosphorus in the Canadian Environment. 1981. 110 pp. $3.00.
17588	Effets du phosphore blanc sur l'environnement canadien. 1981. 112 pp. $3.00.
17589	Zinc in the Aquatic Environment: Chemistry, Distribution, and Toxicology. 1981. 145 pp. $3.00.
17590	Le zinc dans l'environnement aquatique: chimie, répartition et toxicologie. 1981. 152 pp. $3.00.
18128	Intestinal Parasites of Man in the Canadian Environment. 1980. 69 pp. $2.00.
18129	Les parasites intestinaux de l'homme dans l'environnement canadien. 1980. 70 pp. $2.00.
18130	The Ecological Consequences of Dredging and Dredge Spoil Disposal in Canadian Waters. 1982. 142 pp. $5.00.
18132	Effects of Vanadium in the Canadian Environment. 1980. 94 pp. $2.00.
18133	Effets du vanadium dans l'environnement canadien. 1981. 92 pp. $2.00.
18134	Radioactivity in the Canadian Environment. 1980. 129 pp. $3.00.
18135	La radioactivité dans l'environnement canadien. 1981. 133 pp. $3.00.
18156	The Report of the *ad hoc* Panel Convened by the National Research Council of Canada to Review the Spill of Polychlorinated Biphenyls at the Federal Pioneer Ltd. Site in Regina, Saskatchewan. 30 January 1980. 15 pp.
18467	Hydrogen Sulfide in the Atmospheric Environment: Scientific Criteria for Assessing its Effects on Environmental Quality. 1981. 196 pp. $5.00.
18469	Ethylenethiourea: Criteria for the Assessment of its Effects on Man. 1980. 149 pp. $3.00.
18470	Ethylène-thiourée: critères pour evaluer ses effets sur l'homme. 1981. 187 pp. $3.00.

NRCC No. CNRC No.	
18471	Pesticide-Pollinator Interactions. 1981. 190 pp. $5.00.
18472	Interactions entre pesticides et pollinisateurs. 1981. 223 pp. $5.00.
18473	Effects of Aerosols on Atmospheric Processes. 1982. 208 pp. $8.00.
18475	Acidification in the Canadian Aquatic Environment: Scientific Criteria for Assessing the Effects of Acidic Deposition on Aquatic Ecosystems. 1981. 369 pp. $10.00.
18476	Acidification dans l'environnement aquatique au Canada: critères scientifiques pour évaluer les effets du dépôt acide sur les écosystèmes aquatiques. 1982. 377 pp. $10.00.
18566	Thermal Effects Upon Fishes. 1982. 200 pp. $8.00.
18568	Effects of Nickel in the Canadian Environment. 1981. 352 pp. $4.00.
18569	Effets du nickel sur l'environnement canadien. 1982. 347 pp. $4.00.
18570	A Screen for the Relative Persistence of Lipophilic Organic Chemicals in Aquatic Ecosystems - An Analysis of the Role of a Simple Computer Model in Screening. I. A Simple Computer Model as a Screen for Persistence. II. An Introduction to Process Analyses and Their Use in Preliminary Screens of Chemical Persistence. 1981. 302 pp. $8.00.
18572	Effects of Propoxur on Environmental Quality with Particular Reference to its Use for Control of Biting Flies. 1982. 238 pp. $8.00.
18574	Polychlorinated Dibenzo-p-Dioxins: Criteria for Their Effects on Man and his Environment. 1981. 251 pp. $8.00.
18575	Polychlorodibenzo-p-dioxines: critères relatifs à leurs effets sur l'homme et son environnement. 1982. 276 pp. $8.00.
18576	Polychlorinated Dibenzo-p-Dioxins: Limitations to the Current Analytical Techniques. 1981. 184 pp. $8.00.
18578	Chlorinated Phenols: Criteria for Environmental Quality. 1982. 191 pp. $8.00.
18978	Workshop on the Combined Effects of Xenobiotics. Atelier sur les effets combinés des xenobiotiques. 1982. 253 pp. $5.00.
18979	Aminocarb: The Effects of its Use on the Forest and the Human Environment. 1982. 253 pp. $8.00.
19244	Ultrasound: Characteristics and Biological Action. 1981. 284 pp. $8.00.
19245	Les ultrasons: caractéristiques et action biologique. 1982. 284 pp. $8.00.

NRCC No. CNRC n°	
19246	The Effects of Cyanides on Aquatic Organisms with Emphasis upon Freshwater Fishes. 1982. 139 pp. $5.00.
19248	Biting Flies in Canada: Health Effects and Economic Consequences. 1982. 157 pp. $5.00.

Available through prepaid purchase orders from

En vente, moyennant commandes prepayées, au Service des

Publications, NRCC/CNRC
Ottawa, Ontario K1A 0R6

ORGANIZATION CHART

ASSOCIATE COMMITTEE ON SCIENTIFIC CRITERIA FOR ENVIRONMENTAL QUALITY

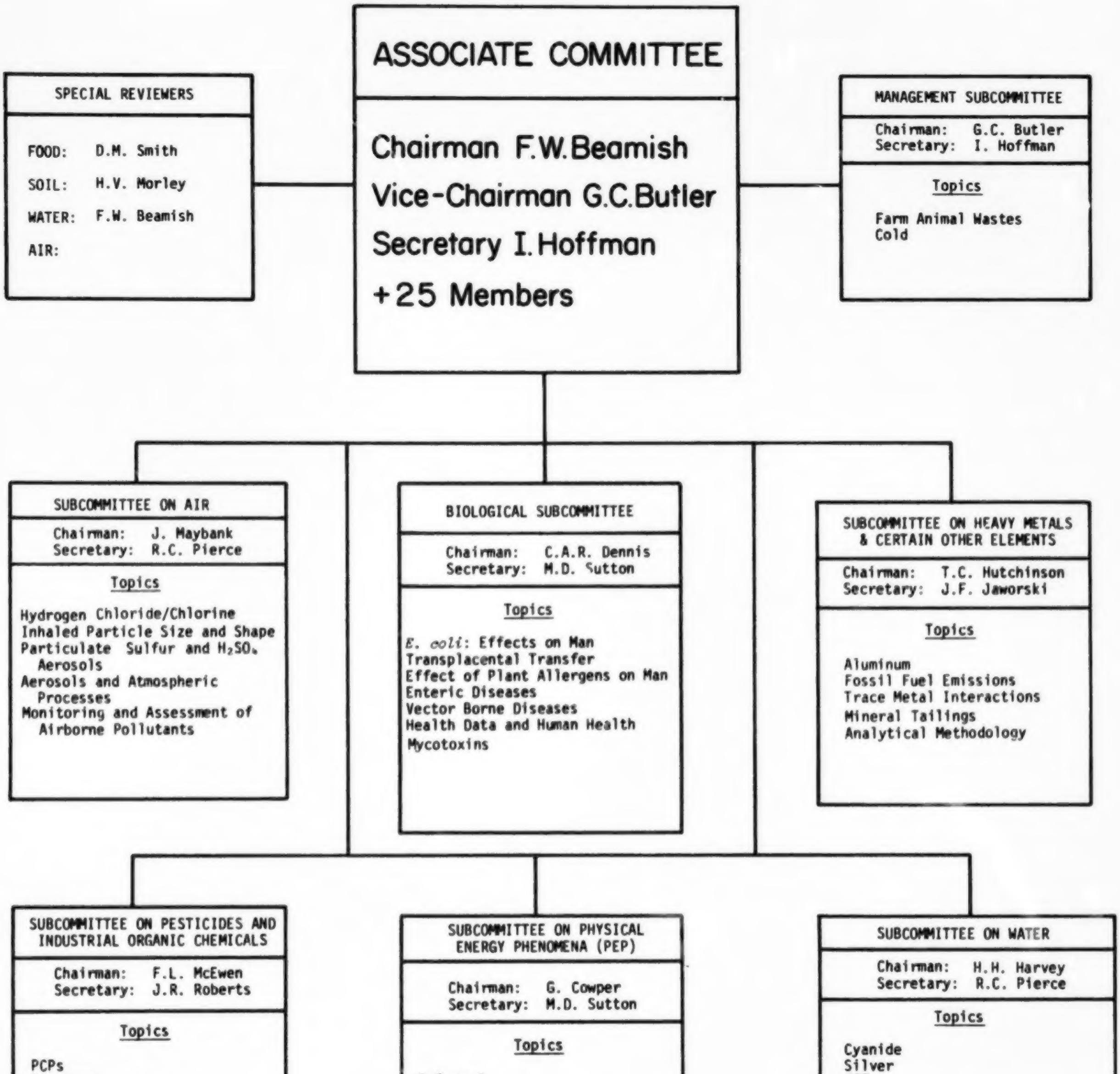

SPECIAL REVIEWERS

FOOD: D.M. Smith
SOIL: H.V. Morley
WATER: F.W. Beamish
AIR:

ASSOCIATE COMMITTEE

Chairman F.W.Beamish
Vice-Chairman G.C.Butler
Secretary I.Hoffman
+25 Members

MANAGEMENT SUBCOMMITTEE

Chairman: G.C. Butler
Secretary: I. Hoffman

Topics

Farm Animal Wastes
Cold

SUBCOMMITTEE ON AIR

Chairman: J. Maybank
Secretary: R.C. Pierce

Topics

Hydrogen Chloride/Chlorine
Inhaled Particle Size and Shape
Particulate Sulfur and H_2SO_4 Aerosols
Aerosols and Atmospheric Processes
Monitoring and Assessment of Airborne Pollutants

BIOLOGICAL SUBCOMMITTEE

Chairman: C.A.R. Dennis
Secretary: M.D. Sutton

Topics

E. coli: Effects on Man
Transplacental Transfer
Effect of Plant Allergens on Man
Enteric Diseases
Vector Borne Diseases
Health Data and Human Health
Mycotoxins

SUBCOMMITTEE ON HEAVY METALS & CERTAIN OTHER ELEMENTS

Chairman: T.C. Hutchinson
Secretary: J.F. Jaworski

Topics

Aluminum
Fossil Fuel Emissions
Trace Metal Interactions
Mineral Tailings
Analytical Methodology

SUBCOMMITTEE ON PESTICIDES AND INDUSTRIAL ORGANIC CHEMICALS

Chairman: F.L. McEwen
Secretary: J.R. Roberts

Topics

PCPs
Propoxur
Methoxychlor (update)
Combined Effects
Aminocarb
Furans
Pyrethroids

SUBCOMMITTEE ON PHYSICAL ENERGY PHENOMENA (PEP)

Chairman: G. Cowper
Secretary: M.D. Sutton

Topics

Infrared
Mechanical Vibration
Lasers
Electrical and Magnetic Fields
Optical Radiation

SUBCOMMITTEE ON WATER

Chairman: H.H. Harvey
Secretary: R.C. Pierce

Topics

Cyanide
Silver
PCPs
Dredge Spoils and Sediments
Waterborne Diseases
Radioactivity
Polynuclear Aromatic Hydrocarbons
Temperature Requirements of Aquatic Species
Underwater Noise
Cadmium in the Aquatic Environment